Cyclic Electromagnetic DNA Simulation (CEDS) can regulate the Functions of Oncogenesis-related miRNAs and DNA Motifs: Protein Signaling Pathways in RAW 264.7 Cells detected by IP-HPLC Analysis

Yeon Sook Kim[1], Suk Keun Lee[2]*

[1] Department of Dental Hygiene, College of Health and Medical Sciences, Cheongju University, Cheongju, South Korea

[2] Department of Oral Pathology, College of Dentistry, Gangneung-Wonju National University, Gangneung; and Institute of Hydrogen Bonding Magnetic Resonance Gene Regulation (Private research center), Daejeon, South Korea

Short title: Cyclic electromagnetic DNA simulation on miRNAs and DNA motifs in RAW 264.7 cells

*Corresponding Authors:

Suk Keun Lee, DDS, MSD, PhD.

Department of Oral Pathology, College of Dentistry, Gangneung-Wonju National University, 7, Jukheon-gil, Gangneung, 25457 South Korea.

E-mail : sukkeunlee2@naver.com

Cyclic Electromagnetic DNA Simulation (CEDS) can regulate the Functions of Oncogenesis-related miRNAs and DNA Motifs: Protein Signaling Pathways in RAW 264.7 Cells detected by IP-HPLC Analysis

Abstract

Based on the hydrogen bonding magnetic resonance (HBMR) in double-stranded DNAs (dsDNAs) exhibiting unique base pair polarities, Cyclic Electromagnetic DNA Simulation (CEDS)[1] was designed to target nine miRNAs and four protein binding site sequences, which are known to have an anti-oncogenic or oncogenic role in cells. RAW 264.7 cells were cultured and treated with CEDS at 20-25 Gauss in a 5% CO_2 and 37°C incubator for 20 min. Besides the cytological observation, the expressions of murine miRNAs and proteins were assessed by quantitative polymerase chain reaction (qPCR) and immunoprecipitation high-performance liquid chromatography (IP-HPLC) using 350 antisera, respectively. The results demonstrated that CEDS was found to increase the number of the corresponding mature and primary miRNAs and influenced the protein signaling in cells. For example, miR-26a-5p*-CEDS was able to downregulate 62 out of 77 target proteins, and induced a strong anti-oncogenic effect by suppressing the proliferation-related, protection-survival-senescence, inflammation-angiogenesis-fibrosis, oncogenesis-glycolysis, telomere-epigenetic modification, and p53- and FAS-mediated apoptosis signaling axis, while it activated the miRNA biogenesis, endoplasmic reticulum (ER) stress, and PARP-mediated apoptosis signaling. Among nine CEDS targeting mature miRNAs, miR-26a-5p*-, miR-126-5p*-, and miR-150-5p*-CEDSs exhibited a potent anti-oncogenic effect on RAW 264.7 cells, while miR-34a-5p*-, miR-181a-5p*-, miR-216a-5p*-, miR-365a-3p*-, and miR-655-3p*-CEDSs exhibited a dual effect, inducing both anti-oncogenic and oncogenic effects. Conversely, miR-155-5p*-CEDS appears to induce marked oncogenic effect, rather than anti-oncogenic effect. Among four CEDS targeting protein binding site sequences, telomere repeat sequence TTAGGG*-CEDS induced a potent anti-oncogenic effect, downregulating the RAS, oncogenesis, and telomere signaling, as well as activating the NFkB signaling, p53- and FAS-mediated apoptosis, and innate and cellular immunity signaling. In contrast, canonical E-box sequence CACGTG*-CEDS exhibited a significant oncogenic effect, which was characterized by the enhancement of RAS and NFkB signaling, and the resulting oncogenesis-glycolysis-chronic inflammation signaling axis. P53

binding site sequence AGACATGCCT*-CEDS induced an oncogenic effect by upregulating proliferation, telomere, and oncogenesis signaling, while concomitantly inducing an anti-oncogenic effect by downregulating RAS and NFkB signaling and upregulating p53- and PARP-mediated apoptosis. Canonical E2Fs binding site sequence TTTC(C/G)CGC*-CEDS facilitated an oncogenic effect by enhancing RAS and NFkB signaling, resulting in the upregulation of proliferation, telomere, and senescence signaling. Consequently, it was found that CEDS using a miRNA or protein binding site sequence impacted the protein signaling in RAW 264.7 cells in a sequence-specific manner. It is therefore proposed that CEDS can target miRNAs and DNA motifs, influencing their hybridization and conformation, and subsequently regulate the protein signaling in the cells.

Keywords: Cyclic electromagnetic DNA simulation, miRNAs, DNA motif, protein signaling,

Introduction

In the previous study, it was demonstrated that CEDS has a DNA hybridization potential by increasing the hydrogen bonding strength between base pairs of short dsDNA depending on CEDS time in a sequence-specific manner[1]. CEDS was found to increase the hybridization of oligo-dsDNAs and induce unique conformations of oligo-dsDNAs based on their sequence-specific base pair polarities. Therefore, it is hypothesized that CEDS can affect the hybridization potential of miRNAs, leading to the activation of miRNA biogenesis and function. However, it remains to be seen whether CEDS has a positive effect on miRNA functions in mammalian cells.

MiRNAs are non-coding small RNAs that can interact with other RNAs and DNAs through hybridization. They play a role in post-transcriptional inhibition of protein translation on mRNAs, as well as transcriptional regulation on genomic DNAs[2]. The primary miRNAs undergo partially mismatched hybridization, resulting in the formation of hairpin-like stem loop structures in the miRNA duplex. The mismatched RNA duplexes may exhibit relatively low hybridization strength between the strands of the miRNA duplex, yet they possess high potential for interaction with other RNAs and DNAs. This environment may present a compelling opportunity for the intervention of CEDS.

CEDS was designed to provide electromagnetic stimulation to base pairs in dsDNA in a cyclic manner. The apparatus sequentially produces a magnetic field targeting each base pair of dsDNA in decagonal or dodecagonal fashion at 20-25 Gauss. To achieve optimal electromagnetic induction, each A-T and G-C pair is stimulated with a different exposure time of 280 and 480 msec, respectively. All the methods are digitally programmed in an electric control apparatus. To increase the efficiency of DNA/RNA hybridization, this study employed both strands of target miRNAs and DNA motifs sequences in CEDS, which were designated as "target sequence*-CEDS." For example, CEDS that utilizes both strands of ds3T3A will be referred to as "3T3A*-CEDS", while CEDS that uses only one strand of ds3T3A is referred to as "3T3A-CEDS".

IP-HPLC has been developed to analyze the protein expression levels in comparison with the controls. It utilizes a simple immunoprecipitation method and is followed by the quantitative analysis of HPLC. The IP-HPLC has been validated through a series of experiments involving cultured cells, animal serum, human saliva, and inflammatory exudate[3-8]. It is believed that the IP-HPLC is adequate to detect multiple proteins simultaneously due to its simple, rapid, inexpensive, accurate, and automatic procedures, and furthermore, its results can be analyzed statistically.

The human genome encodes approximately 2,600 mature miRNAs (miRBase V.22), and it is known that a single miRNA can modulate thousands of genes by recognizing complementary sequences not only at the 3' UTR region but also the 5' UTR and open reading frame regions. Furthermore, miRNA interaction with promoter and enhancer regions also affects the transcription of associated genes[9,10]. It is estimated that over 60% of all mammalian protein-coding genes may be regulated by miRNAs[11]. The present study demonstrated that when the target genes are post-transcriptionally regulated by CEDS using a target miRNA sequence, the reduced expression of target genes can impact the upstream or downstream proteins in the associated signaling. Therefore, it is postulated that miRNAs can regulate the protein signaling more widely than previously assumed[2].

In order to ascertain the fidelity of CEDS, the present study conducted multiple CEDSs targeting oncogenesis-related miRNAs, including miR-26a-5p, miR-34a-5p, miR-126-5p, miR-150-5p, miR-155-5p, 181a-5p, miR-216a-5p, miR-365a-3p, and miR-655-3p. Furthermore, additional CEDSs were performed to target the oncogenesis-related protein binding site sequences, including a telomere repeat sequence (TTAGGG), a canonical E-box sequence (CACGTG), a p53 cluster 1 response element (RE) binding site sequence (AGACATGCCT), and a canonical E2Fs binding site sequence (TTTC(C/G)CGC) in RAW 264.7 cells. These CEDS targets have been the subject of extensive investigation by numerous authors[12-15].

The RAW 264.7 cells, derived from monocytes/macrophage-like cells of Balb/c mice, were utilized in this study by limiting their culture passage number to less than 20, as previously described by Taciak[16]. The cells were cultured in Dulbecco's modified Eagle's medium (WelGene Inc., Korea) supplemented with 10% fetal bovine serum (WelGene Inc., Korea), 100 units/mL penicillin, 100 μg/mL streptomycin, and 250 ng/mL amphotericin B (WelGene Inc., Korea), in a 5% CO_2 incubator at 37.5℃. The cell culture product containing 10^8-10^9 cells was placed at the center of a horizontal type CEDS in the culture incubator and treated with dodecagonal CEDS using a target miRNA or protein binding site sequence for 20 min. Subsequently, the cells were maintained in the culture incubator without CEDS for 30 min of resting time, and then harvested by centrifugation at 150g for 5 min for the following assays. .

1. Quantitative polymerase chain reaction (qPCR) after CEDS targeting different mature and primary miRNAs in RAW 264.7 cells

For quantitative polymerase chain reaction (qPCR) to determine the expression levels of nine miRNAs examined in this study, total miRNAs were extracted from CEDS-treated cells using the miRNeasy kit (Qiagen, USA), and reverse strand cDNAs were generated using the Moloney murine leukemia virus reverse transcriptase (cDNA synthesis kit, Cosmo Genetech, Korea) separately. The cDNAs were then used for qPCR (ChaiBio, USA) with a primer pair targeting an objective miRNA. The unique primer sequences for the mature and primary miRNAs were obtained from the miRBase website by analyzing them with the DNA base pair polarity program (Table 1), and their synthetic primers were purchased from CosmoGenetech Inc. (Seoul, Korea). The qPCR was

carried out with varying annealing temperatures (43–53℃) and different PCR cycles (30–45 cycles) to obtain accurate Cq values. This was followed by a DNA melting process to assess the qPCR fidelity. The exponential growth curve and Cq number of the experimental group were compared to those of the untreated control group.

A series of qPCR experiments were conducted using the primer sets and cDNA templates obtained from the cell culture to determine the expression levels of primary and mature miRNAs after CEDS using a target miRNA sequence. The primary aim of this experiment was to assess the targeting efficiency of CEDS for the specific miRNA of interest among different miRNAs present in cells. The qPCRs were simultaneously conducted for 15 miRNAs selected in this study using the template cDNAs obtained from the RAW 264.7 cells treated with CEDS targeting one miRNA among the 15 miRNAs. The second objective of this experiment was to determine the incremental ratio of mature and primary miRNAs in cells following CEDS treatment compared to the untreated controls. The incremental ratio of mature and primary miRNAs was calculated based on the Cq number.

Table 1. The primer pairs of miRNAs used in quantitative real time PCR (qPCR)

mature mmu-miRNA	primer direction	mature miRNA primer sequences	Primary miRNA primer sequences
miR-26a-5p	Forward	TTCAAGTAACC	AAGCTGGAGGACCGA
	Reverse	AGCCTATCC	ACTCTGTTGTTGCCG
miR-34a-5p	Forward	TAGGCAGTG	CCCGGTGCTCGGTTT
	Reverse	GTACAATCA	GCGGGTGATGCTGTG
miR-126-5p	Forward	CATTATTAC	ACAGCGCGTACC
	Reverse	GCGCGTACC	GAGTGCCAGCCGTGG
miR-150-5p	Forward	CCTGTCTCCCA	CAGCACTGGTAC
	Reverse	CACTGGTAC	CTGGAGTTGTTGCTG
miR-155-5p	Forward	TTAATGCTA	TTAATGCTA
	Reverse	AACCCCTA	CCATTTGTTCCATGT
miR-181a-5p	Forward	TACAATCAACG	TACAATCAACG
	Reverse	ACTCACCGAC	TAGGGTACAATCAAC
miR-216a-5p	Forward	TAATCTCAG	TAATCTCAG
	Reverse	TCACAGTTGCC	TTAGCATAATCCCAG
miR-365a-3p	Forward	TAAGGATTT	ATCTGCCCCT
	Reverse	ATCTGCCCCT	TATCTTACAGAGTTG
miR-655-3p	Forward	AAAGAGGTTA	AAAGAGGTTA
	Reverse	GAACATAACACG	AACTATGCAAGG

qPCR for the expression of mature and primary miRNAs after miR-26a-5p*-CEDS

The qPCR results showed that mmu-miR-26a-5p*-CEDS significantly increased the expression of mature miR-26a-5p and primary miR-26a, with average fold changes of 1.72 and 4.14, respectively, in comparison to untreated controls (Fig. 1 A,B). The multiple qPCRs for 15 miRNAs performed simultaneously showed that miR-26a-5p was moderately expressed compared to other miRNAs, and miR-26a-5p*-CEDS also affected the other miRNA expression by upregulating miR-126-5p and miR-655-3p while downregulating miR-365a-3p compared to untreated control (Figure 1 D,E), indicating the presence of secondary effect through the feedback loop interactions of gene transcription.

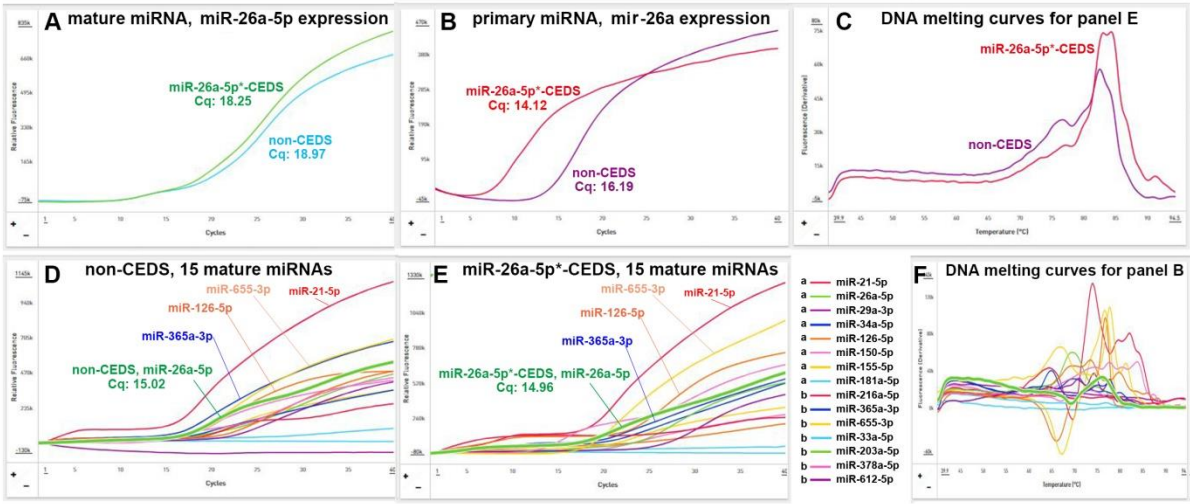

Fig. 1. The effect of miR-26a-5p*-CEDS on the expression of mature miR-26a-5p and primary miR-26a in RAW 264.7 cells was evaluated by qPCR in comparison with other 14 miRNAs. *This figure represents three or more repeated experiments.

qPCR for the expression of mature and primary miRNAs after miR-34a-5p*-CEDS

In the multiple qPCRs for 15 mature miRNAs, mmu-miR-34a-5p sequence TGGCAGTGTCTTAGCTGGTTGT*-CEDS demonstrated a 610% increase in miR-34a-5p expression (Cq=17.34) compared to the untreated control (Cq=14.29) in RAW 264.7 cells. Concurrently, miR-34a-5p*-CEDS was found to significantly increase the expression of miR-126-5p and miR-655-3p compared to the untreated control, while decreasing the expression of miR-21-5p (Fig. 2A and B).

In the qPCR assays conducted to determine CEDS-induced incremental ratio of mature and primary miRNAs, miR-34a-5p*-CEDS demonstrated a significant increase in the expression of mature miR-34a-5p and primary miR-34a, with fold changes of 396% and 688%, respectively, in comparison to the untreated controls (Fig. 2 D and E).

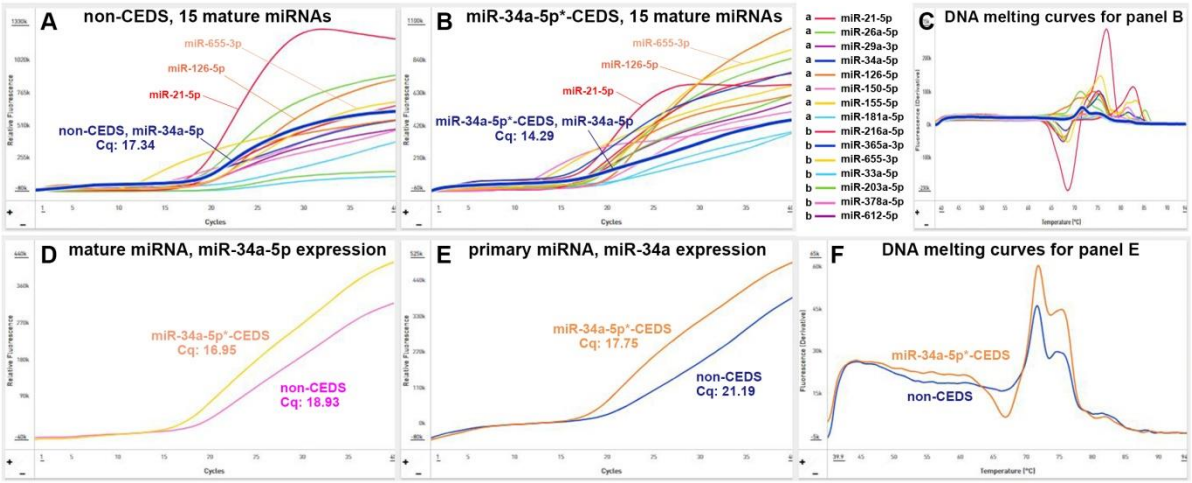

Fig. 2. Quantitative PCR for CEDS effect on the expression of mature miR-34a-5p (D) and primary miR-34a (E) in RAW 264.7 cells. MiR-34a-5p*-CEDS increased the expression of miR-34a-5p along with an influence on the expression of other 14 miRNAs (A and B). Noted the variable melting curves of 15 mature miRNAs and similar melting curves of primary miR-34a (C and F). The representative results were presented based on the findings of triple repeated experiments.

.

qPCR for the expression of mature and primary miRNAs after miR-126-5p*-CEDS

The qPCR results showed that mmu-miR-126-5p*-CEDS increased the expression of mature miR-126-5p and primary miR-126, with average fold changes of 3.36 and 2.56, respectively, in comparison to untreated controls (Fig. 3 A,B). The multiple qPCRs for 15 miRNAs performed simultaneously showed that miR-126-5p was moderately expressed compared to other miRNAs, and miR-126-5p*-CEDS also affected the other miRNA expression by upregulating miR-26a-5p and miR-655-3p compared to untreated control (Fig. 3 D,E), indicating the presence of secondary effect through the feedback loop interactions of gene transcription.

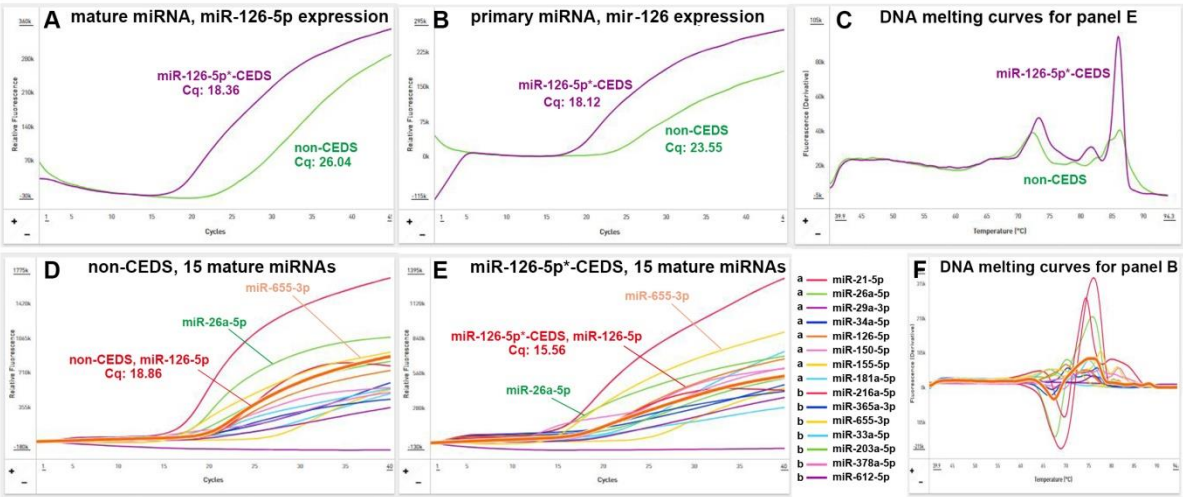

Fig. 3. The effect of miR-126-5p*-CEDS on the expression of mature miR-126-5p and primary miR-126 in RAW 264.7 cells was evaluated by qPCR in comparison with other 14 miRNAs. *This figure represents three or more repeated experiments.

qPCR for the expression of mature and primary miRNAs after miR-150-5p*-CEDS

In the multiple qPCRs for 15 mature miRNAs, mmu-miR-150-5p sequence TCTCCCAACCCTTGTACCAGTG*-CEDS demonstrated a 1080% increase in miR-150-5p expression (Cq=14.94) expression compared to the untreated control (Cq=9.54) in RAW 264.7 cells. Concurrently, miR-150-5p*-CEDS was found to significantly increase the expression of miR-126-5p, miR-365a-3p, and miR-655-3p compared to the untreated control (Fig. 4 A and B).

In the qPCR assays conducted to determine CEDS-induced incremental ratio of mature and primary miRNAs, miR-150-5p*-CEDS demonstrated a significant increase in the expression of mature miR150-5p and primary miR-150, with fold changes of 232% and 340%, respectively, in comparison to the untreated controls (Fig. 4 D and E).

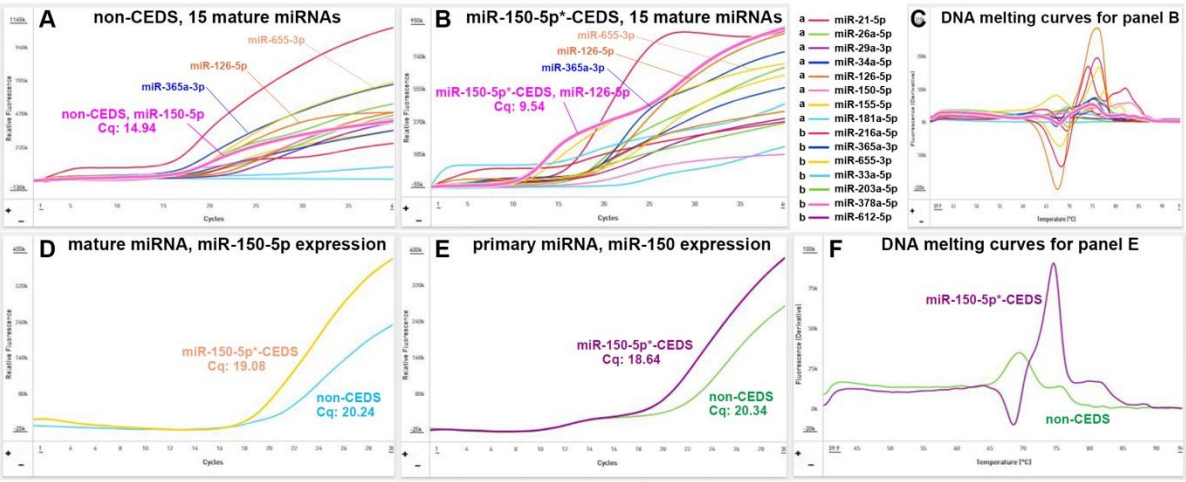

Fig. 4. Quantitative PCR for CEDS effect on the expression of mature miR-150-5p (D) and primary miR-150 (E) in RAW 264.7 cells. MiR-150-5p*-CEDS increased the expression of miR-150-5p along with an influence on the expression of other 14 miRNAs (A and B). Noted the variable melting curves of 15 mature miRNAs and similar melting curves of primary miR-150 (C and F). The representative results were presented based on the findings of triple repeated experiments.

qPCR for the expression of mature and primary miRNAs after miR-155-5p*-CEDS

In the multiple qPCRs for 15 mature miRNAs, mmu-miR-155-5p sequence TTAATGCTAATCGTGATAGGGGTT*-CEDS demonstrated a 924% increase in miR-155-5p expression (Cq=15.83) expression compared to the untreated control (Cq=11.21) in RAW 264.7 cells. Concurrently, miR-155-5p*-CEDS was found to significantly increase the expression of miR-181a-5p, miR-216a-5p, and miR-655-3p compared to the untreated control (Fig. 5 A and B).

In the qPCR assays conducted to determine CEDS-induced incremental ratio of mature and primary miRNAs, miR-155-5p*-CEDS demonstrated a significant increase in the expression of mature miR-155-5p and primary miR-155, with fold changes of 454% and 170%, respectively, in comparison to the untreated controls (Fig. 5 D and E).

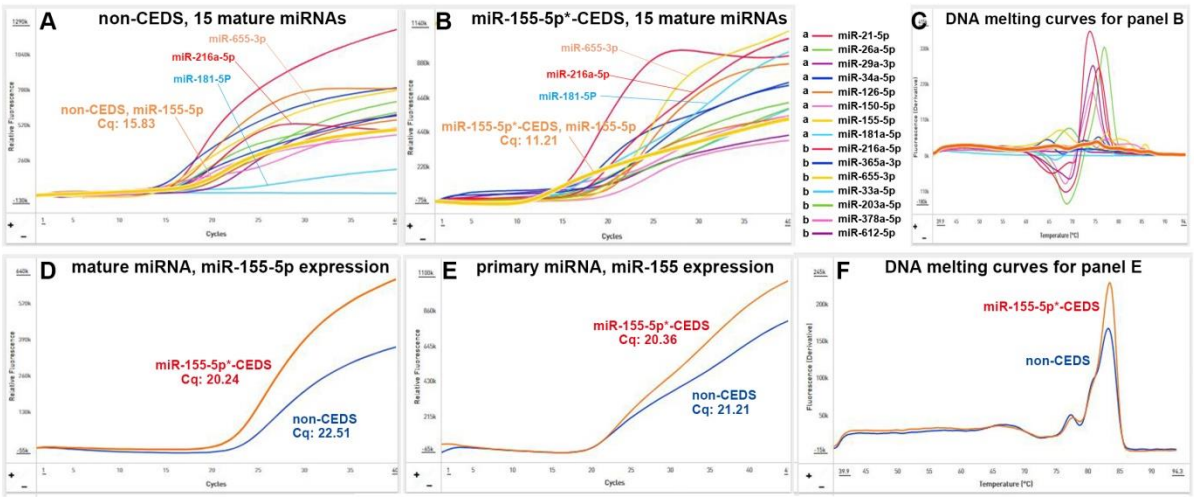

Fig. 5. Quantitative PCR for CEDS effect on the expression of mature miR-155-5p (D) and primary miR-155 (E) in RAW 264.7 cells. MiR-155-5p*-CEDS increased the expression of miR-155-5p along with an influence on the expression of other 14 miRNAs (A and B). Noted the variable melting curves of 15 mature miRNAs and similar melting curves of primary miR-155 (C and F). The representative results were presented based on the findings of triple repeated experiments.

qPCR for the expression of mature and primary miRNAs after miR-181a-5p*-CEDS

In the multiple qPCRs for 15 mature miRNAs, mmu-miR-181a-5p*-CEDS AACATTCAACGCTGTCGGTGAGT*-CEDS demonstrated a 456% increase in miR-181a-5p expression (Cq=16.1) compared to the untreated control (Cq=14.12) in RAW 264.7 cells. Concurrently, miR-181a-5p*-CEDS was found to significantly increase the expression of miR-126-5p, miR-216a-5p, and miR-655-3p compared to the untreated control (Fig. 6 A and B).

In the qPCR assays conducted to determine CEDS-induced incremental ratio of mature and primary miRNAs, miR-181a-5p*-CEDS demonstrated a significant increase in the expression of mature miR-181a-5p and primary miR-181a, with fold changes of 294% and 292%, respectively, in comparison to the untreated controls (Fig. 6 D and E).

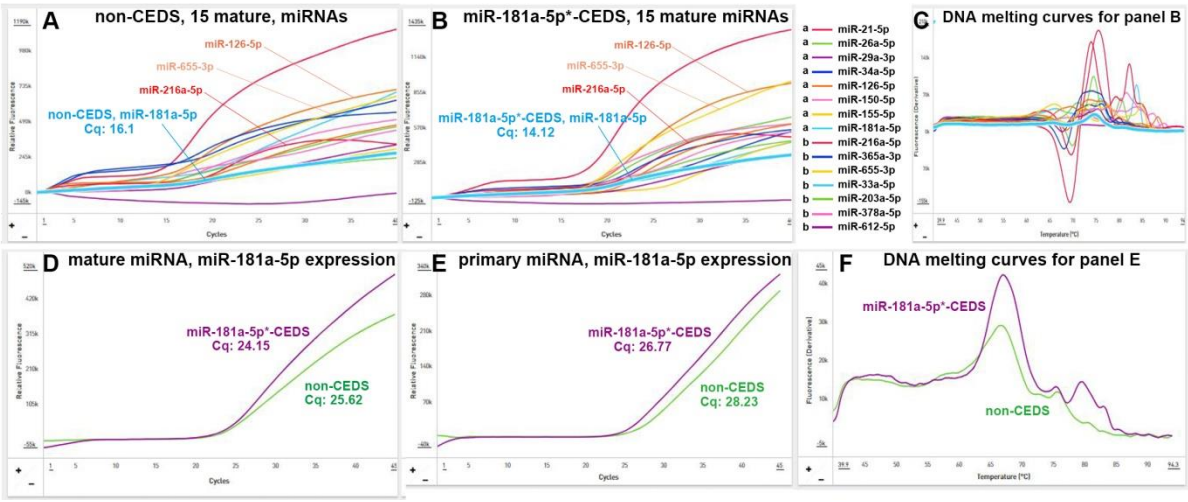

Fig. 6. Quantitative PCR for CEDS effect on the expression of mature miR-181a-5p (D) and primary miR-181a (E) in RAW 264.7 cells. MiR-181a-5p*-CEDS increased the expression of miR-181a-5p along with an influence on the expression of other 14 miRNAs (A and B). Noted the variable melting curves of 15 mature miRNAs and similar melting curves of primary miR-181a (C and F). The representative results were presented based on the findings of triple repeated experiments.

qPCR for the expression of mature and primary miRNAs after miR-216a-5p*-CEDS

In the multiple qPCRs for 15 mature miRNAs, mmu-miR-216a-5p*-CEDS TAATCTCAGCTGGCAACTGTGA*-CEDS demonstrated a 466% increase in miR-216a-5p expression (Cq=16.62) compared to the untreated control (Cq=14.29) in RAW 264.7 cells. Concurrently, miR-216a-5p*-CEDS was found to significantly increase the numbers of miR-26a-5p and miR-126-5p compared to the untreated control (Fig. 7 A and B).

In the qPCR assays conducted to determine CEDS-induced incremental ratio of mature and primary miRNAs, miR-216a-5p*-CEDS demonstrated a significant increase in the expression of mature miR-216a-5p and primary miR-216a, with fold changes of 470% and 112%, respectively, in comparison to the untreated controls (Fig. 7 D and E).

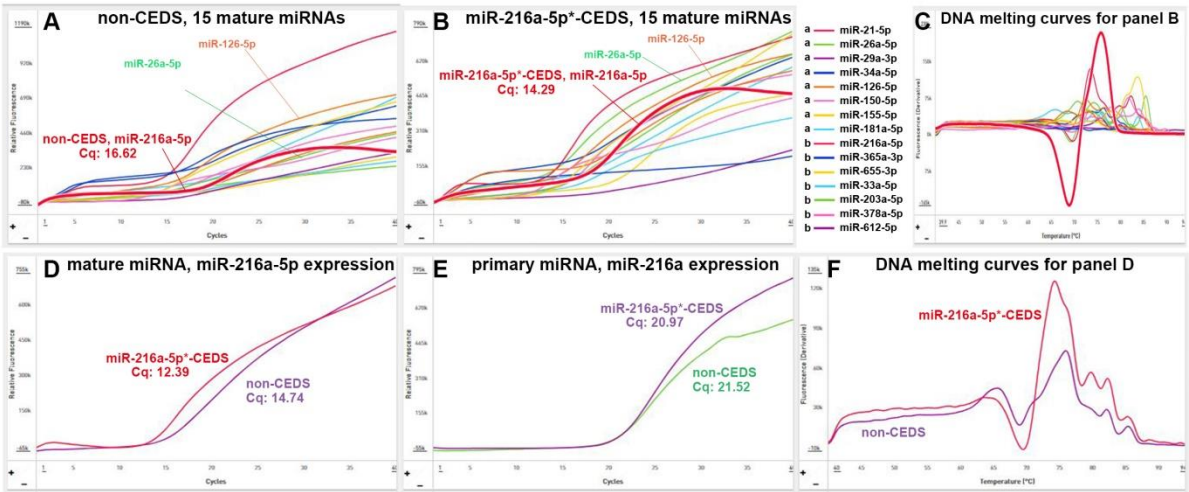

Fig. 7. Quantitative PCR for CEDS effect on the expression of mature miR-216a-5p (D) and primary miR-216a (E) in RAW 264.7 cells. MiR-216a-5p*-CEDS increased the expression of miR-216a-5p along with an influence on the expression of other 14 miRNAs (A and B). Noted the variable melting curves of 15 mature miRNAs and similar melting curves of mature miR-216a-5p (C and F). The representative results were presented based on the findings of triple repeated experiments.

qPCR for the expression of mature and primary miRNAs after miR-365a-3p*-CEDS

In the multiple qPCRs for 15 mature miRNAs, mmu-miR-365a-3p sequence TAATGCCCCTAAAAATCCTTAT*-CEDS demonstrated a 322% increase in miR-365a-3p expression (Cq=17.12) compared to the untreated control (Cq=15.51) in RAW 264.7 cells. Concurrently, miR-365a-3p*-CEDS was found to significantly increase the expression of miR-216a-5p compared to the untreated control, while decreasing the expression of miR-26a-5p and miR-126-5p (Fig. 8 A and B).

In the qPCR assays conducted to determine CEDS-induced incremental ratio of mature and primary miRNAs, miR-365a-3p*-CEDS demonstrated a significant increase in the expression of mature miR-365a-3p and primary miR-365a, with fold changes of 86% and 298%, respectively, in comparison to the untreated controls (Fig. 8 D and E).

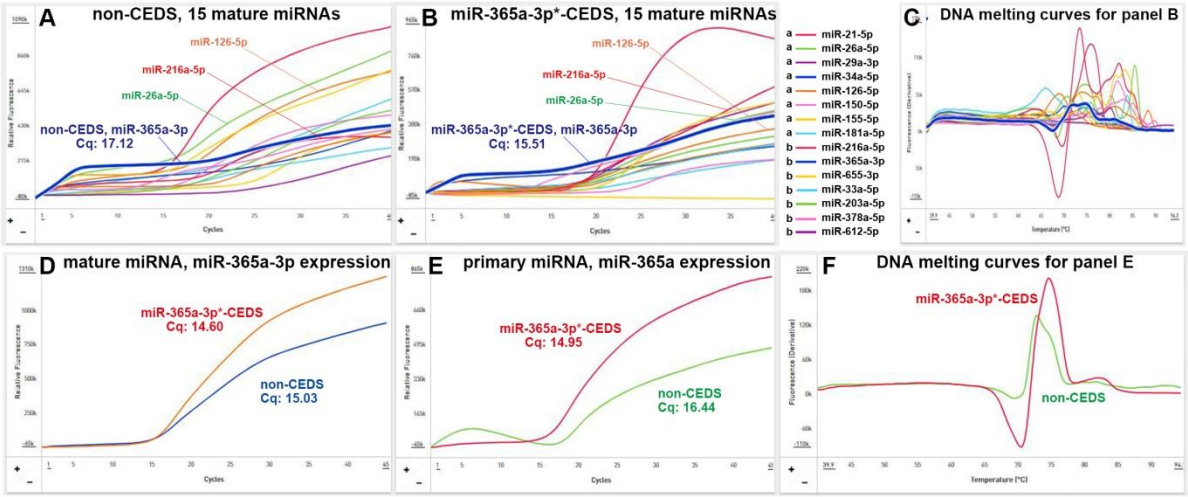

Fig. 8. Quantitative PCR for CEDS effect on the expression of mature miR-365a-3p (D) and primary miR-365a (E) in RAW 264.7 cells. MiR-365a-3p*-CEDS increased the expression of miR-365a-3p along with an influence on the expression of other 14 miRNAs (A and B). Noted the variable melting curves of 15 mature miRNAs and similar melting curves of primary miR-365a (C and F). The representative results were presented based on the findings of triple repeated experiments.

qPCR for the expression of mature and primary miRNAs after miR-655-3p*-CEDS

In the multiple qPCRs for 15 mature miRNAs, mmu-miR-655-3p sequence ATAATACATGGTTAACCTCTTT*-CEDS demonstrated a 124% increase in miR-655-3p expression (Cq=15.52) compared to the untreated control (Cq=14.9) in RAW 264.7 cells. Concurrently, miR-655-3p*-CEDS was found to significantly increase the expression of miR-365a-3p compared to the untreated control, while decreasing the expression of miR-21-5p (Fig. 9 A and B).

In the qPCR assays conducted to determine CEDS-induced incremental ratio of mature and primary miRNAs, miR-655-3p*-CEDS demonstrated a significant increase in the expression of mature miR-655-3p and primary miR-655, with fold changes of 278% and 128%, respectively, in comparison to the untreated controls (Fig. 9 D and E).

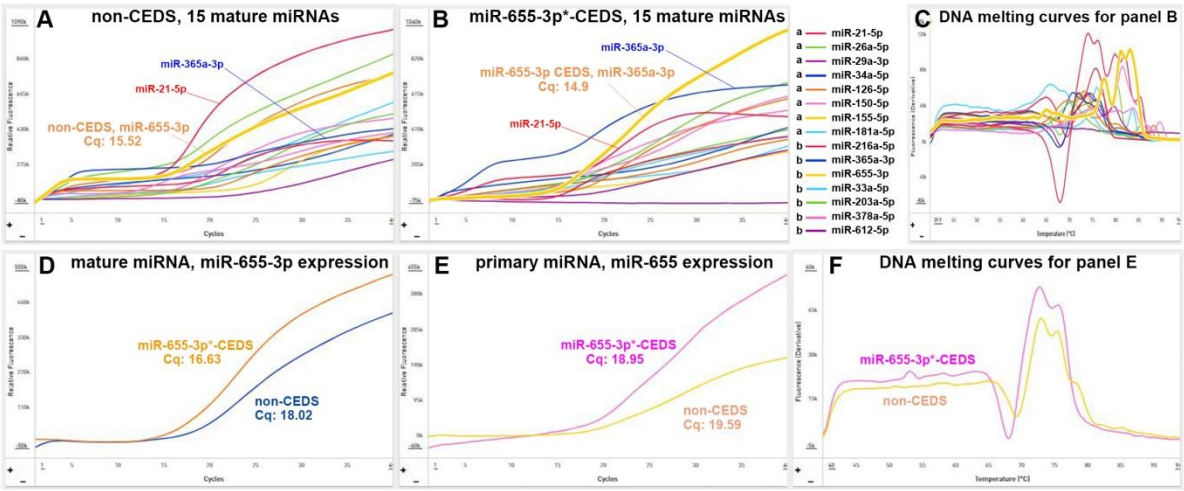

Fig. 9. Quantitative PCR for CEDS effect on the expression of mature miR-655-3p (D) and primary miR-655 (E) in RAW 264.7 cells. MiR-655-3p*-CEDS increased the expression of miR-655-3p along with an influence on the expression of other 14 miRNAs (A and B). Noted the variable melting curves of 15 mature miRNAs and similar melting curves of primary miR-655 (C and F). The representative results were presented based on the findings of triple repeated experiments.

The qPCR results indicated that CEDS has the potential to increase the expression of target mature and primary miRNAs compared to untreated controls. Although the incremental ratios calculated based on the Cq number showed considerable variability in the three replicate qPCRs, there was a consistent trend showing that CEDS increased the expression of target mature and primary miRNAs in the qPCR experiments for nine miRNAs observed in this study.

The sequences of nine miRNAs observed in this study demonstrated no homology with each other in the search of the align sequence nucleotide blast program (NCBI, USA). However, it was found that CEDS targeting a mature miRNA can not only affect the expression of its own miRNA, but also the expression of other mature miRNAs. This phenomenon may be relevant to the common fact that one miRNA can regulate multiple genes, and one gene can be regulated by multiple miRNAs[17].

To illustrate, if A-miRNA and B-miRNA are capable of targeting the same protein-α, an increase of 50% in the expression of A-miRNA may result in the targeting of the entire number of protein-α genes, thereby freeing up the B-miRNA to target other protein genes. Consequently, it is postulated that the increased number of A-miRNA will not impede the functions of B-miRNA, but rather stimulate B-miRNAs to target other protein genes secondarily.

In the present study, the qPCRs were simultaneously performed to assess 15 miRNAs at once, and its results showed a consistent trend, indicating the secondary effect of CEDS, even though the presence of slight variation in the three-times repeated qPCR results. Nevertheless, since the qPCR is the easy and rapid method to identify the secondary effect of CEDS, it would be worthy to note that the secondary effect of CEDS occurs between the relevant miRNAs in their functions as follows.

MiR-26a-5p*-CEDS can increase the expression of miR-126-5p and miR-655-3p while decreasing the expression of miR-365a-3p in RAW 264.7 cells. MiR-34a-5p*-CEDS can increase the expression of miR-126-5p and miR-655-3p while decreasing the expression of miR-21-5p, and that miR-126-5p*-CEDS can increase the expression of miR-26a-5p and miR-655-3p. MiR-150-5p*-CEDS can increase the expression of miR-126-5p, miR-365a-3p, and miR-655-3p, and that miR-155-5p*-CEDS can increase the expression of miR-181a-5p, miR-216a-5p, and miR-655-3p. MiR-181a-5p*-CEDS can increase the expression of miR-126-5p, miR-216a-5p, and

miR-655-3p, and that miR-216a-5p*-CEDS can increase the numbers of miR-26a-5p and miR-126-5p. MiR-365a-3p*-CEDS can increase the expression of miR-216a-5p while decreasing the expression of miR-26a-5p and miR-126-5p. And miR-655-3p*-CEDS can increase the expression of miR-365a-3p while decreasing the expression of miR-21-5p.

The secondary effect of CEDS appeared to increase or decrease the expression of other miRNAs. Therefore, it is postulated that the secondary effect of CEDS may be the result of a complex feedback signaling mechanism involving gene transcription and protein translation. However, it can be said that CEDS can not only exert the primary effect on the target miRNAs, but also the secondary effect on the relevant miRNAs in function at the same time.

IP-HPLC analysis for the changes of the protein signaling after CEDS targeting different miRNAs in RAW 264.7 cells

The RAW 264.7 cells treated with dodecagonal CEDS using a target sequence were collected and lysed using protein lysis buffer (iNtRON Biotechnology INC, Korea), and analyzed by IP-HPLC as follows. Each protein sample was mixed with 5 mL of binding buffer (150mM NaCl, 10mM Tris pH 7.4, 1mM EDTA, 1mM EGTA, 0.2mM sodium vanadate, 0.2mM PMSF and 0.5% NP-40) and incubated with the antibody-bound protein A/G agarose bead column on a rotating stirrer at room temperature for 1 h. Following multiple washes of the columns with Tris-NaCl buffer at a pH of 7.5 and a graded NaCl concentration (0.15–0.3 M), the target proteins were eluted with 300 μL of IgG elution buffer (Pierce, USA). Column elution was conducted using a 0.15 M NaCl/20% acetonitrile solution at a flow rate of 0.5 mL/min.

The immunoprecipitated proteins were subjected to the analysis using a precision HPLC unit equipped with a reverse-phase column and a micro-analytical ultraviolet (UV) detector system (1100 series, Agilent, USA). The control and experimental samples were analyzed in sequence to permit a comparison of their HPLC peaks. The square roots of whole protein peak areas were normalized and compared to the controls to calculate the relative ratio (%) of protein expression level. The ratios of protein levels between the experimental and control groups were divided into five categories, as follows: severe underexpression (below 80%), marked underexpression (80%-below 95%), minimal expression change (95%-below 105%), marked overexpression (105%-120%), and severe overexpression (above 120%).

Table 2. Antibodies used in the IP-HPLC analysis.

Signaling	No.	Antibodies
Proliferation	12	Ki-67, PCNA, PLK4, CDK4, cyclin D2, cdc25A, p14, p15/16, p21, p27, CHK1, nucleolin
cMyc/MAX/MAD network	4 (1)	cMyc, MAX, MAD1, (p27)
Wnt/β-catenin signaling	6	Wnt1, β-catenin, APC, AXIN2, TCF1, Snail
p53/Rb signaling	6(1)	p53, Rb1[#], p-Rb, (CDK4), E2F1, E2F4
SHH/PTCH/GL1 and Notch/Jagged signaling	5	SHH, PTCH, GL1, Notch1, Jagged2
Epigenetic modification	13	Histone H1, KDM4D[$], HDAC10[$], MBD4, DMAP1, DNMT1, EZH2, PCAF, HMGA2, HMGB1, BRG1, Ac-lysine, lamin A/C
Protein translation	6	DOHH[!], DHPS[!], eIF5A1[!], eIF5A2[!], eIF2AK3, eIF2α^
miRNA biogenesis	7	Drosha, Exportin5, Dicer, TRBP2, AGO2, GW182, MTDH
Growth factors	22	GH, GHRH, EGF, EGFR, IGF1, IGF2R, TGFα, TGFβ1[$], TGFβ2, TGFβ3, ALK1, SMAD2/3, SMAD4, SMAD7, HGFα, Met, FGF1, FGF2, FGF7, CTGF, ERβ, progesterone
RAS signaling	26	KRAS[$], HRAS, NRAS[$], pAKT1, PI3K, Rab1, RAF-B, MEKK, ERK1, p-ERK1[$], PTEN[&], STAT3, p-STAT3, PKA1α, AKAP13, AMPKα[@], PGC1α, PLCβ2, c-Fos, JNK1, p-JNK1, PKC, p-PKC1α[@], p-TYK2, JAK2[$], SOS1
NFkB signaling	10	NFkB, IKK, MDR, GADD45, p38, p-p38, SRC1, mTOR[@], NFATc1, NFAT5
p53-mediated apoptosis	18 (1)	(p53), p63, p73, MDM2, BAD, BAK, PUMA, NOXA, BAX, APAF1, BCL2, caspase9, c-caspase9, AIF1, PARP1, c-PARP, caspase3, c-caspase3
FAS-mediated apoptosis	9	FASL, FAS, FADD, TRAIL, FLIP, BID, caspase8, caspase3, c-caspase3
Cytodifferentiation	19	β-actin, α-tubulin, GAPDH, vimentin, TGase2[+], FAK, CaM, calnexin, CRIP1, AP1M1, Ep-CAM, cystatin A, claudin1, caveolin1, VE-cadherin[&], SOX9, DLX2, SOSTDC1, tenascin C
Osteogenesis	11	BMP2, BMP3, BMP4, RUNX2, osterix, OPG, RANKL, osteopontin, osteonectin, osteocalcin, aggrecan
Neuromuscular differentiation	8	NSEγ, GFAP, NK1R, S100, myosin1a, MYH2, desmin, αSMA
Protection	15	HSP27, HSP70, HSP90, SOD1, GSTO1/2, NOS1, HO1, NRF2, hepcidin, SVCT2, leptin, FOXO1, FOXO3, FOXP3, FOXP4
ER stress	10	HSP27, eIF2AK3, eIF2α^, GADD153, p-GADD153, BIP, IRE1α, ATF4, ATF6α, LC3β,
Angiogenesis	16	HIF1α[&], VEGFA, VEGFC, VEGFR2, vWF[$], endocan, CD31, CD106, FLT4[$], LYVE1, TEM8, CMG2[$], angiogenin, endothelin1, PDGFA, FGF2
Survival	8	SP1[@], SP3[@], sirtuin1, sirtuin3, sirtuin6, sirtuin7, survivin[@], XIAP
Fibrosis	11 (2)	collagen3A1, FGF1, CTGF, laminin α5, integrin α5, integrin β1, uPA[+], PAI1, α1-antitrypsin, (tenascin C, claudin1)
Oncogenesis	29 (1)	CEA[$], cMyb, 14-3-3, YAP1, DMBT1, MTDH, CRK, PIM1, AXL, BACH1, BMI1, KLF4, ZEB1, HER2, BRCA1[&], BRCA2[&], NF1, ATR, ATM, PDCD4, CRIP1, TWIST1, XBP1, MTA2, EWSR1, Ets1, Daxx, MALT1, (CRIP1)
Senescence	7 (2)	Klotho, sirtuin1, sirtuin3, sirtuin6, sirtuin7, (p21, caveolin1)
Telomere	3	TERT, TRF1, TIN2
Metabolism	8	HX2, GAPDH, GLUT1, GLUt4, LGR4, PPARγ, TIGAR, LDHA
Acute inflammation	9	TNFα[@], TRAF6, IL1, IL8, MCP1, MIF, CXCR4, MMP1, CRP
Innate immunity	12	CD56, elafin, lactoferrin, LL37, CAMP, β-defensin 1, -2, -3, TLR2, TRL3, TLR4, α1-antitrypsin[&]
Cellular immunity	19	CD3, CD4, CD8, CD20, CD28, CD34, CD40, CD44, CD54, CD80, CD99, IL28, versican, perforin, granzyme B, PD1, PDL1, CTLA4, LTA4H
Chronic inflammation	21 (2)	IL6, IL10, IL12, lysozyme, M-CSF, (CD31), CD68, (CD106), MMP2, MMP3, MMP9, MMP10, MMP12, TIMP1, TIMP2, cathepsin C, cathepsin G, cathepsin K, COX1, COX2, kininogen
Total	**350 (10)**	

( ): Overlapped antibodies.

[#] DAKO, Denmark; [$] Neomarkers, CA, USA; [@] ZYMED, CA, USA; [&]Abcam, Cambridge, UK; ^Cell signaling technology, USA; [!] kindly donated from M. H. Park in NIH, USA [18]; [+] kindly donated from S. I. Chung in NIH, USA [19,20]; no mark; Santa Cruz Biotechnology, USA; the number of antibodies overlapped; ( ).

Abbreviations: 14-3-3: the 14th fraction eluting from a DEAE-cellulose column and in position 3.3 on a starch electrophoresis gel, Ac-lysine: Acetylated-Lysine, AGO2: argonaute 1, Eukaryotic translation initiation factor 2C (eIF2C), AIF1: apoptosis inducing factor 1, AKAP13: A-kinase anchoring proteins 13, ALK1: activin receptor-like kinase 1, AMPKα: AMP-activated protein kinase α, pAKT: v-akt murine thymoma viral oncogene homolog, p-Akt1/2/3 phosphorylated (p-Akt, Thr 308), AP1M1: AP-1 complex subunit mu-1, APAF1: apoptotic protease-activating factor 1, APC: adenomatous polyposis coli, ATF4: activating transcription factor 4, ATM: ataxia telangiectasia caused by mutations, ATR: ataxia telangiectasia and Rad3-related protein, AXIN2: axis inhibition protein 2, AXL: Tyrosine-protein kinase

receptor UFO, BACH1: Transcription regulator protein, BAD: BCL2 associated death promoter, BAK: BCL2 antagonist/killer, BAX: BCL2 associated X, BCL2: B-cell leukemia/lymphoma-2, BID: BH3 interacting-domain death agonist, BIP (GRP 78): binding immunoglobulin protein, BMI1: B lymphoma Mo-MLV insertion region 1 homolog, polycomb group RING finger protein 4, BMP2: bone morphogenesis protein 2, BRCA1: breast cancer type 1 susceptibility protein, BRG1 (SMARCA4): transcription activator, c-caspase 3: cleaved-caspase 3, CaM: calmodulin, CAMP: Cathelicidin antimicrobial peptide, CD3: cluster of differentiation 3, CD31: Platelet endothelial cell adhesion molecule (PECAM-1), CD44 (HCAM): homing cell adhesion molecule, CD54 (ICAM1): intercellular adhesion molecule 1, CD56 (NCAM): neural cell adhesion molecule 1, CD106 (VCAM1): vascular cell adhesion molecule-1, cdc25A: cell division cycle 25A, CDK4: cyclin dependent kinase 4, CEA: carcinoembryonic antigen, CHK1: Checkpoint kinase 1, CMG2: capillary morphogenesis protein 2 (anthrax toxin receptor 2), COX1: cyclooxygenase-2, CRIP1: Cysteine-rich intestinal protein 1, CRK: proto-oncogene c-Crk, CRP: C-reactive protein, CTGF: connective tissue growth factor, CTLA4: cytotoxic T lymphocyte-associatedprotein-4, CXCR4: C-X-C chemokine receptor type 4, Daxx: Death-associated protein 6, DHS: deoxyhypusine synthase, DLX2, homeobox protein Distal-less (Dlx) family, DMAP1: DNA methyltransferase 1 associated protein, DMBT1: deleted in malignant brain tumors 1, DNMT1: DNA 5-cytosine methyltransferase 1, DOHH: deoxyhypusine hydroxylase, E2F1: transcription factor, eIF2AK3 (PERK): protein kinase R (PKR)-like endoplasmic reticulum kinase (PERK), EGF: Epidermal growth factor, EGF: Epidermal growth factor receptor, elF5A1: eukaryotic translation initiation factor 5A-1, EpCAM: Epithelial cell adhesion molecule, ERβ: estrogen receptor beta, ERK1 (extracellular signal-regulated protein kinase 1, MAPK3 (mitogen-activated protein kinase 3)), Ets1: Protein C-ets-1, EZH2 (ENX-1): enhancer of zeste homolog 2, EWSR1: Ewing Sarcoma Breakpoint Region 1 Protein, FADD: FAS associated via death domain, FAK: focal adhesion kinase, FAS: CD95/Apo1, FASL: FAS ligand, FGF1: fibroblast growth factor 1, FLIP: FLICE-like inhibitory protein, FLT4: Fms-related tyrosine kinase 4, FOXO1: Forkhead/winged helix box gene, group O 1, FOXP3: forkhead box P3, GADD45: growth arrest and DNA-damage-inducible 45, GADD153: C/EBP homologous protein (CHOP), GAPDH: glyceraldehyde 3-phosphate dehydrogenase, GFAP: glial fibrillary acidic protein, GH: growth hormone, GHRH: growth hormone-releasing hormone, GL1: Glioma-associated oncogene 1, GLUT1: Glucose transporter 1, GSTO1/2: glutathione S-transferase ω 1/2, GW182: Trinucleotide repeat-containing gene 6A protein, HDAC10: histone deacetylase 10, HER2: EGF receptor tyrosine-protein kinase erbB-2, HGFα: hepatocyte growth factor α, HIF1α: hypoxia inducible factor-1α, HO-1: heme oxygenase 1, HMGA2: High mobility group (HMG) proteins A2, HRAS: GTPase HRAS, HSP70: heat shock protein 70, HX2: hexokinases 2, IGF1: insulin-like growth factor 1, IGF2R: insulin-like growth factor 2 receptor, IKK: ikappaB kinase, IL1: interleukin-1, IRE1α (ERN1): inositol-requiring enzyme 1 α, JAK2: Janus kinase 2, JNK1: Jun N-terminal protein kinase 1, KDM4D: Lysine-specific demethylase 4D, KLF4: Kruppel-like factor 4, KRAS: V-Ki-ras2 Kirsten rat sarcoma viral oncogene homolog, LC3β: microtubule-associated protein 1A/1B-light chain 3β, LDHA: Lactate dehydrogenase A, LGR4: Leucine-rich repeat-containing G-protein coupled receptor 4, LTA4H: leukotriene A4 hydrolase, LYVE1: lymphatic vessel endothelial hyaluronan receptor 1, MAD1: mitotic arrest deficient 1, MALT1: Mucosa-associated lymphoid tissue lymphoma translocation protein 1, MAX: myc-associated factor X, MBD4: methyl-CpG-binding domain protein 4, MCP1: monocyte chemotactic protein 1, M-CSF: macrophage colony-stimulating factor, MDM2: mouse double minute 2 homolog, MDR: multiple drug resistance, MEKK1, MMP1: matrix metalloprotease 1, Met: tyrosine-protein kinase Met, MIF: Macrophage migration inhibitory factor, MMP1: matrix metalloproteinase 1, MTA2: Metastasis-associated protein 2, MTDH: Metadherin, mTOR: mammalian target of rapamycin, cMyc: V-myc myelocytomatosis viral oncogene homolog, MYH2: myosin-2, NF1: neurofibromin 1, NFAT5: nuclear factor of activated T cells 5, NFATc1: nuclear factor of activated T-cells, cytoplasmic 1, NFkB: nuclear factor kappa-light-chain-enhancer of activated B cells, NK1R: neurokinin 1 receptor, NOS1: nitric oxide synthase 1, Notch1: Notch homolog 1, NOXA: Phorbol-12-myristate-13-acetate-induced protein 1, NRAS: neuroblastoma RAS Viral Oncogene homolog, NRF2: nuclear factor (erythroid-derived)-like 2, NSEγ: Neuron specific γ enolase γ, OPG: osteoprotegerin, PAI-1: plasminogen activator inhibitor-1, PARP-1: poly-ADP ribose polymerase 1, c-PARP-1: cleaved-PARP-1, PCAF: p300/CBP-associated factor, PCNA: proliferating cell nuclear antigen, PD-1 (CD279): programmed cell death protein 1, PDCD4: Programmed cell death protein 4, PDGFA: platelet-derived growth factor-A, PDL1: Programmed death-ligand 1, PGC-1α: peroxisome proliferator-activated receptor gamma coactivator 1α, PI3K: phosphatidylinositol-3-kinase, PIM-1: Proto-oncogene serine/threonine-protein kinase 1, PKA1α: protein kinase A 1α, PKC: protein kinase C, PLCβ2: 1-phosphatidylinositol-4,5-bisphosphate phosphodiesterse β-2, PLK4: polo like kinase 4 or serine/threonine-protein kinase, PPARγ: Peroxisome proliferator- activated receptor gamma, PTCH: Protein patched homolog 1, PTEN: phosphatase and tensin homolog, PUMA: p53 upregulated modulator of apoptosis, Rab1: RAS-related protein, Rab GTPases, RAF-B: v-Raf murine sarcoma viral oncogene homolog B, RANKL: receptor activator of nuclear factor kappa-B ligand, Rb-1: retinoblastoma-1, RUNX2: Runt-related transcription factor-2, SHH: sonic hedgehog, sirtuin3: silent mating type information regulation 2 homolog 3, NAD-dependent deacetylase, α-SMA: alpha-smooth muscle actin, SMAD4: mothers against decapentaplegic, drosophila homolog 4, SOD1: superoxide dismutase-1, SOS1: son of sevenless homolog 1, SOSTDC1: sclerostin domain-containing protein 1**,** SOX9: SRY (sex-determining region Y)-related HMG-box transcription factor 9, SP1: specificity protein 1, SRC1: steroid receptor coactivator-1, STAT3: signal transducer and activator of transcription-3, SVCT2: sodium-dependent vitamin C transporter 2, TCF1: T-cell factor-1, TEM8: tumor-specific endothelial marker 8 (anthrax toxin receptor 1), TERT: human telomerase reverse transcriptase, TGase 2: transglutaminase 2, TGF-β1: transforming growth factor-β1, TIGAR: TP53-induced glycolysis and apoptosis regulator, TIMP1: Tissue inhibitor of metalloproteinases 1, TIN2: TERF1-interacting nuclear factor 2, TLR2: toll-like receptor 2, TNFα: tumor necrosis factor-α, TRAF6: TNF receptor associated factor 6, TRAIL: TNF-related apoptosis-inducing ligand, TRBP2, trans-activation-responsive (HIV-1) RNA binding protein 2, TRF1: Telomeric Repeat Factor 1, TWIST1: Twist-related protein 1, p-TYK2: Non-receptor tyrosine-protein kinase, uPA: urokinase-type plasminogen activator, VE-cadherin: vascular endothelial cadherin, VEGFA vascular endothelial growth factor A, VEGFR2: vascular endothelial growth factor receptor 2, p-VEGFR2: phosphorylated vascular endothelial growth factor receptor 2 (Y951), vWF: von Willebrand factor, Wnt1: proto-oncogene protein Wnt1, XBP1: X-box binding protein 1, XIAP: X-linked inhibitor of apoptosis protein, YAP1: Yes-associated protein 1, ZEB1: Zinc finger E-box-binding homeobox 1

MiR-26a-5p*-CEDS influenced the protein signaling in RAW 264.7 cells

RAW 264.7 cells treated with mmu-miR-26a-5p sequence TTCAAGTAATCCAGGATAGGCT*-CEDS showed the characteristic protein expressions by IP-HPLC analysis, resulting in the suppression of proliferation, c-Myc/MAX/MAD network, Wnt/β-catenin signaling, p53/Rb/E2F1 signaling, SHH/PTCH/GLI signaling, Notch/Jagged signaling, epigenetic modification, protein translation, growth factors, cytodifferentiation, osteogenesis, neuromuscular differentiation, RAS signaling, NFkB signaling, angiogenesis, survival, acute inflammation, innate immunity, cellular immunity, chronic inflammation, p53-mediated apoptosis, FAS-mediated apoptosis, fibrosis, senescence, glycolysis, and telomere signaling, as well as the activation of miRNA biogenesis, ER stress, and PARP-mediated apoptosis signaling compared to the untreated controls (Fig. 10A).

The proliferation signaling was suppressed by downregulating miR-26a-5p target proteins PCNA (90.8%), CDK4 (81.8%), cyclin D2 (92.3%), cdc25A (83.6%), and p27 (92. 3%), and miR-26a-5p-responsible protein Ki-67 (88.7%), as well as coincidentally downregulating PLK4 (82.3%), p21 (81.5%), CHK1 (87%) and upregulating p14 (116.5%) and p15/16 (106.9%), despite the upregulation of nucleolin (109.8%).

The cMyc/MAX/MAD network was suppressed by downregulating miR-26a-5p target proteins cMyc (89.7%) and p27 (92.3%) and miR-26a-5p-responsible protein MAX (82.5%) and MAD1 (93.5%).

The Wnt/β-catenin signaling was suppressed by downregulating miR-26a-5p target proteins Wnt1 (85.8%), APC (92.3%), TCF1 (87.6%), and Snail1 (82.9%) and miR-26a-5p-responsible protein β-catenin (81.5%).

The p53/Rb/E2F1 signaling was suppressed by downregulating miR-26a-5p target proteins Rb1 (91.6%), p-Rb (81.2%), CDK4 (81.8%), and E2F1 (86%), and coincidentally upregulating E2F4 (127.1%).

The SHH/PTCH/GLI signaling was suppressed by downregulating miR-26a-5p target proteins SHH (82.2%) and GLI1 (86.6%), despite the upregulation of PTCH1 (114.9%).

The Notch/Jagged signaling was suppressed by downregulating miR-26a-5p target protein Jagged2 (91.6%).

The protein translation signaling appears to be suppressed by significant downregulating miR-26a-5p target protein eIF5A1 (82.6%), despite the upregulation of DHPS (118%), eIF5A2 (124.8%), and eIF2α (114.9%)

The growth factor signaling were suppressed by downregulating miR-26a-5p target proteins IGF1 (83.5%), TGFβ1 (81.4%), HGFα (90.8%), and SMAD7 (92.3%), as well as coincidentally downregulating GHRH (89. 9%), EGFR (73.5%), TGFα (80.9%), and TGFβ3 (91.3%), despite the upregulation of GH (114.3%), EGF (105.6%), IGF2R (105.4%), ALK1 (114.6%), progesterone (133.6%), SMAD4 (108.5%), Met (122.4%), FGF7 (123.7%), and CTGF (109%). SMAD4, Met and CTGF are miR-26a-5p target proteins, but they were unexpectedly upregulated compared to the reference data.

The cytodifferentiation signaling were suppressed by downregulating miR-26a-5p target protein claudin1 (91.7%), as well as coincidentally downregulating GAPDH (86.7%), CaM (87.7%), calnexin (77.7%), CRIP1 (70.8%), AP1M1 (93.8%), Ep-CAM (86.8%), caveolin1 (93.2%), and tenascin C (84%), despite the upregulation of vimentin (107.7%), DLX2 (129.9%), and SOSTDC1 (141.7%). SOSTDC1 is a miR-26a-5p target protein, but it was unexpectedly upregulated compared to the reference data.

The osteogenesis signaling was suppressed by downregulating miR-26a-5p target proteins BMP2 (76.3%) and osteopontin (95%), as well as coincidentally downregulating BMP4 (93%), PTH/PTHrPR (73%), osteocalcin (91.1%), and osteonectin (85.8%), despite the upregulation of OPG (114.7%).

The neuromuscular differentiation signaling appears to be suppressed by downregulating miR-26a-5p target protein αSMA (91.7%) and coincidentally downregulating myosin-1α (85.4%) and MYH2 (89.4%), despite the upregulation of GFAP (111%) and desmin (116.1%).

The RAS signaling was suppressed by downregulating miR-26a-5p target proteins KRAS (91%), NRAS (92.7%), PI3K (76.8%), MEKK (86.5%), AMPKα (93.1%), and p-JNK1 (85.2%) and miR-26a-5p-responsible proteins c-Fos (87.7%) and p-PKC (93.1%), as well as coincidentally downregulating p-STAT3 (73.2%) and SOS1 (91.2%), despite the upregulation of Rab1 (117%), RAF-B (114.3%), ERK1 (134.4%), p-ERK1 (118.3%), PKA1α (120.6%), AKAP13 (114.3%), PKC (109.2%), and PTEN (113.9%). PTEN is a miR-26a-5p target protein, but it was unexpectedly upregulated compared to the reference data.

The NFkB signaling was suppressed by downregulating miR-26a-5p target proteins p38 (85.4%), p-p38 (78%), and mTOR (90%), as well as coincidentally downregulating GADD45 (91.6%), despite the upregulation of IKK (105.5%).

The protection signaling was suppressed by downregulating miR-26a-5p target protein leptin (87.4%) and coincidentally downregulating HSP70 (93.9%), SOD1 (93.8%), GSTO1/2 (84.5%), HO1 (88.5%), and hepcidin (87.3%), despite the upregulation of NOS1 (131.6%), FOXO1 (110.6%), HSP90 (107.2%), NRF2 (105.1%), and ALDH1A1 (105.3%). NOS1 is a miR-26a-5p target protein, but it was unexpectedly upregulated compared to the reference data.

The angiogenesis signaling was suppressed by downregulating miR-26a-5p target proteins VEGFA (86.2%), CD106 (84.3%), and miR-26a-5p-responsible protein PDGFA (75.1%), as well as coincidentally downregulating endocan (93.4%), FLT4 (91%), CMG2 (92.2%), and endothelin1 (86.3%), despite the upregulation of VEGFR2 (141%), vWF (119.9%), LYVE1 (113.1%), TEM8 (113.5%), and angiogenin (105.4%).

The survival signaling was suppressed by downregulating miR-26a-5p target proteins SP1 (81.1%) and SP3 (81.4%), despite the upregulation of sirtuin3 (106.7%).

The acute inflammation signaling was suppressed by downregulating miR-26a-5p target proteins TNFα (84.2%), and IL1 (84.7%), despite the upregulation of TRAF6 (115.8%), IL8 (108.2%), and CXCR4 (110.8%).

The innate immunity signaling was suppressed by downregulating miR-26a-5p target proteins TLR2 (81.4%) and TLR4 (89.6%), as well as coincidentally downregulating CD56 (91.7%), elafin (91.8%), LL37 (93.6%), β-defensin2 (91.7%), and β-defensin3 (81.4%), despite the upregulation of lactoferrin (119.3%), TLR3 (107.3%), and α1-antitrypsin (114.2%).

The cellular immunity signaling was suppressed by downregulating miR-26a-5p-responsible proteins CD44 (87%), and granzyme B (84.1%), as well as coincidentally downregulating CD28 (85.2%), CD34 (81.3%), CD40 (89.7%), CD54 (89.8%), CD80 (83.6%), CD99 (89.3%), IL28 (90.8%), PD1 (91.1%), and LTA4H

(91.6%), despite the upregulation of CD4 (114.2%), CD8 (109.8%), CD20 (121.9%), versican (110.8%), perforin (117.2%), PDL1 (117.9%), and CTLA4 (105.3%).

The chronic inflammation signaling was suppressed by downregulating miR-26a-5p target proteins IL6 (88.2%), CD106 (85.9%), MMP2 (84.2%), and MMP9 (94.7%), as well as coincidentally downregulating IL10 (87.7%), TIMP1 (89.5%), and kininogen (94.3%), despite the upregulation of IL12 (110.9%), lysozyme (117.7%), cathepsin G (107.5%), cathepsin K (119.3%), COX1 (106.6%), and COX2 (118.2%). COX2 is a miR-26a-5p target protein, but it was unexpectedly upregulated compared to the reference data.

The p53-mediated apoptosis signaling was suppressed by downregulating miR-26a-5p target proteins MDM2 (92.7%) and BAK (92.5%), as well as coincidentally downregulating caspase9 (88.5%), c-caspase9 (73.5%), and c-caspase3 (86.9) and upregulating BCL2 (110%), despite the upregulation of miR-26a-5p-responsible proteins p53 (114.3%) and caspase3 (108.1%), and coincidental upregulation of p73 (121.1%), BAD (113%), and PUMA (106.3%).

The FAS-mediated apoptosis signaling was inhibited by downregulating miR-26a-5p target proteins FAS (80.5%) and miR-26a-5p-responsible protein caspase3 (86.9%), as well as coincidentally downregulating FASL (94.7%) and FLIP (88.9%), despite the upregulation of miR-26a-5p-responsible protein caspase3 (108.1%).

The fibrosis signaling was suppressed by downregulating miR-26a-5p target protein claudin1 (91.7%), as well as coincidentally downregulating integrin β1 (90.3%), uPA (93%), and tenascin C (84%) and upregulating FGF7 (123.7%), despite the upregulation of laminin α5 (117.2%), PAI1 (115.2%), α1-antitrypsin (114.2%), CTGF (109%), and integrin α5 (132.1%). CTGF and integrin α5 are miR-26a-5p target proteins, but they were unexpectedly upregulated compared to the reference data.

The senescence signaling was suppressed by downregulating p21 (81.5%) and caveolin1 (93.2%), despite the slight upregulation of sirtuin3 (106.7%).

The glycolysis signaling was suppressed by downregulating miR-26a-5p-responsible protein PPARγ (83.7%), as well as coincidentally downregulating GAPDH (85.7%) and GLUT1 (72.6%), despite the slight

upregulation of TIGAR (114.7%), LDHA (108.8%), HK2 (106.6%), and LGR4 (105.6%). LGR4 is a miR-26a-5p target protein, but it was unexpectedly upregulated compared to the reference data.

The telomere signaling was suppressed by downregulating miR-26a-5p target protein TERT (87%), despite the upregulation of TRF1 (117.3%).

Conversely, **the miRNA biogenesis signaling** was activated by downregulating miR-26a-5p target protein MTDH (85.3%) and coincidentally upregulating Drosha (113.8%), Exportin5 (112%), Dicer (110.3%), TRBP2 (113.6%), AGO2 (117%), and GW182 (116.6%).

The ER stress signaling was activated by upregulating miR-26a-5p-responsible proteins GADD153 (105.6%), ATF4 (106%), and ATF6α (111.4%), as well as coincidentally upregulating eIF2α (113.5%), despite the downregulation of BIP (88.2%) and IRE1α (67.2%).

The PARP-mediated apoptosis signaling was activated by upregulating miR-26a-5p-responsible proteins c-PARP (115.7%) and coincidentally upregulating AIF1 (120.4%).

In addition, miR-26a-5p*-CEDS markedly influenced **the epigenetic modification signaling** by downregulating miR-26a-5p target proteins EZH2 (92.4%), HMGB1 (79.7%), and BRG1 (80.9%) and miR-26a-5p-responsible protein DNMT1 (93.2%), as well as the coincidental downregulation of KDM4D (88.6%), MBD4 (86.9%), DMAP1 (93.5%), PCAF (92.8%), and lamin A/C (94.7%), while it upregulated HDAC10 (138.2%), HMGA2 (118%), and Ac-lysine(107.6"%). HMGA2 is a miR-26a-5p target protein, but it was unexpectedly upregulated compared to the reference data. Consequently, miR-26a-5p*-CEDS induced a trend towards a reduction in the methylation of histones and DNAs, and attenuation of transcriptional repression.

MiR-26a-5p*-CEDS significantly suppressed **the oncogenesis signaling** by downregulating miR-26a-5p target proteins ZEB1 (91.6%), MTDH (85.3%), HER2 (84.9%), ATM (90.9%), and MALT1 (85.8%), while it partly enhanced **the oncogenesis signaling** by upregulating miR-26a-5p-responsible protein XBP1 (121.3%) and coincidentally upregulating KLF4 (141.9%), BRCA1 (123.6%), TWIST1 (135%), NF1 (110.3%), ATR (107.5%), and YAP1 (105.5%). KLF4 is a miR-26a-5p target protein, but it was unexpectedly upregulated

compared to the reference data. Among the 28 oncoproteins, 14 were found to be underexpressed, seven were overexpressed, and seven exhibited minimal change in expression compared to the untreated control.

Consequently, miR-26a-5p*-CEDS significantly impacted the entire protein signaling in RAW 264.7 cells. MiR-26a-5p*-CEDS markedly suppressed the RAS and NFkB signaling axis, leading to the suppression of proliferation-related signaling axis, protection-survival-senescence signaling axis, inflammation-angiogenesis-fibrosis signaling axis, oncogenesis-glycolysis signaling axis, telomere-epigenetic modification signaling axis, and p53- and FAS-mediated apoptosis signaling axis. Conversely, it activated the miRNA biogenesis signaling, ER stress signaling, and PARP-mediated apoptosis signaling (Fig. 10B, Table 3).

The results indicate that miR-26a-5p*-CEDS may provide a potent anti-oncogenic environment in RAW 264.7 cells and exert consistent anti-oncogenic potential to remove cancer cells. Conversely, it attenuates the innate and cellular immunity and cytodifferentiation, which are essential for immune surveillance and cellular maturation.

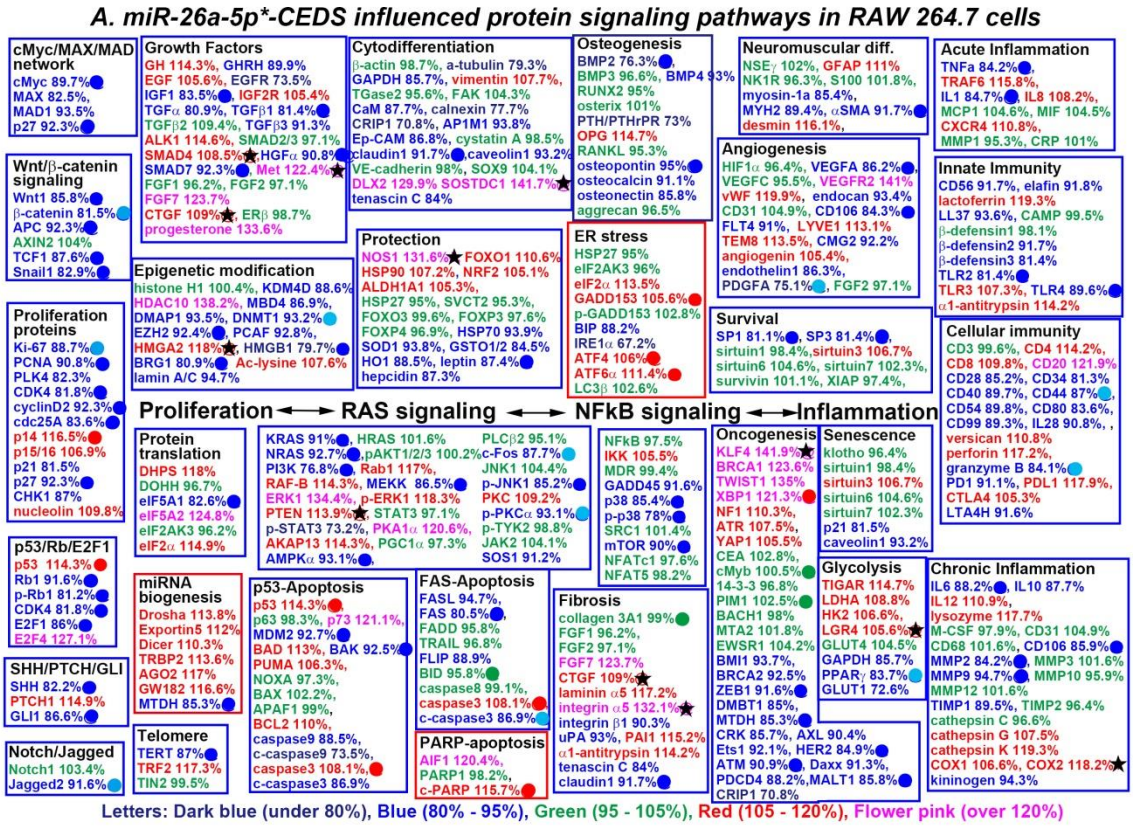

Fig. 10. MiR-26a-5p*-CEDS influenced the protein signaling (A) and axes (B) in RAW 264.7 cells. The IP-HPLC revealed proteins downregulated (**blue**), upregulated (**red**), and minimally changed (**green**) compared to the untreated controls. Dominantly suppressed (**blue square**) and activated (**red square**) signaling. Downregulated proteins by direct targeting (●) and indirect response (●), upregulated proteins by indirect response (●), and minimal changed (±5%) proteins (●). Some target proteins (★) were unexpectedly upregulated contrast to the current manuscripts and data from miRDB and TargetScan websites.

Table 3. Protein expressions in the RAW 264.7 cells treated with miR-26a-5p*-CEDS

Signaling	Downregulated Proteins	Upregulated Proteins
Proliferation	**Ki-67**, **PCNA**, PLK4, **CDK4**, **cyclin D2**, **cdc25A**, p21, **p27**, CHK1	**p14**, p15/16, nucleolin
cMyc/MAX/MAD network	**cMyc**, MAX, MAD1, **p27**,	
Wnt/β-catenin signaling	**Wnt1**, **β-catenin**, **APC**, **TCF1**, **Snail1**	
p53/Rb/E2F1 signaling	**Rb1**, **p-Rb1**, **CDK4**, **E2F1**	**p53**, E2F4
SHH/PTCH/GLI signaling	**SHH**, **GLI1**,	PTCH1
Notch/Jagged signaling	**Jagged2**	
Epigenetic modification	KDM4D, MBD4, DMAP1, **DNMT1**, **EZH2**, PCAF, **HMGB1**, **BRG1**, lamin A/C	HDAC10, **HMGA2★**, Ac-lysine
Protein translation	**eIF5A1**	DHPS, eIF5A2, eIF2α
miRNA biogenesis	**MTDH**	Drosha, Exportin5, Dicer, TRBP2, AGO2, GW182
Growth factors	GHRH, EGFR, **IGF1**, **TGFβ1**, TGFβ3, **HGFα**, **SMAD7**	GH, EGF, IGF2R, ALK1, **SMAD4★**, **Met★**, FGF7, **CTGF★**, progesterone
Cytodifferentiation	α-tubulin, GAPDH, CaM, clanexin, CRIP1, AP1M1, Ep-CAM, cystatin A, **claudin1**, caveolin1, tenascin C	vimentin, DLX2, **SOSTDC1★**
Osteogenesis	**BMP2**, BMP4, PTH/PTHrPR, **osteopontin**, osteocalcin, osteonectin	OPG
Neuromuscular differentiation	Myosin-1a, MYH2, **αSMA**	GFAP, desmin
RAS signaling	**KRAS**, **NRAS**, **PI3K**, **MEKK**, p-STAT3, **AMPKα**, **c-Fos**, **p-JNK1**, **p-PKC1α**, SOS1	Rab1, RAF-B, ERK1, p-ERK1, **PTEN★**, PKA1α, AKAP13, PKC
NFkB signaling	**p38**, **p-p38**, GADD45, **mTOR**	IKK
p53-mediated apoptosis	**MDM2**, **BAK**, caspase9, c-caspase9, c-caspase3	**p53**, p73, BAD, PUMA, BCL2, **caspase3**
FAS-mediated apoptosis	FASL, **FAS**, FLIP, c-caspase3	**caspase3**
PARP-mediated apoptosis		AIF1, **c-PARP**
Protection	HSP70, SOD1, GSTO1/2, HO1, **leptin**, hepcidin	**NOS1★**, FOXO1, HSP90, NRF2, ALDH1A1
ER stress	BIP, IRE1α	eiF2α, **GADD153**, **ATF4**, **ATF6α**
Angiogenesis	**VEGFA**, endocan, **CD106**, FLT4, CMG2, endothelin1, **PDGFA**	VEGFR2, vWF, LYVE1, TEM8, angiogenin, FGF2
Survival	**SP1**, **SP3**	sirtuin3
Acute inflammation	**TNFα**. **IL1**	TRAF6, IL8, CXCR4
Innate immunity	CD56, elafin, LL37, β-defensin2, defensin3, **TLR2**, **TLR4**	lactoferrin, TLR3, α1-antitrypsin
Cellular immunity	CD28, CD34, CD40, **CD44**, CD54, CD80, CD99, IL28, **granzyme B**, PD1, LTA4H	CD4, CD8, CD20, versican, perforin, PDL1, CTLA4
Chronic inflammation	**IL6**, IL10, **CD106**, **MMP2**, **MMP9**, TIPM1, kininogen	IL12, lysozyme, cathepsin G, cathepsin K, COX1, **COX2★**
Glycolysis	GAPDH, **PPARγ**, GLUT1	TIGAR, LDHA, HK2, **LGR4★**
Fibrosis	Integrin β1, uPA, tenascin C, **claudin1**	FGF7, **CTGF★**, laminin α5, **integrin α5★**, PAI1, α1-antitrypsin
Oncogenesis	BMI1, BRCA2, **ZEB1**, DMBT1, **MTDH**, CRK, AXL, Ets1, **HER2**, **ATM**, Daxx, PDCD4, **MALT1**, CRIP1	**KLF4★**, BRCA1, TWIST1, **XBP1**, ATR, YAP1, NF1
Senescence	p21, caveolin1	sirtuin3
Telomere signaling	**TERT**	TRF1

P;;MiR-26a-5p*-CEDS induced the suppression (**blue**) or activation (**red**) of signaling through protein downregulation by direct miRNA targeting (**blue**) or indirect response (**sky blue**) and protein upregulation by indirect response (**red**). Some miRNA target proteins were upregulated (★). The data were compared to the reports of recent manuscripts and miRDB, miRmap, miRPathDB, miRTarBase, and TargetScan websites.

MiR-34a-5p*-CEDS influenced the protein signaling in RAW 264.7 cells

RAW 264.7 cells treated with mmu-miR-34a-5p sequence TGGCAGTGTCTTAGCTGGTTGT*-CEDS showed the characteristic protein expressions, resulting in the suppression of proliferation, cMyc/MAX/MAD network, Wnt/β-catenin signaling, protein translation, miRNA biogenesis, growth factors, cytodifferentiation, neuromuscular differentiation, RAS signaling, NFkB signaling, protection, ER stress, angiogenesis, survival, acute inflammation, cellular immunity, chronic inflammation, FAS-mediated apoptosis, PARP-mediated apoptosis, fibrosis, glycolysis, and telomere signaling, as well as the activation of p53/Rb/E2F1 signaling, SHH/PTCH/GLI signaling, Notch/Jagged signaling, epigenetic modification, osteogenesis, innate immunity, chronic inflammation, p53-mediated apoptosis, oncogenesis, and senescence signaling compared to the untreated controls (Fig. 11A).

The proliferation signaling was suppressed by downregulating miR-34a-5p target proteins CDK4 (76.4%) and cdc25A (89.9%), and p27 (92. 3%), as well as coincidentally downregulating CHK1 (83.8%) and nucleolin (82.5%), despite the upregulation of miR-34a-5p-responsible proteins p14 (111%) and p21 (107.9%) and coincidental upregulation of Ki-67 (106.7%), PCNA (112.8%), and p15/16 (112.9%).

The cMyc/MAX/MAD network was suppressed by downregulating miR-34a-5p target proteins cMyc (77.9%) and MAX (77.5%), and coincidental upregulation of MAD1 (110.3%).

The Wnt/β-catenin signaling was suppressed by downregulating miR-34a-5p target proteins AXIN2 (91.9%) and Snail1 (83.5%), despite the upregulation of Wnt1 (113.8%) and β-catenin (117.7%). Wnt1 and β-catenin are miR-34a-5p target proteins, but they were unexpectedly upregulated compared to the reference data.

The protein translation signaling was suppressed by downregulating miR-34a-5p target proteins eIF5A2 (84.9%) and eIF2AK3 (85.1%), and coincidentally downregulating DHPS (89%) and eIF2α (92.6%), despite the upregulation of DOHH (115.6%).

The miRNA biogenesis signaling appears to be attenuated by downregulating miR-34a-5p-responsible protein AGO2 (94%) and coincidentally downregulating Exportin5 (84.6%), despite the upregulation of Drosha (109.5%) and Dicer (130.4%).

The growth factor signaling appears to be activated by downregulating miR-34a-5p target proteins TGFβ1 (79.4%), SMAD4 (84.4%), and Met (92.4%) and miR-34a-5p-responsible proteins EGFR (85.6%), SMAD7 (76.9%), and CTGF (86.6%), as well as coincidental downregulation of GH (92.5%), EGF (65.8%), TGFβ3 (71.3%), ALK1 (89.3%), and progesterone (92.2%), despite the upregulation of GHRH (111.7%), IGF1 (121.9%), IGF2R (113.1%), TGFβ2 (116.2%), SMAD2/3 (112%), HGFα 137.9%), FGF1 (114.2%), FGF7 (113.6%), and ERβ (120.1%).

The cytodifferentiation signaling appear to be suppressed by downregulating miR-34a-5p-responsible protein FAK (91.9%) and coincidentally downregulating calnexin (85.7%), CRIP1 (85.2%), AP1M1 (92.6%), Ep-CAM (77.9%), elafin (85.1%), and DLX2 (88.1%), despite the upregulation of miR-34a-5p-responsible protein VE-cadherin (108.2%) and coincidental upregulation of β-actin (124.2%), GAPDH (105.5%), cystatin A (115.9%), SOX9 (105.2%), and tenascin C (123.5%).

The neuromuscular differentiation signaling were suppressed by downregulating miR-34a-5p target protein NK1R (78.9%) and coincidentally downregulating GFAP (84.4%), myosin-1a (65.3%), MYH2 (89.1%), and αSMA (91.2%), despite the upregulation of miR-34a-5p-responsible protein desmin (117.2%).

The RAS signaling was suppressed by downregulating miR-34a-5p target proteins pAKT1/2/3 (94.4%), PI3K (85.6%), and PKC (93.6%) and downregulating miR-34a-5p-responsible proteins MEKK (82%), ERK1 (93.2%), PGC1α (60.9%), as well as coincidental downregulation of KRAS (93%), Rab1 (94%), RAF-B (83.9%), p-STAT3 (90.6%), JNK1 (87.4%), and SOS1 (77.8%), despite the upregulation of miR-34a-5p-responsible protein PTEN (121.8%) and coincidental upregulation of NRAS (110.7%), PKA1α (113.2%), PLCβ2 (109.1%), c-Fos (111.4%), p-JNK1 (105.2%), JAK2 (107.5%), and p-PKCα (120.5%).

The NFkB signaling was suppressed by downregulating miR-34a-5p target proteins SRC1 (92.5%) and downregulating miR-34a-5p-responsible proteins MDR (82%) and p38 (90.3%), as well as coincidental downregulation of IKK (88.1%) and NFATc1 (91.1%), despite the upregulation of miR-34a-5p-responsible protein mTOR (106.3%) and coincidental upregulation of NFkB (116.4%) and GADD45 (130.3%).

The protection signaling was suppressed by downregulating miR-34a-5p target protein HSP70 (88%) and downregulating miR-34a-5p-responsible proteins SOD1 (94.2%) and ALDH1A1 (86.6%), as well as GADD153

(105.6%), ATF4 (106%), and ATF6α (111.4%), as well as coincidental downregulation of FOXP4 (93%) and hepcidin (92.6%), despite the upregulation of NOS1 (147.4%), SVCT2 (146%), leptin (136.2%), FOXP (122.3%), NRF2 (115.4%), and FOXO1 (106.3%). NOS1 and NRF2 are miR-34a-5p target proteins, but they were unexpectedly upregulated compared to the reference data.

The ER stress signaling was suppressed by downregulating miR-34a-5p target protein eIF2AK3 (85.1%) and coincidentally downregulating eIF2α (92.6%), GADD153 (82.6%), p-GADD153 (90.5%), ATF6α (93.4%), and LC3β (90.7%), despite the upregulation of BIP (105.3%) and ATF4 (117.3%). BIP is a miR-34a-5p target protein, but it was unexpectedly upregulated compared to the reference data.

The angiogenesis signaling was suppressed by downregulating miR-34a-5p target protein VEGFA (81.2%) and coincidentally downregulating VEGFC (89.9%), VEGFR2 (72.1%), vWF (89.8%), CD31 (92.8%), and CMG2 (79%), despite the upregulation of endocan (116.1%), CD106 (105.6%), FLT4 (110.4%), LYVE1 (113.4%), TEM8 (110.3%), angiogenin (114.4%), endothelin1 (106.6%), and PDGFA (107.2%).

The survival signaling was suppressed by downregulating miR-34a-5p target protein sirtuin1 (93.4%) and downregulating the miR34a-5p-responsible protein SP1 (81.1%), as well as coincidental downregulation of SP3 (81.8%), sirtuin3 (89.5%), and sirtuin7 (85.7%), despite the upregulation of sirtuin6 (105.4%), survivin (109.8%), and XIAP (105%).

The acute inflammation signaling was suppressed by downregulating miR-34a-5p target proteins TRAF6 (85%) and CXCR4 (80.1%), and downregulating miR-34a-5p-responsible proteins MCP1 (84.5%) and MIF (79.3%), and coincidental downregulation of TNFα (91.5%), despite the slight upregulation of IL1 (109.5%), IL8 (107.8%), CRP (110.4%), and MMP1 (137.9%).

The cellular immunity signaling appears to be suppressed by downregulating miR-34a-5p target proteins CD4 (74.6%), CD44 (87.5%) and coincidentally downregulating CD3 (86.9%), CD34 (92.9%), CD80 (86.9%), CD99 (88.2%), IL28 (67.9%), versican (83.3%), perforin (73.2%), and CTLA4 (72.9%) and upregulating PD1 (115%), despite the upregulation of CD8 (121.7%), CD20 (109.1%), CD28 (119.8%), and CD54 (106.2%) and downregulation of miR-34a-5p target protein PDL1 (90.7%).

The FAS-mediated apoptosis signaling was suppressed by downregulating FADD (87.5%) and BID (91.6%), and coincidentally upregulating FLIP (110.6%), despite the upregulation of TRAIL (129.1%) and caspase3 (113.2%). Caspase3 was alternatively upregulated as a miR-34a-5p-responsible protein.

The PARP-mediated apoptosis signaling was suppressed by downregulating miR-34a-5p-responsible proteins PARP1 (87.5%) and c-PARP (90.1%), despite the upregulation of AIF1 (109.2%).

The fibrosis signaling was suppressed by downregulating miR-34a-5p target protein PAI1 (88.6%) and miR-34a-5p-responsible protein CTGF (86.6%), as well as coincidentally downregulating integrin α1 (87.3%) and upregulating FGF7 (113.6%), despite the upregulation of collagen3A1 (109.6%), FGF1 (114.2%), uPA (74.9%), and tenascin C (123.5%). Collagen 3A1 is upregulated as a miR-34a-5p-responsible protein.

The glycolysis signaling was suppressed by downregulating miR-34a-5p-responsible proteins LGR4 (94.5%), PPARγ (94.3%), and miR-34a-5p-responsible protein GLUT4 (94.6%), despite the upregulation of TIGAR (129.7%), LDHA (109%), and GAPDH (105.5%). LDHA is a miR-34a-5p target protein, but it was unexpectedly upregulated compared to the reference data.

The telomere signaling was suppressed by downregulating miR-34a-5p target protein TERT (87%).

Conversely, **the p53/Rb/E2F1 signaling** was activated by upregulating miR-34a-5p target protein E2F1 (112.1%) and upregulating miR-34a-5p-responsible protein p53 (108.7%), as well as coincidental upregulation of Rb1 (107.3%) and E2F1 (112.1%), and downregulating E2F4 (93.6%), despite the downregulation of CDK4 (76.4%). E2F1 is a miR-34a-5p target protein, but it was unexpectedly upregulated compared to the reference data.

The SHH/PTCH/GLI signaling was activated by upregulating GLI1 (113.8%), despite the downregulation of miR-34a-5p-responsible protein SHH (94.9%).

The Notch/Jagged signaling was activated by upregulating Jagged2 (129.2%), despite the downregulation of miR-34a-5p target protein Notch1 (81.2%).

The osteogenesis signaling appears to be activated by upregulating BMP2 (105.2%), BMP3 (125.8%), BMP4 (110.6%), RUNX2 (105.3%), RANKL (111.4%), and osteonectin (122.7%), despite the downregulation

of miR-34a-5p-responsible proteins osteopontin (69%), osteocalcin (84.4%), aggrecan (92.2%), and coincidental downregulation of PTH/PTHrPR (90.6%), and OPG (94.6%).

The innate immunity signaling appear to be activated by upregulating CD54 (106.2%), CD56 (106.1%), β-defensin1 (107.2%), β-defensin2 (108.9%), and β-defensin3 (137.4%), despite the downregulation of miR-34a-5p target protein CD44 (87.5%) and miR-34a-5p-responsible protein TLR4 (91%), as well as the coincidental downregulation of LL37 (85.9%) and versican (83.3%).

The chronic inflammation signaling appears to be activated by upregulating IL12 (140.2%), lysozyme (132%), CD68 (118.7%), CD106 (105.8%), MMP10 (129.7%), MMP12 (110.5%), cathepsin C (123.6%), and COX1 (122.3%) and coincidentally downregulating miR-34a-5p target protein IL10 (85.8%), despite the downregulation of miR-34a-5p target proteins MMP2 (89.8%), MMP3 (91.4%), and MMP9 (87.8%) and coincidental downregulation of TIMP1 (94.5%), cathepsin K (86.4%), and kininogen (88.4%).

The p53-mediated apoptosis signaling was activated by downregulating miR-34a-5p target protein BCL2 (87.5%) and upregulating miR-34a-5p-responsible proteins p53 (108.7%) and caspase3 (113.2%), as well as coincidentally upregulating p63 (127.8%), BAK (109.1%), BAX (120.3%), and MDM2 (106.3%), despite the downregulation of miR-34a-5p target protein p73 (75.4%) and coincidental downregulation of PUMA (93.5%) and c-caspase9 (92.1%).

The senescence signaling was activated by upregulating miR-34a-5p-responsible protein p21 (107.9%) and coincidentally upregulating klotho (112.8%) and sirtuin6 (105.4%), despite the downregulation of miR-34a-5p target protein sirtuin1 (93.4%) and coincidental downregulation of sirtuin3 (89.5%) and sirtuin7 (85.7%). Klotho is a miR-34a-5p target protein, but it was unexpectedly upregulated compared to the reference data.

In addition, miR-34a-5p*-CEDS variably influenced **the epigenetic modification signaling** by downregulating miR-34a-5p target proteins HMGB1 (79.7%) and coincidentally downregulating MBD4 (86.4%) and DMAP1 (87.4%), while it upregulated histone H1 (108.7%), KDM4D (115.4%), HDAC10 (106.4%), EZH2 (124.8%), BRG1 (113.2%), and lamin A/C (118.1%). BRG1 is a miR-34a-5p-responsible protein to be positively regulated. Consequently, miR-34a-5p*-CEDS induced a trend towards an increase in the methylation of histones and DNAs, and promotion of transcriptional repression.

MiR-34a-5p*-CEDS intensively suppressed **the oncogenesis signaling** by downregulating miR-34a-5p target proteins AXL (92.6%), BMI1 (84.4%), MTA2 (82.8%), and PDCD4 (71.1%) and miR-34a-5p-responsible protein YAP1 (86.5%), while it widely enhanced **the oncogenesis signaling** by upregulating Daxx (122.9%), BACH1 (122.7%), ATR (122.3%), Ets1 (119.4%), MALT1 (119.1%), DMBT1 (117.7%), BRCA2 (112.1%), KLF4 (110.5%), BRCA1 (109.8%), CRK (108.6%), ZEB1 (108.6%), and ATM (105.3%). KLF4 is a miR-34a-5p target protein, but it was unexpectedly upregulated compared to the reference data. Among the 28 oncoproteins, 12 were found to be overexpressed, nine were underexpressed, and seven exhibited minimal change in expression compared to the untreated controls.

Consequently, miR-34a-5p*-CEDS markedly affect the whole protein signaling in RAW 264.7 cells. MiR-34a-5p*-CEDS resulted in the attenuation of the RAS-NFkB signaling axis, which subsequently led to the inactivation of proliferation-related signaling axis, protection-ER stress-survival signaling axis, telomere-glycolysis-fibrosis signaling axis, and FAS- and PARP-mediated apoptosis signaling axis. Conversely, miR-34a-5p*-CEDS activated the p53/Rb/E2F1-SHH/PTCH/GLI-Notch/Jagged proliferation signaling axis, epigenetic modification-RAS-p53 associated apoptosis signaling axis, and oncogenesis-senescence-innate immunity-chronic inflammation signaling axis (Fig. 11B, Table 4).

The results indicate that miR-34a-5p*-CEDS induced an anti-oncogenic effect on the cells by suppressing the RAS-NFkB signaling axis, and subsequently attenuating the proliferation, angiogenesis, survival, glycolysis, and FAS- and PARP-mediated apoptosis. Conversely, it also induced an oncogenic effect by activating alternative proliferation, oncogenesis, senescence, chronic inflammation, and p53-mediated apoptosis. It can be concluded that miR-34a-5p*-CEDS exerts a divergent anti-oncogenic or oncogenic effect on RAW 264.7 cells, depending on the specific cellular context.

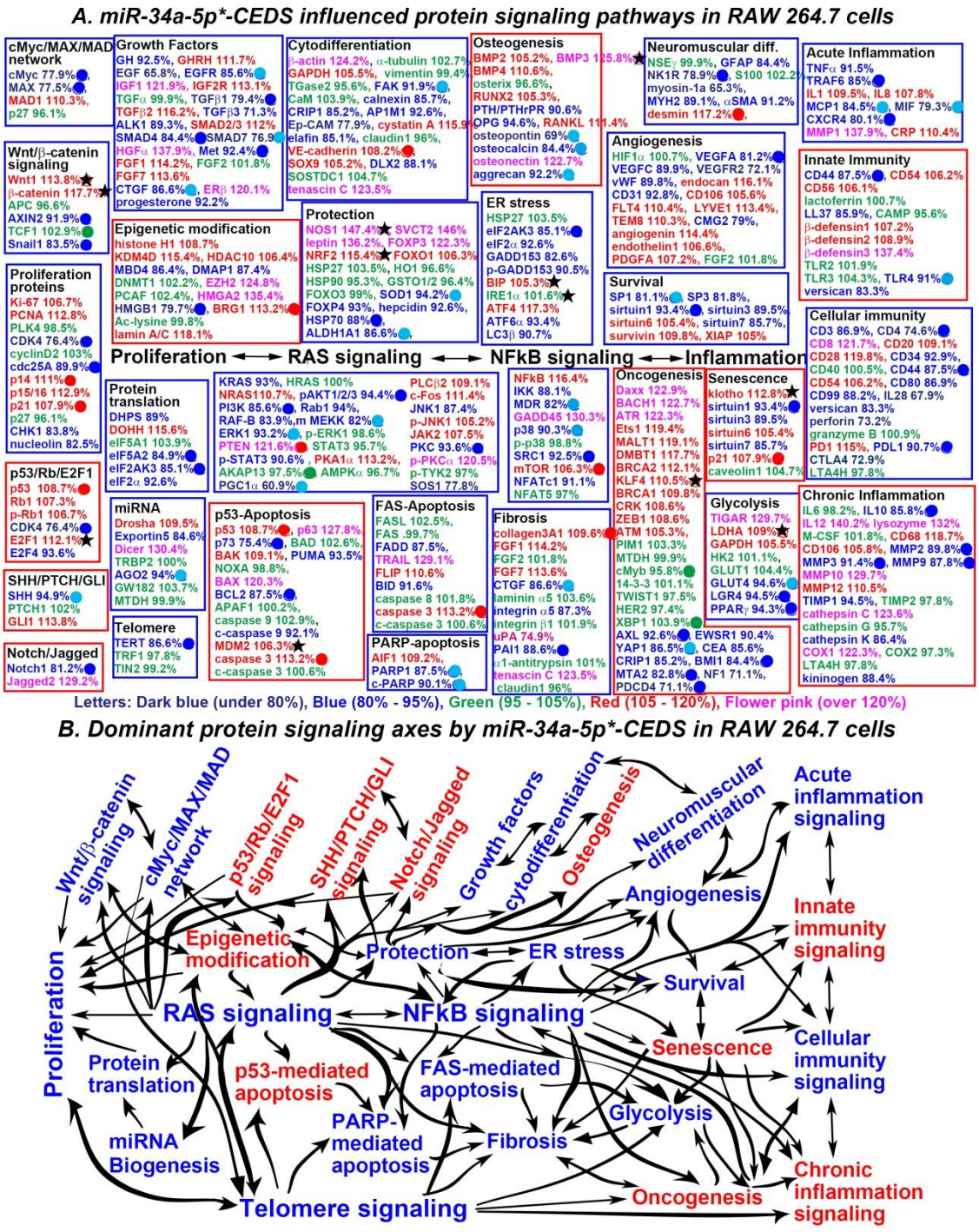

Fig. 11. MiR-34a-5p*-CEDS influenced the protein signaling (A) and axes (B) in RAW 264.7 cells. The IP-HPLC revealed proteins downregulated (**blue**), upregulated (**red**), and minimally changed (**green**) compared to the untreated controls. Dominantly suppressed (**blue square**) and activated (**red square**) signaling. Downregulated proteins by direct targeting (●) and indirect response (●), upregulated proteins by indirect response (●), and minimal changed (±5%) proteins (●). Some target proteins (★) were unexpectedly upregulated contrast to the current manuscripts and data from miRDB and TargetScan websites.

Table 4. Protein expressions in the RAW 264.7 cells treated with miR-34a-5p*-CEDS

Signaling	Downregulated Proteins	Upregulated Proteins
Proliferation	**CDK4, cdc25A**, CHK1, nucleolin	Ki-67, PCNA, **p14**, p15/16, **p21**
cMyc/MAX/MAD network	**cMyc, MAX**	MAD1
Wnt/β-catenin signaling	**AXIN2, Snail**	**Wnt1★, β-catenin★**
p53/Rb/E2F1 signaling	**CDK4**	**p53**, RB1, p-Rb1, **E2F1★**, E2F4
SHH/PTCH/GLI signaling	**SHH**	GLI1
Notch/Jagged signaling	**Notch**	Jagged2
Epigenetic modification	MBD4, DMAP, **HMGB1**	Histone H1, KDM4D, HDAC10, EZH2, HMGA2, **BRG1**, lamin A/C
Protein translation	DHPS, **eIF5A2, eIF2AK3**, eIF2α	DOHH
miRNA biogenesis	Exportin5, **AGO2**	Drosha, Dicer
Growth factors	GH, EGF, **EGFR**, **TGFβ1**, TGFβ3, ALK1, **SMAD4**, **SMAD7, Met, CTGF**, progesterone	GHRH, IGF1, IGFR2, TGFβ2, SMAD2/3, HGFα, FGF1, FGF7, ERβ
Cytodifferentiation	**FAK**, Clanexin, CRIP1, AP1M1, Ep-CAM, elafin, DLX2	β-actin, GAPDH, cystatin A, **VE-cadherin**, SOX9, tenascin C
Osteogenesis	PTH/PTHrPR, OPG**, osteopontin, osteocalcin, aggrecan**	BMP2, **BMP3★**, BMP4, RUNX2, RANKL, osteonectin
Neuromuscular differentiation	GFAP, **NK1/R**, myosin-1a, MYH2, αSMA	**Desmin**
RAS signaling	KRAS, **pAKT1/2/3, PI3K**, Rab1, RAF-B, **MEKK, ERK1**, p-STAT3, **PGC1α**, JNK1, **PKC**	NRAS, **PTEN**, PKA1α, PLCβ2, c-Fos, p-JNK1, JAK2, p-PKCα,
NFkB signaling	IKK, **MDR, p38, SRC1,** NFATc1	NFkB, GADD45, **mTOR**
p53-mediated apoptosis	**p73,** PUMA, **BCL2,** c-caspase9	**p53**, p63, BAK, BAX, **MDM2★**, **caspase3**
FAS-mediated apoptosis	FADD, BID	TRAIL, FLIP, **caspase3**
PARP-mediated apoptosis	**PARP1, c-PARP**	AIF1
Protection	**SOD1**, FOXP4, hepcidin, **HSP70, ALDH1A1**	**NOS1★**, SVCT2, leptin, FOXP3, **NRF2★**, FOXO1
ER stress	**eIF2AK3**, eIF2α, GADD153, p-GADD153, ATF6α, LC3β	**BIP★**, ATF4
Angiogenesis	**VEGFA**, VEGFC, VEGFR2, vWF, CD31, CMG2	endocan, CD106, FLT4, LYVE1, TEM8, angiogenin, endothelin1, PDGFA
Survival	**SP1**, SP3, **sirtuin1**, sirtuin3, sirtuin7	sirtuin6, survivin, XIAP
Acute inflammation	TNFα, **TRAF6**, **MCP1**, **MIF**, **CXCR4**	IL1, IL8, MMP1, CRP
Innate immunity	**CD44,** LL37, **TLR4**, versican	CD54, CD56, β-defensin1, β-defensin2, β-defensin3,
Cellular immunity	CD3, **CD4**, CD34, **CD44,** CD80, CD99, IL28, perforin, **PDL1**, CTLA4	CD8, CD20, CD28, PD1
Chronic inflammation	**IL10, MMP2, MMP3, MMP9**, TIMP1, cathepsin K, kininogen	IL12, lysozyme, CD68, CD106, MMP10, MMP12, cathepsin C, COX1
Glycolysis	**GLUT4, LGR4, PPARγ**	TIGAR, **LDHA★**, GAPDH
Fibrosis	**CTGF**, integrin α5, **PAI1**	**collagen3A1,** FGF1, FGF7, uPA, Tenascin C
Oncogenesis	**AXL,** EWSR1, **YAP1**, CEA, CRIP1, **BMI1**, **MTA2**, NF1, **PDCD4**	Daxx, BACH1, ATR, Ets1, MALT1, DMBT1, BRCA2, **KLF4★**, Daxx, BACH1, ATR, Ets1, MALT1, DMBT1, BRCA2, KLF4, BRCA1, CRK, ZEB1, ATM
Senescence	**sirtuin1**, sirtuin3, sirtuin7	**klotho★**, sirtuin6, **p21**
Telomere signaling	**TERT**	

MiR-34a-5p*-CEDS induced the suppression (**blue**) or activation (**red**) of signaling through protein downregulation by direct miRNA targeting (**blue**) or indirect response (**sky blue**) and protein upregulation by indirect response (**red**). Some miRNA target proteins were upregulated (★). The data were compared to the reports of recent manuscripts and miRDB, miRmap, miRPathDB, miRTarBase, and TargetScan websites.

MiR-126-5p*-CEDS influenced the protein signaling in RAW 264.7 cells

RAW 264.7 cells treated with mmu-miR-126-5p sequence CATTATTACTTTTGGTACGCG*-CEDS showed the characteristic protein expressions, resulting in the suppression of proliferation, cMyc/MAX/MAD network, Wnt/β-catenin signaling, p53/Rb/E2F1 signaling, SHH/PTCH/GLI signaling, Notch/Jagged signaling, epigenetic modification, protein translation, miRNA biogenesis, growth factors, cytodifferentiation, osteogenesis, neuromuscular differentiation, RAS signaling, protection, ER stress, angiogenesis, survival, acute inflammation, chronic inflammation, p53-mediated apoptosis, oncogenesis, glycolysis, and telomere signaling, as well as the activation of NFkB signaling, innate immunity, cellular immunity, FAS-mediated apoptosis, PARP-mediated apoptosis, fibrosis, and senescence signaling compared to the untreated controls (Fig. 12A).

The proliferation signaling was suppressed by downregulating miR-126-5p target protein PLK4 (91.6%) and miR-126-5p-responsible protein CDK4 (92.8%), as well as coincidentally downregulating PCNA (81.7%), p15/16 (90.5%), and nucleolin (94.8%), despite the upregulation of cdc25A (107.5%), p14 (109.3%), p21 (112.1%), and p27 (108%).

The cMyc/MAX/MAD network was suppressed by downregulating MAX (91.6%), despite the slight upregulation of miR-126-5p-responsible protein cMyc (108.4%) and coincidental upregulation of p27 (108.5%).

The Wnt/β-catenin signaling was suppressed by downregulating miR-126-5p target proteins Wnt1 (83%) and TCF1 (76.1%), despite the upregulation of β-catenin (116.6%), APC (110.7%), and AXIN2 (117.8%). APC is a miR-126-5p target protein, but it was unexpectedly upregulated compared to the reference data.

The p53/Rb/E2F1 signaling was suppressed by downregulating miR-126-5p-responsible proteins p53 (90.1%), CDK4 (92.8%), and E2F1 (93.8%) and coincidental upregulation of p-Rb1 (107.7%) and E2F4 (131.4%).

The SHH/PTCH/GLI signaling was suppressed by downregulating miR-126-5p target proteins SHH (86.2%) and coincidental downregulating GLI1 (86.6%).

The Notch/Jagged signaling was suppressed by downregulating Jagged2 (67.9%).

The protein translation signaling was suppressed by downregulating miR-126-5p-responsible protein eIF2α (88.6%) and coincidentally downregulating DHPS (85%) and eIF2AK3 (90.3%), despite the upregulation of DOHH (113.4%).

The miRNA biogenesis signaling appear to be inactivated by downregulating Dicer (69.4%) and TRBP2 (80.2%), despite the upregulation of Exportin5 (131.7%) and AGO2 (110.3%).

The growth factor signaling were suppressed by downregulating miR-126-5p target proteins EGFR (84.2%), TGFβ1 (78.2%), SMAD4 (72.4%), and HGFα (88.4%) and coincidentally downregulating GH (86.9%), IGF1 (78.6%), Met (80.6%), and FGF7 (80.9%), despite the upregulation of GHRH (123.1%), ALK1 (122.9%), FGF1 (111.6%), and ERβ (115%). FGF1 is a miR-126-5p target protein, but it was unexpectedly upregulated compared to the reference data.

The cytodifferentiation signaling appear to be inactivated by downregulating miR-34a-5p target protein claudin1 (88.3%) and coincidentally downregulating GAPDH (88.1%), CaM (81.3%), calnexin (81.3%), CRIP1 (99.3%), Ep-CAM (94.7%), SOSTDC1 (86%), and tenascin C (79.5%), despite the upregulation of α-tubulin (106.8%), vimentin (117.9%), TGase2 (119.1%), FAK (108.7%), AP1M1 (112%), caveolin1 (108.5%), cystatin A (141.2%), and SOX9 (121%).

The osteogenesis signaling was suppressed by downregulating miR-126-5p-responsible proteins BMP2 (82.8%), BMP4 (91.2%), and OPG (71%) and coincidentally downregulating osterix (92.9%), RANKL (80%), and osteonectin (82.7%), despite the upregulation of PTH/PTHrPR (106.8%) and RUNX2 (110.7%). RUNX2 is a miR-126-5p target protein, but it was unexpectedly upregulated compared to the reference data.

The neuromuscular differentiation signaling were inactivated by downregulating NSEγ (89.3%), GFAP (65.7%), NK1R (85.7%), and myosin-1a (83.9%), despite the upregulation of miR-34a-5p target protein αSMA (111%).

The RAS signaling was suppressed the miR- the miR- by downregulating miR-126-5p target proteins HRAS (88.7%), NRAS (82.5%), MEKK (92.4%), ERK1 (89.9%), STAT3 (93.8%), p-STAT3 (65.7%), AKAP13 (94.7%), c-Fos (84.1%), p-JNK1 (87.1%), and SOS1 (84.7%) and coincidentally upregulating RAF-B

(91.3%), PKA1α (94%), and p-TYK2 (94.3%), despite the upregulation of miR-126-5p-responsible protein KRAS (113.8%) and coincidental upregulation of AMPKα (110.5%), PGC1α (111.4%), PLCβ2 (118.1%), JNK1 (109.5%), and PKC (112.9%).

The angiogenesis signaling was suppressed by downregulating miR-126-5p target proteins VEGFA (88.4%), VEGFC (70.2%), angiogenin (85.3%), and CD106 (81.8%) and coincidentally downregulating CD31 (90.1%), despite the upregulation of HIF1α (119.9%), VEGFR2 (105.9%), LYVE1 (115.7%), TEM8 (106.8%), and endothelin1 (126.8%).

The survival signaling was suppressed by downregulating miR-126-5p target protein SP1 (86%) and coincidentally downregulating sirtuin6 (81%), sirtuin7 (93.1%), and survivin (85.9%), despite the upregulation of sirtuin1 (107.3%) and sirtuin3 (105.6%). Sirtuin1 is a miR-126-5p-responsible protein, and slightly upregulated.

The acute inflammation signaling was suppressed by downregulating miR-126-5p target proteins TRAF6 (85.2%), IL1 (84.7%), and CXCR4 (88.9%) and coincidentally downregulating miR-126-5p-responsible protein CRP (83.4%), despite the upregulation of MMP1 (116.9%).

The chronic inflammation signaling was suppressed by downregulating miR-126-5p target proteins IL6 (82.9%) and MMP3 (85.8%) and coincidentally downregulating IL12 (88.4%), lysozyme (89.5%), M-CSF (77.6%), CD31 (90.7%), CD106 (83%), MMP9 (92.9%), cathepsin G (92.5%), and COX2 (80.4%), despite the upregulation of MMP12 (119.6%), TIMP1 (110.7%), and cathepsin K (123%).

The p53-mediated apoptosis signaling was suppressed by downregulating miR-126-5p-responsible proteins p53 (90.3%), BAK (89.5%), caspase9 (86.4%), and c-caspase9 (82.1%) and coincidentally downregulating PUMA (88.2%), despite the upregulation of p73 (105.9%), NOXA (109.8%), BCL2 (115.8%), and c-caspase3 (123.9%). BCL2 is a miR-126-5p target protein, but it was unexpectedly upregulated compared to the reference data.

The glycolysis signaling was suppressed by downregulating miR-126-5p target proteins LGR4 (91.1%) and LDHA (80.4%), and coincidentally downregulating GAPDH (88.1%), despite the slight upregulation of GLUT1 (106.6%).

The telomere signaling was suppressed by downregulating miR-126-5p target protein TERT (91%), despite the upregulation of TRF1 (120.4%).

Conversely, **the innate immunity signaling** was activated by upregulating CD56 (105.5%), lactoferrin (116.2%), LL37 (127.1%), β-defensin1 (114.5%), β-defensin2 (124.8%), TLR2 (110.6%), and TLR4 (114.4%), despite the downregulation of miR-126-5p target protein TLR3 (79.1%) and coincidental downregulation of β-defensin3 (82.5%) and α1-antitrypsin (86.6%). TLR4 is a miR-126-5p target protein, but it was unexpectedly upregulated compared to the reference data.

The cellular immunity signaling was activated by upregulating miR-126-5p-responsible proteins CD4 (121.9%) and CTLA4 (109.2%), and downregulating miR-126-5p target protein PDL1 (90.9%), as well as coincidental upregulation of CD20 (111.9%), CD34 (105.9%), CD44 (113%), CD54 (119%), CD99 (110.6%), perforin (115.1%), and PD1 (105.1%), despite the downregulation of miR-126-5p target protein CD40 (82.5%) and coincidental downregulation of CD3 (84.4%), CD28 (94.4%), IL28 (86.9%), granzyme B (88.9%), and LTA4H (76.8%). CD44 is a miR-126-5p target protein, but it was unexpectedly upregulated compared to the reference data.

The NFkB signaling was activated by upregulating p-p38 (131.7%), mTOR (106.3%), NFATc1 (119.7%), and NFAT5 (118.1%), despite the downregulation of MDR (72.3%), GADD45 (93%), p38 (93.7%), and SRC1 (91.6%). NFAT5 is a miR-126-5p target protein, but it was unexpectedly upregulated compared to the reference data.

The FAS-mediated apoptosis signaling was activated by upregulating miR-126-5p-responsible proteins FASL (126.2%), FADD (118.3%), and c-caspase8 (105.8%) and coincidentally upregulating c-caspase3 (123.9%), despite the downregulation of miR-126-5p target proteins FAS (82.8%) and FLIP (88.2%) and miR-126-5p-responsible protein TRAIL (89.7%).

The PARP-mediated apoptosis signaling was activated by upregulating miR-126-5p-responsible proteins c-PARP (111.9%), despite the downregulation of AIF1 (85.3%) and PARP1 (82.8%).

The fibrosis signaling was activated by upregulating miR-126-5p-responsible protein PAI1 (108%) and coincidentally upregulating collagen3A1 (132.4%), FGF1 (111.6%), and laminin α5 (113.5%) and downregulating FGF7 (80.9%), despite the downregulation of miR-126-5p target protein claudin1 (88.3%) and coincidental downregulation of α1-antitrypsin (86.6%) and tenascin C (79.5%). FGF1 is a miR-126-5p target protein, but it was unexpectedly upregulated compared to the reference data.

The senescence signaling appear to be activated by upregulating miR-34a-5p target protein sirtuin1 (107.3%) and coincidentally upregulating sirtuin3 (105.6%), p21 (112.1%), and caveolin1 (108.5%), despite the downregulation of miR-34a-5p target protein klotho (94.8%) and coincidental downregulation of sirtuin6 (81%) and sirtuin7 (93.1%).

In addition, miR-126-5p*-CEDS variably influenced **the epigenetic modification signaling** by downregulating histone H1 (89.6%), HDAC10 (93.4%), MBD4 (86.8%), DMAP1 (86.4%), EZH2 (88.5%), PCAF (93.5%), and lamin A/C (77.8%), as well as the upregulation of DNMT1 (107.3%), HMGA2 (123.8%), HMGB1 (122.1%), and Ac-lysine (112.1%). DNMT1, HMGA2, and HMGB1 are miR-126-5p target proteins, but they were unexpectedly upregulated compared to the reference data.

MiR-126-5p*-CEDS broadly affected **the oncogenesis signaling** by downregulating miR-126-5p target proteins ATR (90.1%), AXL (89.8%), Ets1 (83.3%) and miR-126-5p-responsible protein BRCA1 (89.4%), as well as the upregulation of BACH1 (127.7%), NF1 (120.8%), Daxx (115.8%), ZEB1 (114.8%), MALT1 (108.5%), and cMyb (106.2%). BACH1 and NF1, and ZEB1 are miR-126-5p target proteins, but they were unexpectedly upregulated compared to the reference data.

Consequently, miR-126-5p*-CEDS significantly impacted the entire protein signaling in RAW 264.7 cells. MiR-126-5p*-CEDS suppressed the RAS signaling, resulting in the inactivation of proliferation-related signaling axis, protection-ER stress-angiogenesis-survival signaling axis, glycolysis-oncogenesis-chronic inflammation signaling axis, and telomere-epigenetic modification-RAS-p53 mediated apoptosis signaling axis.

Conversely, it enhanced NF-kB signaling, which led to the activation of FAS- and PARP-mediated apoptosis-fibrosis signaling axis and senescence-innate and cellular immunity signaling axis (Fig. 12B, Table 5).

The results indicate that miR-126-5p*-CEDS induced a strong anti-oncogenic effect on the cells by suppressing proliferation, angiogenesis, survival, glycolysis, chronic inflammation, and telomere instability. Furthermore, it enhanced the FAS- and PARP-mediated apoptosis and the innate and cellular immunity. It is also noteworthy that miR-126-5p*-CEDS induced senescence and fibrosis as a result.

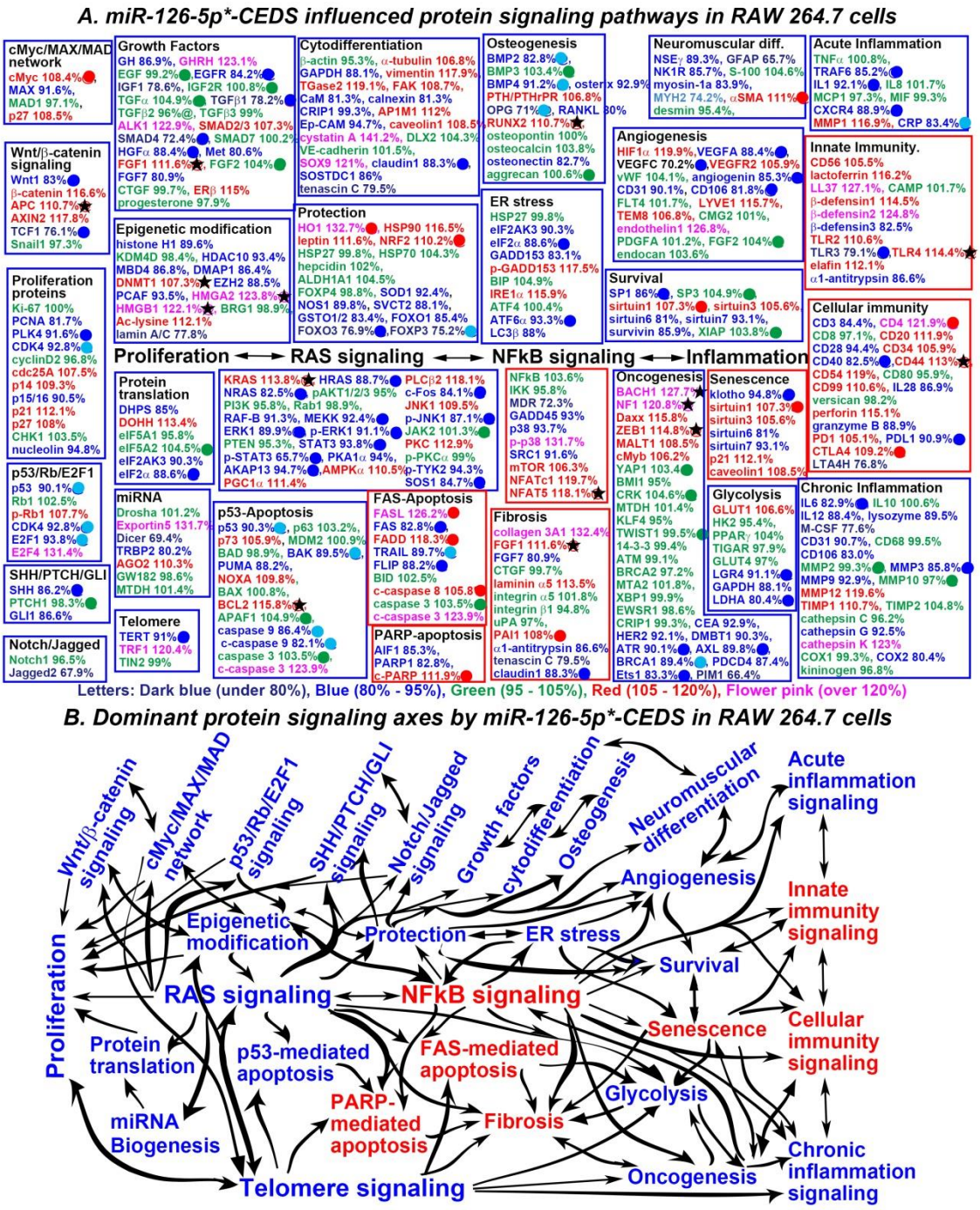

Fig. 12. MiR-126-5p*-CEDS influenced the protein signaling (A) and axes (B) in RAW 264.7 cells. The IP-HPLC revealed proteins downregulated (**blue**), upregulated (**red**), and minimally changed (**green**) compared to the untreated controls. Dominantly suppressed (**blue square**) and activated (**red square**) signaling. Downregulated proteins by direct targeting (●) and indirect response (●), upregulated proteins by indirect response (●), and minimal changed (±5%) proteins (●). Some target proteins (★) were unexpectedly upregulated contrast to the current manuscripts and data from miRDB and TargetScan websites.

Table 5. Protein expressions in the RAW 264.7 cells treated with miR-126-5p*-CEDS.

Signaling	Downregulated Proteins	Upregulated Proteins
Proliferation	PCNA, **PLK4**, **CDK4**, p15/16, nucleolin	cdc25A, p14, p21, p27
cMyc/MAX/MAD network	MAX	**cMyc**, p27
Wnt/β-catenin signaling	**Wnt1**, **TCF1**	β-catenin, APC, AXIN2
p53/Rb/E2F1 signaling	**p53, CDK4, E2F1**	p-Rb1, E2F4
SHH/PTCH/GLI signaling	**SHH**, GLI1	
Notch/Jagged signaling	Jagged	
Epigenetic modification	Histone H, HDAC10, MBD4, DMAP, EZH2, PCAF, lamin A/C	**DNMT1★**, **HMGA2★, HMGB1★**, Ac-lysine
Protein translation	DHPS, eIF2AK3, **eIF2α**	
miRNA biogenesis	Dicer, TRBP2	Exportin5, AGO2
Growth factors	GH, **EGFR**, IGF1, **TGFβ1, SMAD4**, **HGFα,** Met, FGF7	GHRH, TGFα, ALK1, SMAD2/3**, FGF1★**, FGF2, ERβ
Cytodifferentiation	GAPDH, CaM, calnexin, CRIP1, Ep-CAM, **claudin1,** SOSTDC1, tenascin C	α-tubulin, vimentin, TGase2, FAK, AP1M1, caveolin1, cystatin A, SOX9
Osteogenesis	**BMP2, BMP4**, osterix, **OPG,** RANKL, osteonectin	**RUNX2★**, PTH/PTHrPR
Neuromuscular differentiation	NSEγ, GFAP, NK1R, myosin-1a	**αSMA**
RAS signaling	**HRAS**, **NRAS**, RAF-B, **MEKK**, **ERK1, p-ERK1, STAT3, p-STAT3**, PKA1α, AKAP13, **c-Fos**, **p-JNK1**, p-TYK2, **SOS1**	**KRAS★**, AMPKα, PGC1α, PLCβ2, JNK1, PKC
NFkB signaling	MDR, GADD45, p38, SRC1	p-p38, mTOR, NFATc1, **NFAT5★**
p53-mediated apoptosis	**p53, BAK**, PUMA, **caspase9, c-caspase9**	p73, NOXA, **BCL2★**, APAF1, c-caspase3
FAS-mediated apoptosis	**FAS**, **TRAIL**, **FLIP**	**FASL, FADD**, **c-caspase8**, c-caspase3
PARP-mediated apoptosis	AIF1, PARP1	**c-PARP**
Protection	SOD1, NOS1, SVCT2, GSTO1/2, FOXO1, **FOXO3**, **FOXP3**	**HO1,** HSP90, leptin, **NRF2**
ER stress	eIF2AK3, **eIF2α,** GADD153, **ATF6α**, LC3β	p-GADD153, IRE1α
Angiogenesis	**VEGFA**, **VEGFC, angiogenin,** CD31, **CD106**	HIF1α, VEGFR2, LYVE1, TEM8, andothelin1, FGF2
Survival	**SP1**, sirtuin6, sirtuin7, survivin,	SP3, **sirtuin1**, sirtuin3, XIAP
Acute inflammation	**TRAF6, IL1, CXCR4**, **CRP**	MMP1
Innate immunity	β-defensin3, **TLR3**, α1-antitrypsin	CD56, lactoferrin, LL37, β-defensin1, β-defensin2, TLR2, **TLR4★**, elafin
Cellular immunity	CD3, CD28, **CD40**, IL28, granzyme B, **PDL1**, LTA4H	**CD4**, CD20, CD34, **CD44★,** CD54, CD99, perforin, PD1, **CTLA4**
Chronic inflammation	**IL6**, IL12, lysozyme, M-CSF, CD31, CD106, **MMP3**, MMP9, cathepsin G, COX2	MMP12, TIMP1, cathepsin K
Glycolysis	**LGR4**, GAPDH, **LDHA**	GLUT1
Fibrosis	FGF7, α1-antitrypsin, tenascin, **claudin1**	collagen 3A1, FGF1, laminin α5, **PAI1**
Oncogenesis	CEA, HER2, DMBT1, **ATR, AXL**, **BRCA1**, PDCD4, **Ets1**, PIM1	**BACH1★, NF1★**, Daxx, **ZEB1★**, MALT1, YAP1, cMyb
Senescence	**klotho**, sirtuin6, sirtuin7	**sirtuin1**, sirtuin3, p21, caveolin1
Telomere signaling	**TERT**	TRF1

MiR-126-5p*-CEDS induced the suppression (**blue**) or activation (**red**) of signaling through protein downregulation by direct miRNA targeting (**blue**) or indirect response (**sky blue**) and protein upregulation by indirect response (**red**). Some miRNA target proteins were upregulated (★). The data were compared to the reports of recent manuscripts and miRDB, miRmap, miRPathDB,

MiR-150-5p*-CEDS influenced the protein signaling in RAW 264.7 cells

RAW 264.7 cells treated with mmu-miR-150-5p sequence TCTCCCAACCCTTGTACCAGTG*-CEDS showed the characteristic protein expressions, resulting in the suppression of proliferation, cMyc/MAX/MAD network, Wnt/β-catenin signaling, p53/Rb/E2F1 signaling, SHH/PTCH/GLI signaling, epigenetic modification, protein translation, growth factors, cytodifferentiation, osteogenesis, neuromuscular differentiation, RAS signaling, NFkB signaling, angiogenesis, survival, acute inflammation, innate immunity, cellular immunity, chronic inflammation, p53-mediated apoptosis, FAS-mediated apoptosis, oncogenesis, senescence, glycolysis, and telomere signaling, as well as the activation of Notch/Jagged signaling, miRNA biogenesis, protection, PARP-mediated apoptosis, and fibrosis signaling compared to the untreated controls (Fig. 13A).

The proliferation signaling was suppressed by downregulating miR-150-5p target protein cyclin D2 (90.7%) and miR-150-5p-responsible proteins Ki-67 (89.7%), PCNA (93.9%), and p21 (78.9%), as well as the coincidental downregulation of PLK4 (84.7%), cdc25A (84.4%), and CHK1 (88.7%), despite the upregulation of p14 (113.6%), p15/16 (105.7%), and nucleolin (112.2%).

The cMyc/MAX/MAD network was suppressed by downregulating miR-150-5p-responsible protein cMyc (89.7%) and coincidentally downregulating MAX (92.7%) and MAD1 (93.5%).

The Wnt/β-catenin signaling was suppressed by downregulating miR-150-5p target protein β-catenin (75.7%) and miR-150-5p-responsible protein Wnt1 (86.7%), despite the upregulation TCF1 (119.7%) and Snail1 (117.2%). TCF1 could be upregulated through the alternative signaling.

The p53/Rb/E2F1 signaling was suppressed by downregulating p-Rb1 (85.0%), E2F1 (85.8%), and E2F4 (90.5%) and coincidentally upregulating Rb1 (109.8%).

The SHH/PTCH/GLI signaling was suppressed by downregulating SHH (86.1%) and GLI1 (84.5%).

The protein translation signaling was suppressed by downregulating DHPS (90.2%), eIF5A1 (87.3%), despite the upregulation of eIF5A2 (109.7%).

The growth factor signaling were suppressed by downregulating miR-150-5p target proteins IGF1 (81.9%) and TGFβ1 (81.6%) and miR-150-5p-responsible protein SMAD2/3 (85%), as well as coincidentally

downregulating GH (90.4%), GHRH (82.6%), EGFR (76.8%), SMAD7 (92%), and FGF1 (94.3%), despite the upregulation of miR-150-5p-responsible protein SMAD4 (108.3%) and coincidental upregulation of EGF (105.6%), IGF2R (105.6%), TGFα (119.2%), TGFβ2 (112.9%), TGFβ3 (106.1%), ALK1 (118.3%), Met (109.2%), FGF2 (122.2%), FGF7 (107.4%), CTGF (117.4%), and progesterone (129.2%). CTGF is a miR-150-5p target protein, but it was unexpectedly upregulated compared to the reference data.

The cytodifferentiation signaling partially were suppressed by downregulating miR-150-5p target protein tenascin C (90.5%) and miR-150-5p-responsible proteins vimentin (86.1%) and FAK (94.8%) and coincidentally downregulating β-actin (93.8%), α-tubulin (90.7%), GAPDH (86.5%), CaM (90%), calnexin (66.5%), CRIP1 (82%), and caveolin1 (92.9%), despite the upregulation of TGase2 (107.3%), AP1M1 (143.3%), Ep-CAM (110.8%), cystatin A (107%), VE-cadherin (117%), claudin1 (118.3%), DLX2 (137.6%), and SOSTDC1 (143.1%).

The osteogenesis signaling was inactivated by downregulating miR-150-5p target proteins RUNX2 (88.8%), osteonectin (85.4%), and miR-150-5p-responsible protein BMP2 (76.7%), as well as coincidentally downregulating RANKL (84.3%), PTH/PTHrP-R (69.4%), and osteocalcin (84%), despite the upregulation of BMP4 (108.6%), osterix (106.8%), OPG (131.6%), and osteopontin (108%).

The neuromuscular differentiation signaling were inactivated by downregulating miR-150-5p-rsponsible protein αSMA (90.3%) and coincidentally downregulating NK1R (92.3%), MYH2 (92%), and desmin (86%), despite the upregulation of myosin-1a (108.6%).

The RAS signaling was suppressed by downregulating miR-150-5p target proteins STAT3 (84.6%), p-STAT3 (72.7%), AMPKα (94.4%), p-JNK1 (84.1%), and JAK2 (84.9%), as well as coincidentally downregulating KRAS (80.5%), PI3K (90.2%), PLCβ2 (85.7%), c-Fos (93.2%), p-TYK2 (88.8%), and SOS1 (96.4%), despite the upregulation of Rab1 (110.2%), ERK1 (123.7%), AKAP13 (114.9%), and p-PKC1α (113.7%). ERK1 is a miR-150-5p target protein, but it was unexpectedly upregulated compared to the reference data.

The NFkB signaling was suppressed by downregulating miR-150-5p target proteins NFkB (88.1%) and mTOR (88%), as well as coincidentally downregulating MDR (93%) and p-p38 (74.4%), and upregulating IKK (115.4%), despite the upregulation of miR-150-5p-responsible protein SRC1 (130.4%).

The angiogenesis signaling was suppressed by downregulating miR-150-5p target proteins HIF1α (87.9%), VEGFA (83.7%), and miR-150-5p-responsible protein VEGFR2 (94.9%), as well as coincidentally downregulating CD31 (85.3%) and CD106 (87.8%), despite the upregulation of vWF (111.3%), LYVE1 (125.8%), TEM8 (107.3%), CMG2 (108.1%), angiogenin (121.9%), and FGF2 (122.2%).

The survival signaling was suppressed by downregulating miR-150-5p target proteins SP1 (92.8%) and survivin (91.7%), despite the upregulation of SP3 (106.2%), sirtuin1 (105.3%), sirtuin6 (109.1%), sirtuin7 (148.3%), and XIAP (111.1%). Sirtuin1 is a miR-150-5p target protein, but it was unexpectedly upregulated compared to the reference data.

The acute inflammation signaling was suppressed by downregulating miR-150-5p target proteins TNFα (90.2%) and TRAF6 (83.7%), as well as coincidentally downregulating IL1 (78.1%) and MCP1 (90.9%), despite the upregulation of MIF (116.4%).

The innate immunity signaling appears to be inactivated by downregulating miR-150-5p target protein TLR4 (89.9%) and coincidentally downregulating LL37 (86.5%), β-defensin1 (82.8%), β-defensin3 (76.6%), TLR2 (80.9%), and elafin (91%), despite the upregulation of miR-150-5p-responsible protein CD56 (129.6%) and coincidental upregulation of β-defensin2 (127.7%) and α1-antitrypsin (111.3%).

The cellular immunity signaling was suppressed by downregulating miR-150-5p-responsible protein PD1 (87.3%), as well as coincidentally downregulating CD4 (89.5%), CD28 (86%), CD34 (78.6%), CD40 (89%), CD80 (81.3%), CD99 (91%), IL28 (86.3%), granzyme B (93.1%), and LTA4H (93.8%), despite the upregulation of CD8 (117.3%), CD20 (140.8%), versican (118.7%), perforin (112.2%), and CTLA4 (109.3%).

The chronic inflammation signaling was suppressed by downregulating miR-150-5p target proteins IL6 (90.1%) and miR-150-5p-responsible protein IL10 (87.9%), as well as coincidentally downregulating CD31 (86.7%), CD106 (88.8%), MMP3 (84.4%), MMP12 (88.3%), TIMP2 (84.2%), and cathepsin K (94.9%), despite

the upregulation of IL12 (112%), lysozyme (124.4%), CD68 (113.2%), MMP2 (107.7%), COX1 (109.2%), COX2 (110%), and kininogen (134.1%).

The p53-mediated apoptosis signaling was suppressed by downregulating miR-150-5p-responsible proteins caspase9 (89.9%), c-caspase9 (82.3%), and c-caspase3 (88.6%), as well as coincidentally downregulating APAF1(93.5%), despite the upregulation of p73 (105.3%), BAD (119.8%), NOXA (120%), BCL2 (105.9%), and caspase3 (108.4%). BCL2 is a miR-150-5p target protein, but it was unexpectedly upregulated compared to the reference data.

The FAS-mediated apoptosis signaling was inhibited by downregulating miR-150-5p-responsible proteins caspase8 (93%) and c-caspase3 (88.6%), as well as coincidentally downregulating FASL (94.1%), FAS (82.2%), FADD (93.4%), and BID (92.5%), despite the upregulation of TRAIL (111.7%) and caspase3 (108.4%).

The senescence signaling was suppressed by downregulating miR-150-5p-responsible protein p21 (78.9%) and coincidentally downregulating caveolin1 (92.9%), despite the upregulation of sirtuin1 (105.3%), sirtuin6 (109.1%), and sirtuin7 (148.3%). Sirtuin1 is a miR-150-5p target protein, but it was unexpectedly upregulated compared to the reference data.

The glycolysis signaling was suppressed by downregulating miR-150-5p target protein TIGAR (93.5%), PPARγ (89.1%), and GLUT1 (76.7%), as well as coincidentally downregulating GAPDH (86.5%), despite the upregulation of LDHA (116.3%) and HK2 (106%).

The telomere signaling was suppressed by downregulating TERT (84.5%) and TIN2 (91.2%), despite the upregulation of TRF1 (107.3%).

Conversely, **the Notch/Jagged signaling** was activated by upregulating Notch1 (128.3%) and Jagged2 (107.5%). Notch1 is a miR-150-5p target protein, but it was unexpectedly upregulated compared to the reference data**.**

The miRNA biogenesis signaling was activated by upregulating Drosha (106.3%), Exportin5 (122.8%), Dicer (110.5%) and GW182 (108.7%), and downregulating MTDH (93.6%) coincidentally.

The protection signaling was activated by upregulating miR-150-5p-responsible proteins NOS1 (148.7%) and SOD1 (106.2%), as well as coincidentally upregulating leptin (135%), ALDH1A1 (129.9%), FOXO1 (124.5%), FOXO3 (107.5%), and HSP90 (116.6%), despite the downregulation of miR-150-5p-responsible protein HO1 (86.5%) and coincidental downregulation of SVCT2 (94%), FOXP3 (93.5%), GSTO1/2 (82%), and FOXP4 (79.2%).

The PARP-mediated apoptosis signaling was activated by upregulating AIF1 (128.9%), PARP1 (114.2%), and c-PARP (110.9%).

The fibrosis signaling appears to be activated by upregulating FGF2 (122.2%), CTGF (117.4%), lamininα5 (115.8%), integrin α5 (114.9%), uPA (113.5%), α1-antitrypsin (111.3%), and claudin1 (118.3%), despite the downregulation of miR-150-5p target protein tenascin C (90.5%) and miR-150-5p-responsible protein collagen 3A1 (91.3%), as well as coincidentally downregulating FGF1 (94.3%), integrin β1 (88.3%), and PAI1 (86.6%) and upregulating FGF7 (107.4%). CTGF is a miR-150-5p target protein, but it was unexpectedly upregulated compared to the reference data.

In addition, miR-150-5p*-CEDS significantly influenced **the epigenetic modification signaling** by downregulating miR-150-5p target proteins HMGA2 (94.8%), as well as the coincidentally downregulating MBD4 (91.3%), DMAP1 (89.7%), BRG1 (87.4%), and lamin A/C (84.7%), while it upregulated histone H1 (106.5%), EZH2 (110.3%), HMGB1 (131.6%), and Ac-lysine (113.9%). EZH2 is a miR-150-5p target protein, but it was unexpectedly upregulated compared to the reference data. Consequently, miR-150-5p*-CEDS induced a trend towards a reduction in the methylation of histones and DNAs, and attenuation of transcriptional repression.

MiR-150-5p*-CEDS markedly suppressed **the oncogenesis signaling** by downregulating miR-150-5p target proteins PDCD4 (77.9%) and coincidentally downregulating BRCA2 (94.6%), MTDH (93.6%), BACH1 (93.5%), BMI1 (92.4%), ATR (92.1%), CRK (89%), CEA (86.7%), DMBT1 (86.4%), AXL (86.2%), CRIP1 (82%), and ATM (80.4%), while it partly enhanced **the oncogenesis signaling** by upregulating cMyb (131.5%), XBP1 (121%), KLF4 (117.8%), NF1 (107.8%), and Daxx (117.9%). cMyb and XBP1 are miR-150-5p target proteins, but they were unexpectedly upregulated compared to the reference data. Among the 28 oncoproteins,

12 were found to be underexpressed, five were overexpressed, and 11 exhibited minimal change in expression compared to the untreated controls.

Consequently, miR-150-5p*-CEDS had a profound impact on the entire protein signaling in RAW 264.7 cells. MiR-150-5p*-CEDS suppressed the RAS-NFkB signaling axis, subsequently inactivating the majority of proliferation-related signaling axis, growth and cytodifferentiation signaling axis, ER stress-angiogenesis-survival-senescence signaling axis, and so on. MiR-150-5p*-CEDS also impacted the inflammation-immunity signaling axis, glycolysis-oncogenesis-chronic inflammation signaling axis, telomere-epigenetic modification signaling axis, and p53- and FAS-mediated apoptosis signaling. Conversely, it activated protection-Notch/Jagged signaling axis, PARP-mediated apoptosis-fibrosis signaling axis, and miRNA biogenesis signaling (Fig 13B, Table 6).

The results demonstrate that miR-150-5p*-CEDS exerts a potent anti-oncogenic effect on cells by suppressing proliferation, angiogenesis, survival, senescence, glycolysis, oncogenesis, chronic inflammation, and telomere instability. Conversely, it increased the PARP-mediated apoptosis and enhanced the ROS-Notch signaling. Additionally, it is worthy to note that miR-150-5p*-CEDS attenuated innate and cellular immunity, reduced major p53- and FAS-mediated apoptosis, and resulted in fibrosis signaling.

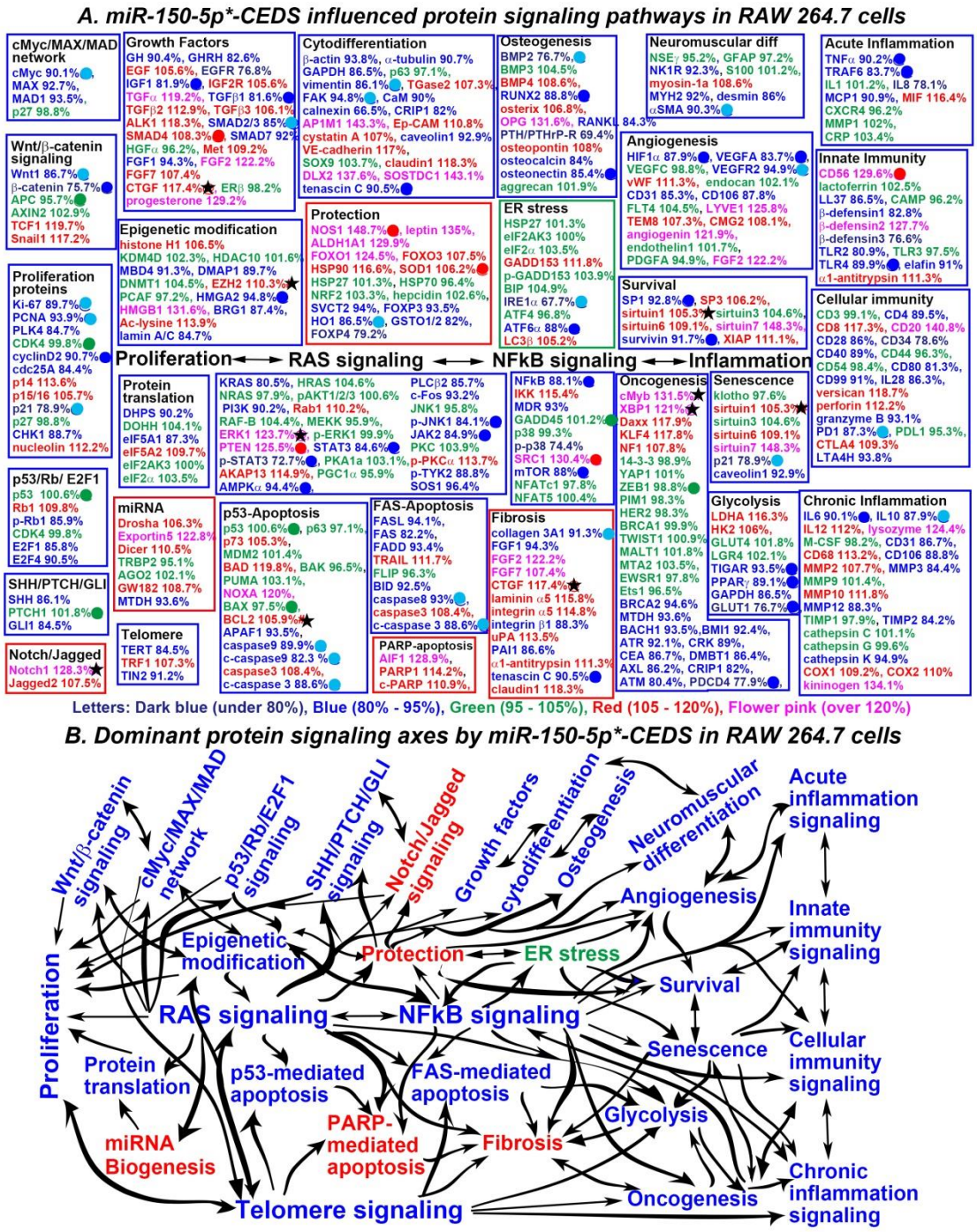

Fig. 13. MiR-150-5p*-CEDS influenced the protein signaling (A) and axes (B) in RAW 264.7 cells. The IP-HPLC revealed proteins downregulated (**blue**), upregulated (**red**), and minimally changed (**green**) compared to the untreated controls. Dominantly suppressed (**blue square**) and activated (**red square**) signaling. Downregulated proteins by direct targeting (●) and indirect response (●), upregulated proteins by indirect response (●), and minimal changed (±5%) proteins (●). Some target proteins (★) were unexpectedly upregulated contrast to the current manuscripts and data from miRDB and TargetScan websites.

Table 6. Protein expressions in the RAW 264.7 cells treated with miR-150-5p*-CEDS.

Signaling	Downregulated Proteins	Upregulated Proteins
Proliferation	**Ki-67, PCNA**, PLK4, **cyclin D2**, cdc25A, **p21**, CHK1	P14, p15/16, nucleolin
cMyc/MAX/MAD network	**cMyc**, MAX, MAD1	
Wnt/β-catenin signaling	**Wnt1**, **β-catenin**	TCF1, Snail
p53/Rb/E2F1 signaling	p-Rb1, E2F1, E2F4	Rb1
SHH/PTCH/GLI signaling	SHH, GLI1	
Notch/Jagged signaling		**Notch1★**, Jagged2
Epigenetic modification	MBD4, DMAP1, **HMGA2**, BRG1, lamin A/C	Histone H1, **EZH2★**, HMGB1, Ac-lysine
Protein translation	DHPS, eIF5A1	eIF5A2
miRNA biogenesis	MTDH	Drosha, Exportin5, Dicer, GW182
Growth factors	GH, GHRH, EGFR, **IGF1, TGFβ1, SMAD2/3**, SMAD7, FGF1	EGF, IGF2R, TGFα, TGFβ2, TGFβ3, ALK1, **SMAD4**, Met, FGF2, FGF7, **CTGF★**, progesterone
Cytodifferentiation	β-actin, α-tubulin, GAPDH, **vimentin, FAK**, CaM, calnexin, CRIP1, caveolin1, **tenascin C**	TGase2, AP1M1, Ep-CAM, cystatin A, VE-cadherin, claudin1, DLX2, SOSTDC1
Osteogenesis	**BMP2**, **RUNX2**, RANKL, PTH/PTHrPR, osteocalcin, **osteonectin**	BMP4, osterix, OPG, osteopontin
Neuromuscular differentiation	NK1R, MYH2, desmin, **αSMA**	myosin-1a
RAS signaling	KRAS, PI3K, **STAT3, p-STAT3**, **AMPKα**, PLCβ2, c-Fos, **p-JNK1, JAK2**, p-TYK2, SOS1	Rab1, **ERK1★**, **PTEN**, AKAP13, p-PKC1α
NFkB signaling	**NFkB**, MDR, p-p38, **mTOR**	IKK, **SRC1**
p53-mediated apoptosis	APAF1, **caspase9, c-caspase9, c-caspase3**	p73, BAD, NOXA, **BCL2★**, caspase3
FAS-mediated apoptosis	FASL, FAS, FADD, BID, **caspase9, c-caspase3**	TRAIL, caspase3
PARP-mediated apoptosis		AIF1, PARP1, c-PARP
Protection	SVCT2, FOXP3, **HO1**, GSTO1/2, FOXP4	**NOS1**, leptin, ALDH1A1, FOXO3, HSP90, **SOD1**,
ER stress	**IRE1α**, **ATF6α**	GADD153, LC3β
Angiogenesis	**HIF1α, VEGFA, VEGFR2**, CD31, CD106,	vWF, LYVE1, TEM8, CMG2, angiogenin, FGF2
Survival	**SP1**, **survivin**,	SP3, **sirtuin1★**, sirtuin6, sirtuin7, XIAP
Acute inflammation	**TNFα**, **TRAF6**, IL8, MCP1	MIF
Innate immunity	LL37, β-defensin1, β-defensin3, TLR2, **TLR4**, elafin,	**CD56**, β-defensin2, α1-antitrypsin
Cellular immunity	CD4, CD28, CD34, CD34, CD40, CD80, CD99, IL28, granzyme B, **PD1**, LTA4H	CD8, CD20, versican, perforin, CTLA4
Chronic inflammation	**IL6**, **IL10**, CD31, CD106, MMP3, MMP12, TIMP2, cathepsin K	IL12, lysozyme, CD68, MMP2, MMP10, COX1, COX2, kininogen
Glycolysis	**TIGAR, PPARγ**, GAPDH, **GLUT1**	LDHA, HK2
Fibrosis	**collagen 3A1**, FGF1, integrin β1, PAI1, **tenascin C**	FGF2, FGF7, **CTGF★**, laminin α5, integrin α5, uPA, α1-antitrypsin, claudin1
Oncogenesis	DMBT1, CRK, MTDH, CEA, AXL, BACH1, BMI1, BRCA2, ATR, ATM, CRIP1, **PDCD4**	**cMyb★**, **XBP1★**, KLF4, NF1, Daxx
Senescence	**p21**, caveolin1	**sirtuin1★**, sirtuin6, sirtuin7
Telomere signaling	TERT, TIN2	TRF1

MiR-150-5p*-CEDS induced the suppression (**blue**) or activation (**red**) of signaling through protein downregulation by direct miRNA targeting (**blue**) or indirect response (**sky blue**) and protein upregulation by indirect response (**red**). Some miRNA target proteins were upregulated (★). The data were compared to the reports of recent manuscripts and miRDB, miRmap, miRPathDB, miRTarBase, and TargetScan websites.

MiR-155-5p*-CEDS influenced the protein signaling in RAW 264.7 cells

RAW 264.7 cells treated with mmu-miR-155-5p sequence TTAATGCTAATCGTGATAGGGGTT*-CEDS showed the characteristic protein expressions, resulting in the suppression of cMyc/MAX/MAD network, Wnt/β-catenin signaling, Notch/Jagged signaling, epigenetic modification, miRNA biogenesis, osteogenesis, NFkB signaling, ER stress, angiogenesis, acute inflammation, chronic inflammation, p53-mediated apoptosis, PARP-mediated apoptosis, oncogenesis, and glycolysis signaling, as well as the activation of proliferation, p53/Rb/E2F1 signaling, SHH/PTCH/GLI signaling, growth factors, cytodifferentiation, neuromuscular differentiation, RAS signaling, protection, survival, innate immunity, cellular immunity, FAS-mediated apoptosis, fibrosis, and senescence compared to the untreated controls (Fig. 14A).

The cMyc/MAX/MAD network was suppressed by downregulating miR-155-5p target protein cMyc (94.1%) and coincidentally downregulating MAX (82.1%) and MAD1 (75.6%).

The Wnt/β-catenin signaling was suppressed by downregulating miR-155-5p target protein APC (92.7%) and miR-155-5p-responsible proteins Wnt1 (89.2%) and TCF1 (79.6%), and coincidental downregulation of AXIN2 (91.9%), despite the upregulation of β-catenin (112.4%) and Snail1 (117.4%).

The Notch/Jagged signaling was suppressed by downregulating miR-155-5p-responsible protein Notch1 (91.2%) and coincidentally downregulating Jagged2 (81.9%).

The miRNA biogenesis signaling was inactivated by downregulating Dicer (78.3%) and TRBP2 (77.1%). despite the upregulation of Exportin5 (123.8%), AGO2 (114.3%), and GW182 (113.9%).

The osteogenesis signaling was suppressed by downregulating BMP2 (78.6%), RUNX2 (82.4%), OPG (72.2%), RANKL (71.9%), osteonectin (88.3%), and aggrecan (87%).

The NFkB signaling was suppressed by downregulating miR-155-5p target proteins NFkB (92.7%), IKK (82.2%), as well as coincidentally downregulating MDR (71.2%), GADD45 (84.3%), despite the upregulation of SRC1 (106.2%) and NFATc1 (131.5%).

The ER stress signaling was suppressed by downregulating HSP27 (94.7%), GADD153 (88.3%), BIP (87%), IRE1α (94.4%), ATF4 (94.7%), despite the upregulation of p-GADD153 (114.4%) and ATF6α (112%).

The angiogenesis signaling was suppressed by downregulating miR-155-5p target protein HIF1α (94.7%) and miR-155-5p-responsible protein VEGFA (94.6%), as well as coincidentally downregulating VEGFC (66.4%), CD106 (83.1%), and endothelin1 (88%), despite the upregulation of vWF (66.4%), FLT4 (132.3%), TEM8 (106.6%), CMG2 (113.6%), and FGF2 (121.3%).

The acute inflammation signaling was suppressed by downregulating miR-155-5p target protein TNFα (92.4%) and TRAF6 (86.8%), despite the upregulation of IL8 (106.7%) and CXCR4 (111%).

The chronic inflammation signaling was suppressed by downregulating miR-155-5p target proteins IL6 (85.9%), M-CSF (83.3%), and COX2 (87.7%), and coincidentally downregulating IL12 (80%), CD106 (84.9%), TIMP1 (93.5%), and cathepsin G (88.1%), despite the upregulation of IL10 (130.7%), lysozyme (116.3%), CD68 (144.8%), MMP2 (105.7%), MMP10 (126%), MMP12 (109.5%), TIMP2 (124.4%), cathepsin K (121.2%), and COX1 (110.7%). IL10 is a miR-155-5p target protein, but it was unexpectedly upregulated compared to the reference data.

The p53-mediated apoptosis signaling appears to be suppressed by downregulating miR-155-5p-responsible protein p53 (88.1%), as well as coincidentally downregulating BAD (89.5%), BAK (94.9%), PUMA (87%), caspase9 (78.7%), and c-caspase9 (91.2%), despite the upregulation of p63 (127.7%), p73 (106.5%), NOXA (117.3%), caspase3 (114.7%), and c-caspase3 (118.6%).

The PARP-mediated apoptosis signaling appears to be suppressed by downregulating miR-155-5p-responsible proteins PARP1 (70.8%) and coincidentally downregulating AIF1 (69.7%), despite the slight upregulation of c-PARP (106.4%).

The glycolysis signaling was suppressed by downregulating miR-155-5p-responsible protein HK2 (86.8%) and LDHA (80.7%) and coincidentally downregulating LGR4 (94.2%), despite the slight upregulation of GLUT1 (110.1%) and GAPDH (107.9%).

Conversely, **the proliferation signaling** appears to be enhanced by the upregulation of cyclin D2 (119.9%), cdc25A (109.7%), and the coincidental downregulation of p14 (92.9%), despite the downregulation of PLK4 (87.1%) and the upregulation of p21 (107.7%) and p27 (124.3%).

The p53/Rb/E2F1 signaling appears to be activated by downregulating miR-155-5p-responsible protein p53 (88.1%) and upregulating E2F1 (105.8%), despite the upregulation of Rb1 (113%) and E2F4 (117.3%), as well as the downregulation of p-Rb1 (84.1%).

The SHH/PTCH/GLI signaling was enhanced by upregulation of SHH (110.3%), PTCH1 (126.1%), and GLI1 (105%). SHH is a miR-155-5p target protein, but it was unexpectedly upregulated compared to the reference data.

The growth factor signaling appears to be activated by upregulating EGF (129.6%), TGFα (108.7%), TGFβ1 (106.5%), SMAD2/3 (142.9%), SMAD7 (114.8%), FGF1 (114%), FGF2 (121.3%), CTGF (107%), and ERβ (109%), and coincidentally downregulating FGF7 (86%), despite the downregulation of miR-155-5p target protein SMAD4 (81.5%) and coincidental downregulation of GH (71.9%), GHRH (82.9%), IGF1 (85.9%), HGFα (94.7%), and Met (56.4%). SMAD4 is a miR-155-5p target protein, but it was unexpectedly upregulated compared to the reference data.

The cytodifferentiation signaling were enhanced by upregulating GAPDH (107.9%), vimentin (105.7%), TGase2 (114.6%), cystatin A (105.2%), VE-cadherin (107.3%), SOX9 (110.9%), claudin1 (138.3%), caveolin1 (109.4%), and DLX2 (107.9%), despite the downregulation of β-actin (89.2%), α-tubulin (94.9%), CaM (94.4%), CRIP1 (86.1%), Ep-CAM (90.1%), SOSTDC1 (80.1%), and tenascin C (85.4%). SOX9 and claudin1 are miR-155-5p target proteins, but they were unexpectedly upregulated compared to the reference data.

The neuromuscular differentiation signaling were activated by upregulating miR-155-5p-responsible protein S100 (108.5%) and coincidentally upregulating MYH2 (128%), αSMA (121.4%), and desmin (121.5%), despite the downregulation of miR-155-5p target protein myosin-1a (82.8%) and coincidental downregulation of NSEγ (83.8%), GFAP (62.1%), and NK1R (90.8%).

The RAS signaling appears to be activated by upregulating miR-155-5p-responsible proteins pAKT1/2/3 (108.1%) and PI3K (107.3%) and coincidentally upregulating KRAS (111.5%), Rab1 (139%), AMPKα (112.9%), PGC1α (120.8%), PLCβ2 (133.6%), JNK1 (106.3%), and PKC (107.7%), despite the downregulation of miR-155-5p target proteins ERK1 (88%), p-ERK1 (91.3%), PTEN (92.3%), STAT3 (84.6%), and c-Fos

(73.7%), as well as the coincidental downregulation of HRAS (89%), AKAP13 (86.1%), and JAK2 (92.8%). KRAS is a miR-155-5p target protein, but it was unexpectedly upregulated compared to the reference data.

The protection signaling appears to be activated by upregulating miR-155-5p-responsible proteins HO1 (119.7%) and NRF2 (109.1%) and coincidentally upregulating FOXO1 (136.8%), FOXP4 (113.8%), hepcidine (111.1%), HSP90 (108%), SOD1 (108.5%), despite the downregulation of miR-155-5p target proteins ALDH1A1 (90.9%), FOXO3 (89.6%), GSTO1/2 (83.3%), and NOS1 (88.7%) and coincidental downregulation of HSP27 (94.7%), HSP70 (94.3%), and leptin (93.9%).

The survival signaling was activated by upregulating miR-155-5p-responsible protein survivin (109.8%) and coincidentally upregulating SP1 (113.6%) and sirtuin3 (112.4%), despite the downregulation of sirtuin1 (89.9%), sirtuin6 (81.5%), and sirtuin7 (84.2%). SP1 is a miR-155-5p target protein, but it was unexpectedly upregulated compared to the reference data.

The innate immunity signaling appears to be activated by upregulating LL37 (109.5%), β-defensin1 (109.8%), β-defensin2 (136.4%), TLR2 (129.5%), and TLR4 (125.7%), despite the downregulation of lactoferrin (93.1%), CAMP (93.7%), β-defensin3 (81.6%), TLR3 (78.9%), and α1-antitrypsin (79.9%).

The cellular immunity signaling was slightly activated by downregulating miR-155-5p target protein PDL1 (92.8%) and coincidentally upregulating CD4 (134.8%), CD20 (149.7%), CD34 (111.8%), IL28 (105.6%), granzyme B (108.6%), CTLA4 (107%), and LTA4H (108.5%). CTLA4 is a miR-155-5p target protein, but it was unexpectedly upregulated compared to the reference data.

The FAS-mediated apoptosis signaling was activated by upregulating FASL (111.6%), FADD (112.1%), caspase3 (114.7%), and c-caspase3 (118.6%), despite the downregulation of TRAIL (91.2%) and BID (93.3%).

The fibrosis signaling was enhanced by upregulating miR-155-5p target protein collagen 3A1 (117%), as well as coincidental upregulation of FGF1 (114%), FGF2 (121.3%), CTGF (107%), laminin α5 (114.5%), integrin β1 (108.5%), PAI1 (114.6%), and claudin1 (138.3%) and downregulating FGF7 (86%), despite the downregulation of integrin α5 (87.7%), uPA (74.8%), α1-antitrypsin (79.9%), and tenascin C (85.4%). Claudin1 is a miR-155-5p target protein, but it was unexpectedly upregulated compared to the reference data.

The senescence signaling was activated by upregulating klotho (121.6%), sirtuin3 (112.4%), p21 (107.7%), and caveolin1 (109.4%), despite the downregulation of miR-155-5p target protein sirtuin1 (89.9%) and the coincidental downregulation of sirtuin6 (81.5%) and sirtuin7 (84.2%).

In addition, miR-155-5p*-CEDS markedly influenced **the epigenetic modification signaling** by downregulating miR-155-5p target proteins HMGB1 (91.6%) and BRG1 (89.3%), as well as the coincidental downregulation of histone H1 (86%), KDM4D (91.5%), HDAC10 (93.9%), MBD4 (83.3%), DMAP1 (79.9%), DNMT1 (83.1%), and HMGA2 (93.3%), while it upregulated EZH2 (108.6%) and lamin A/C (108.2%). Consequently, miR-155-5p*-CEDS induced a trend towards a reduction in the methylation of histones and DNAs, and attenuation of transcriptional repression.

MiR-155-5p*-CEDS significantly suppressed **the oncogenesis signaling** by downregulating miR-155-5p target proteins PDCD4 (92.2%) and Ets (84%), as well as coincidentally downregulating EWSR (94%), BMI (93.9%), AXL (93%), ATR (90.1%), DMBT1 (90.7%), CRIP1 (86.1%), and PIM1 (64.7%), while it enhanced **the oncogenesis signaling** by upregulating TWIST1 (133.6%), NF1 (119.2%), XBP1 (115.4%), CRK (114.2%), Daxx (113.6%), MALT1 (110%), KLF4 (107.7%), and BRCA2 (105.8%). Among the 28 oncoproteins, nine were found to be underexpressed, eight were overexpressed, and 11 exhibited minimal change in expression compared to the untreated controls.

Consequently, miR-155-5p*-CEDS exerted a profound influence on the entire protein signaling in RAW 264.7 cells. MiR-155-5p*-CEDS suppressed the NFkB signaling, inactivating the epigenetic modification-cMyc/MAX/MAD network-Wnt/β-catenin signaling axis, ER stress-angiogenesis-acute inflammation, and glycolysis-oncogenesis-chronic inflammation signaling axis. Conversely, it enhanced the RAS signaling, and subsequently activated proliferation signaling axis, protection-survival-senescence signaling axis, and FAS-mediated apoptosis-fibrosis signaling axis (Fig. 14B, Table 7).

The results indicate that miR-155-5p*-CEDS had an anti-oncogenic effect on RAW 264.7 cells by impeding ER stress, angiogenesis, glycolysis, oncogenesis, and acute and chronic inflammation. Conversely, it also had an oncogenic effect on the cells by increasing proliferation, protection, survival, and senescence. It is

notable that miR-155-5p*-CEDS can enhance the potential of innate and cellular immunity, as well as growth and cytodifferentiation, which are essential for immune surveillance and recovery.

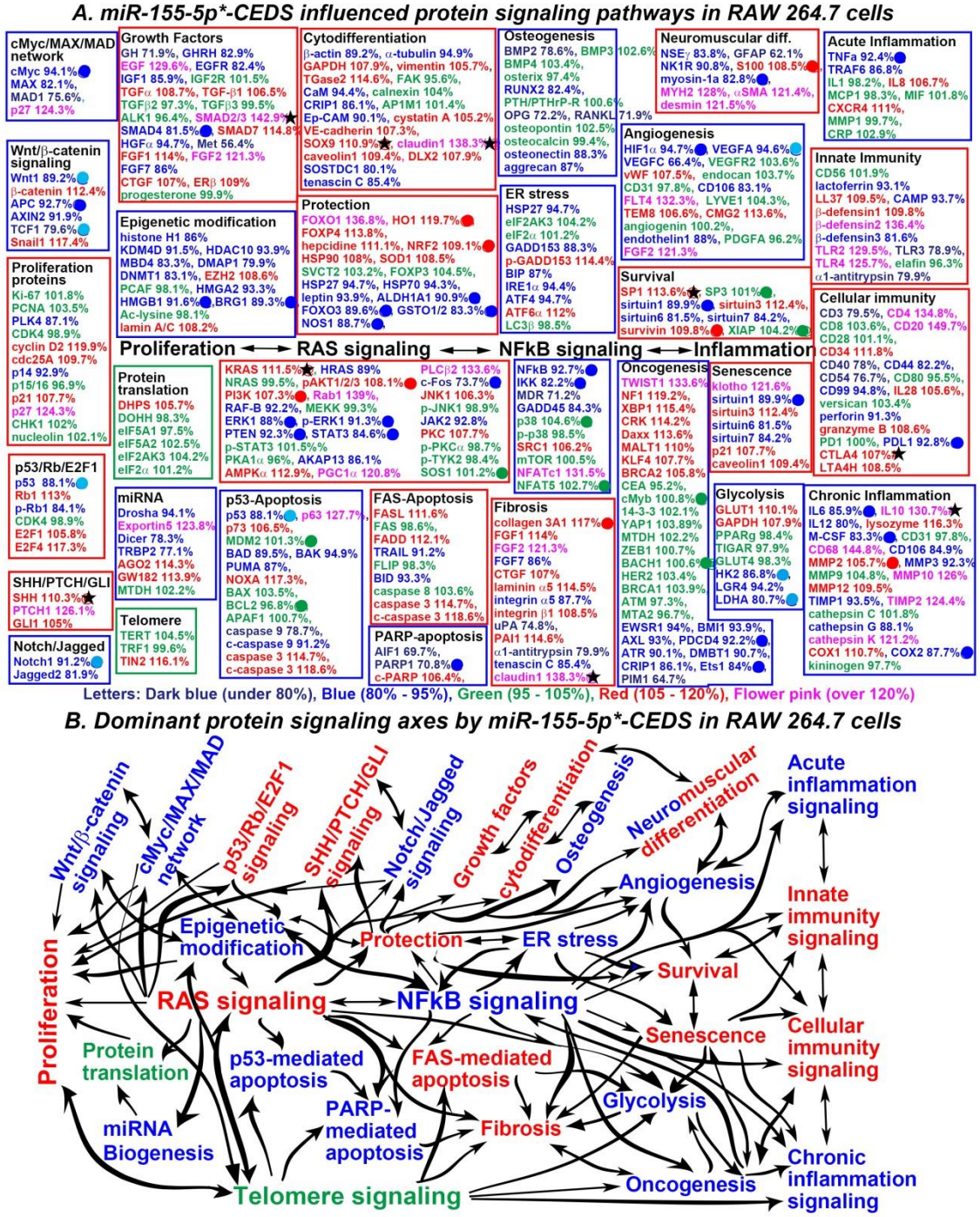

Fig. 14. MiR-155-5p*-CEDS influenced the protein signaling (A) and axes (B) in RAW 264.7 cells. The IP-HPLC revealed proteins downregulated (**blue**), upregulated (**red**), and minimally changed (**green**) compared to the untreated controls. Dominantly suppressed (**blue square**) and activated (**red square**) signaling. Downregulated proteins by direct targeting (●) and indirect response (●), upregulated proteins by indirect response (●), and minimal changed (±5%) proteins (●). Some target proteins (★) were unexpectedly upregulated contrast to the current manuscripts and data from miRDB and TargetScan websites.

Table 7. Protein expressions in the RAW 264.7 cells treated with miR-155-5p*-CEDS.

Signaling	Downregulated Proteins	Upregulated Proteins
Proliferation	PLK4, p14	cyclin D2, cdc25A, p21, p27
cMyc/MAX/MAD network	**cMyc**, MAX, MAD1	p27
Wnt/β-catenin signaling	**Wnt1, APC**, AXIN2, **TCF1**	β-catenin, Snail
p53/Rb/E2F1 signaling	**p53**, p-Rb1,	Rb1, E2F1, E2F4
SHH/PTCH/GLI signaling		**SHH★**, PTCH1, GLI1
Notch/Jagged signaling	**Notch1**, Jagged2	
Epigenetic modification	histone H1, KDM4D, HDAC10, MBD4, CMAP1, DNMT1, HMGA2, **HMGB1**, **BRG1**	EZH2, lamin A/C
Protein translation		DHPS
miRNA biogenesis	Drosha, Dicer, TRBP2	Exportin5, AGO2, GW182
Growth factors	GH, GHRH, EGFR, IGF1, **SMAD4**, HGFα, Met, FGF7	EGF, TGFα, TGFβ1, **SMAD2/3★,** SMA7, FGF1, FGF2, CTGF, ERβ
Cytodifferentiation	β-actin, α-tubulin, CaM, CRIP1, Ep-CAM, SOSTDC1, tenascin C	GAPDH, vimentin, TGase2, cystatin A, VE-cadherin, **SOX9★, claudin1★**, caveolin1, DLX2
Osteogenesis	BMP2, RUNX2, OPG, RANKL, osteonectin, aggrecan	
Neuromuscular differentiation	NSEγ, GFAP, NK1R, **myosin-1a**	**S100**, MYH2, αSMA, desmin
RAS signaling	HRAS, RAF-B, **ERK1, p-ERK1, PTEN, STAT3**, AKAP13, **c-Fos**, JAK2	**KRAS★**, **pAKT1/2/3, PI3K**, Rab1, AMPKα, PGC1α, PLCβ2, JNK1, PKC
NFkB signaling	**NFkB, IKK**, MDR, GADD45	SRC1, NFATc1
p53-mediated apoptosis	**p53**, BAD, BAK, PUMA, caspase9 c-caspase9	p63, p73, NOXA, caspase3, c-caspase3
FAS-mediated apoptosis	TRAIL, BID,	FASL, FADD, caspase3, c-caspase3
PARP-mediated apoptosis	AIF1, **PARP1**	c-PARP1
Protection	HSP27, HSP70, leptin, **ALDH1A1, FOXO3, GSTO1/2, NOS1**	FOXO1, **HO1**, FOXP4, hepcidin, **NRF2**, HSP90, SOD1
ER stress	HSP27, GADD153, BIP, IRE1α, ATF4	p-GADD153, ATF6α
Angiogenesis	**HIF1α, VEGFA**, VEGFC, CD106, endothelin1	vWF, FLT4, TEM8, CMG2, FGF2
Survival	**sirtuin1**, sirtuin6, sirtuin7,	**SP1★**, sirtuin3, **survivin,**
Acute inflammation	**TNFα**, TRAF6	IL1, CXCR4
Innate immunity	lactoferrin, CAMP, β-defensin3, TLR3, α1-antitrypsin	LL37, β-defensin1, β-defensin2, TLR2, TLR4
Cellular immunity	CD3, CD40, CD44, CD54, CD99, perforin, **PDL1**	CD4, CD20, CD34, IL28, granzyme B, **CTLA4★**, LTA4H
Chronic inflammation	**IL6,** IL12, **M-CSF**, CD106, MMP3, TIMP1, cathepsin G, **COX2**	**IL10★**, lysozyme, CD68, **MMP2**, MMP10, MMP12, TIMP2, cathepsin K, COX1
Glycolysis	**HK2**, LGR4, **LDHA**	GLUT1, GAPDH
Fibrosis	FGF7, integrin α5, uPA, α1-antitrypsin, tenascin C	**collagen 3A1,** FGF1, FGF2, CTGF, laminin α5, integrin β1, PAI1, **claudin1★**
Oncogenesis	EWSR1, BMI1, AXL, **PDCD4**, ATR, DMBT1, CRIP1, **Ets1**, PIM1	TWIST1, CRK, NF1, XBP1, Daxx, MALT1, KLF4, BRCA2
Senescence	**sirtuin1**, sirtuin6, sirtuin7	klotho, sirtuin3, p21, caveolin1
Telomere signaling		TIN2

MiR-155-5p*-CEDS induced the suppression (**blue**) or activation (**red**) of signaling through protein downregulation by direct miRNA targeting (**blue**) or indirect response (**sky blue**) and protein upregulation by indirect response (**red**). Some miRNA target proteins were upregulated (★). The data were compared to the reports of recent manuscripts and miRDB, miRmap, miRPathDB, miRTarBase, and TargetScan websites.

MiR-181a-5p*-CEDS influenced the protein signaling in RAW 264.7 cells

RAW 264.7 cells treated with mmu-miR-181a-5p sequence AACATTCAACGCTGTCGGTGAGT*-CEDS showed the characteristic protein expressions, resulting in the suppression of proliferation, p53/Rb/E2F1 signaling, Notch/Jagged signaling, epigenetic modification, protein translation, miRNA biogenesis, growth factors, cytodifferentiation, osteogenesis, RAS signaling, NFkB signaling, ER stress, survival, innate immunity, cellular immunity, chronic inflammation, p53-mediated apoptosis, FAS-mediated apoptosis, PARP-mediated apoptosis, oncogenesis, and senescence signaling, as well as the activation of cMyc/MAX/MAD network, Wnt/β-catenin signaling, SHH/PTCH/GLI signaling, Notch/Jagged signaling, protection, angiogenesis, acute inflammation, fibrosis, glycolysis, and telomere signaling compared to the untreated controls (Fig. 15A).

The proliferation signaling was suppressed by downregulating miR-181a-5p target proteins CDK4 (94%) and cyclin D2 (90.2%) and miR-181a-5p-responsible protein p21 (90.7%), as well as coincidentally downregulating PCNA (94.2%), PLK4 (91.1%), cdc25A (91.9%), CHK1 (92.7%), and nucleolin (92.2%).

The p53/Rb/E2F1 signaling was suppressed by downregulating miR-181a-5p target proteins Rb1 (92.9%) and E2F1 (93.2%) and coincidentally downregulating p-Rb (78.7%) and CDK4 (94%), despite the upregulation of miR-181a target protein p53 (111.1%). P53 is a miR-181a-5p target protein, but it was unexpectedly upregulated compared to the reference data.

The protein translation signaling was appears to be impeded by downregulating DHPS (77.6%) and eIF2AK3 (94.5%), despite the slight upregulation of eIF5A1 (105.4%).

The miRNA biogenesis signaling appears to be suppressed by downregulating miR-181a-5p target protein Dicer (82.8%) and coincidentally downregulating Drosha (90.1%), Exportin5 (93.3%), Dicer (182.8%), and TRBP2 (60.2%), despite the upregulation of miR-181a-5p-responsible protein AGO2 (118.7%), and coincidental upregulation of GW182 (116.5%) and downregulation of MTDH (93%).

The growth factor signaling were partially suppressed by downregulating miR-181a-5p target proteins TGFβ1 (94.6%), SMAD7 (92.6%), and Met (78.8%), as well as coincidentally downregulating TGFα (92.1%), SMAD2/3 (91.8%), ERβ (90.1%), and progesterone (84.6%), despite the upregulation of EFGR (134.3%), IGF1 (112.6%), IGF2R (115.7%), TGFβ2 (120.3%), HGFα (111.1%), FGF2 (117.2%), FGF7 (109.2%), and CTGF

(112.6%). EGFR is a miR-181a-5p target protein, but it was unexpectedly upregulated compared to the reference data.

The cytodifferentiation signaling were partially inactivated by downregulating α-tubulin (91.5%), FAK (82.6%), calnexin (69.4%), CRIP1 (83.8%), SOX9 (71.3%), and SOSTDC1 (68.2%), despite the upregulation of miR-181a-5p-responsible protein VE-cadherin (117.6%) and coincidental upregulation of vimentin (105.8%), CaM (116.9%), AP1M1 (120.4%), DLX2 (131.7%), and tenascin C (129.4%). AP1M1 is a miR-181a-5p target protein, but it was unexpectedly upregulated compared to the reference data.

The osteogenesis signaling was suppressed by downregulating BMP2 (88.9%), BMP3 (91.5%), BMP4 (85.1%), OPG (86.6%), and osteonectin (84.4%), despite the upregulation of RUNX2 (112.6%), PTH/PTHrPR (124.5%), RANKL (109.3%), and osteopontin (109%).

The RAS signaling was markedly suppressed by downregulating miR-181a-5p target proteins KRAS (91.9%), NRAS (90.4%), NRAS (70.7%), p-ERK1 (94%), p-STAT3 (73%), PGC1α (84%), AMPKα (87.5%), JAK2 (81.1%), and PKC (89.2%), as well as coincidentally downregulating PI3K (89.7%), Rab1 (92.2%), PKA1α (92.4%), and PLCβ2 (74.6%), despite the upregulation of pAKT1/2/3 (106%), PTEN (118%), c-FOS (106%), and SOS1 (117.6%). PTEN and c-Fos are miR-181a-5p target proteins, but they were unexpectedly upregulated compared to the reference data.

The NFkB signaling was suppressed by downregulating miR-181a-5p target proteins p-p38 (79.8%), SRC1 (80.8%), and mTOR (77.9%), as well as coincidentally downregulating IKK (94.8%) and MDR (87.2%), despite the slight upregulation of miR-181a-responsible protein NFkB (108.4%).

The ER stress signaling was suppressed by downregulating eIF2AK3 (94.5%), GADD153 (92.2%), IRE1α (94.9%), and LC3β (92.8%), despite the upregulation of p-GADD153 (107.8%) and BIP (129.7%).

The survival signaling was suppressed by downregulating SP1 (92.8%) and XIAP (92.6%), and coincidentally downregulating SP3 (91.2%), despite the upregulation of sirtuin6 (111.1%) and sirtuin7 (116.1%).

The innate immunity signaling appears to be suppressed by downregulating miR-181a-5p target proteins TLR4 (93.4%) and miR-181a-5p-responsible protein CD56 (71.9%), as well as coincidentally downregulating

lactoferrin (79%), LL37 (93%), and β-defensin3 (89%), despite the upregulation of CAMP (106.2%), β-defensin1 (118.5%), β-defensin2 (132.1%), TLR2 (119.7%), elafin (119.7%), and α1-antitrypsin (109.9%).

The cellular immunity signaling was suppressed by downregulating miR-181a-5p-responsible proteins PD1 (87.9%), as well as coincidentally downregulating CD4 (80.2%), CD34 (64.1%), CD40 (79.4%), CD80 (89.1%), CD99 (94.6%), and granzyme B (83.7%), despite the upregulation of CD20 (117%), CD28 (109.2%), and CTLA4 (114.5%).

The chronic inflammation signaling was suppressed by downregulating miR-181a-5p target proteins MMP2 (93.6%) and miR-181a-5p-responsible protein MMP9 (94.9%), as well as coincidentally downregulating IL12 (91%), lysozyme (89%), CD68 (90.8%), CD106 (88.2%), MMP10 (91.7%), MMP12 (86.2%), TIMP1 (88.5%), TIMP2 (77.4%), cathepsin K (94.1%), and kininogen (79.3%), despite the upregulation of MMP3 (108.1%), cathepsin C (106,3%), cathepsin G (105.4%), COX1 (106.4%), and COX2 (115.9%). COX2 is a miR-181a-5p target protein, but it was unexpectedly upregulated compared to the reference data.

The p53-mediated apoptosis signaling appears to be attenuated by downregulating miR-181a-5p target proteins c-caspase3 (91.2%) and coincidentally downregulating caspase9 (84.5%), despite the upregulation of p53 (111.1%), p73 (112%), BAD (116.4%), and NOXA (128.7%). P53 is a miR-181a-5p target protein, but it was unexpectedly upregulated compared to the reference data.

The FAS-mediated apoptosis signaling was inhibited by downregulating miR-181a-5p target proteins c-caspase3 (91.2%) and coincidentally downregulating FASL (89.1%) and FADD (84%), and upregulating FLIP (112%), despite the upregulation of FAS (109.2%) and BID (113%). FAS is a miR-181a-5p target protein, but it was unexpectedly upregulated compared to the reference data.

The PARP-mediated apoptosis signaling was suppressed by downregulating miR-181a-5p target protein PARP1 (93.3%) and coincidentally downregulating AIF1 (83%).

The senescence signaling appears to be suppressed by downregulating miR-181a-5p-responsible protein p21 (90.7%), as well as coincidentally downregulating klotho (93.9%).

Conversely, **the cMyc/MAX/MAD network** was activated by upregulating miR-181a-5p-responsible protein cMyc (109.3%) and coincidentally upregulating MAX (116.6%) and MAD1 (108.9%). MAX is a miR-181a-5p target protein, but it was unexpectedly upregulated compared to the reference data.

The Wnt/β-catenin signaling appears to be activated by upregulating miR-181a-5p-responsible protein Snail1 (112.4%) and coincidental upregulation of TCF1 (108.6%) and APC (106.4%), despite the downregulation of miR-181a target protein Wnt1 (88.3%).

The SHH/PTCH/GLI signaling appears to be alternatively activated by upregulating GLI1 (107%), despite the downregulation of SHH (87.4%).

The Notch/Jagged signaling appear to be activated by upregulating Notch1 (115.7%), despite the downregulation of Jagged2 (81.6%). Notch1 is a miR-181a-5p target protein, but it was unexpectedly upregulated compared to the reference data.

The neuromuscular differentiation signaling were activated by upregulating GFAP (117.4%), S100 (119.1%), and MYH2 (109.9%), despite the downregulation of NSEγ (72.3%), αSMA (71%), and desmin (80.9%).

The protection signaling appears to be activated by upregulating miR-181a-5p-responsible proteins ALDH1A1 (123.6%) and coincidentally upregulating SVCT2 (134.3%), HO1 (124.9%), HSP70 (116.7%), FOXO1 (114.1%), HSP90 (113.3%), GSTO1/2 (109.3%), and hepcidin (108.2%), despite the downregulation of miR-181a-5p target protein NOS1 (79.1%) and miR-181a-5p-responsible protein SOD1 (88%) and NRF2 (83.9%), and the coincidental downregulation of FOXO3 (92.3%). FOXO1 is a miR-181a-5p target protein, but it was unexpectedly upregulated compared to the reference data.

The angiogenesis signaling was activated by upregulating FLT4 (123.2%), TEM8 (109.5%), angiogenin (126.8%), endothelin1 (107.7%), PDGFA (108.9%), and FGF2 (117.2%), despite the downregulation of miR-181a-5p target proteins HIF1α (80.8%) and CD106 (87.1%), as well as coincidental downregulation of LYVE1 (92.5%) and CMG2 (92.3%).

The acute inflammation signaling was activated by upregulating miR-181a-5p-responsible protein TNFα (115%) and coincidentally upregulating IL8 (106.8%), MCP1 (112.2%), MIF (109.7%), and MMP1 (106.1%), despite the downregulation of miR-181a-5p target protein CXCR4 (92.9%) and the coincidental downregulation of CRP (81.4%).

The fibrosis signaling was activated by upregulating FGF2 (177.2%), CTGF (112.6%), integrin α5 (106.6%), integrin β1 (112.5%), uPA (104.9%), α1-antitrypsin (109.9%), and tenascin C (129.4%), despite the downregulation of collagen 3A1 (85.3%), laminin α5 (91.2%), and claudin1 (94.1%) and the upregulation of FGF7 (109.2%).

The glycolysis signaling was activated by upregulating miR-181a-5p-responsible protein LDHA (117.6%), as well as coincidentally upregulating GLUT1 (131.6%), PPARγ (114.4%), and HK2 (105.2%), despite the downregulation of GLUT4 (91.7%). PPARγ and HK2 are miR-181a-5p target proteins, but they are unexpectedly upregulated compared to the reference data.

The telomere signaling was activated by upregulating TERT (111.8%) and TIN2 (105.4%).

In addition, miR-181a-5p*-CEDS markedly influenced **the epigenetic modification signaling** by downregulating miR-181a-5p target proteins EZH2 (81.3%), PCAF (86.6%), HMGA2 (76.9%), and BRG1 (80.9%), as well as the coincidental downregulation of KDM4D (81.4%) and MBD4 (90.8%), while it upregulated miR-181a-5p-responsible protein HMGB1 (105.9%) and coincidental upregulation of histone H1 (106.1%), HDAC10 (124.2%), DMAP1 (107.6%), and lamin A/C 108.7%). Consequently, miR-181a-5p*-CEDS induced a trend towards a reduction in the methylation of histones and DNAs, and attenuation of transcriptional repression.

MiR-181a-5p*-CEDS significantly suppressed **the oncogenesis signaling** by downregulating miR-181a-5p target proteins ATM (94.1%), cMyb (93.7%), PIM1 (92.7%), BACH1 (89.9%), and Daxx (72.7%) and miR-181a-5p-responsible protein BRCA2 (89.2%), while it also activated **the oncogenesis signaling** by upregulating BRCA1 (113.3%), NF1 (113.7%), TWIST1 (113.6%), BMI1 (112.8%), XBP1 (110.1%), EWSR1 (109.6%), Ets1 (106.9%), and AXL (106.6%). BRCA1 and NF1 are miR-181a-5p target proteins, but they were unexpectedly upregulated compared to the reference data. Among the 28 oncoproteins, 11 were found to be

underexpressed, eight were overexpressed, and nine exhibited minimal change in expression compared to the untreated controls.

Consequently, miR-181a-5p*-CEDS exerted a profound influence on the entire protein signaling in RAW 264.7 cells. MiR-181a-5p*-CEDS suppressed the NFkB signaling, inactivating the epigenetic modification-cMyc/MAX/MAD network-Wnt/β-catenin signaling axis, ER stress-angiogenesis-acute inflammation, and glycolysis-oncogenesis-chronic inflammation signaling axis. Conversely, it enhanced the RAS signaling, and subsequently activated proliferation signaling axis, protection-survival-senescence signaling axis, and FAS-mediated apoptosis-fibrosis signaling axis (Fig. 15B, Table 8).

The results indicate that miR-181a-5p*-CEDS had an anti-oncogenic effect on RAW 264.7 cells by impeding ER stress, angiogenesis, glycolysis, oncogenesis, and acute and chronic inflammation. Conversely, it also had an oncogenic effect on the cells by increasing proliferation, protection, survival, and senescence. It is notable that miR-181a-5p*-CEDS can enhance the potential of innate and cellular immunity, as well as growth and cytodifferentiation, which are essential for immune surveillance and recovery.

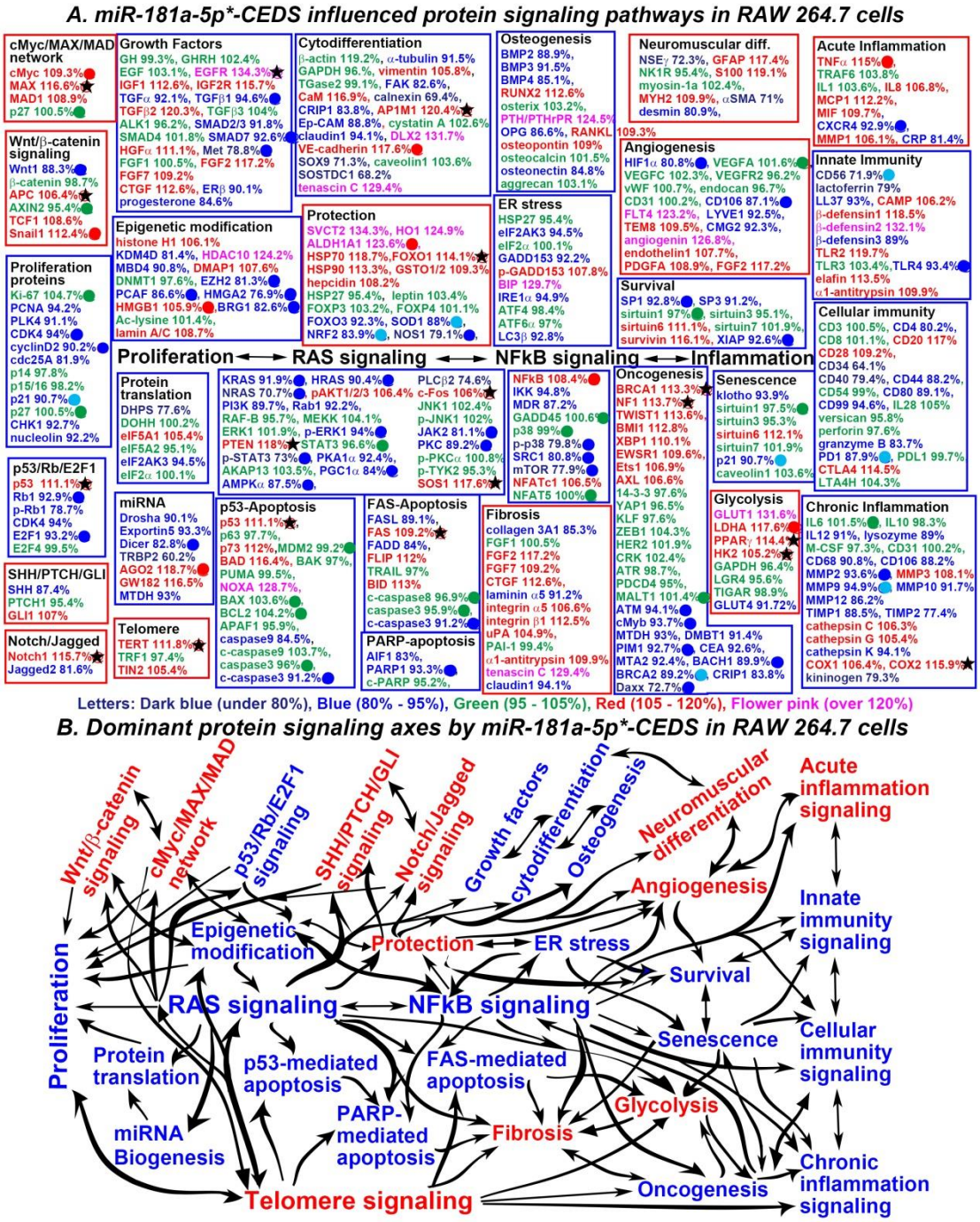

Fig. 15. MiR-181a-5p*-CEDS influenced the protein signaling (A) and axes (B) in RAW 264.7 cells. The IP-HPLC revealed proteins downregulated (**blue**), upregulated (**red**), and minimally changed (**green**) compared to the untreated controls. Dominantly suppressed (**blue square**) and activated (**red square**) signaling. Downregulated proteins by direct targeting (●) and indirect response (●), upregulated proteins by indirect response (●), and minimal changed (±5%) proteins (●). Some target proteins (★) were unexpectedly upregulated contrast to the current manuscripts and data from miRDB and TargetScan websites.

Table 8. Protein expressions in the RAW 264.7 cells treated with miR-181a-5p*-CEDS.

Signaling	Downregulated Proteins	Upregulated Proteins
Proliferation	PCNA, PLK4, CDK4, **cyclin D2**, cdc25A, **p21**, CHK1, nucleolin	
cMyc/MAX/MAD network		**cMyc**, **MAX★**, MAD1
Wnt/β-catenin signaling	Wnt1	**APC★**, **Snail**
p53/Rb/E2F1 signaling	**Rb1**, p-Rb1, CDK4, **E2F1**	**p53★**
SHH/PTCH/GLI signaling	SHH	GLI1
Notch/Jagged signaling	Jagged2	**Notch1★**
Epigenetic modification	KDM4D, MBD4, **EZH2, PCAF, HMGA2, BRG1**	histone H1, HDAC10, DMAP1, **HMGB1**, lamin A/C
Protein translation	DHPS, eIF2AK3	eIF5A1
miRNA biogenesis	Drosha, Exportin5, **Dicer**, TRBP2, MTDH	**AGO2**, GW182
Growth factors	TGFα, **TGFβ1**, SMAD2/3, **SMAD7**, **Met**, ERβ, progesterone	**EGFR★**, IGF1, IGF2R, TGFβ2, HGFα, FGF2, FGF7, CTGF
Cytodifferentiation	α-tubulin, FAK, calnexin, CRIP1, , Ep-CAM, claudin1, SOX9, SOSTDC1	vimentin, CaM, **AP1M1★**, DLX2, **VE-cadherin**, tenascin C
Osteogenesis	BMP2, BMP3, BMP4, OPG, osteonectin	RUNX2, PTH/PTHrPR, RANKL, osteopontin
Neuromuscular differentiation	NSEγ, αSMA, desmin,	GFAP, S100, MYH2
RAS signaling	**KRAS, HRAS**, **NRAS**, PI3K, Rab1, RAF-B, **p-ERK1, p-STAT3**, PKA1α, **PGC1α, AMPKα**, PLCβ2, **JAK2**, **PKC**, p-TYK2	pAKT1/2/3, **PTEN★**, **c-Fos★**, **SOS1★**
NFkB signaling	IKK, MDR, **p-p38, SRC1, mTOR**	**NFkB**, NFATc1
p53-mediated apoptosis	caspase9, c-caspase9	**p53★**, p73, BAD, NOXA
FAS-mediated apoptosis	FASL, FADD, **c-caspase3**	**FAS★**, FLIP, BID
PARP-mediated apoptosis	AIF1, **PARP1**	
Protection	FOXO3, **SOD1, NRF2**, **NOS1**	SVCT2, HO1, **ALDH1A1**, HSP70, **FOXO1★**, HSP90, GSTO1/2, hepcidin
ER stress	eIF2AK3, GADD153, IRE1α, LC3β	p-GADD153, BIP
Angiogenesis	**HIF1α, CD106**, LYVE1, CMG2	FLT4, TEM8, angiogenin, endothelin1, PDGFA, FGF2
Survival	**SP1**, SP3, **XIAP**	sirtuin6, survivin,
Acute inflammation	**CXCR4**, CRP	**TNFα**, IL8, MCP1, MIF, MMP1
Innate immunity	**CD56**, lactoferrin, LL37, β-defensin3, **TLR4**	CAMP, β-defensin1, β-defensin2, TLR2, elafin, α1-antitrypsin
Cellular immunity	CD4, CD34, CD40, CD44, CD80, CD99, granzyme B, **PD1**	CD20, CD28, CTLA4
Chronic inflammation	IL12, lysozyme, CD68, CD106, **MMP2, MMP9**, MMP10, MMP12, TIMP1, TIMP2, cathepsin K, kininogen	MMP3, cathepsin C, cathepsin G, COX1, **COX2★**
Glycolysis	GLUT4	GLUt1, **LDHA**, **PPARγ★, HK2★**
Fibrosis	collagen 3A1, laminin α5, claudin1	FGF2, FGF7, CTGF, integrin α5, integrin β1, uPA, α1-antitrypsin, tenascin C
Oncogenesis	**ATM, cMyb**, MTDH, DMBT1, **PIM1**, CEA, MTA2, **BACH1**, **BRCA2**, CRIP1, **Daxx**	**BRCA1★, NF1★**, TWIST1, BMI1, XBP1, EWSR1, Ets1, AXL, ATM
Senescence	klotho, **p21**,	sirtuin6
Telomere signaling		**TERT★**, TIN2

MiR-181a-5p*-CEDS induced the suppression (**blue**) or activation (**red**) of signaling through protein downregulation by direct miRNA targeting (**blue**) or indirect response (**sky blue**) and protein upregulation by indirect response (**red**). Some miRNA target proteins were upregulated (★). The data were compared to the reports of recent manuscripts and miRDB, miRmap, miRPathDB, miRTarBase, and TargetScan websites.

MiR-216a-5p*-CEDS influenced the protein signaling in RAW 264.7 cells

RAW 264.7 cells treated with mmu-miR-216a-5p sequence TAATCTCAGCTGGCAACTGTGA*-CEDS showed the characteristic protein expressions, resulting in the suppression of proliferation, Wnt/β-catenin signaling, p53/Rb/E2F1 signaling, SHH/PTCH/GLI signaling, Notch/Jagged signaling, epigenetic modification, growth factors, cytodifferentiation, neuromuscular differentiation, RAS signaling, NFkB signaling, angiogenesis, acute inflammation, innate immunity, cellular immunity, chronic inflammation, FAS-mediated apoptosis, PARP-mediated apoptosis, fibrosis, oncogenesis, and senescence, as well as the activation of cMyc/MAX/MAD network, miRNA biogenesis, osteogenesis, protection, ER stress, survival, p53-mediated apoptosis, glycolysis, and telomere signaling compared to the untreated controls (Fig. 16A).

The proliferation signaling was markedly suppressed by downregulating miR-216a-5p target proteins CDK4 (83.7%), cdc25A (78.8%), and CHK1 (94.5%), as well as coincidentally downregulating PCNA (90%), and PLK4 (83.3%), despite the upregulation of cyclin D2 (107.6%) and nucleolin (110.6%) and the downregulation of p15/16 (92.6%) and p21 (87.5%).

The Wnt/β-catenin signaling was markedly suppressed by downregulating miR-216a-5p target proteins Wnt1 (88.9%), β-catenin (88.4%), APC (93.6%), and Snail1 (86.9%).

The p53/Rb/E2F1 signaling was suppressed by downregulating miR-216a-5p target proteins p-Rb (84.8%) and CDK4 (83.7%), as well as the downregulation of E2F1 (94.5%) and upregulation of E2F4 (112.4%), despite the upregulation of p53 (112.8%).

The SHH/PTCH/GLI signaling appears to be inactivated by downregulating SHH (81.9%), despite the upregulation of PTCH1 (116.7%).

The Notch/Jagged signaling was inactivated by downregulating Jagged2 (80.2%).

The growth factor signaling were suppressed by downregulating miR-216a-5p target proteins SMAD2/3 (82.8%), SMAD7 (90.3%), and Met (87.1%) and miR-216a-5p-responsible protein ERβ (86.3%), as well as coincidentally downregulating GHRH (93.99%), CTGF (90%), and progesterone (90.4%), despite the upregulation of GH (112.9%), IGF1 (123.5%), TGFα (111.5%), TGFβ2 (131%), and FGF2 (120.1%). TGFα

(111.5%), TGFβ2 (131%), and FGF2 are miR-216a-5p target proteins, but they were unexpectedly upregulated compared to the reference data.

The cytodifferentiation signaling were suppressed by downregulating miR-216a-5p target proteins claudin1 (83.2%) and SOX9 (72%) and coincidentally downregulating α-tubulin (94%), TGase2 (91.4%), FAK (84.7%), calnexin (68.2%), CRIP1 (88%), AP1M1 (90.5%), cystatin A (85.7%), claudin1 (83.2%), caveolin1 (91.4%), SOX9 (72%), SOSTDC1 (70.2%), and tenascin C (90.1%), despite the upregulation of β-actin (110.8%), GAPDH (109.6%), vimentin (120.7%), VE-cadherin (135.6%), and DLX2 (113.6%). DLX2 is a miR-216a-5p target protein, but it was unexpectedly upregulated compared to the reference data.

The neuromuscular signaling was suppressed by downregulating miR-216a-5p target proteins S100 (94.6%) and αSMA (85.7%) and coincidentally downregulating desmin (65.5%), despite the upregulation of GFAP (114.8%) and myosin-1a (110.9%).

The RAS signaling was suppressed by downregulating miR-216a-5p target proteins pAKT1/2/3 (91.3%), PI3K (94.3%), MEKK (94.4%), ERK1 (94.3%), p-ERK1 (83.1%), JAK2 (86.9%), and p-PKCα (90.4%) and miR-216a-5p-responsible protein p-STAT3 (73%), as well as coincidentally downregulating HRAS (85.3%), NRAS (70.3%), PKA1α (90.4%), PGC1α (85.2%), AMPKα (94.9%), PLCβ2 (90.9%), and JNK1 (94.6%), despite the upregulation of Rab1 (107.5%), RAF-B (105.7%), PTEN (107.2%), AKAP13 (108.8%), p-JNK1 (107.2%), p-TYK2 (112.1%), and SOS1 (119.6%). PTEN is a miR-216a-5p target protein, but it was unexpectedly upregulated compared to the reference data.

The NFkB signaling was suppressed by downregulating miR-216a-5p target proteins NFkB (91.6%), p-p38 (72%), and NFAT5 (91.9%) and miR-216a-5p-responsible protein mTOR (93.4%), as well as coincidentally downregulating MDR (82.4%), SRC1 (79%), and NFATc1 (91%), despite the upregulation of IKK (107.5%) and GADD45 (105.4%).

The angiogenesis signaling was suppressed by downregulating miR-216a-5p target proteins HIF1α (89.4%), VEGFR2 (87.3%), CD106 (89.2%), FLT4 (92.3%), and LYVE1 (95.9%), as well as coincidentally downregulating VEGFA (93.9%), endocan (92.8%), CD31 (92.6%), endothelin1 (88.7%), and PDGFA (90%), despite the upregulation of VEGFC (112.2%), TEM8 (137.4%), angiogenin (106.8%), and FGF2 (120.1%).

The acute inflammation signaling was suppressed by downregulating miR-216a-5p target proteins TRAF6 (94.6%), IL8 (83.7%), and miR-216a-5p-responsible protein IL1 (82.9%), despite the upregulation of TNFα (112.5%) and MIF (117.7%).

The innate immunity signaling was suppressed by downregulating miR-216a-5p target protein TLR3 (94.6%), as well as coincidentally downregulating CD56 (87.6%), lactoferrin (80.6%), β-defensin1 (88.3%), β-defensin2 (90.5%), and elafin (90.6%), despite the upregulation of β-defensin3 (110.5%) and α1-antitrypsin (126.7%).

The cellular immunity signaling was suppressed by downregulating miR-216a-5p-responsible proteins CD40 (84.4%), CD54 (91.2%), and IL2 (84.6%), as well as coincidentally downregulating CD4 (94.3%), CD34 (64.4%), CD80 (89.3%), perforin (85.3%), and granzyme B (85.3%), despite the downregulation of PD1 (83.1%) and PDL1 (89%), and coincidental upregulation of CD20 (118.4%) and CTLA4 (106.8%).

The chronic inflammation signaling appears to be inactivated by downregulating lysozyme (87.1%), CD31 (92.9%), CD106 (89.2%), MMP10 (89.3%), MMP12 (95%), TIMP1 (94%), TIMP2 (80.4%), and COX1 (89%), despite the upregulation of IL10 (106.3%), CD68 (108.1%), MMP2 (107.5%), MMP9 (138.8%), cathepsin C (137.5%), cathepsin K (114.7%), and kininogen (108.4%).

The FAS-mediated apoptosis signaling appears to be inhibited by downregulating miR-216a-5p target protein BID (94.9%) and coincidentally downregulating FADD (81.6%) and upregulating FLIP (122%), despite the upregulation of caspase3 (114.8%). Caspase3 is a miR-216a-5p target protein, but it was unexpectedly upregulated compared to the reference data.

The PARP-mediated apoptosis signaling was suppressed by downregulating miR-216a-5p target protein PARP1 (88.6%) and coincidentally downregulating AIF1 (84.8%).

The fibrosis signaling was inactivated by downregulating miR-216a-5p target protein claudin (83.2%), as well as coincidentally downregulating collagen 3A1 (87.9%), CTGF (90%), laminin α5 (86.7%), and tenascin C (90.1%), despite the upregulation of FGF2 (120.1%), integrin α5 (86.7%), uPA (119.8%), PAI1 (116%), and α1-antitrypsin (126.7%).

The senescence signaling was inactivated by downregulating miR-216a-5p target protein sirtuin3 (93.2%), as well as coincidentally downregulating p21 (87.5%), and caveolin1 (91.4%), despite the slight upregulation of sirtuin6 (108.5%) and sirtuin7 (107.2%).

Conversely, **the cMyc/MAX/MAD network** was activated by upregulating cMyc(106.8%), MAX (115.6%), and MAD1 (110.7%).

The miRNA biogenesis signaling was activated by downregulating miR-216a-5p target proteins MTDH (87.2%) and coincidental upregulating Drosha (114.6%), Exportin5 (117.7%), and AGO2 (132.9%), despite the downregulation of Dicer (81.4%) and TRBP2 (61.4%).

The osteogenesis signaling was activated by upregulating BMP4 (106.8%), RUNX2 (110.7%), PTH/PTHrP-R (127.3%), osterix (137.2%), osteopontin (114%), osteocalcin (116.4%), and osteonectin (107.8%), despite the downregulation of miR-216a-5p target protein BMP2 (75.1%), and coincidental downregulation of OPG (81.3%) and aggrecan (94.1%).

The protection signaling was activated by upregulating SOD1 (135.6%), HO1 (130.6%), SVCT2 (118.6%), HSP27 (111.1%), FOXP3 (110.4%), and FOXO3 (109.1%), despite the downregulation of miR-216a-5p target protein FOXO1 (94.3%), and ALDH1A1 (91.9%) and coincidental downregulation of HSP70 (93%), NOS1 (91.6%), and NRF2 (84.6%).

The ER stress signaling appears to be activated by upregulating HSP27 (111.1%), p-GADD163 (107.3%), and ATF6α (119.7%), despite the downregulation of miR-216a-5p-responsible proteins LC3β (89.4%) and coincidental downregulation of GADD153 (88.1%). ATF6α is a miR-216a-5p target protein, but it was unexpectedly upregulated compared to the reference data.

The survival signaling was activated by upregulating SP1 (112.7%), sirtuin6 (108.5%), sirtuin7 (107.2%), survivin (110.1%) and XIAP (106.9%), despite the downregulation of miR-216a-5p target proteins SP3 (84.4%) and sirtuin3 (93.2%). SP1 and XIAP are miR-216a-5p target proteins, but they were unexpectedly upregulated compared to the reference data.

The p53-mediated apoptosis signaling appears to be activated by upregulating p53 (112.8%), MDM2 (128.4%), BAD (120%), BAK (106.1%), NOXA (115.4%), caspase9 (108.3%), and caspase3 (114.8%), despite the downregulation of miR-216a-5p target proteins p63 (92.8%). Caspase3 is a miR-216a-5p target protein, but it was unexpectedly upregulated compared to the reference data.

The glycolysis signaling was activated by upregulating LDHA (132.4%), GLUT4 (121.5%), GAPDH (109.6%), and LGR4 (106.4%), despite the slight downregulation of miR-216a-5p target protein HK2 (93.2%) and TIGAR (94.7%).

The telomere signaling was activated by upregulating TERT (110.8%) and TIN2 (111.8%).

In addition, miR-216a-5p*-CEDS markedly influenced **the epigenetic modification signaling** by downregulating miR-216a-5p target proteins MBD4 (94.2%), HMGA2 (74.9%), HMGB1 (90.5%), and BRG1 (86.2%), as well as the coincidental downregulation of PCAF (91.4%), while it upregulated histone H1 (105.9%), DNMT1 (107.4%), and EZH2 (77.9%). Consequently, miR-216a-5p*-CEDS induced a trend towards a reduction in the methylation of histones and DNAs, and attenuation of transcriptional repression.

MiR-216a-5p*-CEDS suppressed **the oncogenesis signaling** by downregulating miR-216a-5p target proteins BACH1 (90.5%), MTDH 87.2%), and ATM (79.4%) and miR-216a-5p-responsible protein 14-3-3 (94.7%), as well as coincidentally downregulating PIM1 (90.3%), cMyb (88.8%), CRIP1 (88%), MTA2 (80%), CEA (77.5%), and Daxx (69.8%), while it partly enhanced **the oncogenesis signaling** by upregulating TWIST1 (141.3%), EWSR1 (134.7%), Ets1 (125.1%), ZEB1 (111,7%), HER2 (119.5%), CRK (112%), ATR (110.5%), BMI1 (110.5%), and AXL (105.1%). Ets1 and ZEB1 are miR-216a-5p target proteins, but they were unexpectedly upregulated compared to the reference data. Among the 28 oncoproteins, 10 were found to be underexpressed, nine were overexpressed, and nine exhibited minimal change in expression compared to the untreated controls.

Consequently, miR-216a-5p*-CEDS significantly impacted the entire protein signaling in RAW 264.7 cells. MiR-216a-5p*-CEDS suppressed the RAS-NFkB signaling axis, and subsequently inactivated the proliferation-related signaling axis, angiogenesis-inflammation axis, and senescence-oncogenesis axis.

Conversely, it activated protection-ER stress-survival signaling axis, protection-cMyc-telomere, and p53-mediated apoptosis signaling axis (Fig. 16B, Table 9).

The results indicate that miR-216a-5p*-CEDS had a dual effect on RAW 264.7 cells. It had an anti-oncogenic effect, impeding proliferation, angiogenesis, senescence, inflammation, and oncogenesis. On the other hand, it also exerted an oncogenic effect, enhancing ROS protection, telomere instability, and p53-mediated apoptosis. Therefore, it is postulated that miR-216a-5p*-CEDS may play an oncogenic role through the increase of ROS protection signaling, depending on the context of the cells. However, it is notable that miR-216a-5p*-CEDS could attenuate the capacity of innate and cellular immunity, as well as chronic inflammation.

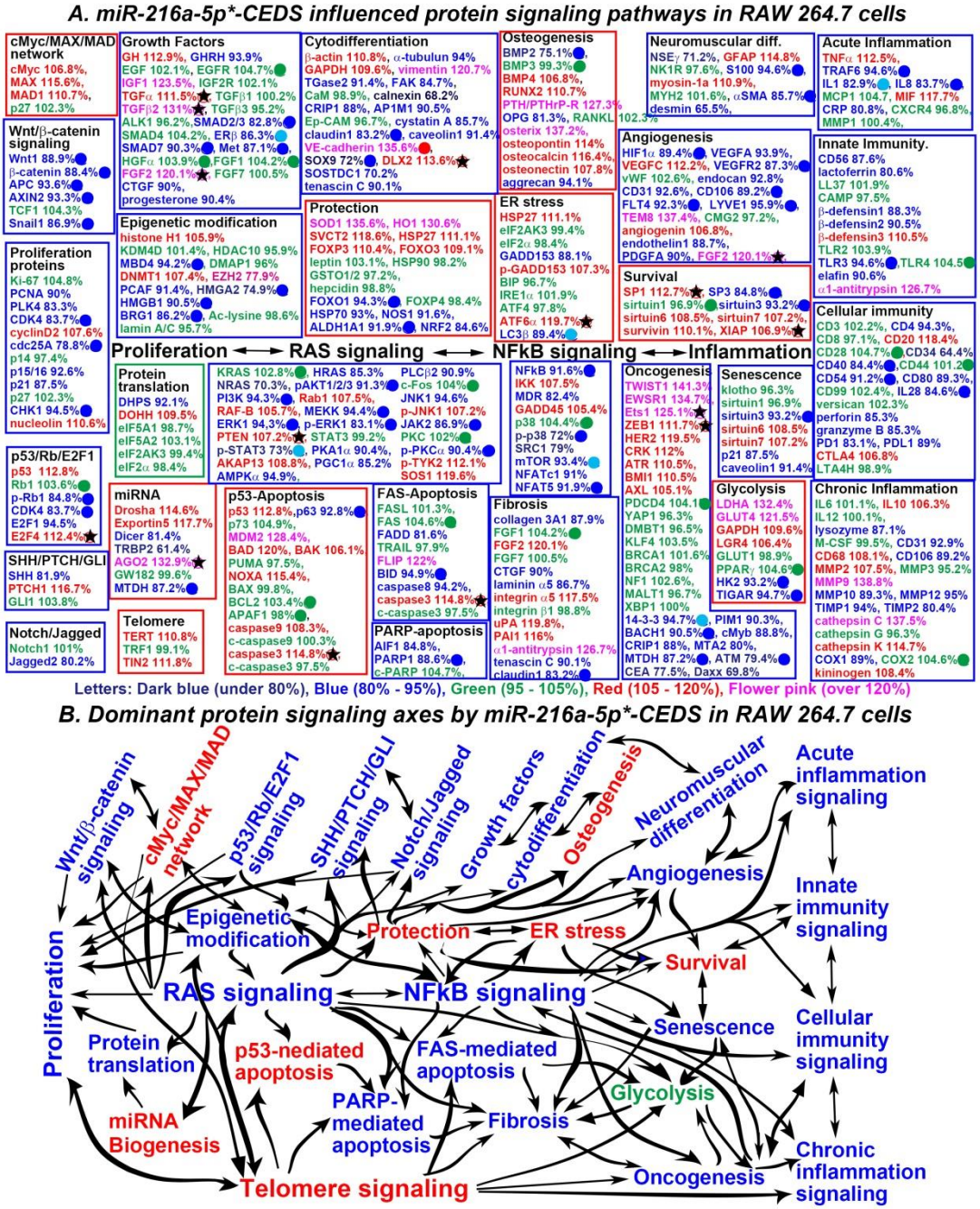

Fig. 16. MiR-216a-5p*-CEDS influenced the protein signaling (A) and axes (B) in RAW 264.7 cells. The IP-HPLC revealed proteins downregulated (**blue**), upregulated (**red**), and minimally changed (**green**) compared to the untreated controls. Dominantly suppressed (**blue square**) and activated (**red square**) signaling. Downregulated proteins by direct targeting (●) and indirect response (●), upregulated proteins by indirect response (●), and minimal changed (±5%) proteins (●). Some target proteins (★) were unexpectedly upregulated contrast to the current manuscripts and data from miRDB and TargetScan websites.

Table 9. Protein expressions in the RAW 264.7 cells treated with miR-216a-5p*-CEDS.

Signaling	Downregulated Proteins	Upregulated Proteins
Proliferation	PCNA, PLK4, **CDK4, cdc25A**, p15/16, p21, **CHK1**	Cyclin D2, nucleolin
cMyc/MAX/MAD network		cMyc, MAX, MAD1
Wnt/β-catenin signaling	**Wnt1, β-catenin, APC, AXIN2, Snail**	
p53/Rb/E2F1 signaling	**p-Rb1, CDK4**, E2F1	p53, E2F4
SHH/PTCH/GLI signaling	SHH	PTCH1
Notch/Jagged signaling	Jagged2	
Epigenetic modification	**MBD4**, PCAF, **HMGA2, HMGB1, BRG1**, Ac-lysine	histone H1, DNMT1, EZH2
Protein translation	DHPS	DOHH
miRNA biogenesis	Dicer, TRBP2, **MTDH**	Drosha, Exportin5, **AGO2★**
Growth factors	GHRH, **SMAD2/3, SMAD7, Met,** CTGF, **ERβ**, progesterone	GH, EGFR, IGF1**, TGFα★, TGFβ2★**, HGFα, FGF1, FGF2
Cytodifferentiation	α-tubulin, TGase2, FAK, calnexin, CRIP1, AP1M1, cystatin A, **claudin1**, caveolin1, **SOX9**, SOSTDC1, tenascin C	β-actin, GAPDH, vimentin, **VE-cadherin**, **DLX2★**
Osteogenesis	**BMP2**, OPG, aggrecan	BMP4, RUNX2, osterix, PTH/PTHrPR, osteopontin, osteocalcin, osteonectin
Neuromuscular differentiation	NSEγ**, S100, αSMA**, desmin	GFAP, myosin-1a
RAS signaling	HRAS, NRAS, **pAKT1/2/3, PI3K, MEKK, ERK1, p-ERK1**, **p-STAT3**, PKA1α, PGC1α, AMPKα, PLCβ2, JNK1, **JAK2, p-PKC1α**	Rab1, RAF-B, **PTEN★**, AKAP13, c-Fos, p-JNK1, p-TYK2, SOS1
NFkB signaling	**NFkB**, MDR, **p-p38,** SRC1, **mTOR,** NFATc1, **NFAT5**	IKK, GADD45
p53-mediated apoptosis	**p63**	p53, MDM2, BAD, BAK, NOXA, BCL2, caspase9**, caspase3★**
FAS-mediated apoptosis	FADD, **BID**, caspase8	FLIP, **caspase3★**
PARP-mediated apoptosis	AIF1, **PARP1**	
Protection	**FOXO1,** HSP70, NOS1, **ALDH1A1**, NRF2	SOD1, HO1, SVCT2, HSP27, FOXP3, FOXO3
ER stress	GADD153, **LC3β**	HSP27, p-GADD153, **ATF6α★**
Angiogenesis	**HIF1α**, VEGFA, **VEGFR2**, endocan, CD31, **CD106, FLT4, LYVE1**, endothelin1, PDGFA	VEGFC, TEM8, angiogenin, **FGF2★**
Survival	**SP3, sirtuin3**	**SP1★**, sirtuin6, sirtuin7, survivin, XIAP
Acute inflammation	**ITRAF6, L1, IL8**, CRP	TNFα, MIF
Innate immunity	CD56, lactoferrin, β-defensin1, β-defensin1, β-defensin2, **TLR3**, elafin	β-defensin3, α1-antitrypsin
Cellular immunity	CD4, CD34, **CD40, CD54,** CD80**, IL28,** perforin, granzyme B,PD1, PDL1	CD20, CD28, CTLA4
Chronic inflammation	Lysozyme, CD31, CD106, MMP10, MMP12, TIMP1, TIMP2, COX1	IL10, CD68, MMP2, MMP9**,** cathepsin C, cathepsin K, COX2, kininogen
Glycolysis	**HK2, TIGAR**	LDHA, GAPDH, LGR4
Fibrosis	collagen 3A1, CTGF, laminin α5, tenascin C, **claudin1**	FGF2, integrin α5, uPA, PAI1, α1-antitrypsin
Oncogenesis	**14-3-3**, PIM1, **BACH1**, cMyb, CRIP1, MTA2, **MTDH, ATM**, CEA, Daxx	TWIST1, EWSR1, **Ets1★**, **ZEB1★**, HER2, CRK, ATR, BMI, PDCD4, AXL
Senescence	**sirtuin3**, p21, caveolin1	sirtuin6, sirtuin7
Telomere signaling		TERT, TIN2

MiR-216a-5p*-CEDS induced the suppression (**blue**) or activation (**red**) of signaling through protein downregulation by direct miRNA targeting (**blue**) or indirect response (**sky blue**) and protein upregulation by indirect response (**red**). Some miRNA target proteins were upregulated (★). The data were compared to the reports of recent manuscripts and miRDB, miRmap, miRPathDB, miRTarBase, and TargetScan websites.

MiR-365a-3p-CEDS influenced the protein signaling in RAW 264.7 cells*

RAW 264.7 cells treated with mmu-miR-365a-3p sequence TAATGCCCCTAAAAATCCTTAT*-CEDS showed the characteristic protein expressions, resulting in the suppression of proliferation, cMyc/MAX/MAD network, Wnt/β-catenin signaling, p53/Rb/E2F1 signaling, SHH/PTCH/GLI signaling, Notch/Jagged signaling, epigenetic modification, protein translation, growth factors, cytodifferentiation, RAS signaling, NFkB signaling, protection, ER stress, innate immunity, cellular immunity, chronic inflammation, FAS-mediated apoptosis, and glycolysis signaling, as well as the activation of miRNA biogenesis, osteogenesis, neuromuscular differentiation, angiogenesis, survival, acute inflammation, p53-mediated apoptosis, PARP-mediated apoptosis, fibrosis, oncogenesis, and senescence compared to the untreated controls (Fig. 17A).

The proliferation signaling appears to be suppressed by downregulating miR-365a-3p target proteins PCNA (80.7%), cyclin D2 (94.3%), and cdc25A (80.9%), as well as coincidentally upregulating p15/16 (118.8%), despite the upregulation of CDK4 (115.5%) and nucleolin (109.8%), and the downregulation of miR-365a-3p target protein p14 (78.9%).

The cMyc/MAX/MAD network was suppressed by downregulating miR-365a-3p target proteins MAX (94.2%), and coincidentally downregulating cMyc (86%) and upregulating MAD1 (109.9%).

The Wnt/β-catenin signaling appears to be inactivated by downregulating AXIN2 (88.2%) and TCF1 (87.1%), despite the upregulation of Wnt1 (120.7%) and β-catenin (108.2%).

The p53/Rb/E2F1 signaling appeared to be inactivated by downregulating p-Rb1 (88.5%) and coincidentally downregulating miR-365a-3p-reponsible protein E2F1 (93.1%), despite the downregulation of miR-365a-3p target protein E2F4 (78.6%), and coincidental upregulation of p53 (108.9%) and CDK4 (115.5%). P53 is a miR-365a-3p target protein, but it was unexpectedly upregulated compared to the reference data.

The SHH/PTCH/GLI signaling was suppressed by downregulating miR-365a-3p target proteins PTCH1 (94.2%), and coincidentally downregulating SHH (87.8%) and GLI1 (83.1%).

The Notch/Jagged signaling appears to be inactivated by downregulating Notch1 (81%).

The protein translation signaling was inactivated by downregulating miR-365a-3p-responsible proteins eIF5A2 (89.9%) and eIF2AK3 (88.4%), and coincidentally downregulating eIF5A1 (89.5%), despite the upregulation of DHPS (107.7%), DOHH (110.8%), and eIF2α (119.5%).

The growth factor signaling appear to be suppressed by downregulating miR-365a-3p target proteins EGF (94.1%), IGF1 (87.1%), TGFα (94.2%), SMAD2/3 (94.1%), SMAD4 (71.7%), HGFα (94.3%), FGF1 (94.9%), FGF2 (93.4%), and FGF7 (86.7%), as well as coincidentally downregulating Met (88.8%), despite the upregulation of GHRH (115.8%), TGFβ1 (118.1%), CTGF (110.7%), and ERβ (113.7%). TGFβ1 is a miR-365a-3p target protein, but it was unexpectedly upregulated compared to the reference data.

The cytodifferentiation signaling appear to be suppressed by downregulating miR-365a-3p target protein SOX9 (94.5%) and tenascin C (93.8%), as well as coincidentally downregulating α-tubulin (94%), GAPDH (83.5%), TGase2 (88.9%), CaM (75.4%), calnexin (93.9%), AP1M1 (83.4%), caveolin1 (94.8%), and SOSTDC1 (84.2%), despite the upregulation of miR-365a-3p-responsible protein VE-cadherin (114.5%) and coincidental upregulation of β-actin (115.4%), vimentin (109.8%), FAK (113.1%), CRIP1 (129.9%), and cystatin A (111%).

The RAS signaling was suppressed by downregulating miR-365a-3p target proteins KRAS (89.8%), pAKT1/2/3 (85.9%), RAF-B (94.7%), p-ERK1 (83.8%), PTEN (89.2%), AMPKα (92.8%), and SOS1 (93.3%), as well as coincidentally downregulating AKAP13 (92.5%) and JNK (94.5%), despite the upregulation of Rab1 (111.1%), STAT3 (119.4%), PLCβ2 (115.8%), c-Fos (110.8%), and p-PKCα (110%). Rab1 is a miR-365a-3p target protein, but it was unexpectedly upregulated compared to the reference data.

The NFkB signaling was suppressed by downregulating miR-365a-3p target proteins NFkB (93.5%), p38 (85.7%), p-p38 (90.9%), SRC1 (94.2%), and NFAT5 (78.8%) and miR-365a-3p-responsible protein mTOR (88.1%), as well as coincidentally downregulating IKK (94.1%), MDR (89%), and NFATc1 (83%).

The protection signaling was suppressed by downregulating miR-365a-3p target proteins FOXP (94.4%), NOS1 (89%), FOXO1 (85.6%), and NRF2 (75.7%), as well as coincidentally downregulating leptin (94.7%), HO1 (92.4%), HSP27 (89.4%), hepcidin (87%), SVCT2 (83%), and SOD1 (71.6%), despite the upregulation of

HSP90 (130%), FOXO3 (123.3%), ALDH1A1 (109.5%), HSP70 (108.4%), and GSTO1/2 (106.5%). FOXO3 is a miR-365a-3p target protein, but it was unexpectedly upregulated compared to the reference data.

The ER stress signaling was suppressed by downregulating miR-365a-3p target proteins eIF2AK3 (88.4%) and ATF6 (81.8%), as well as coincidentally downregulating HSP27 (89.4%), GADD153 (81.3%), ATF4 (80.8%), and LC3β (91.7%), despite the upregulation of eIF2α (119.5%), p-GADD153 (119.5%), BIP (111.3%), and IRE1α (114%).

The innate immunity signaling appear to be inactivated by downregulating miR-365a-3p target proteins TLR2 (93.4%), as well as coincidentally downregulating CAMP (90.6%), β-defensin1 (90.6%), β-defensin3 (94.2%), and elafin (84.4%), despite the upregulation of β-defensin2 (137.6%) and TLR4 (115.8%).

The cellular immunity signaling was suppressed by downregulating miR-365a-3p target proteins CD44 (92%) and CD54 (93.9%), as well as coincidentally downregulating CD4 (92.6%), CD8 (83.9%), CD20 (94.3%), CD34 (89.8%), CD40 (92.4%), granzyme B (77.2%), and CTLA4 (86.8%), despite the upregulation of CD99 (129.4%), versican (122.3%), perforin (111.1%), PDL1 (108.7%), and LTA4H (107.3%).

The chronic inflammation signaling appears to be inactivated by downregulating miR-365a-3p target proteins IL6 (79.9%) and M-CSF (90.7%) and miR-365a-3p-responsible protein COX2 (84.1%), as well as coincidentally downregulating CD68 (94.8%), MMP10 (83.3%), MMP12 (78%), and cathepsin K (92.9%), despite the upregulation of IL12 (105.4%), lysozyme (110.9%), MMP3 (130.4%), MMP9 (109.6%), TIMP2 (110.9%), COX1 (120.7%), and kininogen (140.1%). MMP3 is a miR-365a-3p target protein, but it was unexpectedly upregulated compared to the reference data.

The FAS-mediated apoptosis signaling was suppressed by downregulating miR-365a-3p target proteins BID (94.5%), as well as coincidentally downregulating FAS (86%), FADD (79.8%), and c-caspase3 (81.1%), despite the upregulation of FASL (121%) and caspase3 (111.1%) and coincidental downregulation of FLIP (88.9%).

The glycolysis signaling appears to be suppressed by downregulating miR-365a-3p target protein HK2 (85.5%) and LGR4 (82.1%), as well as coincidentally downregulating GAPDH (83.5%).

Conversely, **the miRNA biogenesis signaling** appears to be activated by upregulating Drosha (108.3%), Exportin5 (120.2%), TRBP2 (135%), and GW182 (106.7%) and coincidentally downregulating MTDH (94.5%), despite the downregulation of miR-365a-3p target protein Dicer (79.8%) and AGO2 (88.7%).

The osteogenesis signaling appears to be activated by upregulating BMP4 (120.5%), OPG (110.2%), PTH/PTHrPR (105.6%), RANKL (105.4%), aggrecan (112.1%), despite the downregulation of miR-365a-3p target protein RUNX2 (87.6%) and coincidental downregulation of osteocalcin (81.9%) and osteonectin (84.2%).

The neuromuscular differentiation signaling appears to be activated by upregulating NK1R (105.1%), S100 (110%), myosin-1a (112.6%), and MYH2 (111.2%), despite the downregulation of αSMA (86.1%).

The angiogenesis signaling appears to be activated by upregulating VEGFR2 (117.4%), TEM8 (124.2%), CMG2 (106.4%), and PDGFA (107.1%), despite the downregulation of miR-365a-3p target proteins FLT4 (87.5%), LYVE1 (87.2%), and FGF2 (93.4%), as well as coincidental downregulation of vWF (83.8%).

The survival signaling appears to be activated by upregulating SP1 (105.6%), sirtuin1 (110.2%), and sirtuin7 (106.8%), despite the downregulation of miR-365a-3p target protein XIAP (89.6%) and coincidental downregulation of sirtuin6 (87.1%). Sirtuin1 is a miR-365a-3p target protein, but it was unexpectedly upregulated compared to the reference data.

The acute inflammation signaling appears to be activated by upregulating TNFα (107.7%), TRAF6 (111.8%), IL8 (119.5%), and MMP1 (115.9%), despite the downregulation of miR-365a-3p target protein CRP (89%) and coincidental downregulation of MIF (78.1%) and CXCR4 (86.7%). TRAF6 is a miR-365a-3p target protein, but it was unexpectedly upregulated compared to the reference data.

The p53-mediated apoptosis signaling appears to be activated by upregulating p53 (108.9%), p63 (108.8%), p73 (112.1%), NOXA (105.1%), caspase9 (110.1%), and caspase3 (111.1%), despite the downregulation of miR-365a-3p target proteins MDM2 (96%), BAX (78.9%), and APAF1 (88.1%), and coincidental downregulation of c-caspase3 (81.1%). P53, p63, and p73 are miR-365a-3p target proteins, but they were unexpectedly upregulated compared to the reference data.

The PARP-mediated apoptosis signaling was activated by upregulating miR-365a-3p-responsible proteins PARP1 (118.4%) and c-PARP (123.6%), as well as coincidentally upregulating AIF1 (105%).

The fibrosis signaling appears to be activated by upregulating collagen 3A1 (107.3%), CTGF (110.7%), laminin α5 (107.7%), and integrin α5 (130.4%) and coincidentally downregulating FGF7 (86.7%), despite the downregulation of miR-365a-3p target proteins FGF1 (94.9%), FGF2 (93.4%), and tenascin C (93.8%), as well as coincidental downregulation of integrin β1 (92.4%), uPA (88.9%), and PAI1 (86.2%). Integrin α5 is a miR-365a-3p target protein, but it was unexpectedly upregulated compared to the reference data.

The senescence signaling appears to be activated by upregulating klotho (114.7%), sirtuin1 (110.2%), and sirtuin7 (106.8%), despite the despite the downregulation of sirtuin6 (87.1%) and caveolin1 (94.8%). Sirtuin1 is a miR-365a-3p target protein, but it was unexpectedly upregulated compared to the reference data.

In addition, miR-365a-3p*-CEDS greatly influenced **the epigenetic modification signaling** by downregulating miR-365a-3p target proteins EZH2 (83.9%), as well as the coincidental downregulation of histone H1 (93.6%), KDM4D (93.7%), HDAC10 (94%), MBD4 (91.9%), DMAP1 (65.5%), DNMT1 (91.3%), PCAF (92.5%), BRG1 (77.7%), Ac-lysine (91.9%), and lamin A/C (94.4%), while it upregulated HMGA2 (118%) and HMGB1 (106.1%). HMGA2 is a miR-365a-3p target protein, but it was unexpectedly upregulated compared to the reference data. Consequently, miR-365a-3p*-CEDS induced a trend towards a reduction in the methylation of histones and DNAs, and attenuation of transcriptional repression.

MiR-365a-3p*-CEDS significantly attenuated **the oncogenesis signaling** by downregulating miR-365a-3p target proteins BMI1 (65%), BACH1 (64.8%), as well as the coincidental downregulation of EWSR1 (91.9%), XBP1 (88.4%), HER2 (85.1%), and CEA (83.2%), while it widely enhanced **the oncogenesis signaling** by upregulating CRIP1 (129.9%), MTA2 (121%), NF1 (115.8%), ATR (117.4%), ZEB1 (119.7%), MALT1 (111.8%), BRCA1 (109.9%), TWIST1 (109.6%), cMyb (109.4%), YAP1 (109%), and KLF4 (106.7%). MTA2, NF1, ZEB1, MALT1, and YAP1 are miR-365a-3p target proteins, but they were unexpectedly upregulated compared to the reference data. Among the 28 oncoproteins, 11 were found to be overexpressed, six were underexpressed, and 11 exhibited minimal change in expression compared to the untreated controls.

Consequently, miR-365a-3p*-CEDS significantly affected the entire protein signaling in RAW 264.7 cells. MiR-365a-3p*-CEDS suppressed the main RAS-NFkB signaling axis, and subsequently inactivated the proliferation-related signaling axis, epigenetic modification-protection-ER stress signaling axis, and FA-mediated apoptosis-glycolysis signaling axis. Conversely, it activated angiogenesis-survival-senescence-acute inflammation signaling axis, and p53- and PARP-mediated apoptosis-fibrosis-oncogenesis signaling axis (Fig. 17B Table 10).

The results indicate that miR-365a-3p*-CEDS exerted an anti-oncogenic effect on RAW 264.7 cells by suppressing proliferation, ROS protection, ER stress, and chronic inflammation. Conversely, CEDS also induced an oncogenic effect by increasing angiogenesis, survival, senescence, fibrosis, and oncogenesis. It is also proposed that miR-365a-3p*-CEDS stimulated p53- and PARP-mediated apoptosis signaling, while simultaneously attenuating the innate and cellular immunity signaling.

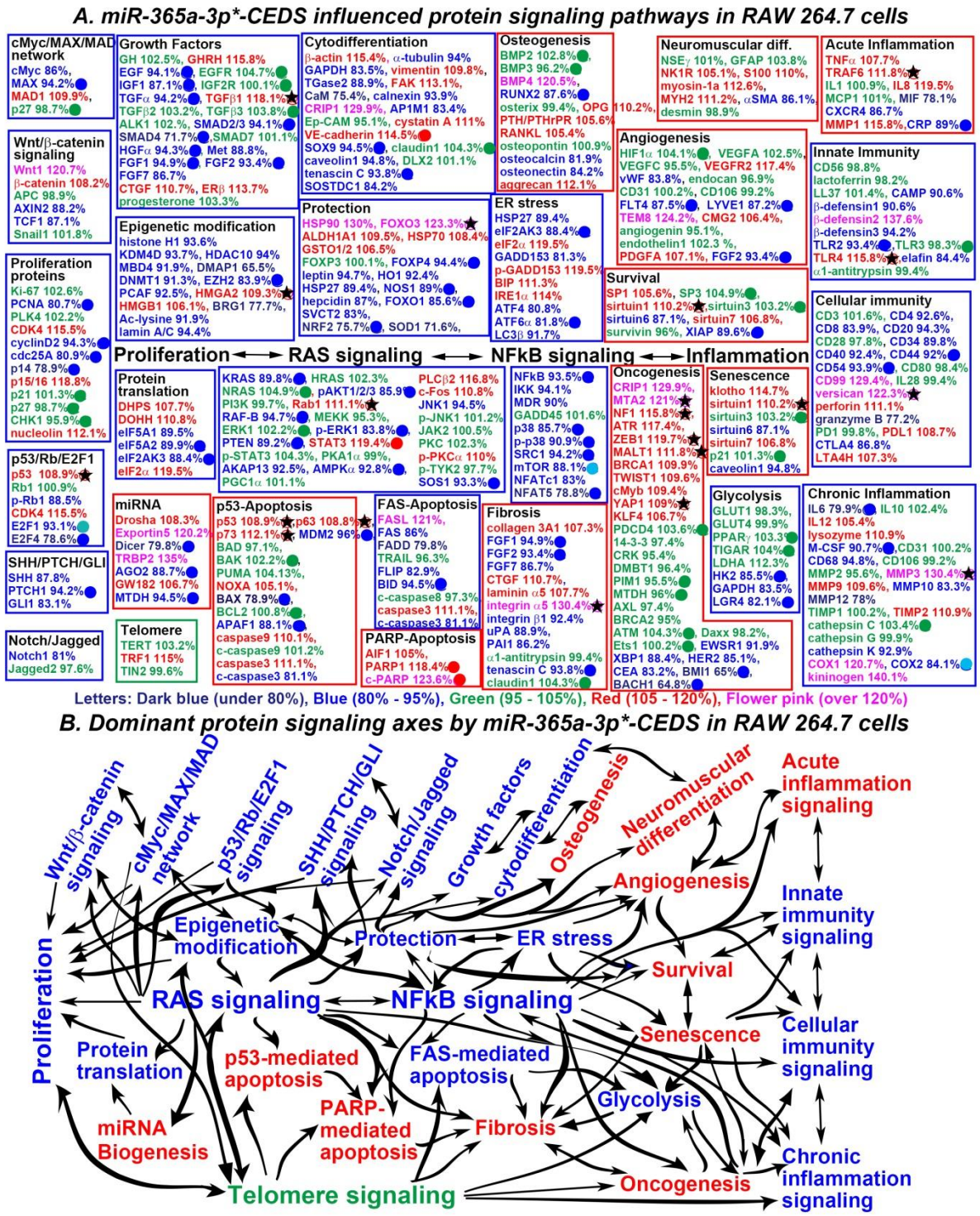

Fig. 17. MiR-365a-3p*-CEDS influenced the protein signaling (A) and axes (B) in RAW 264.7 cells. The IP-HPLC revealed proteins downregulated (**blue**), upregulated (**red**), and minimally changed (**green**) compared to the untreated controls. Dominantly suppressed (**blue square**) and activated (**red square**) signaling. Downregulated proteins by direct targeting (●) and indirect response (●), upregulated proteins by indirect response (●), and minimal changed (±5%) proteins (●). Some target proteins (★) were unexpectedly upregulated contrast to the current manuscripts and data from miRDB and TargetScan websites.

Table 10. Protein expressions in the RAW 264.7 cells treated with miR-365a-3p*-CEDS.

Signaling	Downregulated Proteins	Upregulated Proteins
Proliferation	**PCNA, cyclinD2, cdc25A**, p14, CHK1	CDK4, p15/16, nucleolin
cMyc/MAX/MAD network	cMyc, **MAX**	MAD1
Wnt/β-catenin signaling	AXIN2, TCF1	Wnt1, β-catenin
p53/Rb/E2F1 signaling	p-Rb1, **E2F1, E2F4**	**p53★**
SHH/PTCH/GLI signaling	SHH, **PTCH1**, GLI1	
Notch/Jagged signaling	Notch1	
Epigenetic modification	histone H1, KDM4D, HDAC10, MBD4, DMAP1, DNMT1, **EZH2**, PCAF, BRG1, Ac-lysine, lamin A/C	**HMGA2★**, HMGB1
Protein translation	eIF5A1, **eIF5A2, eIF2AK3**	DOHH, DHPS, eIF2α
miRNA biogenesis	**Dicer, AGO2, MTDH**	Drosha, Exportin5, TRBP2, GW182
Growth factors	**EGF, IGF1, TGFα, SMAD2/3, SMAD4, HGFα**, Met, **FGF1, FDF2**, FGF7	GHRH, **TGFβ1★,** CTGF, ERβ
Cytodifferentiation	α-tubulin, GAPDH, TGase2, CaM, calnexin, AP1M1, **SOX9**, caveolin1, **tenascin C**, SOSTDC1	β-actin, vimentin, FAK, CRIP1, cystatin A, **VE-cadherin**
Osteogenesis	**RUNX2**, osteocalcin, osteonectin,	**BMP2**, BMP4, PTH/PTHrPR, OPG, RANKL, aggrecan
Neuromuscular differentiation	αSMA	NK1R, **S100, myosin-1a, MYH2**
RAS signaling	**KRAS, pAKT1/2/3, RAF-B, p-ERK1, PTEN**, AKAP13, **AMPKα**, JNK1, **SOS1**	NRAS**, Rab1★**, **STAT3**, PLCβ2, c-Fos, p-PKC1α
NFkB signaling	**NFkB**, IKK, MDR, **p38, p-p38, mTOR,** NFATc1, **NFAT5**	
p53-mediated apoptosis	**MDM2, BAX, APAF1**, c-caspase3	**p53★, p63★, p73★**, NOXA, caspase9, caspase3
FAS-mediated apoptosis	FAS, FADD, FLIP, **BID,** c-caspase3	FASL, caspase3
PARP-mediated apoptosis		AIF1, **PARP1, c-PARP**
Protection	**FOXP4**, leptin, HO1, HSP27, **NOS1**, hepcidin, **FOXO1**, SVCT2, **NRF2**, SOD1	HSP90**, FOXO3★**, ALDH1A1, HSP70, GSTO1/2
ER stress	HSP27, **eIF2AK3**, GADD153, ATF4, **ATF6α,** LC3β	eIF2α, p-GADD153, BIP, IRE1α
Angiogenesis	vWF, **FLT4, LYVE1, FGF2**	VEGFR2, TEM8, CMG2, PDGFA
Survival	sirtuin6, **XIAP**	SP1, SP3**, sirtuin1★**, sirtuin7
Acute inflammation	MIF, CXCR4, **CRP**	TNFα, **TRAF6★,** IL8, MMP1
Innate immunity	CAMP, β-defensin1, β-defensin3, **TLR2,** elafin	β-defensin2, TLR3**, TLR4★**
Cellular immunity	CD4, CD8, CD20, CD34, CD40, **CD44, CD54,** granzyme B, CTLA4	CD99, **versican★**, perforin, PDL1, LTA4H
Chronic inflammation	**IL6, M-CSF**, CD68, MMP10, MMP12, cathepsin K, **COX2**	IL12, lysozyme, **MMP3★**, MMP9, TIMP2, COX1, kininogen
Glycolysis	**HK2,** GAPDH, **LGR4**	
Fibrosis	**FGF1, FGF2**, FGF7, Integrin β1, uPA, PAI1, **tenascin C**	collagen 3A1, CTGF, laminin α5, **integrin α5★**
Oncogenesis	EWSR1, XBP1, HER2, CEA, **BMI1, BACH1**	CRIP1, **MTA2★, NF1★,** ATR, **ZEB1★, MALT1★**, BRCA1, TWIST1, cMyb, **YAP1★**, KLF4, PDCD4
Senescence	sirtuin6, caveolin1	klotho, **sirtuin1★**, sirtuin7
Telomere signaling		TRF1

MiR-365a-3p*-CEDS induced the suppression (**blue**) or activation (**red**) of signaling through protein downregulation by direct miRNA targeting (**blue**) or indirect response (**sky blue**) and protein upregulation by indirect response (**red**). Some miRNA target proteins were upregulated (★). The data were compared to the reports of recent manuscripts and miRDB, miRmap, miRPathDB, miRTarBase, and TargetScan websites.

MiR-655-3p*-CEDS influenced the protein signaling in RAW 264.7 cells

RAW 264.7 cells treated with mmu-miR-655-3p sequence ATAATACATGGTTAACCTCTTT*-CEDS showed the characteristic protein expressions, resulting in the suppression of, Wnt/β-catenin signaling, p53/Rb/E2F1 signaling, SHH/PTCH/GLI signaling, Notch/Jagged signaling, protein translation, miRNA biogenesis, growth factors, cytodifferentiation, RAS signaling, NFkB signaling, protection, ER stress, survival, innate immunity, cellular immunity, p53-mediated apoptosis, FAS-mediated apoptosis, and glycolysis signaling, as well as the activation of proliferation, cMyc/MAX/MAD network, epigenetic modification, osteogenesis, neuromuscular differentiation, angiogenesis, acute inflammation, chronic inflammation, PARP-mediated apoptosis, fibrosis, oncogenesis, senescence, and telomere signaling compared to the untreated controls (Fig. 18A).

The Wnt/β-catenin signaling was suppressed by downregulating miR-655-3p target proteins APC (93.7%), AXIN2 (94.1%), and TCF1 (91.7%), despite the upregulation of β-catenin (109.2%).

The p53/Rb/E2F1 signaling was suppressed by downregulating miR-655-3p target protein Rb1 (93.8%) and coincidentally downregulating E2F1 (83.6%), despite the upregulation of p53 (107.3%) and coincidental downregulation of E2F4 (83.4%).

The SHH/PTCH/GLI signaling was suppressed by downregulating miR-655-3p target protein PTCH1 (75.8%) and coincidentally downregulating SHH (87.3%).

The Notch/Jagged signaling was suppressed by downregulating miR-655-3p target protein Notch1 (84.9%).

The protein translation signaling was suppressed by downregulating miR-655-3p target protein eIF5A2 (93.7%) and coincidentally downregulating eIF5A1 (88.8%) and eIF2AK3 (81.6%), despite the upregulation of DOHH (119.8%).

The miRNA biogenesis signaling was suppressed by downregulating miR-655-3p target protein Drosha (90%) and coincidentally downregulating Exportin5 (94.2%), despite the upregulation of TRBP2 (105.2%) and downregulating miR-655 target protein MTDH (94.1%).

The growth factor signaling were partially suppressed by downregulating miR-655-3p target proteins EGF (91.1%), TGFα (91.8%), SMAD2/3 (93.2%), SMAD7 (86.7%), HGFα (91.4%), and FGF7 (93.7%), as well as coincidentally downregulating GH (84.5%) and IGF1 (91.5%), despite the upregulation of GHRH (126.1%), IGF2R (110.8%), TGFβ2 (112.6%), ALK1 (108.1%), SMAD4 (128.6%), FGF2 (110.6%), CTGF (123.8%), and progesterone (106.2%). TGFβ2 and FGF2 are miR-655-3p target proteins, but they were unexpectedly upregulated compared to the reference data.

The cytodifferentiation signaling were partially suppressed by downregulating miR-655-3p target protein SOX9 (88.1%), as well as coincidentally downregulating α-tubulin (92.6%), GAPDH (83.3%), Ep-CAM (94.1%), TGase2 (89.9%), CaM (84.6%), calnexin (94.7%), AP1M1 (88%), and tenascin C (92%), despite the upregulation of β-actin (138.1%), FAK (115.2%), CRIP1 (106.3%), cystatin A (115.5%), VE-cadherin (116.3%), caveolin1 (129.4%), and SOSTDC1 (112.3%).

The RAS signaling was suppressed by downregulating miR-655-3p target proteins pAKT1/2/3 (86%), PTEN (87.9%), AKAP13 (92.9%), c-Fos (94.2%), JAK2 (94.8%), and SOS1 (87.3%) and miR-655-3p-responsible proteins p-ERK1 (92.2%), STAT3 (78.3%), and p-STAT3 (86.3%), as well as coincidentally downregulating KRAS (93%), PKA1α (89.2%), AMPKα (91.7%), PLCβ2 (89.1%), and TYK2 (93%), despite the upregulation of HRAS (108.4%), PKC (108%), and p-PKCα (108%).

The NFkB signaling was suppressed by downregulating miR-655-3p target proteins GADD45 (85.1%), p-p38 (84.7%), SRC1 (93.8%), and NFAT5 (82.8%), as well as coincidentally downregulating IKK (88.9%) and MDR (92.8%).

The protection signaling was suppressed by downregulating miR-655-3p target proteins FOXO1 (94.3%), GSTO1/2 (94%), and SOD1 (73.9%), as well as coincidentally downregulating leptin (93.2%), NOS1 (91.2%), NRF2 (89.9%), SVCT2 (84.4%), and HSP27 (86.5%), despite the upregulation of ALDH1A1 (112.5%), HSP90 (110%), FOXP (108.2%), HO1 (106.3%), and hepcidin (106.2%).

The ER stress signaling was suppressed by downregulating HSP27 (86.5%), eIF2α (81.6%), p-GADD153 (92.6%), BIP (81.6%), ATF4 (79.7%), and LC3β (103.4%), despite the upregulation of IRE1α (106.5%).

The survival signaling was suppressed by downregulating miR-655-3p target protein sirtuin1 (88.5%) and miR-655-3p-responsible protein SP1 (82.5%), as well as coincidentally downregulating sirtuin3 and sirtuin7, despite the upregulation of survivin (115.5%).

The innate immunity signaling appears to be inactivated by downregulating miR-655-3p target proteins TLR3 (92.2%) and TLR4 (92.9%), as well as coincidentally downregulating lactoferrin (94%), CAMP (92.7%), β-defensin1 (86%), and β-defensin3 (77.5%), despite the upregulation of LL37 (115.5%) and β-defensin2 (109.5%).

The cellular immunity signaling was suppressed by downregulating miR-655-3p-responsible proteins CD28 (93.5%), CD40 (92.9%), and versican (93.6%) and miR-655-3p-responsible protein CD80 (83.4%), as well as coincidentally downregulating CD3 (97.6%), CD4 (91.4%), CD8 (78.1%), IL28 (94.6%), granzyme B (89.7%), and CTLA4 (80.9%), despite the upregulation of CD44 (112.6%), CD54 (118.1%), CD99 (107.4%), perforin (135%), PDL1 (108.1%), and LTA4H (111%).

The p53-mediated apoptosis signaling was suppressed by downregulating miR-655-3p target proteins p63 (81.8%), MDM2 (87.2%), BAK (90%), and APAF1 (89.8%), and miR-655-3p-responsible proteins caspase3 (93.9%) and c-caspase3 (84.5%), as well as coincidentally downregulating BAX (83.1%), despite the upregulation of p53 (107.3%) and p73 (106.2). P73 is a miR-655-3p target protein, but it was unexpectedly upregulated compared to the reference data.

The FAS-mediated apoptosis signaling was suppressed by downregulating miR-655-3p target protein FAS (93.8%) and miR-655-3p-responsible proteins caspase3 (93.9%) and c-caspase3 (82.6%), as well as coincidentally downregulating FADD (80.9%) and caspase8 (79.4%), despite the upregulation of TRAIL (132.2%).

The glycolysis signaling was suppressed by downregulating miR-655-3p target proteins LGR4 (89.4%) and LDHA (86.9%), as well as coincidentally downregulating GLUT4 (93.1%) and GAPDH (83.3%), despite the slight upregulation of GLUT1 (108.7%) and HK2 (108.3%). HK2 is a miR-655-3p target protein, but it was unexpectedly upregulated compared to the reference data.

Conversely, **the proliferation signaling** appears to be activated by upregulating Ki-67 (114.6%), PCNA (116.3%), cdc25A (127.7%), and nucleolin (109.5%) and downregulating miR-655-3p target protein p21 (93.9%), as well as coincidental downregulation p14 (90.4%) and p15/16 (93.2%), despite the downregulation of cyclin D2 (83.8%) and upregulation of p27 (106.4%). Cdc25A is a miR-655-3p target protein, but it was unexpectedly upregulated compared to the reference data.

The cMyc/MAX/MAD network appears to be activated by upregulating MAX (106.9%) and p27 (106.4%), despite the downregulation of miR-655-3p target protein cMyc (89.2%).

The osteogenesis signaling appears to be activated by upregulating miR-655-3p-responsible proteins BMP2 (119%) and BMP4 (110%) and coincidentally upregulating OPG (116.9%), RANKL (117.2%), and aggrecan (135.9%), despite the downregulation of RUNX2 (87.7%), PTH/PTHrPR (92.3%), osteocalcin (83.9%), and osteonectin (83.9%).

The neuronal differentiation signaling appears to be inactivated by downregulating NK1R (88.8%), while **the muscular differentiation signaling** was activated by upregulating myosin-1a (144.7%) and desmin (116.2%).

The angiogenesis signaling appeared to be activated by upregulating VEGFC (113.6%), VEGFR2 (111.3%), endocan (116.7%), TEM8 (116.7%), endothelin1 (109.7%), and FGF2 (110.6%), despite the downregulation of miR-655-3p target proteins VEGFA (94%), CD31 (93.5%), and LYVE1 (84.6%), as well as coincidental downregulation of vWF (84.5%) and CMG2 (86%). VEGFC, endocan, and FGF2 are miR-655-3p target proteins, but they were unexpectedly upregulated compared to the reference data.

The acute inflammation signaling appears to be activated by upregulating TNFα (109.2%), TRAF6 (120%), IL1 (124.3%), and IL8 (106.9%), despite the downregulation of miR-655-3p target protein CXCR4 (93.4%) and coincidental downregulation of MCP1 (87.5%) and MIF (88.7%). TRAF6 and IL8 are miR-655-3p target proteins, but they were unexpectedly upregulated compared to the reference data.

The chronic inflammation signaling appears to be activated by upregulating M-CSF (109.9%), lysozyme (132.7%), CD68 (106%), MMP2 (115.4%), MMP3 (114.8%), MMP9 (107%), MMP10 (121.8%), TIMP1

(105%), cathepsin C (130.2%), cathepsin G (109.8%), and COX1 (11.7%), despite the downregulation of miR-655-3p target proteins IL6 (87.3%), CD31 (93.5%), and TIMP2 (93.2%) and coincidental downregulation of IL12 (86.1%), MMP12 (73.9%), and cathepsin K (92.7%). MMP10 is a miR-655-3p target protein, but it was unexpectedly upregulated compared to the reference data.

The PARP-mediated apoptosis signaling was activated by upregulating AIF1 (121.2%) and c-PARP (112.2%). C-PARP is a miR-655-3p target protein, but it was unexpectedly upregulated compared to the reference data.

The fibrosis signaling appears to be activated by upregulating collagen 3A1 (105.9%), FGF2 (110.6%), CTGF (123.8%), laminin α5 (118.4%), integrin α5 (109.2%), and uPA (109.7%) and coincidentally downregulating miR-655-3p target protein FGF7 (93.7%), despite the downregulation of PAI1 (88.8%) and tenascin C (92%). FGF2 and integrin α5 are miR-655-3p target proteins, but they were unexpectedly upregulated compared to the reference data.

The senescence signaling appears to be aberrant by downregulating miR-655-3p target protein sirtuin1 (88.5%) and p21 (93.9%) and coincidentally downregulating sirtuin3 (79.6%) and sirtuin6 (79.3%), even though the upregulation of klotho (126.4%) and caveolin1 (129.4%). Caveolin1 is a miR-655-3p target protein, but it was unexpectedly upregulated compared to the reference data.

The telomere signaling was activated by upregulating TERT (109.1%), TRF1 (113.7%), and TIN2 (116.9%). TERT is a miR-655-3p target protein, but it was unexpectedly upregulated compared to the reference data.

In addition, miR-655-3p*-CEDS significantly influenced **the epigenetic modification signaling** by downregulating miR-655-3p target proteins EZH2 (88.3%) and HMGA2 (92.6%) and coincidentally downregulating DMAP1 (85.7%) and BRG1 (72.5%), while it upregulated KDM4D (113.6%), HDAC10 (107.8%), PCAF (121%), and lamin A/C (132.2%). KDM4D is a miR-655-3p target protein, but it was unexpectedly upregulated compared to the reference data. Consequently, miR-655-3p*-CEDS induced a trend towards an increase in the methylation of histones and DNAs, and affected the transcriptional repression.

MiR-655-3p*-CEDS partially suppressed **the oncogenesis signaling** by downregulating miR-655-3p target proteins MTDH (94.1%), CRK (83.1%), and ZEB1 (93.4%), while it widely enhanced **the oncogenesis signaling** by upregulating Ets1 (133.9%), BRCA1 (117.4%), BRCA2 (115.8%), Daxx (113.8%), AXL (113.3%), ATR (111.5%), YAP1 (111.5%), DMBT1 (107.7%), cMyb (109.9%), ATM (109.8%), PIM1 (109.1%), MTA2 (107.7%), PDCD4 (107.5%), and CRIP (106.3%). ATM is a miR-655-3p target protein, but it was unexpectedly upregulated compared to the reference data. Among the 28 oncoproteins, 14 were found to be overexpressed, 10 were underexpressed, and four exhibited minimal change in expression compared to the untreated controls.

Consequently, miR-655-3p*-CEDS exhibited a variable effect on the entire protein signaling in RAW 264.7 cells. MiR-655-3p*-CEDS suppressed the RAS-NFkB signaling axis, subsequently inactivating the protection-ER stress-survival signaling axis and the p53- and FAS-mediated apoptosis signaling axis. Concurrently, miR-655-3p*-CEDS activated the epigenetic modification-cMyc/MAX/MAD network-proliferation signaling axis, epigenetic modification-telomere-PARP-mediated apoptosis-fibrosis signaling axis, angiogenesis-acute inflammation signaling axis, and oncogenesis-senescence-chronic inflammation signaling axis (Fig. 18B, Table 11).

The results indicate that miR-655-3p*-CEDS exerted an anti-oncogenic effect on RAW 264.7 cells by suppressing ROS protection, ER stress, survival, and glycolysis. However, it also markedly induced an oncogenic effect by increasing proliferation, telomere instability, fibrosis, angiogenesis, senescence, oncogenesis, and acute and chronic inflammation. It is also observed that miR-655-3p*-CEDS inhibited p53- and PARP-mediated apoptosis signaling, while simultaneously stimulating PARP-mediated apoptosis. Additionally, it impaired innate and cellular immunity signaling.

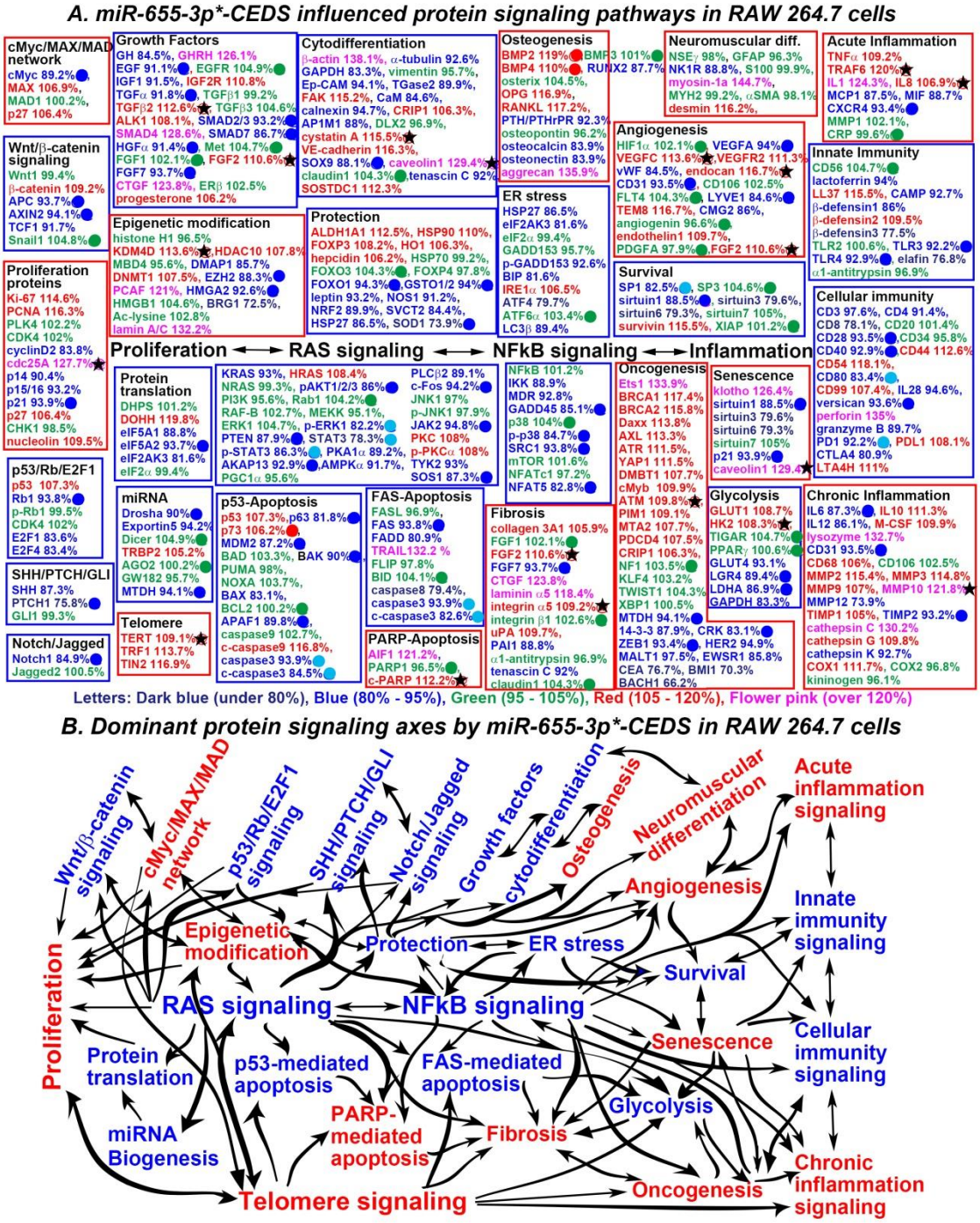

Fig. 18. MiR-655-3p*-CEDS influenced the protein signaling (A) and axes (B) in RAW 264.7 cells. The IP-HPLC revealed proteins downregulated (**blue**), upregulated (**red**), and minimally changed (**green**) compared to the untreated controls. Dominantly suppressed (**blue square**) and activated (**red square**) signaling. Downregulated proteins by direct targeting (●) and indirect response (●), upregulated proteins by indirect response (●), and minimal changed (±5%) proteins (●). Some target proteins (★) were unexpectedly upregulated contrast to the current manuscripts and data from miRDB and TargetScan websites.

Table 11. Protein expressions in the RAW 264.7 cells treated with miR-655-3p*-CEDS.

Signaling	Downregulated Proteins	Upregulated Proteins
Proliferation	cyclin D2, p14, p15/16, **p21**	Ki-67, PCNA, **cdc25A★**, p27, nucleolin
cMyc/MAX/MAD network	**cMyc**	MAX, p27
Wnt/β-catenin signaling	**APC, AXIN2**, TCF1	β-catenin
p53/Rb/E2F1 signaling	**Rb1**, E2F1, E2F4	p53
SHH/PTCH/GLI signaling	SHH, **PTCH1**	
Notch/Jagged signaling	**Notch1**	
Epigenetic modification	DMAP1, **EZH2**, PCAF, **HMGA2**, BRG1	**KDM4D★**, HDAC10, lamin A/C
Protein translation	eIF5A1, **eIF5A2**, eIF2AK3	DOHH
miRNA biogenesis	**Drosha,** Exportin5, **MTDH**	TRBP2
Growth factors	GH, **EGF,** IGF1, **TGFα**, **SMAD2/3, SMAD7, HGFα, FGF7**	GHRH, EGFR, IGF2R, **TGFβ2★**, ALK1, SMAD4, Met, **FGF2★**, CTGF, progesterone
Cytodifferentiation	α-tubulin, GAPDH, claudin1, Ep-CAM, TGase2,CaM, calnexin, APiM1, **SOX9,** tenascin C	β-actin, FAK, CRIP1, **cystatin A★**, VE-cadherin, **caveolin1★**
Osteogenesis	RUNX2, PTH/PTHrPR, osteocalcin, osteonectin	**BMP2**, **BMP4,** OPG, RANKL, aggrecan, SOSTDC1
Neuromuscular differentiation	NK1R	myosin-1a
RAS signaling	KRAS, **pAKT1/2/3, p-ERK1, PTEN, STAT3, p-STAT3**, PKA1α, **AKAP13**, AMPKα, PLCβ2, **c-Fos, JAK2**, TYK2, **SOS1**	HRAS, PKC, p-PKCα
NFkB signaling	IKK, MDR, **GADD45, p-p38, SRC1, NFAT5**	
p53-mediated apoptosis	**p63, MDM2, BAK,** BAX, **APAF1**, **caspase3, c-caspase3**	p53, **p73**, c-caspase9
FAS-mediated apoptosis	**FAS**, FADD, caspase8, **caspase3, c-caspase3**	TRAIL, BID
PARP-mediated		AIF1, **c-PARP★**
Protection	**FOXO1, GSTO1/1**, leptin, NOS1, NRF2, SVCT2, HSP27, **SOD1**	ALDH1A1, FOXP3, HO1, hepcidin
ER stress	HSP27, eIF2AK3, GADD153, p-GADD153, BIP, ATF4, LC3β	IRE1α
Angiogenesis	**VEGFA**, vWF, **CD31, LYVE1**, CMG2	**VEGFC★**, VEGFR2, **endocan★**, FLT4, TEM8, endothelin1**, FGF2★**
Survival	**SP1, sirtuin1**, sirtuin3, sirtuin6	survivin,
Acute inflammation	MCP1, MIF, **CXCR4**	TNFα, **TRAF6★**, IL1, **IL8★**
Innate immunity	Lactoferrin, CAMP, β-defensin1, β-defensin3, **TLR3, TLR4**, elafin	CD56, LL37, β-defensin2,
Cellular immunity	CD3, CD4, CD8, **CD28, CD40, CD80**, IL28, **versican,** granzyme B, **PD1,** CTLA4	CD44, CD54, CD99, perforin, PDL1, LTA4H
Chronic inflammation	**IL6,** IL12, **CD31**, MMP12, **TIMP2**, cathepsin K	IL10, M-CSF, lysozyme, CD31, CD68, MMP2, MMP3, MMP9, **MMP10★**, TIMP1, cathepsin C, cathepsin G, COX1
Glycolysis	GLUT1, **LGR4, LDHA**, GAPDH	GLUT1, **HK2★**, TIGAR
Fibrosis	**FGF7,** PAI1, tenascin C	collagen 3A1, **FGF2★**, CTGF, laminin α5, **integrin α5★**, uPA,
Oncogenesis	**MTDH**, 14-3-3**, CRK, ZEB1,** HER2, MALT1, EWSR1, CEA, BMI1, BACH1	Ets1, BRCA1, BRCA2, Daxx, AXL, ATR, YAP1, DMBT1, cMyb, **ATM★**, PIM1, MTA2, PDCD4, CRIp1
Senescence	**sirtuin1**, sirtuin3, sirtuin6, **p21**	klotho, p21, **caveolin★**
Telomere signaling		**TERT★**, TRF1, TIN2

MiR-655-3p*-CEDS induced the suppression (**blue**) or activation (**red**) of signaling through protein downregulation by direct miRNA targeting (**blue**) or indirect response (**sky blue**) and protein upregulation by indirect response (**red**). Some miRNA target proteins were upregulated (★). The data were compared to the reports of recent manuscripts and miRDB, miRmap, miRPathDB, miRTarBase, and TargetScan websites.

The above protein expression results after CEDS targeting nine mature miRNAs during RAW 264.7 cell culture could be summarized as follows. The RAW 264.7 cells treated with miR-26a-5p*-CEDS showed downregulation of 62 proteins, upregulation of 11 proteins, and minimal expressional change (±5%) of four proteins among 77 miR-26a-5p target proteins, which were identified by the current reports and the data on the miRDB and TargetScan websites. Consequently, the miRNA targeting ratio, defined as the number of downregulated proteins by targeting divided by the number of miR-26a-5p target proteins, was 80.5%. Additionally, CEDS indirectly decreased and increased the expression of 11 and 10 proteins, respectively, which were not targeted by miR-26a-5p (Table 12).

The RAW 264.7 cells treated with miR-34a-5p*-CEDS showed downregulation of 43 proteins, upregulation of 12 proteins, and minimal expressional change (±5%) of four proteins among 59 miR-34a-5p target proteins, which were identified by the current reports and the data on the miRDB and TargetScan websites. Consequently, the miRNA targeting ratio, defined as the number of downregulated proteins by targeting divided by the number of miR-34a-5p target proteins, was 72.9%. Additionally, CEDS indirectly decreased and increased the expression of 26 and 13 proteins, respectively, which were not targeted by miR-34a-5p (Table 12).

The RAW 264.7 cells treated with miR-126-5p*-CEDS showed downregulation of 46 proteins, upregulation of 14 proteins, and minimal expressional change (±5%) of 20 proteins among 80 miR-126-5p target proteins, which were identified by the current reports and the data on the miRDB and TargetScan websites. Consequently, the miRNA targeting ratio, defined as the number of downregulated proteins by targeting divided by the number of miR-126-5p target proteins, was 57.5%. Additionally, CEDS indirectly decreased and increased the expression of 15 and 13 proteins, respectively, which were not targeted by miR-126-5p (Table 12).

The RAW 264.7 cells treated with miR-150-5p*-CEDS showed downregulation of 27 proteins, upregulation of nine proteins, and minimal expressional change (±5%) of eight proteins among 44 miR-150-5p target proteins, which were identified by the current reports and the data on the miRDB and TargetScan websites. Consequently, the miRNA targeting ratio, defined as the number of downregulated proteins by targeting divided by the number of miR-150-5p target proteins, was 61.4%. Additionally, CEDS indirectly

decreased and increased the expression of 22 and four proteins, respectively, which were not targeted by miR-150-5p (Table 12).

The RAW 264.7 cells treated with miR-155-5p*-CEDS showed downregulation of 27 proteins, upregulation of nine proteins, and minimal expressional change (±5%) of nine proteins among 45 miR-155-5p target proteins, which were identified by the current reports and the data on the miRDB and TargetScan websites. Consequently, the miRNA targeting ratio, defined as the number of downregulated proteins by targeting divided by the number of miR-155-5p target proteins, was 60%. Additionally, CEDS indirectly decreased and increased the expression of eight and nine proteins, respectively, which were not targeted by miR-155-5p sequence (Table 12).

The RAW 264.7 cells treated with miR-181a-5p*-CEDS showed downregulation of 21 proteins, upregulation of three proteins, and minimal expressional change (±5%) of one proteins among 25 miR-181a-5p target proteins, which were identified by the current reports and the data on the miRDB and TargetScan websites. Consequently, the miRNA targeting ratio, defined as the number of downregulated proteins by targeting divided by the number of miR-181a-5p target proteins, was 84%. Additionally, CEDS indirectly decreased and increased the expression of four and seven proteins, respectively, which were not targeted by miR-181a-5p (Table 12).

The RAW 264.7 cells treated with miR-216a-5p*-CEDS showed downregulation of 21 proteins, upregulation of two proteins, and minimal expressional change (±5%) of four proteins among 27 miR-216a-5p target proteins, which were identified by the current reports and the data on the miRDB and TargetScan websites. Consequently, the miRNA targeting ratio, defined as the number of downregulated proteins by targeting divided by the number of miR-216a-5p target proteins, was 77.8%. Additionally, CEDS indirectly decreased and increased the expression of seven and two proteins, respectively, which were not targeted by miR-216a-5p (Table 12).

The RAW 264.7 cells treated with miR-365a-3p*-CEDS showed downregulation of 19 proteins, upregulation of five proteins, and minimal expressional change (±5%) of nine proteins among 33 miR-365a-3p target proteins, which were identified by the current reports and the data on the miRDB and TargetScan websites. Consequently, the miRNA targeting ratio, defined as the number of downregulated proteins by targeting divided by the number of miR-365a-3p target proteins, was 57.6%. Additionally, CEDS indirectly

decreased and increased the expression of three and nine proteins, respectively, which were not targeted by miR-365a-3p (Table 12).

The RAW 264.7 cells treated with miR-655-3p*-CEDS showed downregulation of 33 proteins, upregulation of 12 proteins, and minimal expressional change (±5%) of 15 proteins among 60 miR-655-3p target proteins, which were identified by the current reports and the data on the miRDB and TargetScan websites. Consequently, the miRNA targeting ratio, defined as the number of downregulated proteins by targeting divided by the number of miR-655-3p target proteins, was 66%. Additionally, CEDS indirectly increased the expression of five proteins, which were not targeted by miR-655-3p (Table 12).

As a result, the RAW 264.7 cells treated with CEDSs using nine miRNA sequences demonstrated downregulation of 299 proteins (66.4%), upregulation of 77 proteins (17.1%), and minimal expressional change (±5%) of 74 proteins (16.4%) among 450 miRNA target proteins, which were identified by the current reports and the data on the miRDB and TargetScan websites. Consequently, the targeting ratio of miRNA sequence*-CEDS, defined as the number of downregulated miRNA target proteins by CEDS divided by the number of miRNA target proteins examined in this study, was 66.4% on average, with a maximum of 84% and a minimum of 57.5%. In addition, CEDS indirectly decreased and increased the expression of 95 and 72 proteins, respectively, which were not targeted by CEDS examined in this study (Table 12).

The results indicate that CEDS using a miRNA sequence may significantly downregulate the target proteins by approximately 66.4% in ratio, as observed in this study. However, there was still marked variation in the nine cases of CEDS experiments due to the limitation of the number of each miRNA target proteins in this study.

Table 12. The efficiency of CEDS-induced miRNA targeting in the protein expression (n=350) of RAW 264.7 cells

Mature miRNA (murine)	Downregulation of target protein (1)🔵	Indirect downregulation response (2)🔵	Indirect upregulation response (3)🔴	Minimal change (±5%) of target protein (4)🟢	Alternative upregulation of target protein (5)★	Targeting rate (%) $\frac{(1)}{(1)+(4)+(5)}x100$
miR-26a-5p	62	11	10	4	11	80.5%
miR-34a-5p	43	26	13	4	12	72.9%
miR-126-5p	46	15	13	20	14	57.5%
miR-150-5p	27	22	4	8	9	61.4%
miR-155-5p	27	8	9	9	9	60%
miR-181a-5p	21	4	7	1	3	84%
miR-216a-5p	21	7	2	4	2	77.8%
miR-365a-3p	19	3	9	9	5	57.6%
miR-655-3p	33	0	5	15	12	66%
Total number	299	95	72	74	77	66.4%

(1) – (5): number of proteins,

IP-HPLC analysis for the changes of the protein signaling after CEDS targeting different protein binding site sequences in RAW 264.7 cells

In addition to mature miRNA sequences, various protein binding site sequences located throughout genomic DNAs may also be favorable targets for CEDS. Among many protein binding site sequences in murine genomic DNA, four binding site sequences including telomere sequence (TTAGGG), canonical E-box sequence (CACGTG), p53 cluster 1 response element (RE) binding site sequence (AGACATGCCT), and canonical E2Fs binding site sequence (TTTC(C/G)CGC) were selected for the application of CEDS in this study.

The telomere repeat sequence (TTAGGG)*-CEDS influenced the protein signaling in RAW 264.7 cells

Telomere repeat sequences (TTAGGG) facilitate the replication of chromosome ends and the generation of a T-loop with a telomere-binding protein complex, shelterin, to prevent chromosomal degradation. Telomere shortening and instability can induce aging and various diseases due to telomere dysfunction and chromosomal instability. Furthermore, they can form the G-quadruplex structure with the external Hoogsteen bonding strength, which plays an important role in chromatin protection, DNA replication, transcription, and genomic stability. In the present study, a telomere repeat sequence TTAGGG, was selected for CEDS experiment on RAW 264.7 cells (Fig. 19A).

The IP-HPLC results demonstrated that the TTAGGG*-CEDS suppressed protein signaling, including proliferation, the cMyc/MAX/MAD network, Wnt1/β-catenin signaling, p53/Rb/E2F1 signaling, SHH/PTCH/GLI signaling, protein translation, miRNA biogenesis, growth factors, cytodifferentiation, RAS signaling, ER stress, survival, acute inflammation, PARP-mediated apoptosis, fibrosis, oncogenesis, senescence, and telomere signaling. Concurrently, CEDS activated protein signaling, such as Notch/Jagged signaling, epigenetic modification, osteogenesis, neuromuscular differentiation, NFkB signaling, protection, angiogenesis, innate immunity, cellular immunity, chronic inflammation, p53-mediated apoptosis, FAS-mediated apoptosis, and glycolysis signaling compared to the untreated controls.

The proliferating signaling was suppressed by downregulating the telomere-associated proteins Ki-67 (87.9%), PCNA (82.9%), CDK4 (82.9%), p21 (89.8%), and nucleolin (92.8%), as well as coincidentally downregulating PLK4 (92.8%) and p15/16 (89.3%) and upregulating p14 (123.8%) and CHK1 (127.7%).

The cMyc/MAX/MAD network was suppressed by downregulating the telomere-associated protein MAX (92.8%) and coincidentally downregulating MAD1 (91.9%).

The Wnt/β-catenin signaling was suppressed by downregulating the telomere-associated proteins TCF1 (85.2%) and Snail1 (78.1%), and coincidentally downregulating APC (94.6%), despite the upregulation of Wnt1 (121.8%), β-catenin (131.6%), and AXIN2 (111.7%).

The p53/Rb/E2F1 signaling suppressed by downregulating the telomere-associated proteins p53 (77%), Rb1 (93.2%), CDK4 (82.9%), and E2F1 (83.3%), despite the downregulation of E2F4 (80.3%).

The SHH/PTCH/GLI signaling was suppressed by downregulating the telomere-associated proteins GLI (83.3%) and coincidentally downregulating PTCH1 (92%).

The protein translation signaling was suppressed by downregulating the telomere-associated proteins, eIF2α (91.5%), as well as coincidentally downregulating DOHH (89.8%) and eIF5A1 (91.9%), despite the coincidental upregulation of eIF2AK3 (127.4%).

The miRNA biogenesis signaling was suppressed by downregulating the telomere-associated proteins AGO2 (82%), despite the upregulation of TRBP2 (138.8%) and GW182 (105.3%) and the downregulation of MTDH (92.2%).

The growth factor signaling were partially suppressed by downregulating the telomere-associated proteins EGFR (90%), IGF1 (85.8%), TGFβ3 (78.5%), and Met (90.9%), despite the upregulation of the telomere-associated protein FGF2 (106.4%) and coincidental upregulation of GHRH (118.1%), IGF2R (107.1%), ALK1 (105.4%), SMAD2/3 (107%), SMAD4 (110.6%), SMAD7 (109.3%), FGF7 (107.3%), and ERβ (111.1%).

The cytodifferentiation signaling were partially suppressed by downregulating the telomere-associated protein Ep-CAM (85.5%) and coincidentally downregulating β-actin (69.6%), calnexin (96.3%), CRIP1 (88.1%),

AP1M1 (68%), SOSTDC1 (75.5%), and tenascin C (91.3%), despite the upregulation of GAPDH (111.1%), vimentin (108.3%), CaM (105.6%), DLX2 (123%), and caveolin1 (116.2%).

The RAS signaling was suppressed by downregulating the telomere-associated proteins, NRAS (79.6%), PI3K (88.9%), PTEN (79.1%), AMPKα (82.5%), JAK2 (89%), and PKC (86.4%), as well as coincidentally downregulating PKA1α (93.7%), PLC-β2 (84.2%), and TYK2 (90.6%), despite the upregulation of the telomere-associated proteins p-ERK1 (142.5%) and STAT3 (105.3%) and the coincidental upregulation of HRAS (119.5%), Rab1 (108.4%), MEKK (106.1%), AKAP13 (113.3%), p-JNK1 (116%), p-PKC1α (117%), and SOS1 (118.5%).

The ER stress pathway was suppressed by downregulating the telomere-associated proteins eIF2α (91.5%), GADD153 (85%), p-GADD153 (91.3%), IRE1α (94.3%), and LC3β (91.7%), despite the upregulation of HSP27 (135.8%), eIF2AK3 (127.4%), and BIP (124.1%).

The survival signaling was suppressed by downregulating the telomere-associated proteins SP1 (72.4%) and sirtuin6 (85.2%), despite the upregulation of sirtuin1 (111.8%), sirtuin3 (106.5%), and sirtuin7 (116.3%).

The acute inflammation signaling was suppressed by downregulating the telomere-associated proteins IL1 (93.2%), MCP1 (90.5%), and CRP (90.7%), despite the upregulation of TRAF6 (109.2%) and MIF (114%).

The PARP-mediated apoptosis signaling was suppressed by downregulating the telomere-associated proteins, PARP1 (94%) and c-PARP (93.8%).

The fibrosis signaling was suppressed by downregulating collagen 3A1 (90.9%), FGF1 (82.9%), laminin α5 (93.9%), integrin α5 (89.2%), integrin β1 (86.9%), α1-antitrypsin (91.6%), and tenascin C (91.3%), as well as upregulating FGF7 (107.3%), the despite the upregulation of the telomere-associated protein FGF2 and coincidental upregulation of uPA (121%) and PAI1 (113.6%).

The senescence signaling was suppressed by downregulating the telomere-associated proteins klotho (85.1%), sirtuin6 (85.2%), and p21 (89.8%), despite the upregulation of the telomere-associated protein sirtuin1 (111.8%) and the coincidental upregulation of sirtuin3 (106.5%), sirtuin7 (116.3%), and caveolin1 (116.2%).

The telomere signaling was suppressed by downregulating the telomere-associated proteins TERT (88.3%), TRF1 (89.9%), and TIN2 (69.3%).

Conversely, **the Notch/Jagged signaling** was activated by upregulating the telomere-associated proteins Notch1 (109.6%) and coincidentally upregulating Jagged2 (115.9%).

The osteogenesis signaling appears to be activated by upregulating BMP2 (107.4%), BMP3 (133.2%), BMP4 (115%), RUNX2 (106.5%), OPG (112%), and RANKL (122.1%), despite the downregulation of osteocalcin (92.8%) and aggrecan (82.5%).

The neuromuscular differentiation signaling were activated by upregulating NSEγ (120.4%), GFAP (106.2%), NK1R (111.1%), S100 (109.1%), and αSMA (106.1%), despite the downregulation of myosin1a (84.6%) and desmin (78.3%).

The NFkB signaling was activated by upregulating the telomere-associated proteins NFkB (112.4%), p38 (118.1%), and mTOR (113%), as well as coincidentally upregulating IKK (115.7%), MDR (125.7%), and GADD45 (114.4%), despite the downregulation of the telomere-associated proteins NFAT5 (73.8%) and the coincidental downregulation of NFATc1 (94.9%).

The protection signaling was activated by upregulating the telomere-associated proteins HSP27 (135.8%), HO1 (128%), FOXO3 (125.9%), NRF2 (124.1%), HSP70 (121%), and GSTO1/2 (107.3%), as well as coincidentally upregulating SOD1(108.1%) and ALDH1A1 (106.1%), despite the downregulation of the telomere-associated proteins FOXO1 (87.4%) and HSP90 (84.8%), and the coincidental downregulation of leptin (94.8%), FOXP (92.1%), and NOS1 (79.7%).

The angiogenesis signaling was activated by upregulating the telomere-associated proteins VEGFA (111.9%), FGF2 (106.4%), as well as coincidentally upregulating VEGFC (119.1%), vWF (109.7%), LYVE1 (111.6%), TEM8 (127.6%), CMG2 (105.1%), and endothelin1 (116.2%), despite the downregulation of the telomere-associated proteins HIF1α (82.9%), VEGFR2 (85.8%), CD106 (85.6%), angiogenin (72%), and PDGFA (89.2%) and the coincidental downregulation of endocan (74.8%).

The innate immunity signaling appears to be activated by upregulating lactoferrin (110.1%), CAMP (125.8%), β-defensin1 (109.6%), β-defensin2 (111%), TLR2 (108.1%), and elafin (118.5%), despite the downregulation of the telomere-associated proteins CD56 (90.5%) and TLR3 (82%), as well as coincidental downregulation of α1-antitrypsin (91.6%).

The cellular immunity signaling was activated by upregulating the telomere-associated proteins CD44 (129.7%) and coincidentally downregulating the telomere-associated proteins CD34 (80.6%), PD1 (84.3%), and CTLA4 (92.5%), despite the upregulation of CD8 (121.5%), CD20 (118%), CD28 (114.2%), CD40 (139.2%), CD99 (123.8%), and perforin (129.5%).

The chronic inflammation signaling was activated by upregulating the telomere-associated proteins IL6 (123.4%), IL10 (112.5%), and COX2 (133%), as well as coincidentally upregulating lysozyme (111.2%), MMP2 (129.7%), cathepsin C (114.7%), and COX1 (128.2%), despite the downregulation of the telomere-associated proteins CD68 (87.9%) and CD106 (87%), and the coincidental downregulation of M-CSF (79.9%), TIMP1 (85.8%), TIMP2 (92.9%), LTA4H (85.6%), and kininogen (79.6%).

The p53-mediated apoptosis signaling appears to be activated by upregulating p73 (106.1%), PUMA (113.8%), and NOXA (111.7%) and the alternative upregulation of c-caspase9 (111.1%) and caspase3 (130.3%), despite the downregulation of the telomere-associated proteins p53 (77%) and p63 (84.2%), and coincidental downregulation of BAD (94.4%) and APAF1 (94.1%), and upregulation BCL2 (128%).

The FAS-mediated apoptosis signaling was activated by upregulating FAS (115%), BID (114%), caspase8 (109.6%), and caspase3 (130.1%).

The glycolysis signaling was activated by upregulating the telomere-associated proteins LDHA (117%) and GAPDH (111.1%), as well as coincidentally upregulating GLUT1 (124.5%) and HK2 (121.8%), despite the downregulation of LGR4 (89.4%) and TIGAR (86.2%).

In addition, the TTAGGG*-CEDS variably influenced **the epigenetic modification signaling** by upregulating the telomere-associated proteins involved in DNA methylation/acetylation such as KDM4D (107.1%), M BD4 (112.4%), and HMGB1 (116.3%), while downregulating EZH2 (73.2%), PCAF (90.9%), and

HMGA2 (83.6%). Consequently, the TTAGGG*-CEDS induced a trend towards an increase in the methylation of histones and DNAs, and transcriptional repression.

The TTAGGG*-CEDS broadly affected **the oncogenesis signaling** by upregulating the telomere-associated proteins such as BRCA1 (126.5%), cMyb (127.7%), ATM (118.2%), YAP1 (111.6%), and PIM1 (108%), as well as coincidentally upregulating CEA (130.8%), AXL (125%), NF1 (112.7%), and ZEB1 (112. 4%), while it also downregulated telomere-associated proteins such as ATR (85%), Ets1 (78.4%), and BACH1 (74%), as well as coincidentally downregulated CRK (94. 8%), 14-3-3 (92.6%), MTDH (92.2%), KLF4 (91.4%), MTA2 (90.1%), CRIP1 (88.1%), HER2 (81.5%), EWSR (86.4%), (84.5%), PDCD4 (84.2%), and TWIST1 (74.1%). Among the 28 oncoproteins, 14 were found to be underexpressed, 10 were overexpressed, and four exhibited minimal change in expression compared to the untreated controls.

Consequently, the telomere sequence (TTAGGG)*-CEDS significantly impacted the entire protein signaling in RAW 264.7 cells. The TTAGGG*-CEDS primary inhibited the RAS signaling, subsequently inactivating the protection-ER stress-survival signaling axis, the p53- and FAS-mediated apoptosis signaling axis, and the telomere-oncogenesis-PARP-associated apoptosis-fibrosis axis. Conversely, the TTAGGG*-CEDS activated NF-kB signaling, subsequently stimulating epigenetic modification-protection-angiogenesis signaling axis, p53- and FAS-mediated apoptosis-glycolysis-chronic inflammation signaling axis (Fig. 19B, Table 13).

The results demonstrate that the TTAGGG*-CEDS significantly inhibited cell proliferation, ER stress, survival, cellular senescence, telomere instability, and oncogenesis. Concurrently, it enhanced ROS protection, angiogenesis, apoptosis, glycolysis, and chronic inflammation. It is found that the TTAGGG*-CEDS induced cellular stress in the absence of survival and proliferation, which resulted in the anti-oncogenic effect with extensive apoptosis. It is noteworthy that the TTAGGG*-CEDS has the potential to enhance innate and cellular immunity.

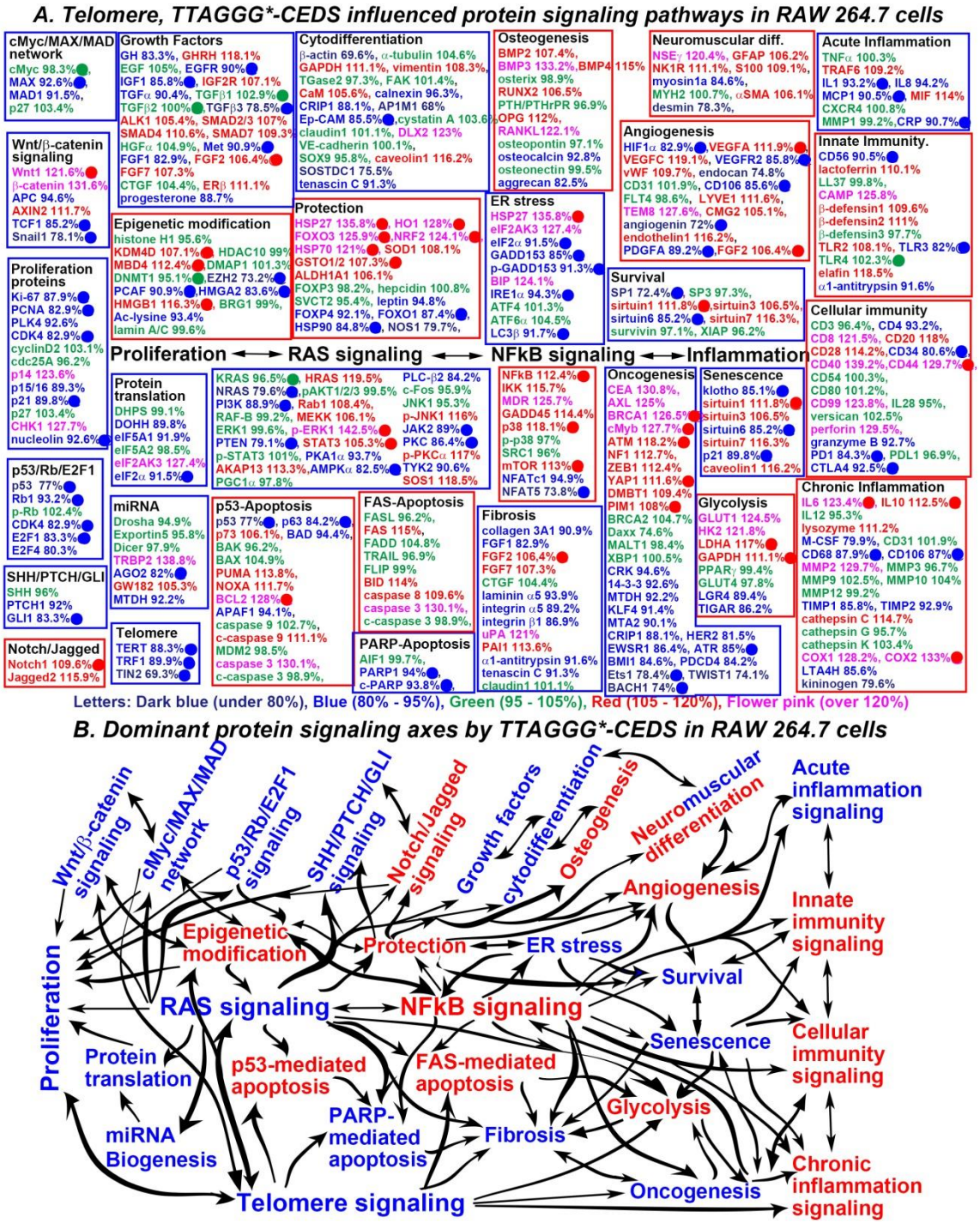

Fig. 19. The telomere sequence (TTAGGG)*-CEDS influenced the protein signaling (A) and axes (B) in RAW 264.7 cells. The IP-HPLC results revealed proteins that were downregulated (blue), upregulated (red), and minimally changed (green) compared to the untreated controls. Dominantly suppressed (blue square) and activated (red square) signaling. Telomere-associated proteins (Harmonizome 3.0), downregulated (●) or upregulated (●) by the TTAGGG*-CEDS.

Table 13. Protein expressions in the RAW 264.7 cells treated with telomere sequence (TTAGGG)*-CEDS.

Signaling	Downregulated Proteins	Upregulated Proteins
Proliferation	**Ki-67, PCNA**, PLK4, **CDK4**, p15/16, **p21**, **nucleolin**	p14, CHK1
cMyc/MAX/MAD network	**MAX**, MAD1	
Wnt/β-catenin signaling	APC, **TCF1, Snail**	**Wnt1**, β-catenin, AXIN2
p53/Rb/E2F1 signaling	**p53**, **Rb1**, **CDK4**, **E2F1,** E2F4	
SHH/PTCH/GLI signaling	PTCH1, **GLI1**	
Notch/Jagged signaling		**Notch1**, Jagged2
Epigenetic modification	**EZH2, PCAF, HMGA2**, Ac-lysine	**KDM4D**, **MBD4, HMGB1**
Protein translation	DOHH, eIF5A1, **eIF2α**	eIF2AK3
miRNA biogenesis	**AGO2**, MTDH	TRBP2, GW182
Growth factors	GH, **EGFR, IGF1**, TGFα, **TGFβ3**, **Met,** FGF1, progesterone	GHRH, IGF2R, ALK1, SMAD2/3, SMAD4, SMAD7, HGFα, **FGF2**, FGF7, ERβ
Cytodifferentiation	β-actin, calnexin, CRIP1, AP1M1**, Ep-CAM,** SOSTDC1, tenascin C	GAPDH, vimentin, CaM, DLX2, caveolin1
Osteogenesis	osteocalcin, aggrecan	BMP2, BMP3, BMP4, RUNX2, OPG, RANKL
Neuromuscular differentiation	myosin-1a, desmin	NSEγ, GFAP, NK1R, S100, αSMA
RAS signaling	**NRAS, PI3K, PTEN**, PKA1α, **AMPKα**, PLCβ2, **JAK2, PKC**, TYK2	HRAS, Rab1, MEKK, **p-ERK1, STAT3**, AKAP13, p-JNK1, p-PKC1α, SOS1
NFkB signaling	SRC1, NFATc1, **NFAT5**	**NFkB**, IKK, MDR, GADD45, **p38, mTOR**
p53-mediated apoptosis	**p53, p63,** BAD, APAF1	p73, BAK, PUMA, NOXA**, BCL2,** x-xaspase9, caspase3
FAS-mediated apoptosis	FASL	FAS, FADD, BID, caspase8, caspase3
PARP-mediated apoptosis	**PARP1, c-PARP**	
Protection	leptin, FOXP4, **FOXO1, HSP90**, NOS1	**HSP27**, **HO1, FOXO3, NRF2, HSP70**, SOD1, **GSTO1/2**, ALDH1A1
ER stress	**eIF2α, GADD153, p-GADD153, IRE1α, LC3β**	**HSP27**, eIF2AK3, BIP
Angiogenesis	**HIF1α, VEGFR2**, endocan, **CD106, angiogenin**, **PDGFA**	**VEGFA**, VEGFC, vWF, LYVE1, TEM8, CMG2, enthelin1, FGF2
Survival	**SP1**, **sirtuin6**	**sirtuin1**, sirtuin3, sirtuin7
Acute inflammation	**IL1**, IL8, **MCP1**, **CRP**	TRAF6, MIF
Innate immunity	**CD56, TLR3**, α1-antitrypsin	Lactoferrin, CAMP, β-defensin1, β-defensin2, TLR2, elafin
Cellular immunity	CD4, **CD34**, granzyme B, **PD1, CTLA4**	CD8, CD20, CD28, CD40, **CD44**, CD99, perforin
Chronic inflammation	M-CSF, **CD68, CD106**, TIMP1, TIMP2, LTA4H, kininogen	**IL6, IL10**, lysozyme, MMP2, cathepsin C, COX1, **COX2**
Glycolysis	LGR4, PPARγ, TIGAR,	GLUT1, HK2, **LDHA, GAPDH**
Fibrosis	collagen 3A1, FGF1, laminin α5, integrin α5, integrin β1, α1-antitrypsin, tenascin C	**FGF2,** FGF7, uPA, PAI1
Oncogenesis	CRK, 14-3-3, MTDH, KLF4, MTA2, CRIP1, HER2, EWSR1, **ATR**, BMI1, PDCD4, **Ets1,** TWIST1, **BACH1**	CEA, AXL, **BRCA1, cMyb, ATM**, NF1, ZEB1, **YAP1**, DMBT1, **PIM1**
Senescence	**klotho, sirtuin6, p21**	**sirtuin1**, sirtuin3, sirtuin7, caveolin1
Telomere signaling	**TERT, TRF1, TIN2**	

The telomere sequence*-CEDS, TTAGGG*-CEDS induced the suppression (**blue**) and activation (**red**) of signaling by downregulating (**blue**) and upregulating (**red**) the proteins, respectively. The data were compared to the reports of recent manuscripts and Harmonizome 3.0 website.

The canonical E-box sequence (CACGTG)*-CEDS influenced the protein signaling in RAW 264.7 cells

The E-box binding proteins play a pivotal role in regulating transcription activity for genome-wide transcription of numerous genes. Their numbers and types vary depending on the binding specificity of E-box. In the consensus sequences of E-box, CANNTG, the canonical E-box sequence CACGTG, was selected for the present CEDS study. As the canonical E-box is preferentially bound by cMyc, it is hypothesized that the canonical E-box sequence (CACGTG)*-CEDS may affect the interaction between cMyc and the canonical E-box sequence, resulting in transcriptional changes of the cMyc target protein genes (Fig. 20A).

The IP-HPLC results demonstrated that the CACGTG*-CEDS suppressed protein signaling, including proliferation, the cMyc/MAX/MAD network, Wnt1/β-catenin signaling, p53/Rb/E2F1 signaling, SHH/PTCH/GLI signaling, epigenetic modification, protein translation, miRNA biogenesis, growth factor, cytodifferentiation, ER stress, angiogenesis, survival, acute inflammation, innate immunity, FAS-mediated apoptosis, fibrosis, senescence, and telomere signaling. Concurrently, CEDS activated protein signaling, such as Notch/Jagged signaling, osteogenesis, neuromuscular differentiation, RAS signaling, NFkB signaling, protection, cellular immunity, chronic inflammation, p53-mediated apoptosis, PARP-mediated apoptosis, oncogenesis, and glycolysis signaling compared to the untreated controls.

The proliferating signaling was partially inactivated by downregulating the cMyc target proteins PCNA (90.6%), PLK4 (82.9%), and CDK4 (86.6%) and coincidentally upregulating p14 (116.1%), despite the downregulation of the cMyc target protein p15/16 (89.3%), p21 (91.7%), p27 (91.4%) and CHK1 (67.9%), and coincidental upregulation of nucleolin (116.5%).

The cMyc/MAX/MAD network was suppressed by downregulating the cMyc target protein cMyc (91.6%), MAX (87.7%), and p27 (91.4%) and coincidentally downregulating MAD1 (86.6%).

The Wnt/β-catenin signaling appears to be inactivated by downregulating the cMyc target proteins Wnt1 (92.2%) and TCF1 (82.4%), despite the upregulation of the cMyc target proteins β-catenin (107.5%) and APC (110.4%), and coincidental upregulation of AXIN2 (115%).

The p53/Rb/E2F1 signaling suppressed by downregulating the cMyc target proteins p53 (80.6%), CDK4 (86.6%), and E2F1 (91%) and upregulating Rb1 (107%), despite the downregulation of E2F4 (78.1%).

The SHH/PTCH/GLI signaling was suppressed by downregulating the cMyc target proteins SHH (89.8%), PTCH1 (90.1%), and GLI (83.5%).

The protein translation signaling appears to be inactivated by downregulating the cMyc target protein DHPS (90.6%) and coincidentally downregulating eIF2AK3 (73.4%).

The miRNA biogenesis signaling was inactivated by downregulating the cMyc target protein Drosha (88.4%) and coincidentally downregulating Exportin5 (92.1%), despite the upregulation of TRBP2 (128.8%) and the coincidental downregulation of the cMyc target protein MTDH (88.7%).

The growth factor signaling were partially inactivated by downregulating the cMyc target proteins, EGFR (92.2%) and Met (89.2%), and coincidentally downregulating EGF (85.5%), TGFβ3 (70.7%), SMAD2/3 (94.3%), and progesterone (92.7%), despite the upregulation of the cMyc target proteins SMAD4 (108.4%) and coincidental upregulation of GH (109.3%), IGF1 (111.9%), SMAD7 (104.4%), FGF7 (110.5%), CTGF (125.1%), and ERβ (110.8%).

The cytodifferentiation signaling were partially suppressed by downregulating the cMyc target proteins CRIP1 (83.5%) and Ep-CAM (85.9%), as well as coincidentally downregulating β-actin (85.3%), TGase2 (89.2%), AP1M1 (87.6%), DLX2 (94.4%), VE-cadherin (93.1%), SOSTD1 (79%), and tenascin C (90.5%), despite the upregulation of the cMyc target proteins FAK (106%), claudin1 (107.5%), and caveolin1 (109.5%) and coincidental upregulation of α-tubulin (108.3%), vimentin (125.3%), and calnexin (130.4%).

The ER stress pathway was inactivated by downregulating the cMyc target proteins eIF2AK3 (67%), p-GADD153 (90.6%), IRE1α (90.4%), and LC3β (92.9%), despite the upregulation of HSP27 (109.4%), BIP (130%), ATF4 (123.1%), and ATF6α (107.8%).

The angiogenesis signaling appears to be inactivated by downregulating VEGFR2 (89.9%), endocan (74.8%), CD31 (92%), CD106 (91%), LYVE1 (90.7%), CMG2 (94.1%), and angiogenin (77.4%), despite the upregulation of the cMyc target protein HIF1α (119.1%) and coincidentally upregulating VEGFC (109.6%), vWF (108%), endothelin1 (95.2%), and PDGFA (109.8%).

The survival signaling was suppressed by downregulating the cMyc target proteins SP1 (72.3%) and XIAP (91.1%), and coincidentally downregulating sirtuin6 (81.9%), despite the upregulation of sirtuin3 (118.6%) and sirtuin7 (106.7%).

The acute inflammation signaling appears to be inactivated by downregulating the cMyc target proteins IL1 (81.4%) and CXCR4 (93%), and coincidentally downregulating IL8 (89.4%), despite the slight upregulation of the cMyc target protein TRAF6 (107.4%) and coincidental upregulation of TNFα (106.3%), MCP1 (107.7%), and MIF (107.6%).

The innate immunity signaling appears to be inactivated by downregulating CD56 (87.3%), TLR2 (77.1%), TLR3 (71.5%), and α1-antitrypsin (93.3%), despite the upregulation of the cMyc target protein TLR4 (108.9%) and coincidental upregulation of lactoferrin (127.5%) and elafin (116.5%).

The chronic inflammation signaling was inactivated by downregulating the cMyc target proteins IL12 (85.3%), M-CSF (82.1%), and LTA4H (81.9%) and coincidentally downregulating IL10 (92.3%), CD31 (92.4%), CD106 (91.5%), TIMP1 (91.8%), TIMP2 (86.6%), cathepsin K (91.9%), COX1 (79%), and kininogen (84.7%), despite the upregulation of the cMyc target protein COX2 (106.1%) and coincidental upregulation of lysozyme (127.2%), MMP2 (105%), MMP9 (111.4%), MMP10 (125.6%), MMP12 (122.3%), cathepsin C (113.1%), and cathepsin G (126.9%).

The FAS-mediated apoptosis signaling was suppressed by downregulating the cMyc target proteins FASL (83.6%), FAS (89.3%), FLIP (94.5%), and caspase8 (90.3%), despite the upregulation of the cMyc target proteins TRAIL (136.7%) and caspase3 (116.2%), and coincidental upregulation of FADD (126.7%).

The fibrosis signaling was suppressed by downregulating the cMyc target proteins collagen 3A1 (82.9%), integrin α5 (88.4%), integrin β1 (82.7%), and PAI1 (94.4%) and coincidentally downregulating laminin α5 (87.1%), α1-antitrypsin (93.3%), and tenascin C (91.3%) and upregulating FGF7 (110.5%), despite the upregulation of CTGF (125.1%).

The senescence signaling appears to be was suppressed by downregulating the cMyc target proteins klotho (80.7%) and p21 (91.7%), and coincidentally downregulating sirtuin6 (81.9%), despite the upregulation

of the cMyc target protein caveolin1 (109.5%) and coincidental upregulation of sirtuin3 (118.6%) and sirtuin7 (106.7%).

The telomere signaling was suppressed by downregulating the cMyc target proteins TERT (87.1%), TRF1 (87.6%), and TIN2 (67.6%).

Conversely, **the Notch/Jagged signaling** was activated by upregulating the cMyc target proteins Notch1 (109.6%) and coincidentally upregulating Jagged2 (115.9%).

The osteogenesis signaling was activated by upregulating the cMyc target proteins BMP2 (134.8%), RUNX2 (109.1%), and RANKL (113.7%) and coincidentally upregulating BMP4 (130.8%), osterix (108.9%), OPG (110.3%), osteopontin (105.8%), and osteonectin (105.4%), despite the downregulation of PTH/PTHrPR (74.5%), osteocalcin (94.7%), and aggrecan (82.7%).

The neuronal differentiation signaling was activated by upregulating the cMyc target protein S100 (109.1%) and coincidentally upregulating NSEγ (105.5%) and NK1R (108.9%), despite the downregulation of GFAP (91.7%) , while **the muscular differentiation signaling** was inactivated by downregulating the cMyc target protein MYH2 (86.1%) and coincidental downregulation of myosin-1a (86.2%), MYH2 (86.1%), and desmin (77.4%).

The RAS signaling appears to be activated by upregulating the cMyc target proteins NRAS (105.5%), pAKT1/2/3 (113.9%), p-STAT3 (110.3%), PKA1α (112.9%), c-Fos (115.3%), JAK2 (113.1%), p-PKCα (119.5%), and SOS1 (125.4%) and coincidentally upregulating PLCβ2 (111.7%), despite the downregulation of the cMyc target proteins PI3K (89.9%), p-ERK1 (78.7%), PTEN (85.2%), and AMPKα and coincidental downregulation of Rab1 (88.5%) and p-TYK2 (75.8%).

The NFkB signaling was activated by upregulating the cMyc target proteins NFkB (123.4%), MDR (125.6%), GADD45 (121%), p38 (117%), SRC1 (108%), and mTOR (108.4%), despite the downregulation of the cMyc target proteins p-p38 (86.5%), NFATc1 (94.9%), and NFAT5 (76.4%).

The protection signaling appears to be activated by upregulating the cMyc target protein FOXO3 (122.4%) and coincidentally upregulating FOXP4 (124.2%), HSP27 (109.4%), NRF2 (109.4%), HO1 (108%),

GSTO1/2 (107%), and SOD1 (106.9%), despite the downregulation of the cMyc target proteins FOXO1 (86.4%), HSP70 (87%), and HSP90 (79.1%) and coincidental downregulation of NOS1 (80.7%).

The cellular immunity signaling appears to be activated by upregulating the cMyc target proteins CD54 (105.6%) and PDL1 (105.8%) and coincidentally upregulating CD28 (112.8%), CD40 (141.2%), IL28 (119%), and perforin (138.6%), despite the downregulation of the cMyc target proteins PD1 (82.2%) and coincidental downregulation of CD8 (91.2%), CD20 (86.9%), and CD34 (81.7%).

The p53-mediated apoptosis signaling was activated by upregulating the cMyc target proteins p73 (121.5%), BAK (105%), PUMA (106.5%), NOXA (107.8%), BAX (114.3%), BCL2 (106%), and caspase3 (116.2%) and coincidentally upregulating BAD (105%), caspase9 (114.8%), and c-caspase9 (114.3%), despite the downregulation of p53 (80.6%) and p63 (86.3%).

The PARP-mediated apoptosis signaling was activated by upregulating PARP1 (110.6%) and c-PARP (118.9%).

The glycolysis signaling appears to be activated by upregulating the cMyc target proteins HK2 (129.6%), LDHA (109%) and coincidentally upregulating GAPDH (104.8%) and GLUT1 (106%), despite the downregulation of the cMyc target protein TIGAR (79%) and coincidental downregulation of GLUT4 (88.4%).

In addition, the canonical E-box sequence*-CEDS, CACGTG*-CEDS, markedly influenced **the epigenetic modification signaling** by downregulating the cMyc target proteins KDM4D (87.2%), EZH2 (91.9%), and BRG1 (93.2%) and coincidentally downregulating histone H1 (94.4%) and PCAF (93.5%), while it upregulated the cMyc target protein DNMT1 (118%) and lamin A/C (105.6%), as well as coincidentally upregulated MBD4 (118%) and Ac-lysine (122%). Consequently, the CACGTG*-CEDS induced a trend towards a reduction in the methylation of histones and DNAs, and attenuation of transcriptional repression.

The canonical E-box sequence*-CEDS significantly suppressed **the oncogenesis signaling** by downregulating the cMyc target proteins TWIST (94%), BRCA1 (93.3%), PDCD4 (92.9%), MTA2 (90.5%), MTDH (88.7%), ATR (84.9%), HER2 (83.9%), CRIP1 (83.5%), BRCA2 (83.2%), and Ets1 (80.9%) and coincidentally downregulating BMI1 (94.8%), while it widely enhanced **the oncogenesis signaling** by

upregulating the cMyc target proteins ZEB1 (127.2%), cMyb (118.1%), YAP1 (116.7%), and KLF4 (113.2%) and coincidentally upregulating XBP1 (133.8%), NF1 (133.3%), ATM (130.9%), CEA (128.9%), AXL (122.2%), EWSR1 (120.1%), PIM1 (117.2%), DMBT1 (113%), 14-3-3 (111%), and CRK (109.2%). Among the 28 oncoproteins, 14 were found to be overexpressed, 11 were underexpressed, and three exhibited minimal change in expression compared to the untreated controls.

Consequently, the canonical E-box sequence (CACGTG)*-CEDS strongly impacted the entire protein signaling in RAW 264.7 cells. The CACGTG*-CEDS primary enhanced the RAS-NFkB signaling axis, subsequently activating epigenetic modification-protection-Notch/Jagged-osteogenesis signaling axis, p-53 and PARP- mediated apoptosis signaling axis, glycolysis-oncogenesis-chronic inflammation, and cellular immunity signaling axis, while it inactivated proliferation-related signaling axis, ER stress-angiogenesis-survival-senescence-acute inflammation-innate immunity signaling axis, and FAS-mediated apoptosis-fibrosis-telomere signaling axis (Fig. 20B, Table 14).

The results indicate that the CACGTG*-CEDS increased ROS protection, p53- and PARP-mediated apoptosis, glycolysis, oncogenesis, and chronic inflammation in RAW 264.7 cells, but decreased proliferation, ER stress, angiogenesis, survival, senescence, acute inflammation, FAS-mediated apoptosis, and telomere instability, thereby, providing oncogenic environment with a reduced potential of cytodifferentiation, regeneration, wound healing, and innate and cellular immunity in the cells.

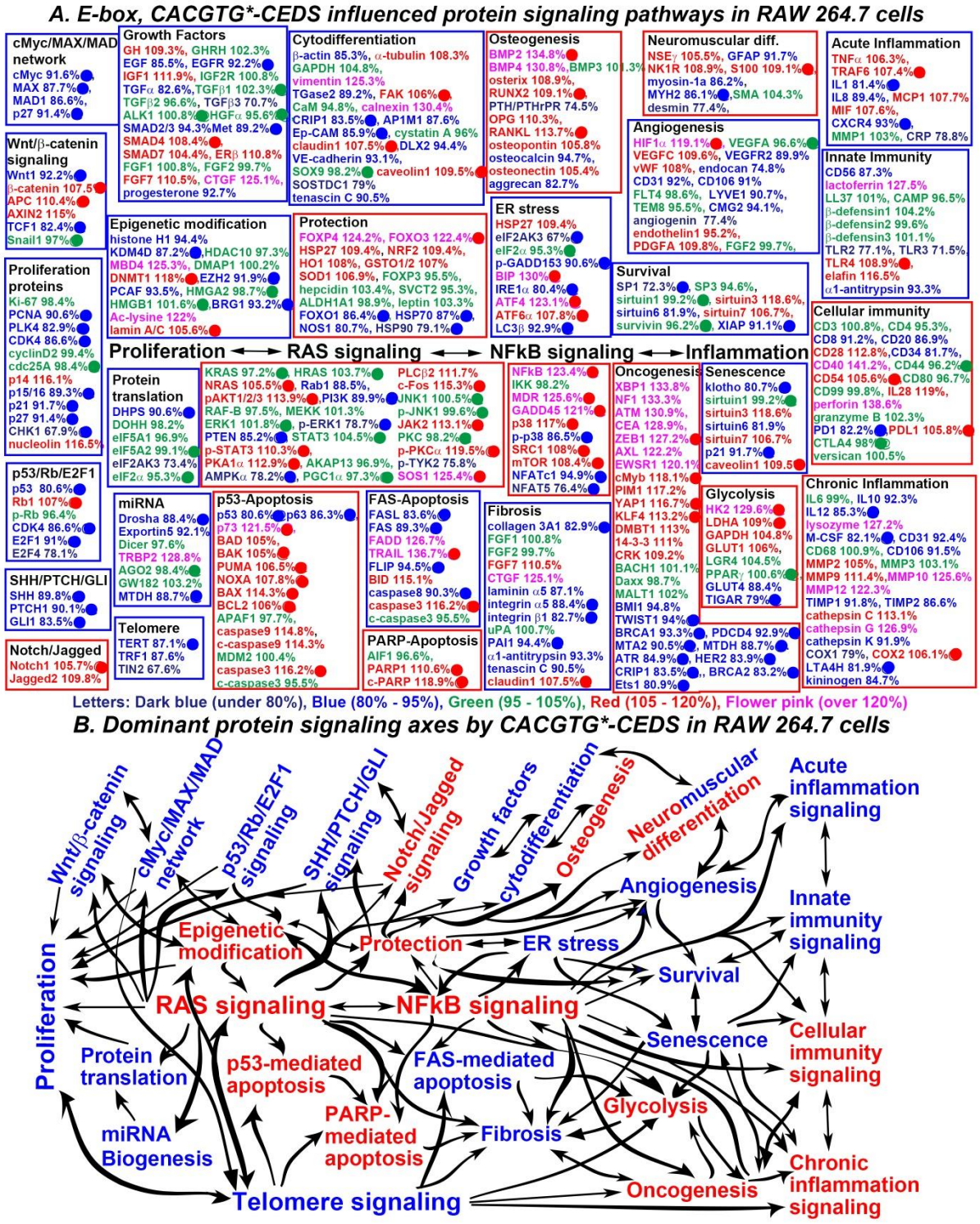

Fig. 20. The canonical E-box sequence (CACGTG)*-CEDS influenced the protein signaling (A) and axes (B) in RAW 264.7 cells. The IP-HPLC results revealed proteins that were downregulated (**blue**), upregulated (**red**), and minimally changed (**green**) compared to the untreated controls. Dominantly suppressed (**blue square**) and activated (**red square**) signaling. cMyc target proteins (Harmonizome 3.0), downregulated (●) or upregulated (●) by the CACGTG*-CEDS.

Table 14. Protein expressions in the RAW 264.7 cells treated with canonical E-box sequence (CACGTG)*-CEDS.

Signaling	Downregulated Proteins	Upregulated Proteins
Proliferation	**PCNA, PLK4, CDK4, p15/16, p21, p27, CHK1**	p14, nucleolin
cMyc/MAX/MAD network	**cMyc, MAX**, MAD1, **p27**	
Wnt/β-catenin signaling	**Wnt1, TCF1**	**β-catenin, APC**, AXIN2
p53/Rb/E2F1 signaling	**p53, CDK4, E2F1**, E2F4	**Rb1**
SHH/PTCH/GLI signaling	**SHH, PTCH1, GLI1**	
Notch/Jagged signaling		**Notch1**, Jagged2
Epigenetic modification	histone H1, **KDM4D, EZH2, BRG1**	MBD4, **DNMT1**, Ac-lysine, **lamin A/C**
Protein translation	**DHPS**, eIF2AK3	
miRNA biogenesis	**Drosha**, Exportin5, **MTDH**	TRBP2
Growth factors	EGF, **EGFR**, TGFα, TGFβ3, SMAD2/3, **Met**, progesterone	GH, IGF1, **SMAD4**, SMAD7, FGF7, CTGF, ERβ
Cytodifferentiation	β-actin, TGase2, **CRIP1**, AP1M1, **Ep-CAM**, cystatin A, DLX2, VE-cadherin, SOSTDC1, tenascin C	α-tubulin, vimentin, **FAK**, calnexin, **claudin1**, **caveolin1**
Osteogenesis	PTH/PTHrPR, osteocalcin, aggrecan	**BMP2**, BMP4, osterix, **RUNX2**, OPG, **RANKL**, osteopontin, osteonectin
Neuromuscular differentiation	GFAP, myosin-1a, **MYH2**, desmin	NSEγ, NK1R, **S100**
RAS signaling	**PI3K**, Rab1, **p-ERK1, PTEN, AMPKα**, p-TYK2	**NRAS, pAKT1/2/3, p-STAT3, PKA1α**, PLCβ2, **c-Fos, JAK2, p-PKC1α, SOS1**
NFkB signaling	**p-p38, NFATc1, NFAT5**	**NFkB, MDR, GADD45, p38, SRC1, mTOR**
p53-mediated apoptosis	**p53, p63**	**P73, BAD, BAK, PUMA, NOXA, BAX, BCL2**, caspase9, c-caspase9, **caspase3**
FAS-mediated apoptosis	**FASL, FAS, FLIP, caspase8**	FADD, **TRAIL**, BID, **caspase3**
PARP-mediated apoptosis		**PARP1, c-PARP**
Protection	**FOXO1, HSP70**, NOS1, **HSP90**	**FOXP4**, FOXO3, HSP27, NRF2, HO1, GSTO1/2, SOD1
ER stress	**eIF2AK3, p-GADD153, IRE1α, LC3β**	HSP27, **BIP, ATF4, ATF6α**
Angiogenesis	VEGFR@, endocan, CD31, CD106, LYVE1, CMG2, angiogenin	**HIF1α**, VEGFC, vWF, endothelin1, PDGFA
Survival	**SP1**, sirtuin6, **XIAP**	sirtuin3, sirtuin7
Acute inflammation	**IL1**, IL8, **CXCR4**	TNFα, **TRAF6**, MCP1, MIF
Innate immunity	CD56, TLR2, TLR3, α1-antitrypsin	Lactoferrin, **TLR4**, elafin
Cellular immunity	CD8, CD20, CD34, **PD1**	CD28, CD40, **CD54**, IL28, perforin, **PDL1**
Chronic inflammation	IL10, **IL12, M-CSF**, CD31, CD106, TIMP1, TIMP2, cathepsin K, COX1, **LTA4H**, kininogen	Lysozyme, MMP2, MMP9, MMP10, MMP12, cathepsin C, cathepsin G, **COX2**
Glycolysis	GLUT4, **TIGAR**	**HK2, LDHA**, GAPDH, GLUT1
Fibrosis	**collagen 3A1**, laminin α5, **integrin α5, integrin β1, PAI1**, α1-antitrypsin, tenascin C	FGF7, CTGF, claudin1
Oncogenesis	BMI1, **TWIST1, BRCA1, PDCD4, MTA2, MTDH, ATR, HER2, CRIP1, BRCA2, Ets1**	XBP1, NF1, ATM, CEA, **ZEB1**, AXL, EWSR1, **cMyb**, PIM1, **YAP1, KLF4**, DMBT1, 14-3-3, CRK
Senescence	**klotho**, sirtuin6, **p21**	sirtuin3, sirtuin7, **caveolin1**
Telomere signaling	**TERT**, TRF1, TIN2	

The canonical E-box sequence*-CEDS, CACGTG*-CEDS induced the suppression (**blue**) and activation (**red**) of signaling by downregulating (**blue**) and upregulating (**red**) the proteins, respectively. The data were compared to the reports of recent manuscripts and Harmonizome 3.0 website.

The p53 binding site sequence (AGACATGCCT)*-CEDS influenced the protein signaling in RAW 264.7 cells

The consensus binding site of p53 response elements (REs) is comprised of two decameric DNA motifs, RRRCWWGYYY (R = A, G; W = A, T; Y = C, T), which are redundant, approximately palindromic, and separated by 0–18 bps[12]. In the present study, the decameric binding site sequence for p53 cluster 1 RE[21], AGACATGCCT was selected for CEDS experiment on KE cells.

The IP-HPLC results demonstrated that the AGACATGCCT*-CEDS suppressed protein signaling, including SHH/PTCH/GLI signaling, Notch/Jagged signaling, miRNA biogenesis, growth factors, neuromuscular differentiation, RAS signaling, NFkB signaling, protection, cellular immunity, chronic inflammation, FAS-mediated apoptosis, and senescence signaling. Concurrently, CEDS activated protein signaling, such as proliferation, cMyc/MAX/MAD network, Wnt/β-catenin signaling, p53/Rb/E2F1 signaling, epigenetic modification, protein translation, cytodifferentiation, osteogenesis, angiogenesis, survival, acute inflammation, innate immunity, p53-mediated apoptosis, PARP-mediated apoptosis, fibrosis, glycolysis, and telomere signaling compared to the untreated controls (Fig. 21A).

The SHH/PTCH/GLI signaling appear to be inactivated by downregulating the p53 target protein (GLI1 94.1%), despite the upregulation of the p53 target protein SHH (111.3%).

The Notch/Jagged signaling was suppressed by downregulating the p53 target protein Notch1 (90.6%) and coincidentally downregulating Jagged2 (92.8%).

The miRNA biogenesis signaling was suppressed by downregulating the p53 target proteins Dicer (83.9%) and AGO2 (92.4%), as well as coincidentally downregulating Drosha (93.4%), Exportin5 (85.4%), and GW182 (88.6%).

The growth factor signaling partially was partially inactivated by downregulating the p53 target proteins EGF (86.5%), EGFR (83.1%), TGFα (89.1%), SMAD4 (93.8%), SMAD7 (90%), Met (91.3%), and FGF2 (92.9%) and coincidentally downregulating TGFβ2 (89%), ALK1 (90.0%), and progesterone (87.9%), despite the upregulation of the p53 target proteins IGF2R (137%), TGFβ1 (108.8%), SMAD2/3 (117.8%), FGF7 (106.3%), and CTGF (109.2%) and coincidental upregulation of GH (124%), GHRH (129.1%), and FGF1 (128.6%).

The neuromuscular differentiation signaling appears to be inactivated by downregulating the p53 target proteins GFAP (91.5%) and coincidentally downregulating NSEγ (87.6%), myosin-1a (80.2%), and desmin (80.6%), despite the upregulation of the p53 target protein S100 (109.8%) and coincidental upregulation of NK1R (110.4%), MYH2 (108.5%), and αSMA (108.5%).

The RAS signaling was suppressed by downregulating the p53 target proteins KRAS (92.8%), HRAS (78.1%), pAKT1/2/3 (89.4%), PI3K (90.4%), MEKK (89.7%), and PGC1α (92.6%) and coincidentally downregulating p-JNK1 (94.2%), despite the upregulation of the p53 target proteins RAF-B (106.3%), ERK1 (112%), and PTEN (119.6%) and coincidental upregulation of PKA1α (112.6%), AKAP13 (121.6%), PLCβ2 (117.3%), JNK1 (120.6%), p-PKCα (132.6%), TYK2 (127.5%), and SOS1 (106%).

The NFkB signaling appears to be inactivated by downregulating the p53 target proteins NFkB (92.3%), GADD45 (92.6%), SRC1 (87%), and NFATc1 (86.7%) and coincidentally downregulating IKK (92.9%), despite the upregulation of the p53 target proteins p-p38 (111.3%), mTOR (108%), and NFAT5 (131.8%) and coincidental upregulation of MDR (125%).

The protection signaling was inactivated by downregulating the p53 target proteins SOD1 (93.5%), FOXP3 (92.4%), FOXO1 (91%), HSP90 (83.6%), and HSP70 (80.8%), as well as coincidentally downregulating GSTO1/2 (93.5%), NRF2 (93.9%), and leptin (90.3%), despite the upregulation of hepcidin (125.9%), ALDH1A1 (121%), and NOS1 (109.5%).

The cellular immunity signaling appear to be inactivated by downregulating the p53 target proteins CD54 (93.7%) and versican (93.1%), and coincidental downregulation of CD40 (86.9%) and perforin (67%), despite the upregulation of CD4 (142.6%), CD8 (121.1%), CD20 (110.7%), CD99 (114.2%), IL28 (111.9%), and granzyme B (111%) and downregulation of the p53 target proteins PDL1 (91.1%) and CTLA4 (91%).

The chronic inflammation signaling appears to be suppressed by downregulating the p53 target proteins IL6 (91.3%), IL12 (84.4%), MMP2 (84.8%), MMP9 (84%), and TIMP2 (93.8%), as well as coincidentally downregulating CD68 (76.9%), cathepsin C (88.4%), and COX1 (72.1%), despite the upregulation of the p53 target protein COX2 (113.7%) and coincidental upregulation of lysozyme (137.5%), M-CSF (114.1%), CD106 (110.3%), cathepsin C (88.4%), and COX1 (72.1%).

The FAS-mediated apoptosis signaling was suppressed by downregulating the p53 target proteins FASL (74.6%), FAS (87%), FADD (93.4%), and BID (85.2%) and coincidentally downregulating TRAIL (93.7%) and FLIP (89.7%), despite the alternative upregulation of the p53 target proteins caspase3 (119.8%) and c-caspase3 (117.3%).

The senescence signaling was suppressed by downregulating the p53 target proteins klotho (89.6%), sirtuin3 (93.5%), and sirtuin6 (92.2%), despite the upregulation of the p53 target protein sirtuin1 (116.5%).

Conversely, **the proliferating signaling** appears to be activated by upregulating the p53 target proteins PLK4 (105.1%), CDK4 (111.3%), cyclinD2 (127.7%), and CHK1 (112.6%) and downregulating p15/16 (93.8%), despite the downregulation of PCNA (91.2%) and nucleolin (74.8%).

The cMyc/MAX/MAD network was activated by upregulating the p53 target proteins MAX (95.1%) and downregulating MAD1 (88.9%).

The Wnt/β-catenin signaling was activated by upregulating the p53 target proteins β-catenin (111.7%), APC (109.3%), AXIN2 (112%), and Snail1 (117.3%).

The p53/Rb/E2F1 signaling appears to be activated by upregulating the p53 target proteins CDK4 (111.3%) and downregulating p53 (91.2%).

The protein translation signaling was activated by upregulating the p53 target proteins eIF5A1 (111.4%) and coincidentally upregulating DHPS (107%) and eIF2α (112.7%), despite the downregulation of the p53 target protein eIF5A2 (80.5%) and coincidental downregulation of DOHH (90.4%).

The cytodifferentiation signaling were partially activated by upregulating the p53 target protein CaM (132%) and coincidentally upregulating β-actin (128.8%), α-tubulin (107.4%), AP1M1 (108.4%), claudin1 (108%), SOX9 (113%), DLX2 (100.8%), and tenascin C (111.5%), despite the downregulation of TGase2 (81.7%), calnexin (93.9%), and VE-cadherin (87.1%).

The osteogenesis signaling was activated by upregulating BMP2 (114.7%), PTH/PTHrP-R (139.2%), OPG (139.5%), osteocalcin (106.6%), and aggrecan (129.8%), despite the downregulation of BMP3 (76.1%) and upregulation of SOSTDC1 (125.1%).

The angiogenesis signaling was activated by upregulating the p53 target protein HIF1α (147.1%) , as well as coincidentally upregulating VEGFC (118.3%), VEGFR2 (104.9%), vWF (110.3%), CD106 (110.3%), FLT4 (106.6%), LYVE1 (132.6%), and endothelin1 (115.1%), despite the downregulation of the p53 target protein endocan (91.4%), angiogenin (83.6%), and FGF2 (92.9%).

The survival signaling was activated by upregulating the p53 target proteins SP1 (107.8%), sirtuin1 (116.5%), and survivin (113%), despite the downregulation of the p53 target proteins sirtuin3 (93.5%) and sirtuin6 (92.2%).

The acute inflammation signaling was activated by upregulating the p53 target proteins IL1 (134.1%) and (CXCR4 125.1%), and coincidentally upregulating TRAF6 (106.8%), despite the downregulation of MCP1 83.1%.

The innate immunity signaling appears to be activated by upregulating the p53 target protein TLR3 (109.2%) and coincidentally upregulating TLR2 (110.4%), TLR4 (112.7%), and β-defensin1 (113.4%), despite the downregulation of the p53 target proteins lactoferrin (74.3%) and LL37 (81.1%), and coincidental downregulation of β-defensin2 (85.3%), β-defensin3 (94.2%), and α1-antitrypsin (66.7%).

The p53-mediated apoptosis signaling appears to be activated by upregulating the p53 target proteins BAD (111.9%), BAK (105.1%), caspase9 (105.2%), c-caspase9 (110%), caspase3 (119.8%), and c-caspase3 (117.3%), despite the downregulation of the p53 target proteins p53 (91.2%) and BCL2 (92.1%). **The PARP-mediated apoptosis signaling** was activated by upregulating the p53 target protein c-PARP (107.1%) and coincidentally upregulating AIF1 (109%).

The fibrosis signaling appears to be activated by upregulating the p53 target protein CTGF (109.2%), as well as coincidentally upregulating collagen 3A1 (117.9%), FGF1 (128.6%), laminin α5 (112.4%), tenascin C (111.5%), and claudin1 (108%) and upregulating the p53 target protein FGF7 (106.3%), despite the downregulation of the p53 target proteins FGF2 (92.9%), integrin α5 (90.9%), and integrin β1 (87.7%), and coincidental downregulation of uPA (91.2%), PAI1 (94.9%), and α1-antitrypsin (66.7%).

The glycolysis signaling was activated by upregulating the p53 target proteins TIGAR (116.1%), PPARγ (108.3%) and coincidentally upregulating HK2 (117.3%), despite the downregulation of the p53 target protein LDHA (80.8%).

The telomere signaling was activated by upregulating the p53 target protein TERT (126.9%), despite of slight downregulation of the p53 target protein TRF1 (93.7%).

In addition, the p53 binding site sequence*-CEDS significantly influenced **the epigenetic modification signaling** by downregulating the p53 target protein KDM4D (83.4%) and coincidentally downregulating histone H1 (92.4%) and HDAC10 (94.3%), while it upregulated the p53 target proteins EZH2 (133.5%), HMGA2 (128%), and lamin A/C (106.5%) and coincidentally upregulated MBD4 (108.4%), PCAF (111.6%), and Ac-lysine (109.7%). Consequently, the AGACATGCCT*-CEDS induced a trend towards an increase in the methylation of histones and DNAs, and transcriptional repression.

The p53 binding site sequence*-CEDS significantly suppressed **the oncogenesis signaling** by downregulating the p53 target proteins cMyb (87.6%), NF1 (84.5%), ZEB1 (83.6%), Daxx (77.1%), and TWIST1 (75.3%) and coincidentally downregulating CRK (92.6%), BACH1 (90.9%), CRIP1 (88.2%), and AXL (88.4%), while it widely enhanced **the oncogenesis signaling** by upregulating the p53 target proteins XBP1 (130.1%), BRCA1 (125.6%), 14-3-3 (120%), YAP1 (120%), PDCD4 (119.1%), BRCA2 (114.1%), KLF4 (113.4%), EWSR1 (110.3%), and MTA2 (109.8%). Among the 28 oncoproteins, nine were found to be overexpressed, nine were underexpressed, and ten exhibited minimal change in expression compared to the untreated controls.

Consequently, the p53 binding site sequence (AGACATGCCT)*-CEDS significantly impacted the protein signaling in RAW 264.7 cells. The AGACATGCCT*-CEDS primary suppressed the RAS and NFkB signaling axis, subsequently inactivated the protection-Notch/Jagged-SHH/PTCH/GLI signaling axis, FAS- and PARP-mediated apoptosis signaling axis, and senescence-glycolysis-cellular immunity-chronic inflammation signaling axis. In contrast, it enhanced the epigenetic modification-proliferation-related signaling axis, angiogenesis-survival-innate immunity-acute inflammation signaling axis, and epigenetic modification-telomere-p53-mediated apoptosis-fibrosis-oncogenesis signaling axis (Fig. 21B, Table 15).

The results indicate that the AGACATGCCT*-CEDS had both anti-oncogenic and oncogenic effects on RAW 264.7 cells. The anti-oncogenic effect was weak and was found to decrease ROS protection, senescence, and glycolysis. In contrast, the oncogenic effect was strong and was found to increase cellular proliferation, angiogenesis, survival, fibrosis, oncogenesis, and telomere instability. It was additionally observed that the AGACATGCCT*-CEDS can diminish the capacity of FAS- and PARP-mediated apoptosis and cellular immunity in the cells.

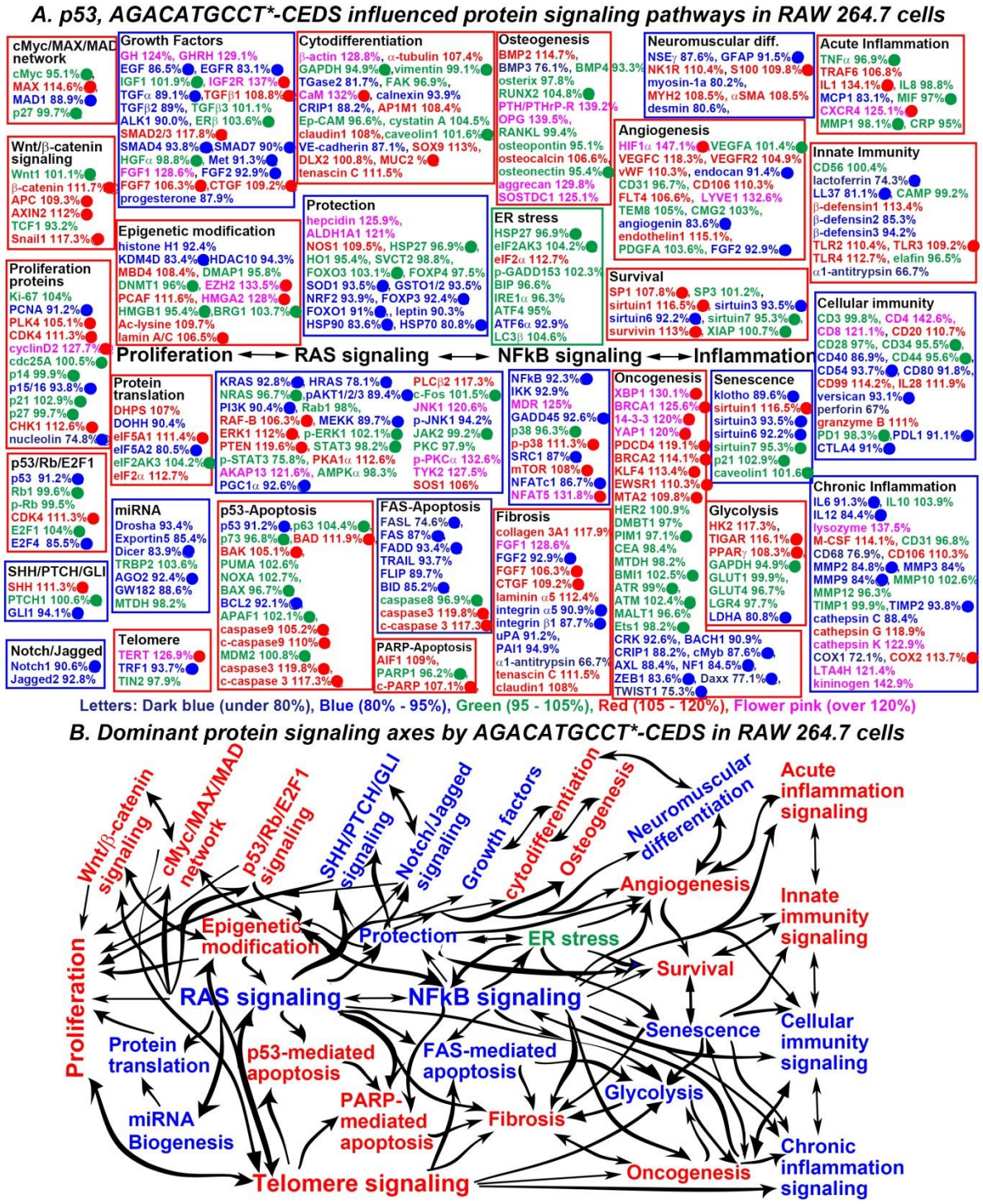

Fig. 21. The p53 binding site sequence (AGACATGCCT)*-CEDS influenced the protein signaling (A) and axes (B) in RAW 264.7 cells. The IP-HPLC results revealed proteins that were downregulated (**blue**), upregulated (**red**), and minimally changed (**green**) compared to the untreated controls. Dominant trend of suppressed (**blue square**) and activated (**red square**) signaling. p53 target proteins (Harmonizome 3.0), downregulated (●) or upregulated (●) by AGACATGCCT*-CEDS.

Table 15. Protein expressions in the RAW 264.7 cells treated with p53 binding site sequence (AGACATGCCT)*-CEDS

Signaling	Downregulated Proteins	Upregulated Proteins
Proliferation	**PCNA, p15/16**, nucleolin	**PLK4, CDK4, cyclin D2, CHK1**
cMyc/MAX/MAD network	**MAD1**	**MAX**
Wnt/β-catenin signaling		**β-catenin, APC, AXIN2, Snail**
p53/Rb/E2F1 signaling	**p53, E2F4**	**CDK4**
SHH/PTCH/GLI signaling	**GLI1**	**SHH**
Notch/Jagged signaling	**Notch1**, Jagged	
Epigenetic modification	histone H1, **KDM4D**, HDAC10	MBD4, **EZH2**, PCAF, **HMGA2**, Ac-lysine, **lamin A/C**
Protein translation	DOHH, **eIF5A2**	DHPS, **eIF5A1**, eIF2α
miRNA biogenesis	Drosha, Exportin5, **Dicer, AGO2**, GW182	
Growth factors	**EGF, EGFR, TGFα**, TGFβ2, ALK1, **SMA4, SMAD7, Met, FGF2**, progesterone	GH, GHRH, **IGF2R, TGFβ1, SMAD2/3**, FGF1, **FGF7, CTGF**
Cytodifferentiation	TGase2, calnexin, CRIP1, VE-cadherin	β-actin, α-tubulin, **CaM**, AP1M1, claudin1, SOX9, DLX2, tenascin C
Osteogenesis	BMP3	BMP2, PTH/PTHrPR, OPG, osteocalcin, aggrecan, SOSTDC1
Neuromuscular differentiation	NSEγ, **GFAP**, myosin-1a, desmin	NK1R, **S100**, MYH2, αSMA
RAS signaling	**KRAS, HRAS, pAKT1/2/3, PI3K, MEKK, PGC1α**, p-JNK1	**RAF-B, ERK1, PTEN**, PKA1α, AKAP13, PLCβ2, JNK1, p-PKC1α, TYK2, SOS1
NFkB signaling	**NFkB**, IKK, **GADD45, SRC1, NFATc1**	MDR, p-p38, **mTOR, NFAT5**
p53-mediated apoptosis	**p53, BCL2**	**BAD, BAK, caspase9, c-caspase9, caspase3, c-caspase3**
FAS-mediated apoptosis	**FASL, FAS, FADD**, TRAIL, FLIP, **BID**	**caspase3, c-caspase3**
PARP-mediated apoptosis		AIF1, **c-PARP**
Protection signaling	**SOD1**, GSTO1/2, NRF2, **FOXP3, FOXO1**, leptin, **HSP90, HSP70**	hepcidin, ALDH1A1, NOS1
ER stress signaling	ATF6α	eIF2α
Angiogenesis signaling	**endocan, angiogenin, FGF2**	**HIF1α**, VEGFC, VEGFR2, vWF, CD106, FLT4, LYVE1, endothelin1
Survival signaling	**sirtuin3, sirtuin6**	**SP1, sirtuin1, survivin**
Acute inflammation	MCP1	TRAF6, **IL1, CXCR4**
Innate immunity	**lactoferrin**, LL37, β-defensin2, β-defensin3, α1-antitrypsin	β-defensin1, TLR2, **TLR3**, TLR4
Cellular immunity	CD40, **CD54**, CD80, **versican**, perforin, **PDL1, CTLA4**	CD4, CD8, CD20, CD99, IL28, granzyme B
Chronic inflammation	**IL6, IL12**, CD68, **MMP2**, MMP3, **MMP9, TIMP2**, cathepsin C, COX1	Lysozyme, M-CSF, CD106, cathepsin G, cathepsin K, **COX2**, LTA4H, kininogen
Glycolysis	**LDHA**	HK2, **TIGAR, PPARγ,**
Fibrosis	**FGF2, integrin α5, integrin β1**, uPA, PAI1, α1-antitrypsin	collagen 3A1, FGF1, **FGF7, CTGF**, laminin α5, tenascin C claudin1
Oncogenesis	CRK, BACH1, CRIP1, **cMyb**, AXL, **NF1, ZEB1, Daxx, TWIST1**	**XBP1, BRCA1, 14-3-3, YAP1, PDCD4, BRCA2, KLF4, EWSR1, MTA2**
Senescence	**klotho, sirtuin3, sirtuin6**	**sirtuin1**
Telomere signaling	**TRF1**	**TERT**

The p53 binding site sequence*-CEDS, AGACATGCCT*-CEDS induced the suppression (**blue**) and activation (**red**) of signaling by downregulating (**blue**) and upregulating (**red**) the proteins, respectively. The data were compared to the reports of recent manuscripts and Harmonizome 3.0 website.

The canonical E2Fs binding site sequence (TTTC(C/G)CGC)*-CEDS influenced the protein signaling in RAW 264.7 cells

E2Fs are a family of transcription factors found in higher eukaryotes. They encode eight genes, with E2F1, E2F2, and E2F3a functioning as transcription activators and E2F3b, E2F4, E2F5, E2F6, E2F7, and E2F8 functioning as transcription repressors. On the other hand, the typical E2Fs with DP proteins, including E2F1, E2F2, E2F3a, E2F3b, E2F4, E2F5, and E2F6, are known to bind to a canonical sequence TTTC(C/G)CGC, in contrast to the atypical E2Fs with no DP protein, including E2F7 and E2F8[22]. The present study utilized the canonical E2Fs binding site sequence TTTC(C/G)CGC, for CEDS on RAW 264.7 cells. It is therefore anticipated that the TTTC(C/G)CGC*-CEDS will affect the transcriptional roles of both transcription activators (E2F1, E2F2, and E2F3a) and transcription repressors (E2F3b, E2F4, E2F5, and E2F6).

E2Fs are a family of transcription factors found in higher eukaryotes. They encode eight genes, with E2F1, E2F2, and E2F3a acting as transcriptional activators and E2F3b, E2F4, E2F5, E2F6, E2F7, and E2F8 acting as transcriptional repressors. On the other hand, the typical E2Fs with DP proteins, including E2F1, E2F2, E2F3a, E2F3b, E2F4, E2F5, and E2F6, are known to bind to a canonical sequence TTTC(C/G)CGC, in contrast to the atypical E2Fs with no DP protein, including E2F7 and E2F8. In the present study, the canonical E2F binding site sequence TTTC(C/G)CGC, was used for CEDS on RAW 264.7 cells. Therefore, it is expected that the TTTC(C/G)CGC*-CEDS will affect the transcriptional roles of both transcriptional activators (E2F1, E2F2, and E2F3a) and transcriptional repressors (E2F3b, E2F4, E2F5, and E2F6).

The IP-HPLC results demonstrated that the TTTC(C/G)CGC*-CEDS suppressed protein signaling, including the Wnt1/β-catenin signaling, SHH/PTCH/GLI signaling, protein translation, miRNA biogenesis, osteogenesis, ER stress, survival, innate immunity, FAS-mediated apoptosis, PARP-mediated apoptosis, fibrosis, oncogenesis, and glycolysis signaling. Concurrently, CEDS activated protein signaling, such as the proliferation, cMyc/MAX/MAD network, p53/Rb/E2F1 signaling, Notch/Jagged signaling, epigenetic modification, growth factors, cytodifferentiation, neuromuscular differentiation, RAS signaling, NFkB signaling, protection, angiogenesis, acute inflammation, cellular immunity, chronic inflammation, p53-mediated apoptosis, senescence, and telomere signaling compared to the untreated controls (Fig. 22A).

However, the canonical E2Fs binding site sequence*-CEDS increased E2F1 expression (107.4%) while decreased E2F4 expression (78%) in RAW 264.7 cells. Therefore, this study focused on observing the expression changes of E2F1 targeting proteins in the cells after CEDS.

The Wnt/β-catenin signaling was suppressed by downregulating the E2F1 target proteins Wnt1 (93.7%), β-catenin (75.4%), AXIN2 (93.2%), despite the upregulation of the E2F1 target protein APC (122.1%).

The protein translation signaling was suppressed by downregulating the E2F1 target proteins eIF5A1 (88.1%), eIF5A2 (92.1%), and eIF2α (81.6%), despite the upregulation of the E2F1 target protein DHPS (108.8%) and coincidental upregulation of eIF2AK3 (127%).

The miRNA biogenesis signaling appears to be inactivated by downregulating the E2F1 target protein Dicer (73.5%) and coincidentally downregulating Exportin5 (87.9%) and GW182 (88.3%), despite the upregulation of TRBP2 (106.3%) and MTDH (106.5%).

The osteogenesis signaling appears to be inactivated by downregulating the E2F1 target protein BMP2 (74.9%) and coincidentally downregulating BMP3 (92.5%), OPG (92.9%), and RANKL (92.5%), as well as coincidentally upregulating SOSTDC1 (133.2%), despite the upregulation of RUNX2 (130.6%), PTH/PTHrPR (111.6%), osteocalcin (116.4%), and aggrecan (128.7%).

The ER stress pathway was suppressed by downregulating the E2F1 target proteins eIF2a (81.6%), p-GADD153 (89.3%), and IRE1α (91.8%) and coincidentally downregulating BIP (91.2%) and ATF4 (91.3%), despite the upregulation of the E2F1 target proteins HSP27 (129.6%) and ATF6α (118.4%), and the coincidental upregulation of eIF2AK3 (127%).

The survival signaling appears to be inactivated by downregulating the E2F1 target proteins sirtuin1 (91.9%), sirtuin6 (84.4%), and survivin (77.4%), despite the upregulation of the E2F1 target protein sirtuin7 (109.2%) and coincidental upregulation of sirtuin3 (110.7%).

The innate immunity signaling appears to be inactivated by downregulating lactoferrin (73.8%), LL37 (84.9%), β-defensin2 (77%), β-defensin3 (85.9%), TLR3 (86.3%), and α1-antitrypsin (71.5%), despite the coincidental upregulation of β-defensin1 (133%), TLR4 (112.6%), and elafin (114.8%).

The FAS-mediated apoptosis signaling was suppressed by downregulating the E2F1 target proteins FASL (88.2%), FAS (90%), BID (65.3%), caspase8 (88.4%), and caspase3 (93.8%) and coincidentally downregulating TRAIL (87.9%).

The PARP-mediated apoptosis signaling was suppressed by downregulating the E2F1 target protein PARP1 (80.4%).

The fibrosis signaling was suppressed by downregulating collagen 3A1 (90.9%), FGF1 (82.9%), laminin α5 (93.9%), integrin α5 (89.2%), integrin β1 (86.9%), α1-antitrypsin (91.6%), and tenascin C (91.3%).

The glycolysis signaling was activated by upregulating the E2F1 target proteins collagen 3A1 (94.5%), CTGF (94.7%), integrin α5 (93.7%), integrin β1 (87.5%), and α1-antitrypsin (71.5%), despite the downregulation of the E2F1 target proteins FGF1 (119.3%), FGF2 (119.6%), claudin1 (108.4%) and coincidental downregulation of tenascin C (109.1%).

Conversely, **the proliferating signaling** was activated by upregulating the E2F1 target proteins Ki-67 (115.5%), CDK4 (110.7%), p21 (114.8%), and CHK1 (112.2%), despite the downregulation of the E2F1 target proteins PCNA (85.5%), p14 (92.4%), and nucleolin (79.9%) and coincidental downregulation of PLK4 (82.7%).

The cMyc/MAX/MAD network was suppressed by downregulating the E2F1 target protein cMyc (107.2%) and coincidentally downregulating MAX (111.8%), as well as the downregulation of MAD1 (92.4%) and p27 (91.8%).

The p53/Rb/E2F1 signaling was activated by upregulating the E2F1 target proteins p53 (109.4%), CDK4 (110.7%), and E2F1 (107.4%) and downregulating the E2F1 target proteins p-Rb1 (93.9%) and E2F4 (78%).

The SHH/PTCH/GLI signaling appears to be activated by upregulating SHH (105.7%), despite downregulation of the E2F1 target protein GLI1 (94.1%).

The Notch/Jagged signaling was activated by upregulating the E2F1 target proteins Notch1 (116%) and Jagged2 (107.5%).

The growth factor signaling were partially activated by upregulating the E2F1 target proteins TGFβ1 (125.6%), TGFβ2 (137.4%), SMAD2/3 (132.7%), FGF1 (119.3%), and FGF2 (119.6%) and coincidentally upregulating GH (113.2%), GHRH (107.6%), EGF (117.3%), despite the downregulation of the E2F1 target proteins SMAD4 (94.3%), SMAD7 (88.8%), and CTGF (94.7%) and coincidental downregulation of IGF2R (94.7%), TGFβ3 (85.5%), and ALK1 (97.4%).

The cytodifferentiation signaling were partially activated by upregulating the E2F1 target proteins α-tubulin (112.4%), FAK (105.4%), CaM (113%), claudin1 (108.4%), DLX (114.9%) and coincidentally upregulating Ep-CAM (124.7%), cystatin A (127.5%), SOX9 (108.8%), tenascin C (109.1%), despite the downregulation of the E2F1 target protein CRIP1 (84.3%) and coincidental downregulation of β-actin (87.1%), GAPDH (90.9%), and VE-cadherin (83.1%).

The RAS signaling was weakly activated by upregulating the E2F1 target proteins HRAS (118.9%), PI3K (142.6%), Rab1 (106.6%), and JNK1 (123.5%) and coincidentally upregulating PKA1α (111.3%), PLCβ2 (118.4%), PKC (105.2%), p-PKCα (116.2%), and SOS1 (114.6%), despite the downregulation of the E2F1 target proteins KRAS (88.6%), PTEN (92.8%), STAT3 (86.5%), and c-Fos (93.2%), and coincidental downregulation of p-STAT3 (92.7%), p-JNK1 (89.8%), and p-TYK2 (87.3%).

The NFkB signaling was activated by upregulating the E2F1 target proteins MDR (136.1%), GADD45 (132.7%), p38 (124.6%), mTOR (110.7%), and NFAT5 (107.3%), despite the downregulation of the E2F1 target protein NFATc1 (93.1%) and coincidental downregulation p-p38 (94.8%).

The protection signaling appears to be activated by upregulating the E2F1 target proteins HSP27 (129.6%), HSP70 (119%), and ALDH1A1 (116.3%) and coincidentally upregulating hepcidin (126.4%), GSTO1/2 (109.5%), SOD1 (109.2%), and SVCT2 (106.2%), despite the downregulation of the E2F1 target protein HO1 (93.5%), FOXO1 (89.4%), and HSP90 (84.9%) and coincidental downregulation of FOXP4 (90.2%) and NOS1 (80.9%).

The angiogenesis signaling appears to be activated by upregulating the E2F1 target proteins HIF1α (111.8%), PDGFA (127.5%), and FGF2 (119.6%) and coincidentally upregulating VEGFR2 (120%), vWF (111.4%), FLT4 (106.5%), LYVE1 (110.2%), and endothelin1 (106.2%), despite the downregulation of the

E2F1 target proteins VEGFC (93.2%) and angiogenin (74.2%), and coincidental downregulation of endocan (92.9%) and CD31 (91.1%).

The acute inflammation signaling appears to be activated by upregulating the E2F1 target protein TRAF6 (115.6%) and coincidentally upregulating MIF (112.5%) and CXCR4 (111.8%), despite the downregulation of MCP1 (90.2%) and CRP (89.9%).

The cellular immunity signaling appears to be activated by upregulating the E2F1 target proteins CD8 (144.7%), and CD99 (112.3%) and coincidentally upregulating CD28 (116%), CD34 (127.7%), IL28 (110.3%), and granzyme B (133.7%) and downregulating CTLA4 (91.7%), despite the downregulation of the E2F1 target protein CD4 (94.6%) and upregulation of PDL1 (118%), as well as the coincidental downregulation of CD3 (93.4%), versican (90.5%), and perforin (69.6%).

The chronic inflammation signaling was activated by upregulating the E2F1 target protein cathepsin C (114.2%) and coincidentally upregulating IL12 (106.8%), lysozyme (107.5%), MMP10 (119.1%), MMP12 (110.9%), TIMP1 (116.5%), TIMP2 (146.5%), cathepsin G (120.2%), cathepsin K (114.3%), LTA4H (122.5%), and kininogen (128.2%), despite the downregulation of the E2F1 target proteins CD68 (83.8%) and MMP2 (93.5%), and coincidental downregulation of IL10 (86.7%), CD31 (91.6%), MMP3 (79.5%), and COX1 (68.6%).

The p53-mediated apoptosis signaling appears to be activated by upregulating the E2F1 target proteins p53 (109.4%), BAD (124.2%), BAK (105.4%), PUMA (106.8%), NOXA (115.6%), and BAX (106.7%) and coincidentally downregulating MDM2 (89.5%), despite the downregulation of the E2F1 target proteins p73 (88.2%) and caspase3 (93.8%), and upregulation of BCL2 (109.7%), as well as coincidental downregulation of p63 (90.6%).

The senescence signaling was activated by upregulating the E2F1 target proteins klotho (115.8%), sirtuin7 (109.2%), and p21 (114.8%) and coincidentally upregulating sirtuin3 (110.7%), despite the downregulation of the E2F1 target proteins sirtuin1 (91.9%) and sirtuin6 (84.4%).

The telomere signaling was activated by upregulating the E2F1 target protein TERT (118.1%) and coincidentally upregulating TIN2 (133.4%), despite the downregulation of the E2F1 target protein TRF1 (86.9%).

In addition, the E2Fs binding site sequence*-CEDS significantly influenced **the epigenetic modification signaling** by downregulating the E2F1 target protein HMGA2 (93.8%) and coincidentally downregulating HDAC10 (89.8%), while it upregulated the E2F1 target proteins KDM4D (115%), DNMT1 (107.8%), BRG1 (111.4%), and lamin A/C (108.8%) and coincidentally upregulated Ac-lysine (113.7%). Consequently, the TTTC(C/G)CGC CEDS induced a trend towards an increase in the methylation of histones and DNAs, and transcriptional repression.

The E2Fs binding site sequence*-CEDS significantly suppressed **the oncogenesis signaling** by downregulating the E2F1 target proteins BRCA1 (93.9%), PIM1 (93.7%), BRCA2 (93.4%), ZEB1 (91.9%), cMyb (90.5%), CRK (89.2%), TWIST1 (87.1%), NF1 (87%), CRIP1 (84.3%), and Daxx (72.4%) and coincidentally downregulating MTA2 (89.4%), BMI1 (87.8%), and BACH1 (84.8%). while it also enhanced **the oncogenesis signaling** by upregulating the E2F1 target proteins MALT1 (112.6%), YAP1 (106.4%), and XBP1 (105.8%) and coincidentally upregulating DMBT1 (122.1%), 14-3-3 (115.2%), CEA (112.1%), EWSR1 (109.9%), MTDH (106.5%), and HER2 (105.8%). Among the 28 oncoproteins, 14 were found to be underexpressed, nine were overexpressed, and five exhibited minimal change in expression compared to the untreated controls.

Consequently, the canonical E2Fs binding site sequence (TTTC(C/G)CGC)*-CEDS strongly impact the protein signaling in RAW 264.7 cells. The TTTC(C/G)CGC*-CEDS primary enhanced the RAS-NFkB signaling axis, subsequently activated proliferation-related signaling axis, epigenetic modification-protection, cytodifferentiation-angiogenesis-acute inflammation signaling axis, senescence-cellular immunity-chronic inflammation signaling axis, and epigenetic modification-p53-mediated apoptosis-telomere signaling axis, while it inactivated the ER stress-survival-innate immunity signaling axis and the FAS- and PARP-mediated apoptosis-fibrosis-glycolysis-oncogenesis signaling axis (Fig. 22B, Table 16).

The results indicate that TTTC(C/G)CGC*-CEDS had a strong potential of oncogenic effect on RAW 264.7 by activating proliferation, ROS protection, angiogenesis, senescence, chronic inflammation, and telomere instability, while it had a weak potential of anti-oncogenic effect by attenuating ER stress, survival, fibrosis, glycolysis, and oncogenesis. It was also found that the TTTC(C/G)CGC*-CEDS can induce acute and chronic inflammation but diminish the FAS- and PARP-mediated apoptosis.

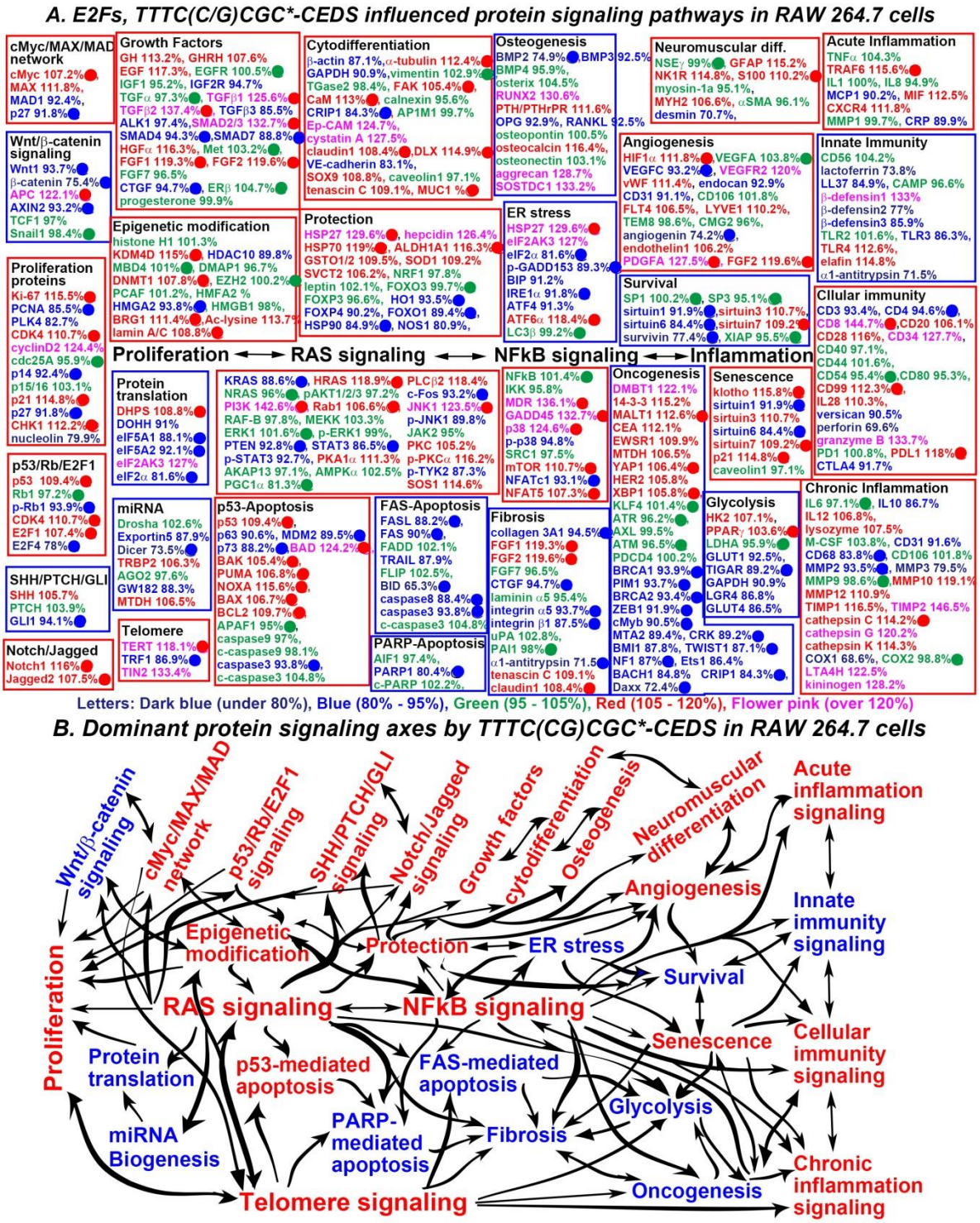

Fig. 22. The E2Fs binding site sequence (TTTC(C/G)CGC)*-CEDS influenced the protein signaling (A) and axes (B) in RAW 264.7 cells. The IP-HPLC results revealed proteins downregulated (**blue**), upregulated (**red**), and minimally changed (**green**) compared to the untreated controls. Dominant trend of suppressed (**blue square**) and activated (**red square**) signaling to be defined. E2F1 target proteins (Harmonizome 3.0), downregulated (●) or upregulated (●) by (TTTC(C/G)CGC)*-CEDS.

Table 16. Protein expressions in the RAW 264.7 cells treated with canonical E2Fs binding site sequence (TTTC(C/G)CGC)*-CEDS

Signaling	Downregulated Proteins	Upregulated Proteins
Proliferation	**PCNA, PLK4, p14, p27**, nucleolin	**Ki-67**, **CDK4,** cyclin D2, **p21, CHK1**
cMyc/MAX/MAD network	MAD1, **p27**	**cMyc,** MAX
Wnt/β-catenin signaling	**Wnt1, β-catenin, AXIN2**	**APC**
p53/Rb/E2F1 signaling	**p-Rb1, E2F4**	**p53, CDK4, E2F1**
SHH/PTCH/GLI signaling	**GLI1**,	SHH
Notch/Jagged signaling		**Notch1, Jagged2**
Epigenetic modification	HDAC10, **HMGA2**	**KDM4D, DNMT1, BRG1,** Ac-lysine**, lamin A/C**
Protein translation	DOHH, **eIF5A1, eIF5A2, eIF2α**	**DHPS,** eIF2AK3
miRNA biogenesis	Exportin5, **Dicer**, GW182	TRBP2, MTDH
Growth factors	IGF2R, TGFβ3, ALK1, **SMAD4, SMAD7, CTGF**	GH, GHRH, EGF, **TGFβ1, TGFβ2, SMAD2/3**, HGFα, **FGF1, FGF2,**
Cytodifferentiation	β-actin, GAPDH, **CRIP1,** VE-cadherin	**α-tubulin, FAK**, **CaM**, Ep-CAM, cystatin A, **claudin1, DLX2**, SOX9, tenascin C
Osteogenesis	BMP2, **BMP3**, OPG, RANKL	RUNX2, PTH/PTHrPR, osteocalcin, aggrecan, SOSTDC1
Neuromuscular differentiation	Desmin	GFAP, NK1R, **S100**, MYH2
RAS signaling	**KRAS**, **PTEN, STAT3**, p-STAT3, **c-Fos**, p-JNK1, p-TYK2	**HRAS**, **PI3K, Rab1**, PKA1α, PLCβ2, **JNK1**, PKC< p-PKC1α, SOS1
NFkB signaling	p-p38, **NFATc1**	**MDR, GADD45, p38, mTOR, NFAT5**
p53-mediated apoptosis	p63, **p73, MDM2, caspase3**	**p53**, **BAD, BAK**, PUMA, NOXA, **BAX, BCL2**
FAS-mediated apoptosis	**FASL, FAS**, TRAIL, **BID, caspase8, caspase3**	
PARP-mediated apoptosis	**PARP1**	
Protection	**HO1**, FOXP4, **FOXO1, HSP90**, NOS1	**HSP27**, hepcidin, **HSP70, ALDH1A1**, GSTO1/2, SOD1, SVCT2
ER stress	**eIF2α, p-GADD153**, BIP, **IRE1α**, ATF4	**HSP27**, eIF2AK3, **ATF6α**
Angiogenesis	**VEGFC**, endocan, CD31, **angiogenin**	**HIF1α**, VEGFR2, vWF, FLT4, LYVE1, angiogenin, **PDGFA, FGF2**
Survival	**sirtuin1, sirtuin6, survivin**	sirtuin3, **sirtuin7**
Acute inflammation	MCP1, CRP	**TRAF6**, MIF, CXCR4
Innate immunity	Lactoferrin, LL37, β-defensin2, β-defensin3, TLR3, α1-antitrypsin	β-defensin1, TLR4, elafin
Cellular immunity	CD3, CD4, versican, perforin, CTLA4	CD8, CD20, CD28, CD34, **CD99**, IL28, granzyme B, **PDL1**
Chronic inflammation	IL10, CD31, **CD68, MMP2**, MMP3, COX1	IL12, lysozyme, MMP10, MMP12, TIMP1, TIMP2, **cathepsin C**, cathepsin G, cathepsin K, LTA4H, kininogen
Glycolysis	GLUT1, **TIGAR**, GAPDH, LGR4, GLUT4	HK2, **PPARγ,**
Fibrosis	**collagen 3A1, CTGF, integrin α5, integrin β1, α1-antitrypsin**	**FGF1, FGF2**, tenascin C, **claudin1**
Oncogenesis	BRCA1, **PIM1, BRCA2, ZEB1, cMyb,** MTA2, **CRK,** BMI1, **TWIST1**, NF1, BACH1, CRIP1, Daxx	DMBT1, 14-3-3, **MALT1**, CEA, EWSR1, MTDH, **YAP1**, HER2, XBP1
Senescence	**sirtuin1, sirtuin6**	**klotho,** sirtuin3**, sirtuin7**, **p21**
Telomere signaling	**TRF1**	**TERT**, TIN2

The canonical E2Fs binding site sequence*-CEDS, TTTC(C/G)CGC*-CEDS induced the suppression (**blue**) and activation (**red**) of signaling by downregulating (**blue**) and upregulating (**red**) the proteins, respectively. The data were compared to the reports of recent manuscripts and Harmonizome 3.0 website.

The poly-A sequence (12A)*-CEDS influenced the protein signaling in RAW 264.7 cells

The poly-A sequences (4A-12A) are ubiquitously distributed throughout the mouse genome. Therefore, the poly-A sequence may play a role in gene transcription in different regions of the genome, but its function will be variable and nonspecific depending on the context of the genomic environment. In the present study, the poly-A sequence (12A) was selected for CEDS experiment as a nonspecific control to compare with other CEDSs using different miRNA and DNA motif sequences that have been shown to be essential for gene expression.

RAW 264.7 cells treated with the 12A*-CEDS exhibited changes in protein expression throughout essential signaling, both positively and negatively. However, each protein signaling exhibited unique trends of activation or inactivation. As a result, the 12A*-CEDS increased protein signaling related to proliferation, cMyc/MAX/MAD network, p53/Rb/E2F1 signaling, SHH/PTCH/GLI signaling, Notch/Jagged signaling, miRNA biogenesis, growth factors, cytodifferentiation, RAS signaling, ER stress, angiogenesis, survival, acute inflammation, PARP-mediated apoptosis, and fibrosis. On the other hand, it activated protein signaling related to Wnt/β-catenin signaling, epigenetic modification, protein translation, osteogenesis, neuromuscular differentiation, NFkB signaling, protection, innate immunity, cellular immunity, chronic inflammation, p53-mediated apoptosis, FAS-mediated apoptosis, oncogenesis, senescence, glycolysis, and telomere signaling (Fig. 23A).

In RAW264.7 cells treated with the 12A*-CEDS, **the proliferation signaling** appears to be inactivated by downregulating PCNA (up to 90.5%), PLK4 (83.5%), CDK4 (84.2%), and nucleolin (80.6%), and upregulating p15/16 (112.5%), p21 (115.7%), and p27 (110.1%), despite the upregulation of Ki-67 (107.4%) and cyclinD2 (106.2%).

The cMyc/MAX/MAD network appears to be inactivated by downregulating MAX (86.7%), and upregulating p27 (110.1%).

The p53/Rb/E2F1 signaling was inactivated by downregulating Rb1 (86.1%), CDK4 (84.2%), and E2F1 (85.9%), as well as coincidentally upregulating p53 (105.8%) and E2F4 (136.1%).

The SHH/PTCH/GLI signaling was inactivated by downregulating GLI1 (76.1%) despite the slight upregulation of SHH (109%).

The Notch/Jagged signaling appears to be inactivated by downregulating Jagged2 (86%) despite the upregulation of Notch1 (119.7%).

The growth factor signaling were partially inactivated by downregulating EGF (73.9%), TGFβ1 (79.3%), TGFβ2 (93.8%), TGFβ3 (74.1%), ERβ (81.2%), SMCD7 (69.7%), and FGF2 (93.3%), despite the upregulation of GHRH (116.7%), IGF1 (106.9%),, ALK1 (109.3%), SMAD2/3 (117.5%), HGFα (120.4%), FGF7 (115.4%), and progesterone (106.7%).

The cytodifferentiation signaling were partially inactivated by downregulating vimentin (94.5%), TGase2 (87.6%), calnexin (78.7%), CRIP1 (81.6%), AP1M1 (89.1%), caveolin1 (94.7%), and DLX2 (89.7%), despite the upregulation of β-actin (110.2%), GAPDH (107.7 %), FAK (106.1%), Ep-CAM (136.9%), VE-cadherin (114.2%), SOX9 (110.6%), and tenascin C (108.7%).

The RAS signaling appears to be inactivated by downregulating HRAS (82.2%), pAKT1/2/3 (94.1%), RAF-B (80.8%), MEKK (80.6%), ERK1 (86.2%), PTEN (77.2%), STAT3 (86%), PGC1α (93%), PKC (86. 7%), JAK2 (93.8%), p-TYK2 (82.2%), and SOS1 (83.6%), despite the upregulation of KRAS (105.1%), PI3K (107.7%), Rab1 (121.7%), p-ERK1 (108.8%), p-STAT3 (115.4%), PKA1α (120.3%), AMPKα (111.9%), p-JNK1 (105.1%), and p-PKCα (118.8%).

The ER stress signaling was inactivated by downregulating HSP27 (77.5%), eIF2α (84.5%), and p-GADD153 (82.5%), and BIP (94.4%), despite the upregulation of ATF4 (113.2%) and LC3β (105%).

The angiogenesis signaling was suppressed by downregulating HIF1α (94.7%), VEGFA (67%), vWF (86.4%), CD31 (90.3%), CMG2 (78.9%), PDGFA (91.8%), and FGF2 (03.3%), despite the upregulation of FLT4 108.9%), LYVE1 (110.7%), and angiogenin (115%).

The survival signaling was suppressed by downregulating SP1 (75%), sirtuin1 (80.5%), sirtuin6 (89.6%), sirtuin7 (82.9%), and survivin (84.1%), despite the upregulation of SP3 (141.3%).

The acute inflammation signaling appears to be inactivated by downregulating TNFα (93.1%), TRAF6 (83.6%), and CXCR4 (85.5%), despite the upregulation of IL8 (122.6%), MCP1 (106.2%), MMP1 (129.2%), and CRP (111.7%).

The PARP-mediated apoptosis signaling was inactivated by downregulating PARP1 (92.9%), despite the upregulation of AIF1 (108.6%).

The fibrosis signaling was inactivated by downregulating FGF2 (93.3%), integrin α5 (88.5%), uPA (73.6%), PAI1 (81.6%), and α1-antitrypsin (88.4%), despite the upregulation of FGF7 (115.4%), integrin β1 (117.5%), and tenascin C (108.7%).

Conversely, **the Wnt/β-catenin signaling** appears to be activated by upregulating Wnt1 (112.1%) and β-catenin (112%).

The protein translation signaling appears to be activated by upregulating DHPS (133.5%) and eIF5A1 (109%), despite the downregulation of eIF5A2 (90.6%) and eIF2α (84.5%).

The osteogenesis signaling was activated by upregulating BMP2 (110.9%), BMP3 (128.4%), BMP4 (114.2%), OPG (106%), RANKL (116.5%), osteonectin (118.5%), and aggrecan (111.4%), despite the downregulation of RUNX2 (88.7%), osteopontin (72.7%), and osteocalcin (83.4%).

The neuronal differentiation signaling was activated by upregulating NSEγ (106.3%), GFAP (118.9%), despite the downregulation of NK1R (75.4%), while cellular differentiation signaling appeared to be inactivated by downregulating myosin-1a (73.9%) and MYH2 (87.8%), despite the upregulation of αSMA (119%).

The NFkB signaling appears to be activated by upregulating p-p38 (116%), mTOR (113.2%), NFATc1 (119%), and NFAT5 (128.9%) and coincidentally upregulating IKK (93.7%), despite the downregulation of MDR (87.3%), GADD45 (91.5%), and SRC1 (87.5%).

The protection signaling appears to be inactivated by upregulating SVCT2 (126%), SOD1 (123.5%), HO1 (113.7%), FOXP3 (112.8%), GSTO1/2 (108.7%), and NRF2 (108.3%), despite the downregulation of FOXP4 (92.4%), HSP70 (88.8%), FOXO1 (88.6%), hepcidin (86.1%), and HSP27 (77.5%).

The innate immunity signaling was activated by upregulating CD56 (114.5%), lactoferrin (134.8%), β-defensin1 (128%), TLR2 (115%), TLR3 (120.2%), and TLR4 (116.2%), despite the downregulation of LL37 (75.6%), CAMP (94.1%), and α1-antitrypsin (88.4%).

The celluar immunity signaling appears to be activated by upregulating CD3 (up to 114.7%), CD8 (110.6%), CD20 (108.4%), CD44 (105.7%), granzyme B (111.7%), and PDL1 (114.1%), despite the downregulation of CD40 (89.8%), CD40 (89.8%), IL28 (68.8%), versican (70.5%), perforin (68%), and PD1 (90%).

The chronic inflammation signaling appear to be activated by upregulating IL12 (112%), lysozyme (137.5%), MMP2 (121.5%), MMP9 (119.3%), MMP10 (108.2%), COX1 (122.9%), COX2 (115.9%), and LTA4H (125%), despite the downregulation of IL10 (75.3%), M-CSF (91.5%), CD31 (90.9%), CD68 (88.6%), MMP12 (93.9%), TIMP1 (85.5%), and TIMP2 (86.3%).

The p53-mediated apoptosis signaling was activated by upregulating p53 (105.8%), BAK (118.9%), BAX (108.9%), BCL2 (146%), MDM2 (114.3%), caspase3 (109.1%), and c-caspase3 (110.4%), despite the downregulation of p73 (81.6%), APAF1 (84.1%), and caspase9 (83.8%).

The FAS-mediated apoptosis signaling appears to be activated by upregulating FASL (124.1%), caspase8 (109.4%), caspase3 (109.1%), and c-caspase3 (110.4%), despite the downregulation of FAS (80.6%) and BID (81.2%).

The senescence signaling appears to be activated by upregulating klotho (142.3%) and p21 (115.7%), despite the downregulation of sirtuin1 (82.9%), sirtuin6 (90.3%), sirtuin7 (82.9%), and caveolin1 (94.7%).

The glycolysis signaling appears to be activated by upregulating LGR4 (113%), GLUT1 (112.7%), and GAPDH (107.7%), despite the downregulation of TIGAR (90.1%) and PPARγ (83.9%).

The telomere signaling was activated by upregulating TERT (up to 113.2%), and downregulating TRF1 (92.9%).

In addition, the 12A*-CEDS markedly influenced **the epigenetic modification signaling** by downregulating HDAC10 (91.5%), DMAP1 (89.9%), and DNMT1 (94.1%), as well as coincidentally upregulating KDM4D (112.2%), MBD4 (106.3%), PCAF (108.1%), HMGB1 (127.8%), BRG1 (115.9%), Ac-lysine (108.5%), and lamin A/C (105.5%). Consequently, the 12A*-CEDS induced a trend towards an increase in the methylation of histones and DNAs, and transcriptional repression.

The 12A*-CEDS significantly suppressed **the oncogenesis signaling** by downregulating HER2 (94.5%), PIM1 (89.9%), EWSR1 (86%), CRIP1 (81.6%), NF1 (73.9%), PDCD4 (73.6%), BMI1 (70.6%), and MTA2 (67%), while it widely activating **the oncogenesis signaling** by upregulating KLF4 (135.8%), MALT1 (135.7%), CRK (129.8%), DMBT1 (128.1%), Daxx (126.6%), BACH1 (118.5%), MTDH (116.4%), Ets1 (116.3%), ATM (110.8%), ZEB1 (110.5%), 14-3-3 (109.2%), and BRCA2 (107.4%). Among the 28 oncoproteins, 12 were found to be overexpressed, eight were overexpressed, and eight exhibited minimal change in expression compared to the untreated controls.

Consequently, the nonspecific sequence (12A)*-CEDS significantly impacted the protein signaling in RAW 264.7 cells. The 12*-CEDS suppressed the RAS signaling, subsequently inactivating proliferation-related signaling axis, ER stress-angiogenesis-survival-acute inflammation signaling axis, and PARP-mediated apoptosis-fibrosis signaling axis. In contrast, it enhanced the NFkB signaling, subsequently activating the p53- and FAS-mediated apoptosis signaling axis, and senescence-glycolysis-oncogenesis-innate immunity-chronic inflammation signaling axis (Fig. 23B, Table 17).

The results indicate that the 12*-CEDS also affects the protein signaling in a similar manner to the above experiments, due to the existence of numerous poly-A sequences (4A-12A) in the mouse genome. The 12A*-CEDS resulted in imbalanced protein signaling in RAW 264.7 cells, activating epigenetic methylation, oncogenesis, and telomere instability, leading to chronic inflammation and apoptosis, in the absence of cellular growth and differentiation, wound healing, and ROS protection. Therefore, it is postulated that the 12A*-CEDS may influence the cells to undergo aging and retrogressive changes with a high potential of oncogenesis.

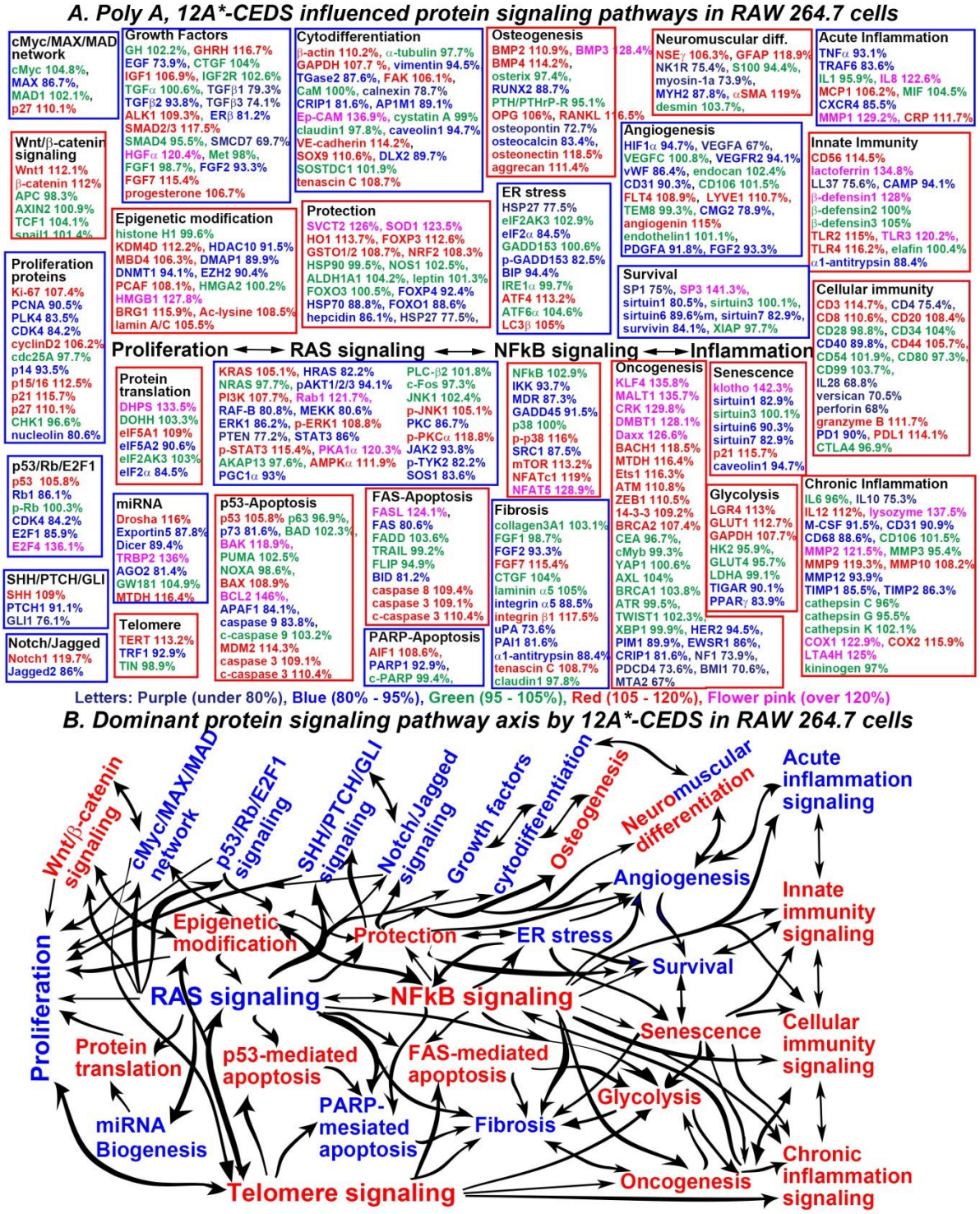

Fig. 23. The nonspecific sequence (12A)*-CEDS influenced the protein signaling (A) and axes (B) in RAW 264.7 cells. The IP-HPLC results revealed proteins that were downregulated (blue), upregulated (red), and minimally changed (green) compared to the untreated controls. This allowed the dominant trend of suppressed (blue square) and activated (red square) signaling to be defined.

Table 17. Protein expressions in the RAW 264.7 cells treated with nonspecific sequence (12A)*-CEDS

Signaling	Downregulated Proteins	Upregulated Proteins
Proliferation	PCNA, PLK4, CDK4, p14, nucleolin	Ki-67, cyclin D2, p15/16, p21, p27
cMyc/MAX/MAD network	MAX	p27
Wnt/β-catenin signaling		Wnt1, β-catenin
p53/Rb/E2F1 signaling	Rb1, CDK4, E2F1	p53, E2F4
SHH/PTCH/GLI signaling	PTCH1, GLI1	SHH
Notch/Jagged signaling	Jagged2	Notch1
Epigenetic modification	HDAC10, DMAP1, DNMT1, EZH2	KDM4D, MBD4, PCAF, HMGB1, BRG1, Ac-lysine, lamin A/C
Protein translation	eIF5A2, eIF2α	DHPS, eIF5A1
miRNA biogenesis	Exportin5, Dicer, AGO2,	Drosha, TRBP, MTDH
Growth factors	EGF, TGFβ1, TGFβ2, TGFβ3, SMCD7, FGF2, ERβ	GHRH, NF1, ALK1, SMCD2/3, HGFα, FGF7, progesterone
Cytodifferentiation	Vimentin, TGase2, calnexin, CRIP1, AP1M1, caveolion1, DLX2	β-actin, GAPDH, FAK, Ep-CAM, VE-cadherin, SOX9, tenascin C
Osteogenesis	RUNX2, osteopontin, osteocalcin,	BMP2, BMP3, BMP4, OPG, RANKL, osteonectin, aggrecan
Neuromuscular differentiation	NK1R, myosin-1a, MYH2	NSEγ, GFAP, αSMA
RAS signaling	HRAS, pAKT1/2/3, RAF-B, MEKK, ERK1, PTEN, STAT3, PGC1α, PKC, JAK2, p-TYK2, SOS1	KRAS, PI3K, Rab1, p-STAT3, PKA1α, AMPKα, p-JNK1, p-PKC1α
NFkB signaling	IKK, MDR, GADD45, SRC1	p-p38, mTOR, NFATc1, NFAT5
p53-mediated apoptosis	p73, APAF1, caspase9	p53, BAK, BAX, BCL2, MDM2, caspase3, c-caspase3
FAS-mediated apoptosis	FAS, BID	FASL, caspase8, caspase3, c-caspase3
PARP-mediated apoptosis	PARP1	AIF1
Protection	FOXP4, HSP70, FOXO1, hepcidin, HSP27	SVCT2, SOD1, HO1, FOXP3, GSTO1/2, NRF2,
ER stress	HSP27, eIF2α, p-GADD153, BIP	ATF4, LC3β
Angiogenesis	HIF1α, VEGFA, VEGFR2, vWF, CD31, CMG2, PDGFA, FGF2	FLT4, LYVE1, angiogenin
Survival	SP1, sirtuin1, sirtuin1, sirtuin6, sirtuin7, survivin	SP3
Acute inflammation	TNFα, TRAF6, CXCR4	IL8, MCP1, MMP1, CRP
Innate immunity	LL37, CAMP, α1-antitrypsin	CD56, lactoferrin, TLR2, TLR3, TLR4
Cellular immunity	CD4, CD40, IL28, versican, perforin, PD1	CD3, CD8, CD20, CD44, granzyme B, PDL1
Chronic inflammation	IL6, IL10, M-CSF, CD31, CD68, MMP12, TIMP1, TIMP2	IL12, lysozyme, MMP2, MMP9, MMP10, COX1, COX2, LTA4H
Glycolysis	TIGAR, PPARγ	LGR4, GLUT1, GAPDH
Fibrosis	FGF2, integrin α5, uPA, PAI1, α1-antitrypsin	FGF7, integrin β1, tenascin C
Oncogenesis	HER2, PIM1, EWSR1, CRIP1, NF1, PDCD4, BMI1, MTA2	KLF4, MALT1, CRK, DMBT1, Daxx, BACH1, MTDH, Ets1, ATM, ZEB1, 14-3-3, BRCA2
Senescence	sirtuin1, sirtuin6, sirtuin7, caveolin1	klotho, p21
Telomere signaling	TRF1	TERT

The nonspecific sequence*-CEDS, 12A*-CEDS induced induced the suppression (**blue**) and activation (**red**) of signaling by downregulating (**blue**) and upregulating (**red**) the proteins, respectively.

The IP-HPLC analysis utilizing 350 antisera demonstrated that CEDS, which employ different DNA motif sequences, can influence the protein expression of global protein signaling in RAW 264.7 cells. The telomere repeat sequence (TTAGGG)*-CEDS upregulated 34 proteins (31.6%), downregulated 67 proteins (62.6%), and exhibited minimum effect on six proteins (5.6%) among the 107 telomere-associated proteins observed in this study (Table 19).

The canonical E-box sequence (CACGTG)*-CEDS upregulated 69 proteins (41.8%), downregulated 66 proteins (40%), and exhibited minimum effect on 30 proteins (18.2%) among 165 cMyc targeting proteins. The p53 (cluster 1 response element) binding site sequence (AGACATGCCT)*-CEDS upregulated 61 proteins (32.3%), downregulated 70 proteins (37%), and exhibited minimum effect on 58 proteins (30.1%) among 189 p53 targeting proteins. And the canonical E2Fs binding site sequence (TTTC(C/G)CGC)*-CEDS upregulated 69 proteins (41.3%), downregulated 67 proteins (40.1%), and exhibited minimum effect on 31 proteins (18.6%) among 167 E2F1 targeting proteins observed in this study (Table 19).

Consequently, the telomere repeat sequence (TTAGGG)*-CEDS demonstrated a greater tendency to downregulate the telomere-associated proteins (62.6%) than to upregulate them (31.6%) in RAW 264.7 cells. Conversely, the canonical E-box sequence (CACGTG)*-CEDS, the p53 (cluster 1 response element) binding site sequence (AGACATGCCT), and the canonical E2Fs binding site sequence (TTTC(C/G)CGC) demonstrated a relatively similar ratio of targeting efficiency between the upregulation versus downregulation of their targeting proteins, with 41.8% versus 40%, 32.3% versus 37%, and 41.3% versus 40.1%, respectively.

It is therefore postulated that the telomere repeat sequence*-CEDS can strongly induce the conformational changes of abundant telomere dsDNA compared to the other protein binding site sequence*-CEDSs. This may result in the stabilization of the G-quadruplex structure of the telomere sequence, which in turn may lead to an anti-oncogenic effect on RAW 264.7 cells. Conversely, CEDS using other protein binding site sequences, such as the canonical E-box sequence, the p53 (cluster 1 response element) binding site sequence, and the canonical E2Fs binding site sequence, may induce the conformational changes of target dsDNA to a lesser extent. This can lead to inappropriate upregulation and downregulation of target proteins, resulting in cellular stress and oncogenesis in RAW 264.7 cells.

Table 19. The targeting efficiency of CEDS using a different DNA motif sequence in RAW 264.7 cells

Protein binding site sequence*-CEDS	Up-regulation (over 105%)	Down-regulation (under 95%)	Minimal change (±5%)	Total target proteins
TTAGGG*-CEDS (telomere repeat sequence)	34	67	6	107
	31.6%	62.6%	5.6%	100%
CACGTG*-CEDS (canonical E-box sequence)	69	66	30	165
	41.8%	40%	18.2%	100%
AGACATGCCT*-CEDS (p53 binding site sequence)	61	70	58	189
	32.3	37%	30.1%	100%
TTTC(C/G)CGC*-CEDS (canonical E2Fs binding site sequence)	69	67	31	167
	41.3%	40.1%	18.6%	100%
Total	232	268	125	625
	37.1%	42.9%	20%	100%
12A*-CEDS (nonspecific sequence)	130	122	98	350
	37.1%	34.9%	28%	100%

Cytological and immunocytochemical observation of CEDS-treated cells

Cytological observation of RAW 264.7 cells treated with miRNA sequence*-CEDS

RAW 264.7 cells were cultured on cell culture slides (Hybridwell™, SPL Life Science, Korea) using the same method as the above experiment. Approximately 50% confluent RAW 264.7 cells grown on culture slide surfaces were treated with murine mature miRNA sequence*-CEDS at 23-25 Gauss for 20 min and once more in 12 hours. After a culture period of 24 hours, the cells were fixed with 10% buffered formalin, stained with hematoxylin and eosin, and also underwent immunocytochemical staining for c-caspase 3.

Immunocytochemical (ICC) staining was performed using the indirect triple sandwich method on the Vectastatin system (Vector Laboratories, USA), and visualized using a 3-amino-9-ethylcarbazole solution (Santa Cruz Biotechnology, USA) with no counter staining. The results were observed by optical microscope, and their characteristic images were captured (DP-73, Olympus Co., Japan) and illustrated.

The control group which was not treated with CEDS showed many cells diffusely scattered on culture dish surface, and the cells were occasionally positive for c-caspase 3. Whereas CEDS using mmu-miR-21-5p sequence TAGCTTATCAGACTGATGTTGA*-CEDS, showed proliferative cells which were frequently aggregated into multicellular spheroids. The cells were weakly positive for c-caspase 3. CEDS using mmu-miR-26a-5p sequence, TTCAAGTAATCCAGGATAGGCT*-CEDS showed marked decrease of cell number, and strong immunoreaction of c-caspase 3 in the remaining cells. CEDS using mmu-miR-29a-3p sequence, TAGCACCATCTGAAATCGGTTA*-CEDS showed relatively abundant cells which were partly aggregated. Some cells were positive for c-caspase 3 (Fig. 24 A-P).

CEDS using mmu-miR-126-5p sequence, TTCAAGTAATCCAGGATAGGCT*-CEDS showed marked decrease of cells, and strong immunoreaction of c-caspase 3 in the remaining cells. CEDS using mmu-miR-150-5p sequence, TCTCCCAACCCTTGTACCAGTG*-CEDS showed slight decrease of cell number, and positive immunoreaction of c-caspase 3 in some cells. CEDS using mmu-miR-155-5p sequence, TTCAAGTAATCCAGGATAGGCT*-CEDS showed significant decrease of cell number, and showed strong immunoreaction of c-caspase 3 (Fig. 24 Q-BB)

The cytological results demonstrated that miR-26a-5p or miR-126-5p*-CEDS induced a strong anti-proliferative and apoptotic effect on RAW 264.7 cells compared to the untreated controls. The anti-proliferative

and apoptotic effect was found to be diminished in CEDS using miR-155-5p, miR-150-5p, and miR-29a-3p sequence in order, while CEDS using miR-21-5p sequence was observed to induce the proliferation and aggregation of cells, thereby exerting an oncogenic effect.

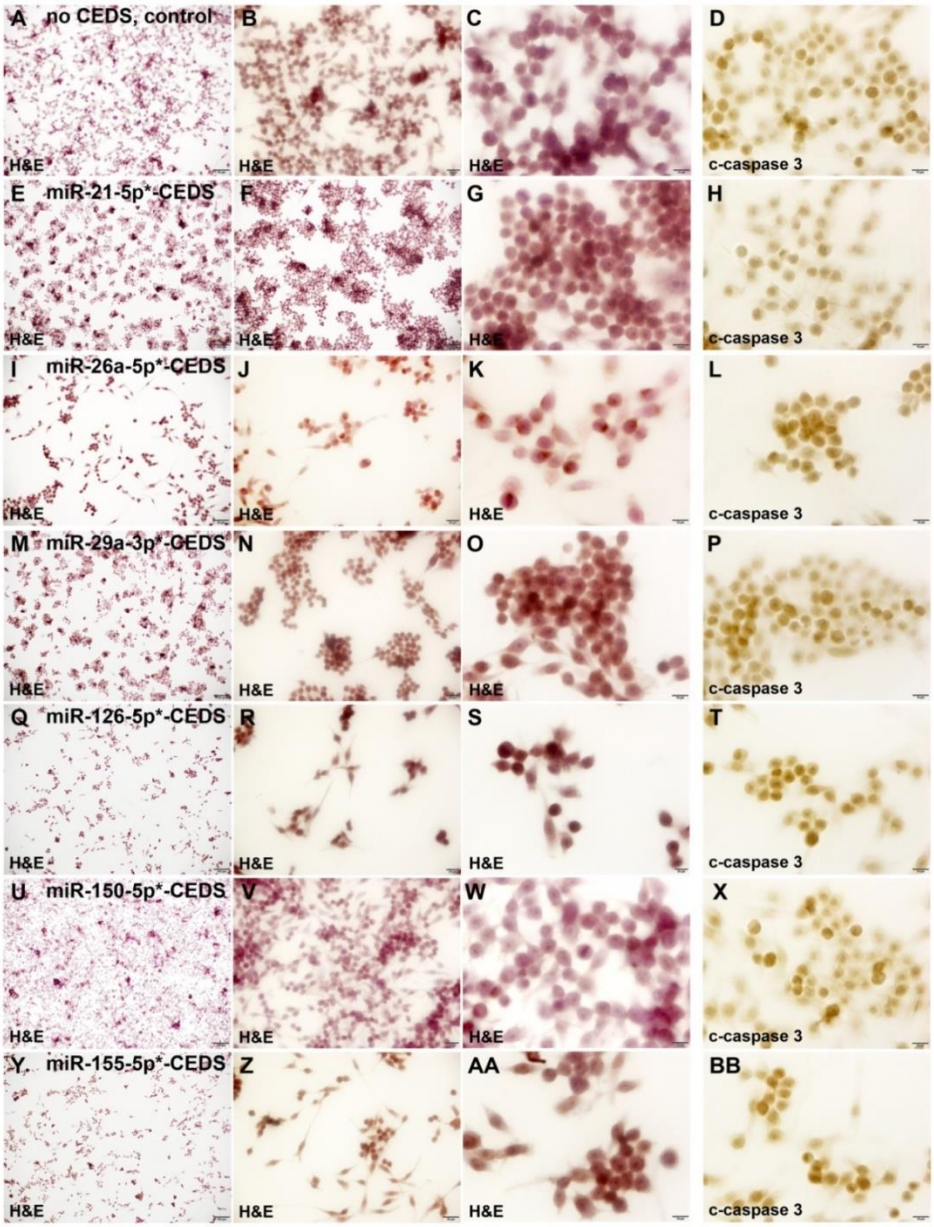

Fig. 24. Cytological and immunocytochemical staining on RAW 264.7 cells treated with CEDS using murine mature miRNA sequence. A-D: Control, no CEDS, diffuse spread of cells (A-C), and occasional immunoreaction of c-caspase 3 (D). E-H: MiR-21-5p*-CEDS, marked aggregation of cells (E-G), and weak immunoreaction of c-caspase 3(H). I-L: MiR-26a-5p*-CEDS, marked decrease of cell number (I-K), and strong immunoreaction of c-caspase 3(L). M-P: MiR-29a-3p*-CEDS, slight aggregation of cells (M-O), and occasional immunoreaction of c-caspase 3 (P). Q-T: MiR-126-5p*-CEDS, marked decrease of cell number (Q-S), and strong immunoreaction of c-caspase 3 (T). U-X: MiR-150-5p*-CEDS, slight decrease of cell number (U-W), and slight immunoreaction of c-caspase 3 (X). Y-BB: MiR-155-5p*-CEDS, significant decrease of cell number (Y-AA), moderate immunoreaction of c-caspase 3 (BB).

Cytological observation of KB cells treated with telomere repeat sequence*-CEDS

The KB cells derived from human epithelial cell (ATCC, USA) were cultured on culture dishes (90 mm diameter, SPL Life Science, Korea) using the same method as the aforementioned experiment. Approximately 50% confluent KB cells grown on culture dish surfaces were treated with CEDS using telomere repeat sequence (TTAGGG) at 23-25 Gauss for 20 min twice a day. Following a three-day incubation period, the cells were fixed with 10% buffered formalin and stained with hematoxylin and eosin.

Telomere repeat sequences are able to facilitate the replication of chromosome ends and to generate a T-loop with a telomere-binding protein complex, shelterin, to prevent chromosomal degradation. Telomere shortening and instability can induce aging and various diseases due to telomere dysfunction and chromosomal instability. The present study selected a telomere repeat sequence, TTAGGG, for CEDS experiment on KB cells.

CEDS using telomere repeat sequence, TTAGGG*-CEDS exhibited a notable reduction in cell density on the culture dish, as observed grossly, and a comparable decline in the number of KB cells, as observed microscopically, in comparison to CEDS using random sequence, 2(ACGT)*-CEDS. Conversely, the KB cells that were not treated with CEDS exhibited robust growth and occupied the entire surface area of the culture dish. The KB cells that were treated with the 2(ACGT)*-CEDS demonstrated similar growth patterns in the gross observation to the KB cells that were not treated with CEDS (Fig. 25).

In the high-magnification view, the KB cells that had not been treated with CEDS were distributed in a compact manner and exhibited frequent mitotic features with hyperchromatic nuclei. In contrast, the cells that had been treated with the 2(ACGT)*-CEDS exhibited a slight decrease in cell number and a lower mitotic feature compared to the cells that had not been treated with CEDS. In contrast, the cells treated with the TTAGGG*-CEDS exhibited a notable reduction in cell number, accompanied by a higher prevalence of pyknotic cells undergoing apoptosis compared to the cells not treated with CEDS and the cells treated with the 2(ACGT)*-CEDS (Fig. 25 C, F, and I).

o

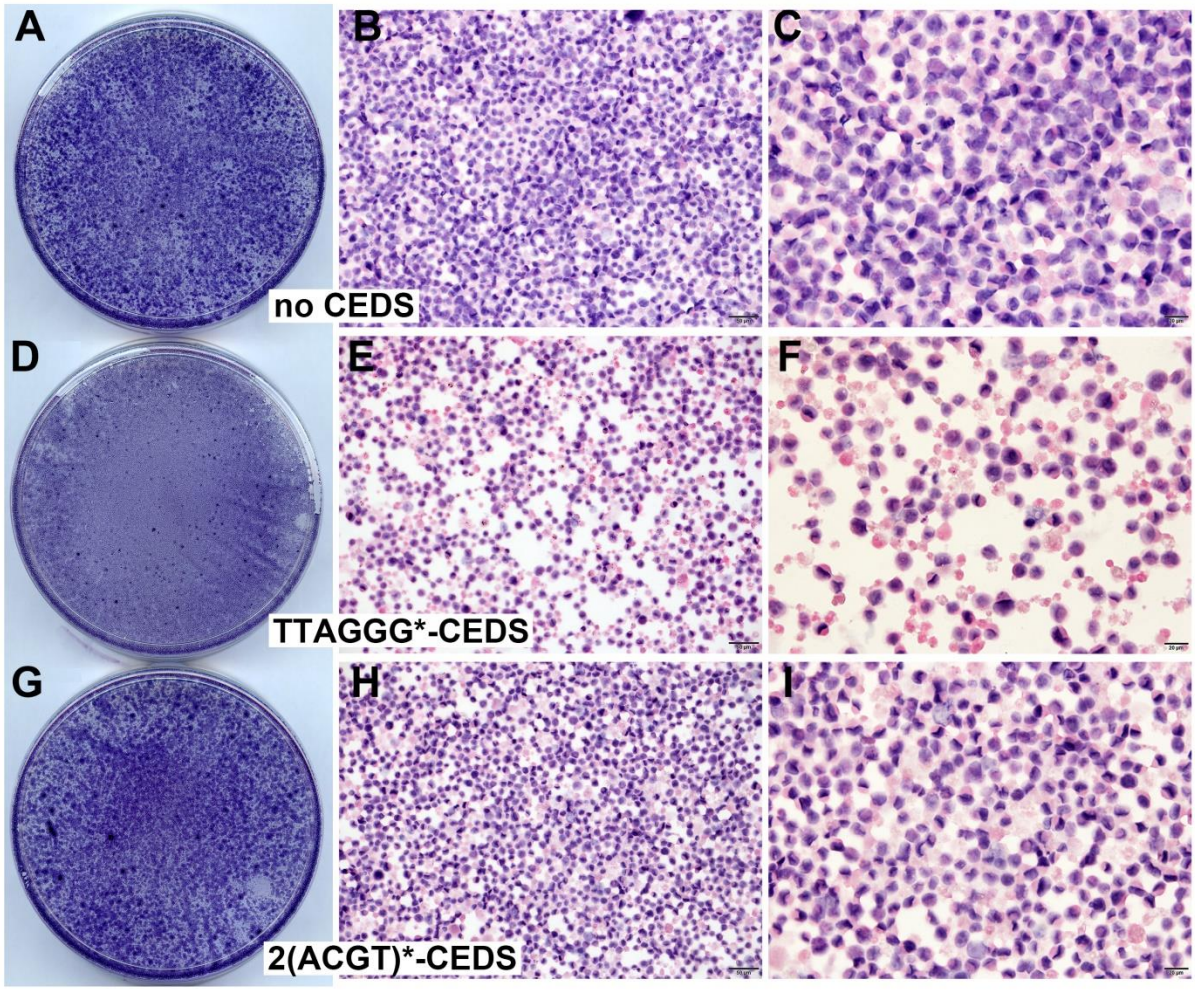

Fig. 25. Cytological observation of KB cells after CEDS treatment. H&E stain. A-C: The control with no CEDS showed the abundant growth of cells on Petri dish (A) and in the microscopic observation (B and C), exhibiting hyperchromatic nuclei and frequent mitosis. D-F: The telomere sequence TTAGGG*-CEDS produced marked cell loss with frequent apoptotic cell death. G-I: The random sequence 2(ACGT)*-CEDS resulted the similar features to the untreated control (A-C).

Cytological observation of KB cells treated with telomere repeat sequence*-, canonical E-box sequence*-, and p53 binding site sequence*-CEDS separately

The KB cells were cultured on culture dishes (90 mm diameter) using the same method as the aforementioned experiment. Approximately 50% confluent KB cells grown on culture dish surfaces were treated with CEDS using a miRNA sequence at 23-25 Gauss for 20 min twice a day in the culture incubator. Following a three-day incubation period, the cells were fixed with 10% buffered formalin and stained with toluidine blue, a basic thiazine metachromatic dye with high affinity for acidic tissue components, likely DNA and RNA. Subsequently, gross and microscopic observations were performed.

A comparison of CEDS effect between the telomere repeat sequence (TTAGGG)*-CEDS and the mutant telomere repeat sequence (TTTGGG)*-CEDS revealed that the TTAGGG*-CEDS markedly decreased the cell density and metachromasia in toluidine blue versus the untreated control. In contrast, the TTTGGG*-CEDS exhibited a weaker effect on cell density and metachromasia in toluidine blue stain than the TTAGGG*-CEDS (Fig. 26 A-C).

The results show that the telomere repeat sequence (TTAGGG)*-CEDS strongly induces cell death, while the mutant telomere repeat sequence (TTTGGG)*-CEDS induces cell death to a lesser extent due to a base pair inversion from A-T to T-A. Therefore, it is postulated that the telomere repeat sequence (TTAGGG)*-CEDS may affect the conformation of unique telomere sequences more effectively than the mutant telomere repeat sequence (TTTGGG)*-CEDS, thereby strongly inhibiting proliferation and simultaneously inducing apoptosis in KB cells.

The E-box binding proteins play a pivotal role in regulating transcription activity for genome-wide transcription of numerous genes. Their numbers and types vary depending on the binding specificity of E-box. In the consensus sequences of E-box, CANNTG, the canonical E-box sequence, CACGTG, was selected for the present CEDS study. The canonical E-box sequence (CACGTG)*-CEDS exhibited a slight decrease in cell density and cell number in toluidine blue stain, as observed both grossly and microscopically, in comparison to the random sequence (2(ACGT))*-CEDS and the untreated control. Furthermore, the cells treated with the

CACGTG*-CEDS demonstrated less metachromasia in toluidine blue stain than the cells treated with 2(ACGT)*-CEDS and no CEDS (Fig. 26 D-F).

The results indicate that the CACGTG*-CEDS attenuates DNA and RNA transcription and induces cell death, while the 2(ACGT)*-CEDS rarely affects DNA and RNA transcription and does not induce any features of cell death similar to the untreated control. Therefore, it can be postulated that the canonical E-box sequence (CACGTG)*-CEDS affects the conformation of the E-box
CACGTG, and subsequently impairs the binding of c-Myc to E-boxes in KB cells.

The consensus binding site of p53 response elements (REs) is comprised of two decameric DNA motifs, RRRCWWGYYY (R = A, G; W = A, T; Y = C, T), which are redundant, approximately palindromic, and separated by 0–18 bp. In the present study, the decameric binding site sequence for p53 cluster 1 RE[21], AGACATGCCT was selected for CEDS experiment on KE cells.

The p53 binding site sequence (AGACATGCCT)*-CEDS demonstrated a weak reduction in cell density and metachromasia in toluidine blue staining, both grossly and microscopically, in comparison to the random sequence (2(ACGT))*-CEDS and the untreated control. In the high-magnification view, the cells treated with the AGACATGCCT*-CEDS exhibited monotonous, round nuclei with reduced metachromasia, while the cells treated with the 2(ACGT)*-CEDS displayed pleomorphic and hyperchromatic nuclei with strong metachromasia, similar to those observed in the untreated control (Fig. 26 G-I).

The results indicate that the p53 cluster 1 RE binding site sequence (AGACATGCCT)*-CEDS may exert a differential influence on the binding of the tetrameric p53 protein complex, contingent on the transcriptional context of each gene. This results in a weak anti-oncogenic effect on KB cells in this study. However, it is postulated that the protein binding specificity on the binding site DNA sequence may be influenced by the unique base pair polarities of the binding site dsDNA conformation in a more intricate manner than previously anticipated, interacting with various responsible materials.

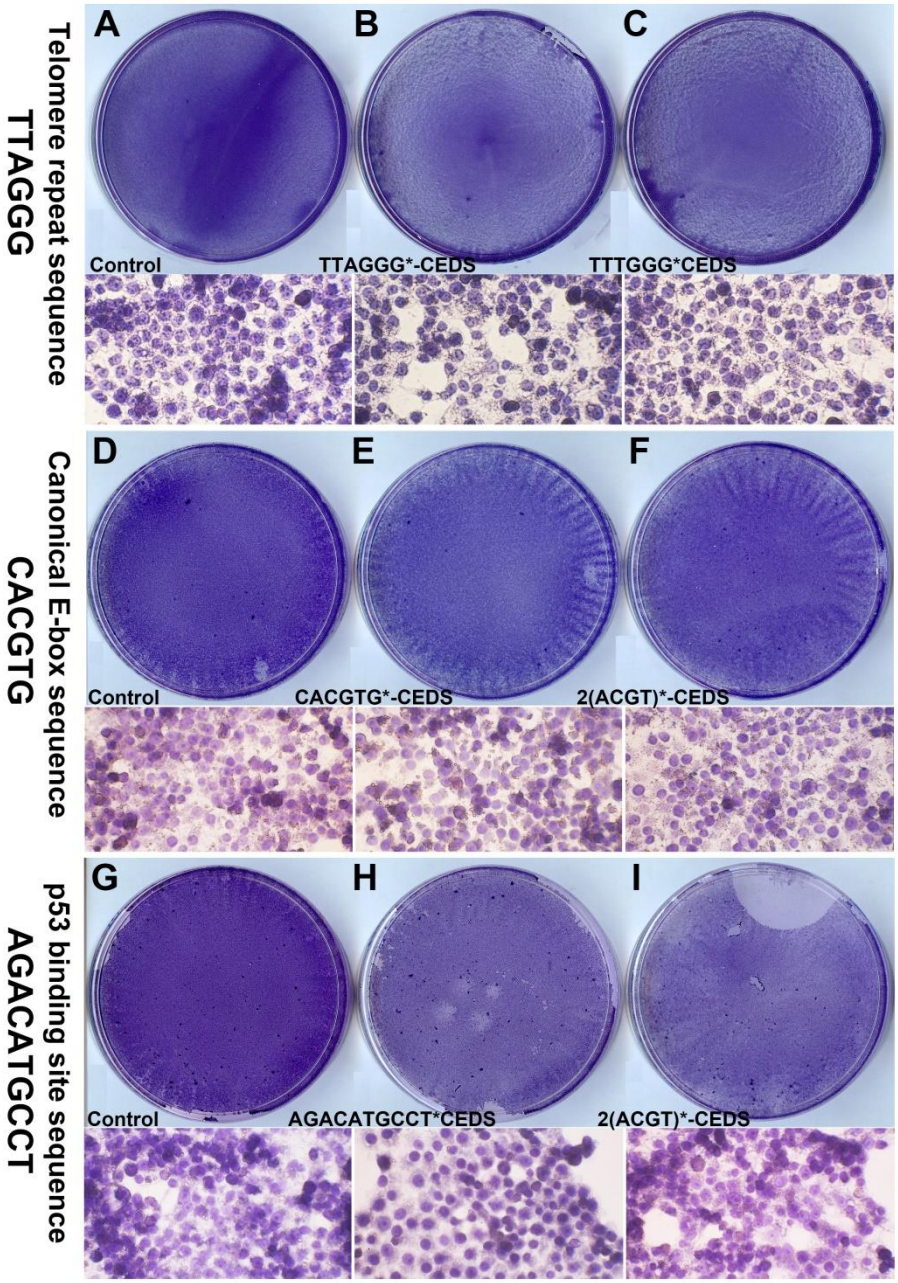

Fig. 26. Cytological observation of KB cells treated with different CEDS at 20-25 Gauss, 20 min per a day, for 3 days during the cell culture with toluidine blue stain. The control was not treated with CEDS. A-C: The telomere repeat sequence (TTAGGG)*-CEDS was found to induce greater apoptotic cell death than the mutant telomere sequence (TTTGGG)*-CEDS. The KB cells treated with the TTAGGG*-CEDS exhibited lower metachromasia in toluidine blue stain than the TTTGGG*-CEDS as well as the untreated control. D-F: The canonical E-box sequence (CACGTG)*-CEDS was found to induce a slight apoptotic cell loss compared to the random sequence (2(ACGT))*-CEDS and the untreated control. G-I: The p53 binding site sequence (AGACATGCCT)*-CEDS demonstrated a similar cell number and a lower metachromasia in toluidine blue stain compared to the untreated control and the 2(ACGT)*-CEDS.

The DNA and RNA are the central reservoir in cells, which can modulate cellular structures and functions through DNA/RNA transcription and protein translation. It is thought that they have special biological signals to function as distinctive modulators. The nucleotides themselves are amphoteric, but become acidic when the cryptic internalization of base pairs occurs after hybridization. The acidity of hybridized nucleotide complexes, including dsDNA and dsRNA, may be relevant to the strength of the hybridization. Therefore, it can be postulated that the slight acidity of dsDNA and dsRNA may exert the intramolecular electric conductivity, which is controllable by the level of hydrogen bonding strength between base pairs.

In another sense, the dsDNA and dsRNA may exhibit semiconducting properties that are dependent on changes in the hydrogen bonding strength between base pairs. It is therefore reasonable to postulate that the unique semi-conductive properties of dsDNA and dsRNA will enable them to carry out the full range of biological signaling processes associated with DNA and RNA transcription and protein translation, and that it could be readily affected by CEDS in a sequence-specific manner.

CEDS utilized in this study was designed to regulate the hydrogen bonding strength between base pairs of dsDNA and dsRNA. CEDS is available due to the regular cyclic arrangement of base pairs in dsDNA and dsRNA. It can target a specific sequence of dsDNA and dsRNA by CEDS due to the same angular momentum between macroscale and ultramicroscale structures of dsDNA and dsRNA. The preceding study demonstrated that the targeting efficiency of CEDS to randomly arranged dsRNA or dsRNA is approximately 25%.

The objective of this study is to identify the cellular changes that occur following CEDS targeting nine mature miRNAs and four protein binding site sequences in RAW 264.7 cells. The gross and cytological observations were initially conducted, and subsequently, the protein expression changes that influence the entire protein signaling were examined through IP-HPLC using monospecific 350 antisera.

It was hypothesized that CEDS could enhance the hydrogen bonding strength between DNA/RNA base pairs and induce the native base pair polarities of DNA/RNA, which are required for DNA/RNA transcription. The present study investigated the changes in the expression of mature and primary miRNAs through the real-time qPCR method. The qPCR results demonstrated that both mature and primary miRNAs were increased in number after CEDS. It appears that the mature miRNAs exhibited a greater increase than the primary miRNAs

in response to CEDS treatment. These findings suggest that CEDS may facilitate not only the production of mature miRNAs from primary miRNAs but also the formation of primary miRNAs from miRNA gene transcripts.

The nine miRNA sequence*-CEDSs investigated in this study demonstrated a significant impact on the expression of target proteins, with an average reduction of 66.4%. MiR-26a-5p*-CEDS exhibited a pronounced anti-oncogenic effect, accompanied by a reduced potential for apoptosis, innate and cellular immunity in RAW 264.7 cells. MiR-126-5p*-CEDS induced a potent anti-oncogenic effect, accompanied by a strong potential for apoptosis, innate and cellular immunity in RAW 264.7 cells. However, it also exhibited a potential for fibrosis and senescence. MiR-150-5p*-CEDSs exhibited a potent anti-oncogenic effect, accompanied by a strong anti-inflammatory effect, but a reduced potential for apoptosis, innate and cellular immunity in RAW 264.7 cells. In contrast, miR-34a-5p, miR-181a-5p, miR-216a-5p, miR-365a-3p, and miR-655-3p*-CEDSs exhibited a dual effect, inducing both anti-oncogenic and oncogenic effects. MiR-155-5p*-CEDS demonstrated a tendency to induce a marked oncogenic effect, with an elevated potential of proliferation, survival, senescence, and fibrosis, rather than an anti-oncogenic effect on RAW 264.7 cells.

The telomere repeat sequence (TTAGGG)*-CEDS was found to have a tendency to downregulate the telomere-associated proteins (62.6%), in contrast to the canonical E-box sequence (CACGTG)*-CEDS (40%), the p53 cluster 1 response element binding site sequence (AGACATGCCT)*-CEDS (37%), and the canonical E2Fs binding site sequence (TTTC(C/G)CGC)*-CEDS (40.1%). It is noteworthy that the telomere repeat sequence*-CEDS demonstrated a robust anti-oncogenic effect in both IP-HPLC and cytological observation, inhibiting proliferation, survival, oncogenesis, senescence, and telomere instability signaling while concomitantly enhancing apoptosis and innate and cellular immunity signaling.

The abundant distribution of telomere repeat sequences (TTAGGG) at both ends of each chromosome may contribute to the higher response of the TTAGGG*-CEDS compared to the other protein binding site sequence*-CEDSs observed in this study. However, it is thought that the TTAGGG*-CEDS may affect the G-quadruplex structure of telomere by increasing the hydrogen bonding strength between base pairs of dsTTAGGG rather than the external Hoogsteen bonding strength of the G-quadruplex. Consequently, the

TTAGGG*-CEDS can stabilize telomere G-quadruplexes, which play a critical role in chromatin protection, DNA replication, transcription and genomic stability, and resulted in anti-oncogenic effect on RAW 264.7 cells.

Furthermore, it has been demonstrated that CEDS using a single miRNA sequence can influence the expression of other miRNAs that are linked to it through a feedback loop involving gene transcription and protein translation in qPCR and IP-HPLC analysis. For instance, miR-26a-5p*-CEDS was observed to increase the expression of miR-126-5p and miR-655-3p while concomitantly decreasing the expression of miR-365a-3p. Similarly, miR-34a-5p*-CEDS was found to elevate the expression of miR-126-5p and miR-655-3p, while concurrently reducing the expression of miR-21-5p. MiR-126-5p*-CEDS increased the expression of miR-26a-5p and miR-655-3p. MiR-150-5p*-CEDS increased the expression of miR-126-5p, miR-365a-3p, and miR-655-3p. MiR-155-5p*-CEDS increased the expression of miR-181a-5p. MiR-181a-5p*-CEDS increased the expression of miR-126-5p, miR-216a-5p, and miR-655-3p. MiR-216a-5p*-CEDS increased the expression of miR-26a-5p and miR-126-5p. MiR-365a-3p*-CEDS was observed to increase the expression of miR-216a-5p while concomitantly decreasing the expression of miR-26a-5p and miR-126-5p. And miR-655-3p*-CEDS was found to increase the expression of miR-365a-3p while concomitantly decreasing the expression of miR-21-5p.

In this study, the 12A sequence was employed as a control sequence in CEDS experiments to be compared with other specific motif sequences, including those of nine oncogenesis-related miRNAs, the telomere repeat, the E-box, the p53 binding site, and the E2Fs binding site. However, the 12A sequence may exhibit homology to numerous poly-A dsDNA sequences (4A-12A) within the genome DNAs of RAW 264.7 cells. Consequently, the 12A*-CEDS is also capable of influencing gene transcription and protein expression by targeting nA (n = 4~12) sequences within genomic DNA and miRNAs, respectively, which are almost impossible to be identified. It is therefore proposed that the 12A*-CEDS be considered a nonspecific positive control in comparison to the other CEDSs performed in this study.

CEDS has been designed to stimulate the DNA base pair polarities of target dsDNA, leading to a change in the DNA conformation. This enables CEDS to exert a regulatory effect on the target dsDNA safely. Therefore, it is suggested that CEDS can influence the target dsDNA in a sequence-specific manner with minimum biohazard, and that its results should be assessed by the probability of targeting, rather than by the mechanical targeting. Although CEDS is a non-invasive method that requires no additional medication and is relatively easy

to use with a variety of procedures for multiple CEDS treatments to target specific miRNAs and DNA motifs in cells with minimal electromagnetic exposure, CEDS showed variable targeting efficiency depending on the context and cell types and also showed the secondary effect on other gene via sequence homology or feedback loop of gene transcription and protein translation. Therefore, it is highly recommended that the effect of CEDS should be explored through *in vitro* culture experiments before application in animals and patients, using the hydrogen bonding magnetic resonance (HBMR)-based gene regulation (HBMR-GR) system consisting of CEDS device, IP-HPLC analysis, and big data for gene targeting.

Acknowledgments

We would like to express our gratitude to the late Professor Je Geun Chi and the late Dr. Soo Il Chung, who contributed to this research in part.

References

1 Lee, S. K., Lee, D. G. & Kim, Y. S. Development of Hydrogen Bonding Magnetic Reaction-based Gene Regulation through Cyclic Electromagnetic DNA Simulation in Double-Stranded DNA. *arXiv*, arXiv:1210.7091 (2024).

2 Komatsu, S., Kitai, H. & Suzuki, H. I. Network Regulation of microRNA Biogenesis and Target Interaction. *Cells* **12**, doi:10.3390/cells12020306 (2023).

3 Kim, S. M., Eo, M. Y., Cho, Y. J., Kim, Y. S. & Lee, S. K. Differential protein expression in the secretory fluids of maxillary sinusitis and maxillary retention cyst. *European archives of oto-rhino-laryngology : official journal of the European Federation of Oto-Rhino-Laryngological Societies* **274**, 215-222, doi:10.1007/s00405-016-4167-2 (2017).

4 Kim, S. M., Eo, M. Y., Cho, Y. J., Kim, Y. S. & Lee, S. K. Immunoprecipitation high performance liquid chromatographic analysis of healing process in chronic suppurative osteomyelitis of the jaw. *Journal of cranio-maxillo-facial surgery : official publication of the European Association for Cranio-Maxillo-Facial Surgery* **46**, 119-127, doi:10.1016/j.jcms.2017.10.017 (2018).

5 Lee, I. S. *et al.* Effects of 4-Hexylresorcinol on Craniofacial Growth in Rats. *International journal of molecular sciences* **22**, doi:10.3390/ijms22168935 (2021).

6 Seo, M. H., Kim, D. W., Kim, Y. S. & Lee, S. K. Pentoxifylline-induced protein expression change in RAW 264.7 cells as determined by immunoprecipitation-based high performance liquid chromatography. *PloS one* **17**, e0261797, doi:10.1371/journal.pone.0261797 (2022).

7 Yoon, C. S., Kim, M. K., Kim, Y. S. & Lee, S. K. In vivo protein expression changes in mouse livers treated with dialyzed coffee extract as determined by IP-HPLC. *Maxillofacial plastic and reconstructive surgery* **40**, 44, doi:10.1186/s40902-018-0183-z (2018).

8 Yoon, J. H., Kim, D. W., Lee, S. K. & Kim, S. G. Effects of 4-hexylresorcinol administration on the submandibular glands in a growing rat model. *Head & face medicine* **18**, 16, doi:10.1186/s13005-022-00320-7 (2022).

9 Dharap, A., Pokrzywa, C., Murali, S., Pandi, G. & Vemuganti, R. MicroRNA miR-324-3p induces promoter-mediated expression of RelA gene. *PloS one* **8**, e79467, doi:10.1371/journal.pone.0079467 (2013).

10 Xiao, M. *et al.* MicroRNAs activate gene transcription epigenetically as an enhancer trigger. *RNA biology* **14**, 1326-1334, doi:10.1080/15476286.2015.1112487 (2017).

11 Friedman, R. C., Farh, K. K., Burge, C. B. & Bartel, D. P. Most mammalian mRNAs are conserved targets of microRNAs. *Genome research* **19**, 92-105, doi:10.1101/gr.082701.108 (2009).

12 Bao, F., LoVerso, P. R., Fisk, J. N., Zhurkin, V. B. & Cui, F. p53 binding sites in normal and cancer cells are characterized by distinct chromatin context. *Cell cycle* **16**, 2073-2085, doi:10.1080/15384101.2017.1361064 (2017).

13 Carson, L. M. & Flynn, R. L. Highlighting vulnerabilities in the alternative lengthening of telomeres pathway. *Current opinion in pharmacology* **70**, 102380, doi:10.1016/j.coph.2023.102380 (2023).

14 Gong, H., Lu, F., Zeng, X. & Bai, Q. E2F transcription factor 1 (E2F1) enhances the proliferation, invasion and EMT of trophoblast cells by binding to Zinc Finger E-Box Binding Homeobox 1 (ZEB1). *Bioengineered* **13**, 2360-2370, doi:10.1080/21655979.2021.2023793 (2022).

15 Pan, Y., van der Watt, P. J. & Kay, S. A. E-box binding transcription factors in cancer. *Frontiers in oncology* **13**, 1223208, doi:10.3389/fonc.2023.1223208 (2023).

16 Taciak, B. *et al.* Evaluation of phenotypic and functional stability of RAW 264.7 cell line through serial passages. *PloS one* **13**, e0198943, doi:10.1371/journal.pone.0198943 (2018).

17 Hashimoto, Y., Akiyama, Y. & Yuasa, Y. Multiple-to-multiple relationships between microRNAs and target genes in gastric cancer. *PloS one* **8**, e62589, doi:10.1371/journal.pone.0062589 (2013).

18 Park, M. H. & Wolff, E. C. Hypusine, a polyamine-derived amino acid critical for eukaryotic translation. *The Journal of biological chemistry* **293**, 18710-18718, doi:10.1074/jbc.TM118.003341 (2018).

19 Chung, S. I. Comparative studies on tissue transglutaminase and factor XIII. *Annals of the New York Academy of Sciences* **202**, 240-255, doi:10.1111/j.1749-6632.1972.tb16338.x (1972).

20 Chung, S. I., Shrager, R. I. & Folk, J. E. Mechanism of action of guinea pig liver transglutaminase. VII. Chemical and stereochemical aspects of substrate binding and catalysis. *The Journal of biological chemistry* **245**, 6424-6435 (1970).

21 Lim, J. H., Latysheva, N. S., Iggo, R. D. & Barker, D. Cluster Analysis of p53 Binding Site Sequences Reveals Subsets with Different Functions. *Cancer informatics* **15**, 199-209, doi:10.4137/CIN.S39968 (2016).

22 Morgunova, E. *et al.* Structural insights into the DNA-binding specificity of E2F family transcription factors. *Nature communications* **6**, 10050, doi:10.1038/ncomms10050 (2015).